IAEA-TECDOC-421

MATERIALS RELIABILITY IN THE BACK END OF THE NUCLEAR FUEL CYCLE

PROCEEDINGS OF A TECHNICAL COMMITTEE MEETING
ON MATERIALS RELIABILITY IN THE BACK END
OF THE NUCLEAR FUEL CYCLE
ORGANIZED BY THE
INTERNATIONAL ATOMIC ENERGY AGENCY
AND HELD IN VIENNA, 2–5 SEPTEMBER 1986

A TECHNICAL DOCUMENT ISSUED BY THE
INTERNATIONAL ATOMIC ENERGY AGENCY, VIENNA, 1987

MATERIALS RELIABILITY IN THE BACK END
OF THE NUCLEAR FUEL CYCLE
IAEA, VIENNA, 1987
IAEA-TECDOC-421

Printed by the IAEA in Austria
May 1987

PLEASE BE AWARE THAT
ALL OF THE MISSING PAGES IN THIS DOCUMENT
WERE ORIGINALLY BLANK

The IAEA does not normally maintain stocks of reports in this series. However, microfiche copies of these reports can be obtained from

INIS Clearinghouse
International Atomic Energy Agency
Wagramerstrasse 5
P.O. Box 100
A-1400 Vienna, Austria

Orders should be accompanied by prepayment of Austrian Schillings 100,– in the form of a cheque or in the form of IAEA microfiche service coupons which may be ordered separately from the INIS Clearinghouse.

FOREWORD

Past and current materials advances have provided a basis for the successful development of the nuclear industry. Operating experience of nuclear fuel cycle facilities has proved that the performance and availability of key equipment largely depend on the reliability of its construction materials. In general, the materials of construction have performed well in accordance with the design criteria of equipment. In some cases, however, materials failure problems have been encountered, the causes of which are related to their corrosion and mechanical degradation.

For more efficient and safe operation of nuclear fuel cycle facilities, the increase of materials reliability becomes one of the common tasks in a number of IAEA Member States. This situation is more important in the back-end of the nuclear fuel cycle which involves higher levels of radioactivity, higher temperatures and corrosive chemicals in various service environments.

In response to the growing interest in these topics, the IAEA convened the Technical Committee Meeting on "Materials Reliability in the Back-End of the Nuclear Fuel Cycle" at its Headquarters from September 2 to 5, 1986 with the attendance of 26 participants from 13 Member States. This Technical Document contains the 15 papers presented during the Meeting. Material aspects of the following fields of the back-end of the nuclear fuel cycle are covered: interim and long-term storage of spent fuel; final disposal of spent fuel; storage and vitrification of High Level Liquid Wastes (HLLW); long-term storage of High Level Wastes (HLW); and spent fuel treatment.

The Agency wishes to thank all the scientists, engineers and institutions who contributed to this Meeting with their papers and their participation. Special thanks are due to the Session Chairmen, Messrs. S. Leistikow (Federal Republic of Germany), H.A.W. Tas (Belgium), T. Yamanouchi (Japan), G.R. Balasubramanian (India), and to the Chairmen of Panel Discussions, Messrs. F.W. Popp (Federal Republic of Germany), G. Turluer and R. Demay (France). The officer of the IAEA, responsible for the organization of the meeting and for editing the document, was Mr. M. Ugajin of the Nuclear Materials and Fuel Cycle Technology Section.

EDITORIAL NOTE

In preparing this material for the press, staff of the International Atomic Energy Agency have mounted and paginated the original manuscripts as submitted by the authors and given some attention to the presentation.

The views expressed in the papers, the statements made and the general style adopted are the responsibility of the named authors. The views do not necessarily reflect those of the governments of the Member States or organizations under whose auspices the manuscripts were produced.

The use in this book of particular designations of countries or territories does not imply any judgement by the publisher, the IAEA, as to the legal status of such countries or territories, of their authorities and institutions or of the delimitation of their boundaries.

The mention of specific companies or of their products or brand names does not imply any endorsement or recommendation on the part of the IAEA.

Authors are themselves responsible for obtaining the necessary permission to reproduce copyright material from other sources.

CONTENTS

Corrosion studies on selected packaging materials for disposal of high level wastes..... 7
E. Smailos, R. Köster

Compatibility of candidate overpack materials with deep argillaceous HLW disposal environments..... 25
H.A.W. Tas, W. Debruyn, J. Dresselaers

Selection of canister materials: Electrochemical corrosion tests of Hastelloy C4 and other Ni-Cr(-Mo) alloys in chloride containing solutions..... 37
I. Wolf, H. Bort

Material corrosion under spent nuclear fuel storage conditions..... 51
V.G. Kritsky, V.V. Morozov, A.F. Nechaev, Yu.A. Khitrov, N.G. Petrik, N.N. Kalyazin, T.F. Makarchuk

Material selection for final storage of spent fuel in a salt repository — The Pollux cask system as an example..... 63
K. Einfeld, F.W. Popp, U. Knapp

HLLW storage tank materials: Technical options and operating experience..... 83
J. Bachelay, J. Decours, R. Demay, M. Pelras, L. Rozand, G. Turluer

Glass melter materials: Technical options for the French vitrification process and operating experience..... 97
R. Bonniaud, R. Demay, R. Richter, L. Rozand

Selection of suitable stainless steels for nuclear reprocessing plants: Application of chemical and electrochemical testing methods to austenitic CrNi steel AISI type 304L in various chemical compositions..... 107
S. Leistikow, R. Kraft, R. Simon, M. Schneider

Austenitic stainless steels: Assessment of progress in materials performance for reprocessing applications..... 117
J. Decours, J.-C. Decugis, R. Demay, M. Pelras, G. Turluer

Experience of corrosion problems and material developments in the Tokai Reprocessing Plant..... 129
T. Yamanouchi, A. Aoshima, N. Sasao, S. Takeda, N. Ishiguro

Study of the chemical structure of films formed during transpassive to passive transitions on a cathodically protected AISI 430 ferritic stainless steel..... 147
M. Ben Haim, U. Atzmony, N. Shamir, J. Yahalom

Long-term storage problems of spent LWR fuel elements..... 155
B. Čech, E. Kadeřábek, J. Koutský

Zirconium use for large process components..... 165
H. Chauve, J. Decours, R. Demay, M. Pelras, J. Simonnet, G. Turluer

Materials reliability in the back-end of the nuclear fuel cycle: Argentine experience..... 193
M.C. Geldstein

Selection of materials for various systems in reprocessing fast reactor fuels — Present status and future programme..... 207
J.B. Gnanamoorthy, G.R. Balasubramanian

Panel Discussions..... 215

List of Participants..... 219

CORROSION STUDIES ON SELECTED PACKAGING MATERIALS FOR DISPOSAL OF HIGH LEVEL WASTES

E. SMAILOS, R. KÖSTER
Institut für Nukleare Entsorgungstechnik,
Kernforschungszentrum Karlsruhe GmbH,
Karlsruhe, Federal Republic of Germany

Abstract

In order to qualify corrosion resistant materials for high level waste (HLW) packagings acting as a long-term barrier in a rock salt repository, the corrosion behaviour of the preselected materials Ti 99.8-Pd, Hastelloy C4 and two unalloyed steels was investigated. The resistance of the materials to general corrosion, local corrosion and stress corrosion cracking was examined under postulated accident conditions in the repository by long-term immersion tests of up to 4 years duration and electrochemical methods. The parameters investigated were different salt brines, temperatures of 90°C, 170°C and 200°C as well as a gamma radiation field of 10^3Gy/h (10^5rad/h).

Among the materials studied, Ti 99.8-Pd exhibited the highest corrosion resistance. This material corroded at a very low rate (<1µm/a) both with and without gamma radiation, and proved to be resistant to local corrosion and stress corrosion cracking. Further work is needed to assess its susceptibility to hydrogen embrittlement. Hastelloy C4 exhibited a good general corrosion behaviour (≤2µm/a) but was susceptible to crevice corrosion, and pitting corrosion occured at 200°C. Under gamma irradiation i.e. in the presence of strong oxidants (e.g. H_2O_2, ClO_3^-) the susceptibility of Hastelloy C4 to local corrosion increased and strong pitting and crevice corrosion was observed at 90°C. The electrochemical studies confirmed the tendency of this material to local corrosion. They show that the stability of the protective passive layer is greatly reduced with increasing temperature. More anodic potentials than the passivated zone (e.g. 50 to 250 mV at 90°C) give rise to local attacks.

The two unalloyed steels (fine-grained steel and cast steel) were resistant to local and stress corrosion cracking in the absence of gamma radiation so that their corrosion behaviour due to general corrosion is predictable. However, the steels must be sufficiently protected against gamma radiation. In this case their corrosion rates are in the order of 30-40 µm/a at 90°C and 100-140 µm/a at 170°C and thus acceptable for a "corrosion allowance concept". With the temperature increasing to 200°C the steels corroded at rates of 500-600 µm/a so that thick-walled self-shielding packagings will be required in order to ensure long-term stability. Further studies will be necessary to determine the treshold value below which the gamma dose rate must decline to avoid a significant influence on the corrosion of steels, and to evaluate the risk of hydrogen embrittlement.

Due to the predictable corrosion behaviour and considering easy manufacturing of containers, quality assurance concept and material costs, an unalloyed steel seems to be the most promising material for a long-term HLW-packaging.

---

1. INTRODUCTION

According to the waste management concept developed in the Federal Republic of Germany high level wastes (HLW) will be solidified in borosilicate glass, packed into Cr-Ni steel canisters and disposed of in rock salt formations. To provide an additional protection of HLW forms against radionuclide mobilization by a postulated attack of corrosive salt brines, the use of a corrosion resistant packaging acting as a barrier during the high temperature phase in the disposal area is being investigated.

In order to qualify corrosion resistant packaging materials investigations were performed within the Research Programme of the European Communities on different materials which had been

preselected in a first phase of the test programme /1,2/. On the basis of these studies the materials Ti 99.8-Pd, Hastelloy C4, and the unalloyed steels fine-grained steel and cast steel were selected for further long-term corrosion tests and electrochemical investigations. This paper describes mainly results of long-term immersion tests on the corrosion behaviour of the above materials performed in six salt brines which may be present in a repository in rock salt under specified hypothetical accident conditions. Further parameters were the temperatures of 90°C, 170°C and 200°C as well as a gamma radiation field of 10^3Gy/h (10^5rad/h). Besides the results of immersion tests, some results of electrochemical studies will be reported. They relate to the stability of passive layers of Ti 99.8 Pd and Hastelloy C4 in salt brines and to the influence exerted by oxidising radiolytic products (e.g. H_2O_2, ClO_3^-) as well as by some salt impurities (e.g. Fe^{3+},Cu^{2+}) and thermally released products (H_2S, HCl) on the corrosion behaviour of Hastelloy C4.

2. MATERIALS AND TEST CONDITIONS

The materials investigated had the following chemical compositions:

- Ti 99.8 Pd (DIN No. 3.7025.10):
  0.18 wt% Pd, 0.05 wt% Fe, 0.04 wt% O_2, 0.001 wt% H_2, BAL Ti;
- Hastelloy C4 (DIN No. 2.4610):
  15.4 wt% Cr, 15.2 wt% Mo, 0.79 wt% Fe, 0.24 wt% Ti, BAL Ni;
- fine-grained steel (DIN No. 1.0566):
  0.17 wt% C, 0.44 wt% Si, 1.49 wt% Mn, BAL Fe;
- cast steel (DIN No. 1.1131):
  0.16 wt% C, 0.61 wt% Si, 1.51 wt% Mn, BAL Fe.

The materials were tested in six salt brines. The test media were selected on the basis of common knowledge of brines possibly occuring in the Zechstein bodies of rock salt in Lower Saxony in the FRG. The compositions of the brines at 55°C and their pH

values measured at 25°C were:

- $NaCl-H_2O$ (wt%) : 26.9 NaCl, 73.1 H_2O (pH = 7.2).
- $NaCl-CaSO_4-H_2O$ (wt%) : 26.9 NaCl, 0.5 $CaSO_4$, 72.6 H_2O (pH = 6.8).
- $KCl-H_2O$ (wt%) : 30.7 KCl, 69.3 H_2O (pH = 6.4).
- $CaCl_2-H_2O$ (wt%) : 57.4 $CaCl_2$, 42.6 H_2O (pH = 2.9).
- $NaCl-KCl-MgCl_2-MgSO_4-H_2O$ (Z-brine):
  0.2 NaCl, 0.66 KCl, 36.4 $MgCl_2$, 0.87 $MgSO_4$, 61.87 H_2O (pH = 3.6).
- $NaCl-KCl-MgCl_2-MgSO_4-H_2O$ (Q-brine):
  1.4 NaCl, 4.7 KCl, 26.8 $MgCl_2$, 1.4 $MgSO_4$, 65.7 H_2O (pH = 4.9).

In order to simulate the additional uptake of NaCl in a HLW borehole at the higher disposal temperatures (200°C at the maximum), 1.7 g NaCl was added per 100 g of solution. The saturation oxygen content of the salt brines between 25°C and 55°C was in the range from 0.2 mg/l to 5 mg/l.

The majority of the corrosion tests related to the quinary Q-brine because this brine is considered to be the most relevant solution encountered in an accident in a repository in rock salt. The influence of temperature and gamma radiation of 10^3Gy/h (10^5rad/h) on the long-term corrosion behaviour of the materials was investigated in this medium by immersion tests of up to 4 years duration. The study of the influence exerted by gamma-radiation on the corrosion behaviour of the materials is important because it can influence the corrosion mechanism. On the one hand, radiolytic dissociation of the brines produces reducing/oxidising reactive particles and stable products such as e^-_{aq}, Cl_2^-, H_2O_2, O_2, ClO_4^-, ClO_3^-, ClO^-, Cl_2 /3,4,5/ which are capable of accelerating or inhibiting the process of corrosion. On the other hand, the semi-conductor properties of oxide protective films on metals may undergo changes as a result of absorption of the gamma-radiation (photoelectric effect) /5/.

The test temperatures in Q-brine without irradiation were 90°C, 170°C and 200°C. The experiments were carried out at normal pressure at 90°C and equilibrium pressure of 0.55 MPa and 0.9

MPa at 170°C and 200°C, respectively. The temperature of 200°C corresponds to the maximum surface temperature of the HLW canisters according to the German borehole concept. The influence of gamma radiation on the corrosion behaviour of the materials in Q-brine was tested at 90°C. The selected radiation dose of 10^3Gy/h corresponds to the dose rate on the surface of a thin-walled (about 5 mm) HLW canister. The radiation source was Co-60 of about 1.1×10^{14}Bq (3000 Ci). In the other five salt brines comparative studies were performed at 170°C in order to investigate the influence of brine composition on the corrosion behaviour of the materials. All corrosion tests were performed with a specimen-surface to medium-volume ratio (S/V) of 1 $cm^2/5cm^3$, i.e. for the case of an excess in corrodant. For the experiments at 90°C glass vessels and at 170°C and 200°C pressure vessels were used.

After immersion in the salt brines the specimens were freed from the adhering salts and corrosion products, and their resistance to general corrosion, pitting and crevice corrosion as well as stress corrosion cracking was investigated. The general corrosion was examined on plain specimens (40 mm x 20 mm x 3-4 mm, for cast steel 40 mm x 20 mm x 10 mm) and the stress corrosion cracking on TIG-welded U-specimens (80 mm x 15 mm x 3-4 mm). On both specimen types also the resistance to pitting corrosion was investigated. The crevice corrosion attack was examined on plain specimens by contact metal/metal and metal/PTFE. In order to investigate the influence of welding on the corrosion behaviour of the materials TIG-welded plain specimens were used in addition to welded U-specimens. The general corrosion (weight changes) of the specimens in the brines was determined gravimetrically, local corrosion attacks by an electronic depth gauge and by taking surface profiles and metallographic micrographs.

Electrochemical studies were performed in order to get information on the stability of passive layers of Ti 99.8-Pd and Hastelloy C4 in Q-brine as well as on the influence of oxidising radiolytic products (H_2O_2, ClO^-, ClO_3^-, ClO_4^-), of some salt impurities (Br^-,J^-,Fe^{3+},Ca^{2+}/6/), and of thermally released products from rock salt (H_2S, HCl/7/).

3. RESULTS AND DISCUSSION

3.1 Influence of temperature on material corrosion in the quinary Q-brine

The time-temperature behaviour of the general corrosion rates of the materials investigated in Q-brine is shown in Figs. 1 and 2. The data are average values of 3-6 comparative specimens and have been calculated from the weight losses. The ranges indicated for the general corrosion rates show the standard variation of the specimens.

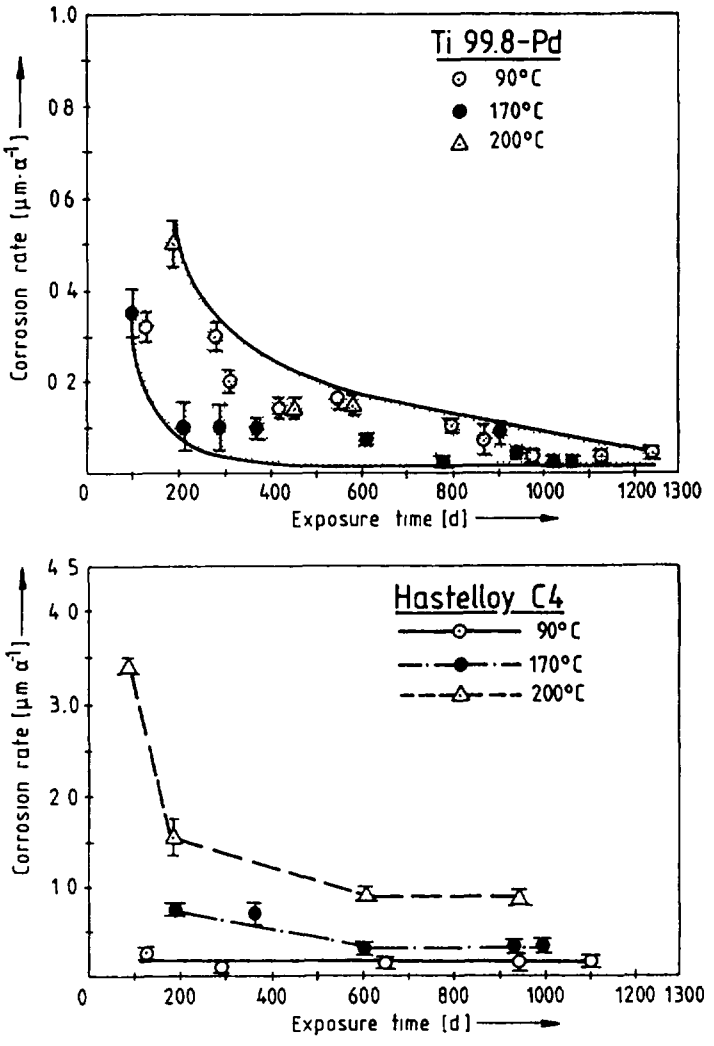

Fig. 1 General corrosion rates of Ti 99.8-Pd and Hastelloy C4 in Q-brine at different temperatures

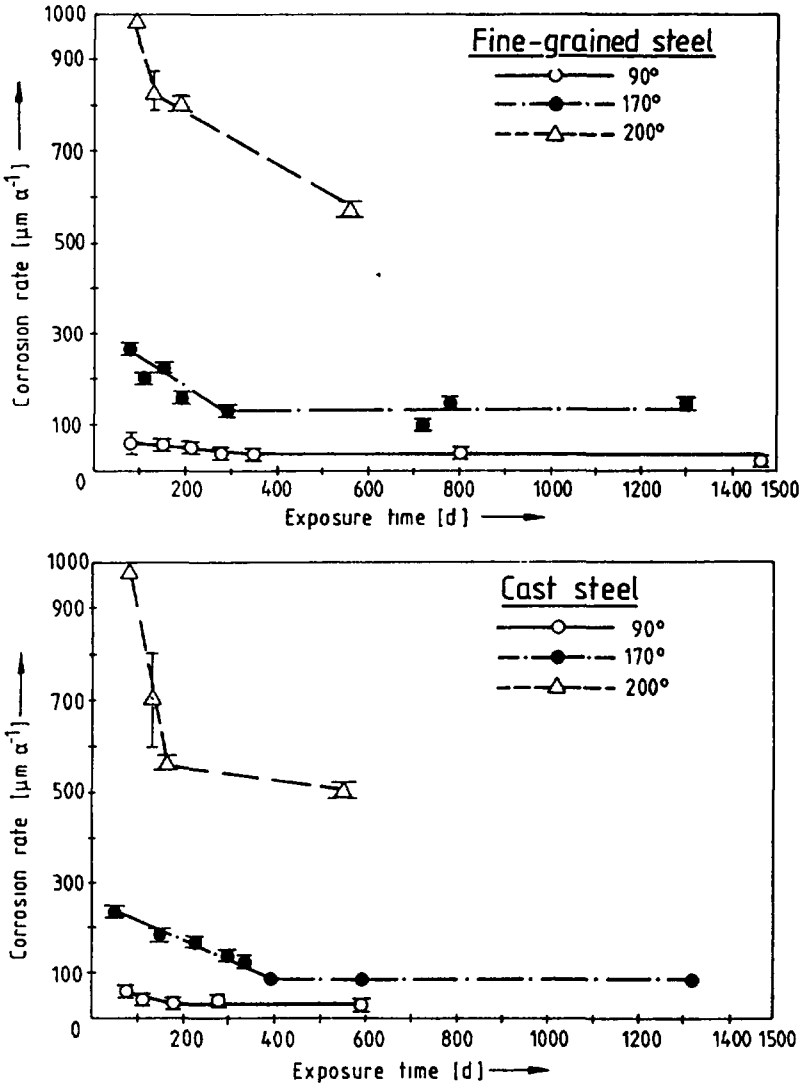

Fig. 2 General corrosion rates of fine-grained steel and cast steel in Q-brine at different temperatures

The material Ti 99.8-Pd corroded over a test period of about 4 years in Q-brine at an extremely low general corrosion rate (Fig.1). The final corrosion rate is in the order of 0.1-0.2 µm/a and seems to approach a constant value. The corrosion rate was not influenced noticeably by test temperatures up to 200°C. The material corroded uniformly; pitting corrosion, crevice corrosion or stress corrosion cracking was not encountered. The optical micrograph in Fig.3 shows the uniform corrosion of Ti 99.8-Pd by the example of a specimen immersed in brine for 420 days at 200°C.

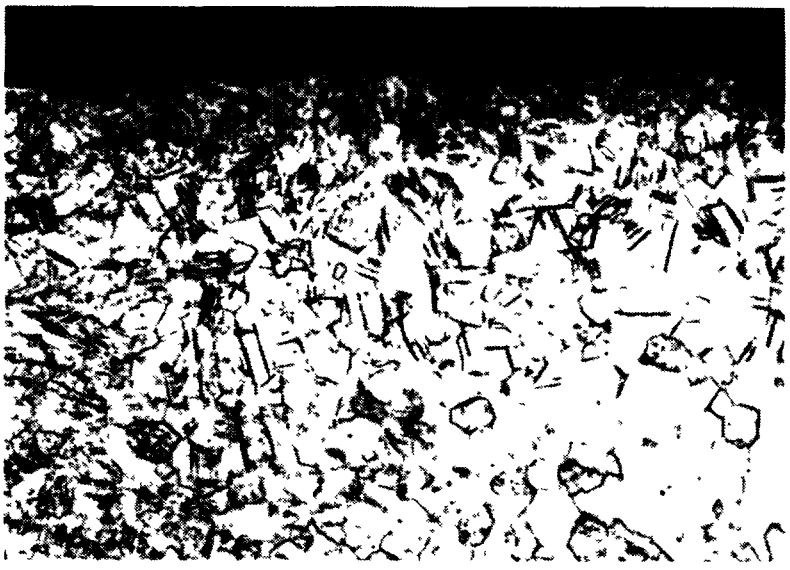

FIG. 3 OPTICAL MICROGRAPH OF Ti 99.8-Pd AFTER 420 DAYS IMMERSION IN Q-BRINE AT 200° C

(X 200)

The high corrosion resistance exhibited by Ti 99.8-Pd in brines to general corrosion and local corrosion is known to be due to the formation of stable protective surface layers of titanium oxides. The electrochemical study of the potential-time behaviour (E/t) and the current density-potential behaviour (I/E) of the material in Q-brine at 25°C and 90°C shows that Ti 99.8 Pd has a wide stable passive zone. No indications of local corrosion can be seen from the I/E plot up to E=+3.0 V vs. AG/AgCl (3M KCl). Metallographic post-examinations support this result.

Surface examinations /8/ of corroded Ti 99.8-Pd specimens with polished surfaces by means of electron spectroscopy (XPS) revealed at all test temperatures the presence of a passive layer consisting mainly of TiO_2. The thickness of the layer (TiO_2 and Ti-suboxides) formed on the metal surface by oxidation in air increased after corrosion from about 2 nm to 4-6 nm.

The general corrosion rate of Hastelloy C4 (Fig.1) increased with rising temperature but even at the maximum test temperature of 200°C it remained low, about 1 µm/a. After long immersion times the corrosion rates seem to remain constant with time.

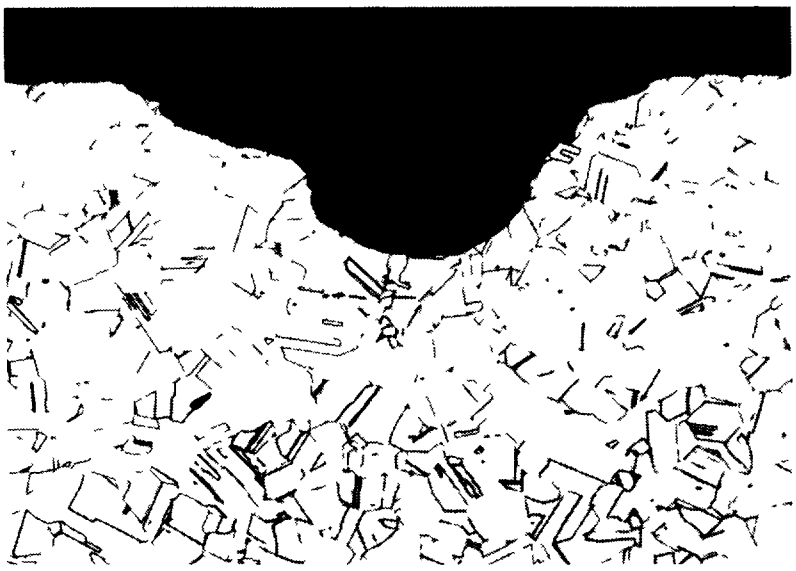

FIG. 4 OPTICAL MICROGRAPH OF HASTELLOY C 4 AFTER 700 DAYS IMMERSION IN Q-BRINE at 200° C (X 100)

At 90°C and 170°C the material was resistant to pitting corrosion and stress corrosion cracking but suffered from crevice attack. At 200°C, besides crevice corrosion, pitting attack occured to a depth of about 200 µm in tests exceeding 700 days duration (micrograph Fig.4). The electrochemical studies confirm the sensitivity of Hastelloy C4 to local corrosion at elevated temperatures in Q-brine. The study of the current density-potential behaviour (I/E) of the material at T = 25°C and 90°C shows that with rising temperature the stability of the passive layer spontaneously developing in Q-brine gets heavily reduced. The passive zone extending above 900 mV at 25°C shrinks to about 50-250 mV at 90°C. More anodic potential values than the passive zone cause local attack of the material at 90°C which become a non-uniform general corrosion while the potential rises further. Figure 5 shows the I/E behaviour of Hastelloy C4 in Qbrine at 90°C.

The unalloyed steels fine-grained steel and cast steel showed qualitatively and quantitatively a very similar corrosion behaviour. The general corrosion rates of the actively corroded /9/ steels (Fig.2) rose with increasing test temperature. The final corrosion rates were in the range of 30-40 µm/a at 90°C, 100-140 µm/a at 170°C, and 500-600 µm/a at 200°C, respectively.

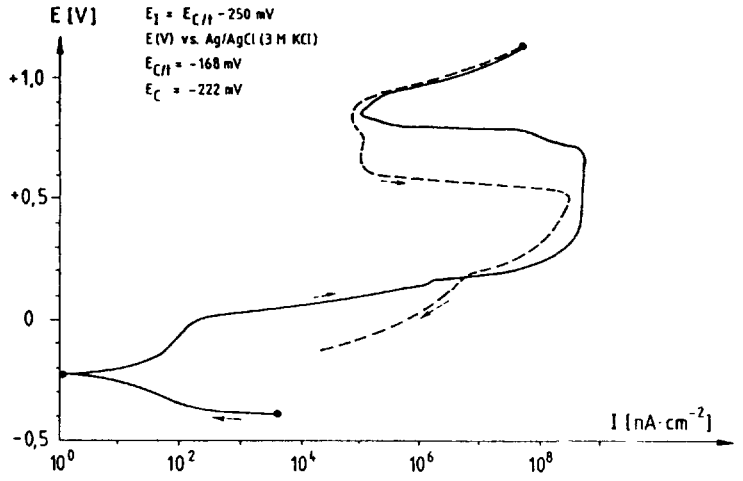

Fig. 5 Current density-potential behaviour of Hastelloy C4 in Q-brine at 90°C

At 90°C and 170°C the corrosion rates seem to approach a value which is constant with time. At 200°C a further decrease of the corrosion rate after longer time is suggested. The increase in the corrosion rate with temperature is attributed to a thermally activated process and decreasing pH of the solution with rising temperature. Acid corrosion is considered to be the dominant process because at the temperatures investigated the measured pH-values of the Q-brine were less than 4 (e.g. pH (90°C) = 3.6). The influence of oxygen on corrosion over the long test period (i.e. $>$ 50 days) must be small because the low oxygen content of the brine (i.e. $<$ 0.1 ppm at 90°C) will be consumed by corrosion in the first few days of the test.

Both steels were resistant to pitting and crevice corrosion as well as to stress corrosion cracking after an exposure period of up to 4 years. After short exposure periods in Q-brine they corroded non-uniformly. After extended exposure time corrosion became nearly uniform. Figures 6 and 7 show characteristic micrographs of fine-grained steel and cast steel after long immersion times in Q-brine at 170°C.

The TIG-welding had no influence on the corrosion rate of Ti 99.8-Pd. The corrosion rate of the welded Hastelloy C4 and steel specimens was higher than of unwelded ones by about 30-50%.

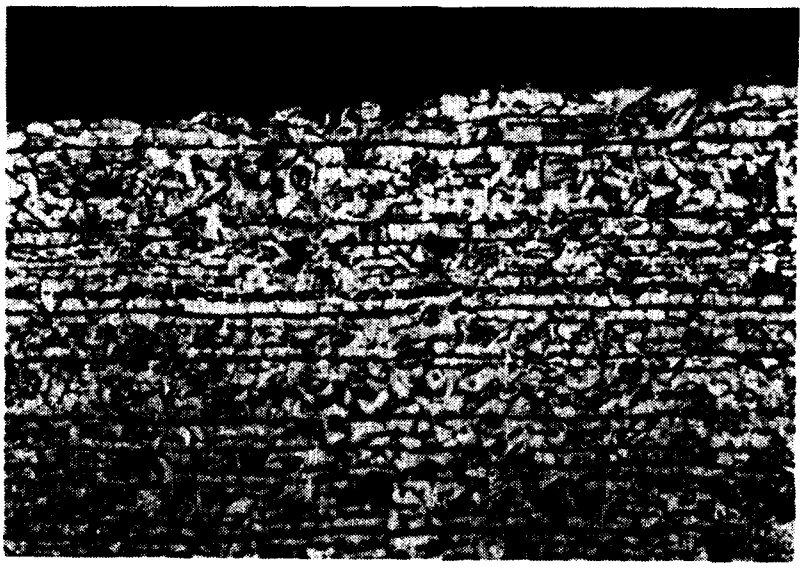

FIG. 6 OPTICAL MICROGRAPH OF FINE-GRAINED STEEL AFTER 720 DAYS IMMERSION IN Q-BRINE AT 170° C (X 200)

FIG. 7 OPTICAL MICROGRAPH OF CAST STEEL AFTER 580 DAYS IMMERSION IN Q-BRINE AT 170° C (X 50)

3.2 Influence of gamma radiation on material corrosion in the quinary Q-brine

The Ti 99.8-Pd specimens immersed in Q-brine at 90°C and a gamma dose rate of 10^3Gy/h (10^5rad/h) showed a slight gain in weight. Its value was 0.2 mg/cm² and remained fairly constant over a test period of 610 days. According to the results of surface investigations /8/ this weight gain can be explained by the formation of a corrosion layer under the impact of irradiation which obviously develops faster than it decomposes. It was shown on these investigations that the oxide covering layer formed in the presence of radiation has a thickness of 600 nm after 610 days and therefore it is much thicker than in the absence of radiation. Overlying the TiO_2 layer, which is typical of non-irradiation conditions a layer consisting of Mg and O was built up. The specimens of Hastelloy C4 and both steels investigated under irradiation showed weight losses which were much higher than without irradiation.

Figure 8 shows a comparison of the general corrosion rates of the materials investigated in Q-brine at 90°C with and without gamma irradation. For the estimation of the corrosion rate of Ti 99.8-Pd under irradiation it was assumed that the oxide covering layer consists only of TiO_2. The error caused by neglecting the MgO contribution is small on account of the low thickness of the oxide layer and the minor differences in the densities of TiO_2 (4.1 g.cm^{-3}) and MgO (3.7 g.cm^{-3}). On the basis of this calculation the corrosion of Ti 99.8-Pd is only 0.7 µm/a and remains fairly constant over an immersion time of 610 days. Furthermore, this material corroded uniformly and local corrosion was not encountered (micrograph Fig.9). The corrosion rates of Hastelloy C4 and both steels under conditions of irradiation were by about the factor 10-20 higher than without irradiation. In addition, Hastelloy C4 was subjected to severe pitting (maximum pit depth 1 mm after 610 days) and crevice corrosion and the steels underwent non-uniform corrosion accompanied by shallow pit formation. However, the maximum depth of shallow pits formed in the steels is only slightly higher than the

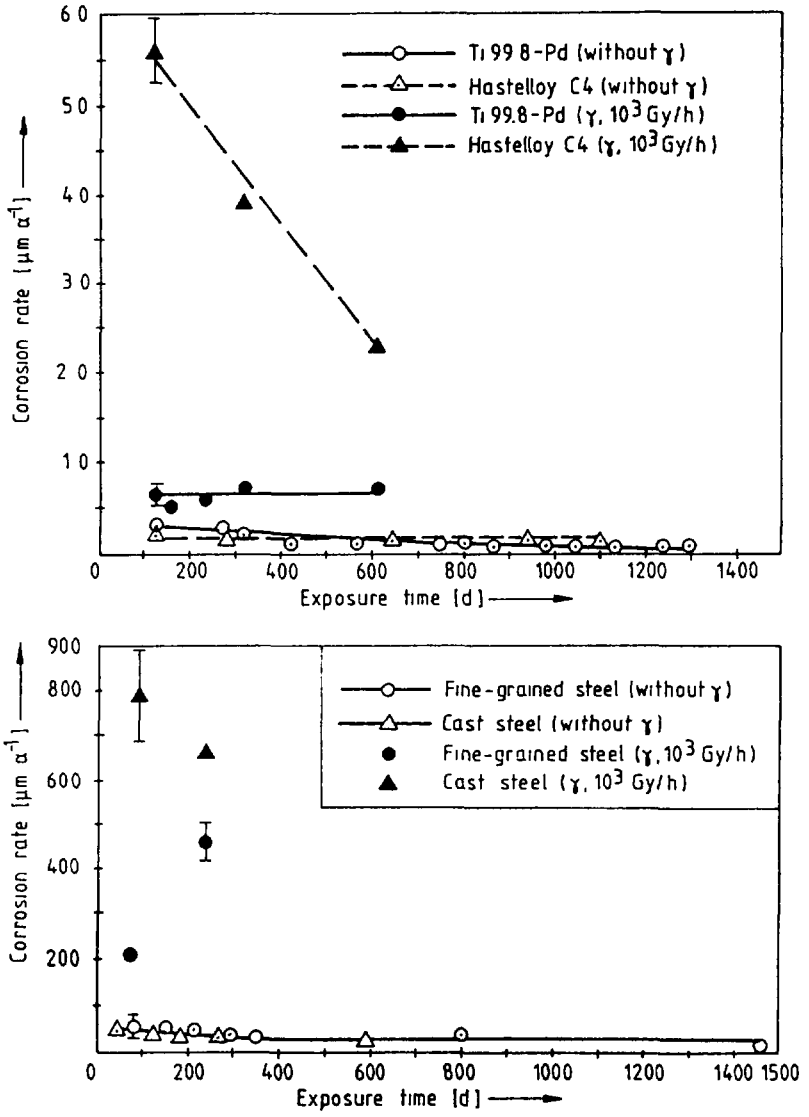

Fig.8 General corrosion rates in Q-brine at 90°C with and without γ-irradiation

average general corrosion rate. The micrograph in Fig.10 shows by way of example pitting corrosion of Hastelloy C4.

Under gamma irradiation the corrosion rate of Hastelloy C4 decreased with time, while without irradiation and at a comparable temperature (90°C) a constant corrosion rate was observed. This fact is not fully understood. A general statement of the time dependence of the corrosion rate of steels under gamma irradiation cannot yet be made from the few experimental data available so far.

FIG. 9 OPTICAL MICROGRAPH OF Ti 99.8-Pd AFTER 606 DAYS IMMERSION IN Q-BRINE AT 90° C WITH GAMMA-IRRADIATION (10^3 Gy/h)

(X 200)

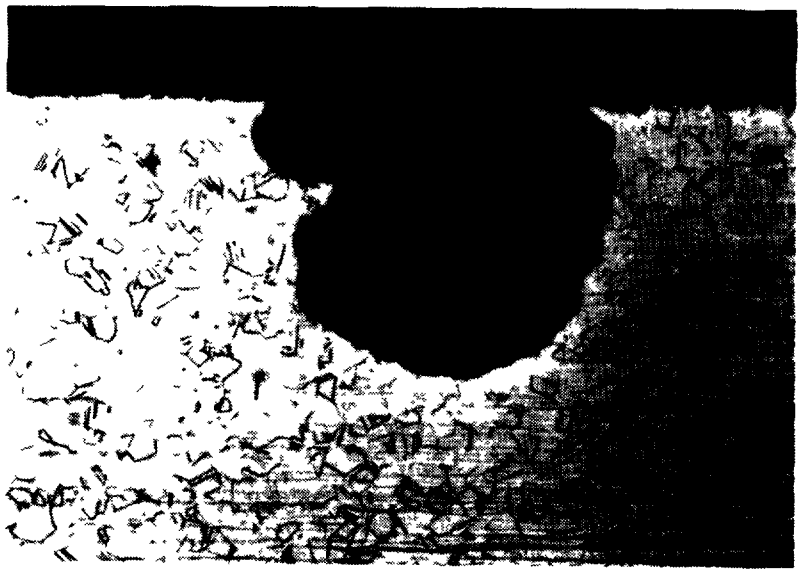

FIG.10 OPTICAL MICROGRAPH OF HASTELLOY C4 AFTER 606 DAYS IMMERSION IN Q-BRINE AT 90° C WITH GAMMA-IRRADIATION (10^3 Gy/h)

(X 50)

According to electrochemical investigations the increase in the corrosion rate and in the sensitivity of Hastelloy C4 to local corrosion in Q-brine exposed to gamma-irradiation is attributable to the formation of the oxidants H_2O_2, ClO^- and ClO_3^-. At 90°C and accident relevant concentrations of $C \leq 5 \times 10^{-2}$ M/l, H_2O_2, ClO^- and ClO_3^- added in Q-brine und 1M NaCl solution moved the corrosion potential into the vicinity or even beyond the zone of local corrosion. The same is true for Fe^{3+} and Cu^{2+} which might be present as impurities of the salt, as well as for the thermally released product HCl ($pH \leq 2$). In S^{2-} bearing solutions no passive behaviour is observed but increased corrosion rates and local attacks. In contrary, the radiolytic product ClO_4^- and possible impurities of the salt in Q-brine such as Br^-, I^- and Mn^{2+} obviously have no additional influence on the corrosion behaviour of Hastelloy C4 at 90°C.

The strong increase in the corrosion rate of the steels exposed to gamma irradiation suggests, according to indications in reference /10/, that the strong oxidants formed (e.g. H_2O_2, ClO_3^-) act as cathodic depolarizers. Therefore new cathodic reactions occure which, in turn, cause an acceleration of the anodic process.

3.3 Influence of the composition of salt brines on materials corrosion

The results of corrosion in the various brines after six months of immersion at 170°C have been compiled in Table 1. The influence of brine composition on the corrosion behaviour of Ti 99.8-Pd and Hastelloy C4 was not significant. Both materials corroded in all media in a slightly uniform mode and were resistant to pitting corrosion. The reduction in thickness of the materials (0.03 µm-0.16 µm for Ti 99.8-Pd and 0.08 µm-0.37 µm for Hastelloy C4) after six months of immersion in the various brines differs by only the factor 5. Likewise, study of the I/E-behaviour does not suggest a noticeable influence of the composition of the brines investigated on the electrochemical corrosion behaviour of Ti 99.8-Pd. The same is true for Hastelloy C4, except in Z-brine. In this brine the passive zone of $E \leq 100$ mV

TABLE 1 INFLUENCE OF BRINE COMPOSITION ON THE CORROSION OF TI 99.8-PD, HASTELLOY C4 AND FINE-GRAINED STEEL AFTER 6 MONTHS IMMERSION AT 170° C

CORRODANT	REDUCTION IN THICKNESS[1] (µM)		
	TI 99.8-PD	HASTELLOY C4	FINE-GRAINED STEEL
$NaCl-H_2O$	0.03 ± 0.02	0.08 ± 0.01	7.6[2]
$NaCl-CaSO_4-H_2O$	0.07 ± 0.02	0.08 ± 0.01	3.9[3]
$KCl - H_2O$	0.05 ± 0.02	0.08 ± 0.01	5.5
$CaCl_2-H_2O$	0.12 ± 0.02	0.11 ± 0.01	12.9[2]
$NaCl-KCl-MgCl_2-MgSO_4-H_2O$ (Q-BRINE)	0.16 ± 0.02	0.37 ± 0.01	112.0
$NaCl-KCl-MgCl_2-MgSO_4-H_2O$ (Z-BRINE)	0.08 ± 0.02	0.37 ± 0.01	128.0

1) FOR TI 99.8-PD AND HASTELLOY C4 UNIFORM CORROSION, FOR FINE-GRAINED STEEL SHALLOW PIT FORMATION IN SOME MEDIA AS INDICATED.

2) MAXIMUM PIT DEPTH 25 µM; 3) MAXIMUM PIT DEPTH 200 µM.

is smaller than in the other brines which is an indication of the higher risk of local corrosion.

The corrosion behaviour of fine-grained steel in the various test media differed greatly both qualitatively and quantitatively. In the KCl-, NaCl- and $CaCl_2$-brine the material corroded by slight general corrosion (5.5-13 µm) and the corrosion attack was uniform (KCl-brine) or slightly non-uniform (maximum depth: 25-30 µm). General corrosion was likewise slight in the NaCl-$CaSO_4$ solution; nevertheless, in this medium shallow pit formation occured with a maximum depth of 200 µm. By contrast, in the Q- and Z-brines the fine-grained steel corroded almost uniformly with a high general corrosion of 110-130 µm.

4. Conclusions

- Among the materials studied under postulated accident conditions Ti 99.8-Pd exhibited the highest corrosion resistance in salt brines. Under the applied experimental conditions a general corrosion rate by less than 1 µm/a can be anticipated, even in the presence of a high gamma radiation

field of 10^3Gy/h (10^5rad/h). The results obtained after up to 4 years test duration did not indicate a susceptibility to local corrosion or stress corrosion cracking.

Nevertheless, further investigations will be necessary to provide final evidence of the suitability of Ti 99.8-Pd as a material for long-term HLW packagings. These will mainly involve the clarification of questions relating to embrittlement in the presence of radiolytic hydrogen and low tensile stresses.

- In the immersion tests Hastelloy C4 was sensitive to crevice corrosion at a temperature as low as 90°C and to pitting corrosion at 200°C. The electrochemical investigations show that after long periods the material could be attacked by pitting corrosion even at 90°C. In the presence of strong oxidants (H_2O_2, ClO^-, ClO_3^-, Fe^{3+}, Cu^{2+}), which may appear as a result of gamma irradiation or in the form of impurities of the salt, heavy pitting and crevice corrosion must be anticipated.

- For the unalloyed steels neither stress corrosion cracking nor local corrosion occurred without irradiation (absence of oxidants) so that their behaviour due to general corrosion is predictable. However, unalloyed steels must be sufficiently protected against gamma-radiation. In that case the corrosion rates for S/V = 1:5 cm^{-1} at 90°C (30-40 µm/a) and 170°C (100-140 µm/a) in a period of e.g. 300 years lead to corrosion allowances which are in the order of container wall thickness of about 12 mm and 40 mm, respectively. These values are relatively low compared to an estimated wall thickness of 100 mm in order to ensure mechanical stability against the resulting rock pressure of 35 MPa. At 200°C, (corrosion rate: 500-600 µm/a) the necessary corrosion allowance will be greater than that for mechanical protection. Investigations are in progress to determine the wall thickness required to ensure that the gamma dose rate at the container surface and, consequently, the radiolysis of brines is reduced to negligible levels. In addition to

these studies, further investigations will be necessary to qualify structural steels as HLW container material. This includes above all the determination of their susceptibility to H_2 embrittlement.

Due to the predictable corrosion behaviour and considering material costs, easy manufacturing and quality assurance concept, an unalloyed steel seems to be the most promising material for a long-term HLW-packaging.

5. REFERENCES

/1/ SMAILOS, E., KIENZLER, B., KÖSTER, R. "HAW-Behälter als Barriere im Endlager", Proc. Int. Seminar on Chemistry and Process Engineering for High Level Liquid Waste Solidification, Jülich, 1981, Kernforschungsanlage Jülich, GmbH, Rep. Jül-Conf. 42 Vol. 2 (1981), 917.

/2/ Köster, R. "Near-field phenomena in geological repositories for radioactive wastes", Proc. Int. Conf., Seattle, 1983, Radioactive Waste Management, 4 (1984), 303.

/3/ JENKS, G.H., Radiolysis and Hydrolysis in Salt Mine Brines, ORNL/TM-3717 (1972).

/4/ JENKS, G.H., Review of Information on the Radiation Chemistry of Materials around Waste Canisters in Salt and Assessment of the Need for Additional Experimental Information, ORNL-5607 (1980).

/5/ GLASS, R.S., Effect of Radiation on the Chemical Environment Surrounding Waste Canisters in Proposed Repository Sites and Possible Effects on the Corrosion Process, SAND 81-1677 (1981).

/6/ HERRMANN, A.G., Über das Vorkommen einiger Spurenelemente in Salzlösungen aus dem deutschen Zechstein; Kali und Steinsalz 3 (1961) 209.

/7/ JOCKWER, N., Gesellschaft für Strahlen- und Umweltforschung, unpublished report (1981)

/8/ PFENNIG, G., MOERS, H., KLEWE-NEBENIUS H., KIRCH, G., ACHE, H.J., Surface Analytical Investigation of Corroded Ti-Pd Proposed as Container Material for the Disposal of High Level Wastes, Poster presented at Intern. Conf. on Nuclear and Radiochemistry, Lindau, Federal Republic of Germany, 1984.

/9/ SCHMITT, R.E., CANADILLAS, F., KÖSTER; R., Elektrochemische Untersuchung des Korrosionsverhaltens von Feinkornbaustahl 1.0566 und Weicheisen in chloridhaltigen wäßrigen Lösungen, KfK-3729 (1984).

/10/ BJALOBZESKIJ, A.V., "Korrosion durch radioaktive Strahlung", in K.Schwabe (ed.), Akademie Verlag, Berlin (1971) 82.

COMPATIBILITY OF CANDIDATE OVERPACK MATERIALS WITH DEEP ARGILLACEOUS HLW DISPOSAL ENVIRONMENTS

H.A.W. TAS, W. DEBRUYN, J. DRESSELAERS
Centre d'étude de l'énergie nucléaire (SCK/CEN),
Mol, Belgium

Abstract

The Belgian R&D programme on the disposal of high level radioactive waste has been focused on the qualification of deep argillaceous formations for HLW disposal, because they have a number of inherent attractive characteristics and also because they are sufficiently abundant to cover the Belgian needs.

A large number of corrosion resistant materials as well as some corrosion allowance materials have been tested. The laboratory test program included accelerated tests as well as exposure tests in simulated repository conditions.

Initial "field" experiments have been performed in a near surface clay quarry. However, in order to obtain realistic corrosion rate estimates corrosion experiments with simultaneous monitoring of the clay environment parameters have been started in a 230 meters deep underground laboratory constructed in the Boom clay formation at Mol. Two types of experimental devices have been designed. In the first type coupons are mounted on an internally heated tubular holder and are directly exposed to the solid clay. In a second type of test a purge gas is used to extract corrosive products from the clay and circulate them subsequently over a number of metal coupons. Relevant parameters such as pH and Eh are continuously monitored for evaluating the evolution of soil agressivity

after the initial chemical and mechanical disturbance of the clay, caused by the operations required for the introduction of the experimental devices.

---

1. INTRODUCTION

The Belgian R&D programme on the disposal of high level radioactive waste has been focused on the qualification of deep argillaceous formations for HLW disposal, because they have a number of inherent attractive characteristics and also because they are sufficiently abundant to cover the Belgian needs.

Corrosion damage experiments of candidate overpack materials and of candidate gallery lining materials have been performed in different environments, which may prevail in an engineered repository in the Boom clay. These environments include : direct contact with clay, interstitial clay water, humid clay atmospheres loaded with corrosive products escaping from the clay under influence of thermal effects and ground waters immediately adjacent to the argillaceous layers. Most of the tests have been conducted in aerated and non-aerated conditions. For the overpack, which should have a lifetime of 500 to 1000 years, a large number of corrosion resistant materials as well as some corrosion allowance materials have been tested ; for the galleries, with a projected lifetime less than 50 years, concrete or a sliding steel lining are considered only. The laboratory test programme included accelerated tests as well as exposure tests in simulated repository conditions. "Field" experiments have been performed in a near surface clay quarry in Terhaegen. Cast iron samples, which have been recovered from coal mine underground structures, after

being exposed to argillaceous formations for very long times, have been submitted to metallographic analysis.

In order to evaluate the corrosion behaviour of candidate overpack materials under realistic repository conditions, different experiments were initiated in the 230 meters deep underground laboratory at the Mol site. These experiments are aimed at obtaining both on-site corrosion rate data and clay environment evolution patterns, which develop after the disturbance caused by container introduction and subsequent exposure to the hot waste containers.

2. EXPERIMENTAL

2.1. Laboratory Experiments

The clay environment is very sensitive to aeration. The pH of fresh Boom clay is situated between 10.1 and 10.5 but can shift to values as low as 2.95 after one year of exposure to air. At the same time large shifts of the redox potential occur form initial values close to -400 mV (versus hydrogen electrode) to + 600 mV in fully oxidized condition. An air stream passing over a clay surface not only picks up moisture but also important amounts of CO_2 and small but relevant amounts of SO_2, NO, NO_2 and CO.

Exposing ductile iron or carbon steel directly to clay at room temperature gives rise to general corrosion rates ranging from 10 to 50 μm per year. A three year exposure of different grades of ductile iron in a surface clay quarry at Terhaegen gave rise to a mean corrosion rate of 50 μm per year for the low alloy ductile irons whereas for high silicon and high nickel grades corrosion rates lower by a factor of 2 to 4 were found.

Exposure of the low alloy ductile iron to aerated clay and non-aerated clay in sealed pots with an air respectively argon cover gas yielded corrosion rate values of about 10 µm per year. No significant difference could be found between the corrosion rates obtained in anoxic or aerated conditions.

Immersion tests performed at 90°C on a reference carbon steel in interstitial claywater typical for aerated clay conditions and in interstitial claywater typical for anoxic clay conditions yielded a noticeable difference : 25 µm per year for aerated conditions versus 10 µm per year for anoxic conditions. The extent of corrosion observed after 9 months of exposure was not significantly higher than the damage observed after 4 months of exposure. This means that initial corrosion rates are very high (linear extrapolation gives values as high as 75 µm per year) but that the process then slows down considerably due to the formation of a relatively stable protective layer. The stability of this protective layer is the key parameter for the evaluation of the long term corrosion resistance of this material.

Similar exposure tests in Antwerpiaen groundwater performed in anoxic conditions yielded corrosion rates lower than 1 µm per year.

Exposure tests in humid clay atmospheres yielded generally corrosion rates between 50 and 150 µm per year provided a sufficiently high relative humidity was present in the system. Two years exposure in a gas corrosion chamber at 25°C, 75% relative humidity and 75 ppm of SO_2 yielded corrosion rates of ductile irons not larger than 60 µm per year. Exposure of the same materials in a corrosion

chamber with alternating wet and dry cyclic operation (aerated type interstitial claywater addition) induced an 150 µm per year mean corrosion rate. Corrosion rates of a reference carbon steel exposed to a relatively dry atmosphere at 150°C (air stream with aerated type interstitial claywater addition) did not surpass 2 µm per year.

All evidence available seems to indicate that ductile iron or carbon steel corrosion remains limited to approximately 50 µm per year for all experiments performed except for the extremely harsh conditions of a cyclic operating corrosion chamber. Although a meaningfull decrease was generally observed in experiments, performed under anoxic conditions, corrosion rates as low as one would expect them to be under these conditions, and which were for example obtained in Antwerpiaen groundwater, were not observed. This could be due to the fact that corrosive species other than oxygen are responsible for the attack observed or that the oxygen potential has not sufficiently been reduced in the experiments.

It is also possible that after initial fast corrosion, extremely low corrosion rates will be established. This seems to be confirmed by the examination of cast iron samples recovered from coal mine underground structures. Indeed, a corrosion rate estimate based on the analysis of coal mine shaft material (grey iron) exposed up to 90 years in a marl environment yielded a general corrosion rate not larger than 3 µm per year.

A selected number of candidate canister materials (Hastelloy C-4, different titanium alloys Inconel 625, UHB 904L and others) has been examined after 2 years of exposure

in direct contact with clay. Hastelloy C had corrosion and deposition products at isolated locations. The extent of the reaction layer was limited to a maximum thickness of 0.01 μm. The attack occurred mainly by oxygen and all alloying elements took part in the reaction. The titanium alloys were covered by a more uniform corrosion layer and oxygen penetration up to a depth of 0.1 μm was observed.

After 49 months of exposure to a synthetic clay atmosphere at 150°C a number of ferritic and austenitic steels, nickel alloys and titanium alloys were examined by scanning electron microscopy. With the exception of the Ti-alloys all samples suffered from pitting, the extent differing with composition. The Ni-alloys also showed some reaction initiating at the grain bounderies. Ti and its alloys showed a certain roughening of the surface only, which seemed to indicate a relation between reaction susceptibility and grain orientation.

For a similar "synthetic clay atmosphere" type of experiment performed during 5 years at 300°C post-corrosion analyses were made by means of Auger spectroscopy. This revealed a maximum corrosion layer thickness of 0.08 μm for all alloys tested. The corrosion products were sulphides and oxysulphides.

As to the influence of stress on corrosion, only a few materials have shown susceptibility to this type of failure. Cracking has been found on a few samples of AISI 316 and AISI 304 type steels.

2.2 Corrosion experiments in the underground experimental room at 230 meters depth.

Two types of experiments were designed to investigate the corrosion behaviour of various materials in the clay environment. In the first type of experiment the effect of direct contact with clay is considered; the second type of test is related to the interaction between confinement materials and a gaseous atmosphere in equilibrium with clay.

For the direct contact experiments tubes (Fig. 1) with a length of 5.3 meter were constructed and loaded with candidate overpack and structural materials and also with different simulated vitrified waste specimens. The corrosion tests will be carried out at 15°C, 90°C and 170°C. Heating is provided by a furnace situated inside the tube. Exposure times up to 50,000 hours are planned. Figure 2 shows one of the pressure tubes during installation.

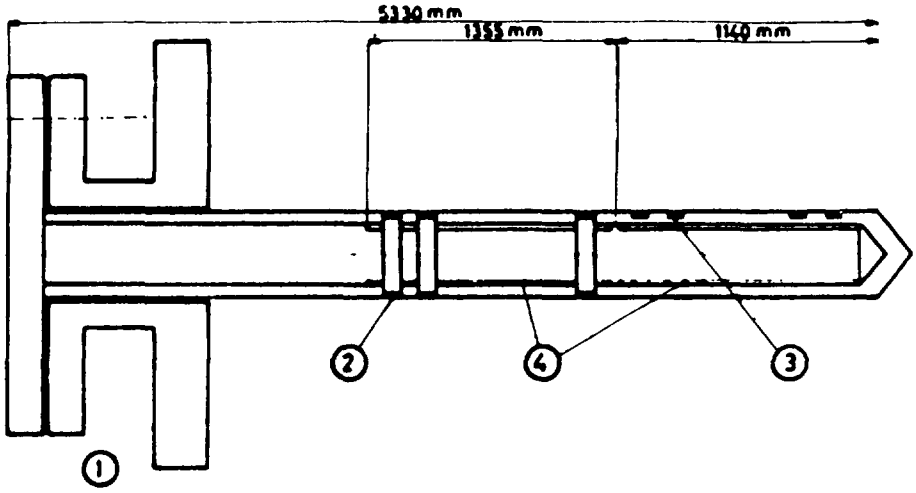

Fig. 1 : Schematic view of experimental device for "in situ" corrosion experiments in direct contact with clay. 1: gallery; 2: container samples; 3: waste form samples; 4: heating elements.

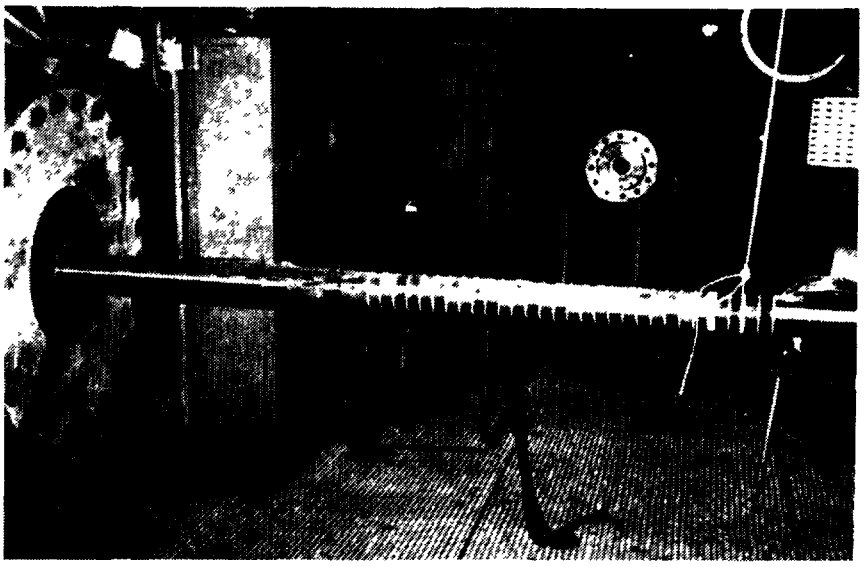

Fig. 2 : Introduction of a direct-contact corrosion probe into the clay from the experimental underground room at 230 meters depth.

The pressure tubes are equipped with sensors to give an electrochemical characterization of the clay surrounding the exposed material. Redox potential and pH will be monitored continously at all temperatures considered. These two electrochemical parameters have a major impact on the soil agressivity. In this way it is possible to gain information on the effect of :

- the disturbance of the clay by the drilling operations and the introduction of oxygen associated with it
- the heating of the clay
- the diffusion of corrosion products into the clay.

Each pressure tube is equipped with Pt and Au measuring electrodes. A solid body type Ag/AgCl reference electrode was introduced at the nearest gallery perforation. This reference electrode is filled with a KCl containing acrylic polymer, which does not need to be renewed regularly

and which is pressure resistant and hence does not require complicated additional external pressure compensation such as traditional systems require.

The pH in the immediate vicinity of the pressure tubes is monitored with commercial high-pressure resistant glass electrodes, which have been modified to resist local high pressures caused by, e.g. pyrite particles present in the clay.

Knowledge of the evolution of these electrochemical parameters under disposal site conditions is essential for the development of a mathematical model which can predict the corrosion susceptibility of selected materials for the very long exposure periods anticipated.

A second experimental device (Fig. 3) was designed to gain information on corrosion in a clay atmosphere. The tubes have a porous plug and have heating elements and test

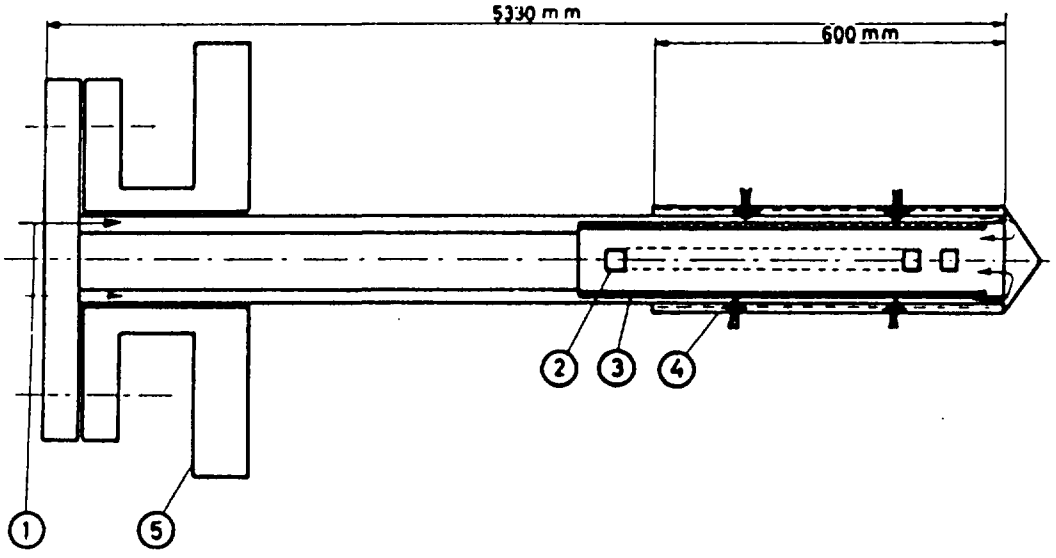

Fig. 3 : Schematic view of experimental device for "in situ" corrosion experiments in contact with clay atmosphere extracted across a porous outer tube.
1: gas inlet; 2: container and waste form samples; 3: heating elements; 4: porous filter; 5: gallery.

specimens inside. Helium or air will be used as purge gas to take up corrosive products penetrating the plug and to circulate these over the test samples. The outcoming flow will be collected and continuously monitored for its dew point. Afterwards the condensable products will be extracted at 8°C and -80°C for off-line chemical analysis. Test temperatures are 15°C, 50°C, 90°C and 170°C.

Three automated systems for direct measurement of corrosion rates were adapted for the underground experiments:

- corrator measurements: the method is based on the measurement of the linear polarization resistance,
- corrosometer: the device measures accurately the increase of electrical resistance due to the reduction of the cross-sectional area of the metallic sample as it is corroding in the environment,
- PAIR technique: this "polarization admittance instantaneaous rate" method is based on the same principles as the polarization resistance technique. Corrosion rates as low as 0.25 µm per year can be measured with this method.

3. CONCLUSIONS

Based on the experimental results obtained so far the following preliminary conclusions can be drawn :

- carbon steel and cast irons exposed to clay atmospheres in the temperature range between 50°C and 150°C corrode at a fast rate, given a sufficiently high relative humidity (up to 150 µm per year). This effect is enhanced under wet/dry cycling conditions,

- in contact with solid clay corrosion rates between 50 µm per year and a few µm per year have been measured for carbon steel. Aeration enhances corrosion. However, also under anoxic conditions relatively high corrosion rates are observed,
- initial corrosion rates of carbon steels in claywater are very high, but decrease to very low rates after a few months. A similar behaviour is not observed during exposure to common groundwaters,
- corrosion resistant materials such as titanium alloys and Hastelloy C build up passivation layers at a rate well below 1 µm per year.

Real site experiments need to be performed in order to elucidate the following important aspects of container behaviour in a clay repository :

- Build-up and stability of passivation layers on corrosion resistant materials over long exposure periods.
- Evolution of the clay environment as disturbed by container introduction, exposure to the hot waste containers and gamma-radiation.
- Behaviour of candidate canister materials under these non-equilibium clay conditions.

SELECTION OF CANISTER MATERIALS: ELECTROCHEMICAL CORROSION TESTS OF HASTELLOY C4 AND OTHER Ni-Cr(-Mo) ALLOYS IN CHLORIDE CONTAINING SOLUTIONS

I. WOLF
Kernforschungszentrum Karlsruhe GmbH,
Karlsruhe

H. BORT
Siecor,
Neustadt-Coburg

Federal Republic of Germany

Abstract

Several Ni-Cr (-Mo) alloys (HASTELLOY C4, INCONEL 625, SANICRO 28, INCOLOY 825, INCONEL 690) were tested by electrochemical methods to characterize their corrosion behaviour in chloride containing solutions at various temperatures and pH-values in respect to their application as canister materials for final radioactive waste storage.

Especially, HASTELLOY C4 which proved to have the highest corrosion resistance of all tested alloys was tested by the following electrochemical methods:

(1) Poteniodynamic measurements to determine the characteristic potentials, passive current densities and critical pitting potentials.
(2) Potentiostatic measurements in order to evaluate the duration of the incubation period at various potentials.
(3) Galvanostatic measurements in order to characterize critical pitting potentials.

As electrolyte 1 m H_2SO_4 was used, as parameters temperature, chloride content and pH-value were varied.

Variation of temperature gives the following results: an increase in temperature leads to an increase of the critical passivation current density, the passive potential bandwidth decreases slightly and the passive current density increases with rising temperature.

The addition of different chloride contents to the H_2SO_4 solution shows the following effects: the critical passivation current density and the passive current density increase with increasing chloride concentration and both, the critical pitting potentials and the pitting nucleation potentials, shift towards negative values.

As third parameter the pH-value was varied. As expected, an increase of the pH-value extends the passive region to more negative values, the passive current density decreases. The

variation of the pH-value does not affect the critical pitting potential.

All tested alloys showed a clearly limited resistance against pitting corrosion phenomena.

However, the best corrosion behaviour is shown by HASTELLOY C4, which has of all tested alloys the lowest passivation current density and the largest potential region with protection against local corrosion phenomena.

---

1. Introduction

The aim of the presented work was to find a ranking order for a group of alloys in respect to their corrosion behaviour when applied for the production of waste packages for final storage of high radioactive waste. Several Ni-Cr (-Mo) alloys (HASTELLOY C4, INCONEL 625, SANICRO 28, INCOLOY 825, INCONEL 690) were tested by electrochemical methods to characterize their corrosion behaviour in chloride containing solutions at various temperatures and pH-values in respect to their application as canister materials for final storage especially in rock salt formations.

The high level radioactive waste considered is the one left by the reprocessing of spent fuel elements from which the fissile and fertile nuclides have been extracted in view of their recycling. This waste is immobilized by incorporating it in an inert solid, which can be either glass- or ceramic matrix. At the present stage of technology, glasses (i.e. borosilicates) are the only operational process available [1].

The hazardous nuclides are:

- the fission products with a very high activity,
- the uranic and transuranic nuclides with a lower activity but with a much longer life.

Total isolation of the high level waste by disposal in geological stable formations seems to be achievable for 300 to 1000 years. For the period beyond 1000 years, it has been proposed that the isolation be only partial and that the release rate of activity per year should then not be higher than 10^{-5} of the total activity [1].

The prevailing concept on which the final waste disposal is based is the so called multibarrier concept:

The first barrier of this concept is the waste form, i.e. the glass matrix, whose functions are to immobilize the radiotoxic elements and to dilute them in order to keep the heat generation at a sufficiently low level.

The second barrier is the canister which provides mechanical support to the waste during the transportation, handling and

encapsulation operations and serves as a crucible in which the liquid glass is cast.

The third barrier may be a gamma shield surrounding the canister in order to protect the external space from the gamma-radiation of the waste.

The next barrier is the overpack which encloses all the preceding components. Its purpose is to provide the necessary corrosion resistance to the container.

The backfill placed around the container in the repository and the host rock (salt, granite etc., according to the geology) complete the isolation concept.

1.1 Corrosion prevention

In general, the corrosion conditions in the repository are determined by the rock temperatures which may range from about 100 to 200°C, lithostatic pressure, radiation and, in case of final storage in rock salt repositories, high chlorides concentrations. Corrosion damages to the overpack canisters can theoretically be avoided in several ways:

A first one is absolute immunity, i.e. the thermodynamical impossibility of a reaction between the corroding media and the material exposed to it. The only two absolutely corrosion immune metals are gold and platinum; the costs of plating a container are economically not acceptable.

A second way for an alloy to practically avoid corrosion is to develop a superficial layer which protects the underlying metal from further corrosion; such an alloy is usually called corrosion resistant. Aluminium alloys, stainless steels, Ni- based alloys which are the subject of this investigation as already mentioned above, Zr- based alloys and Ti- based alloys have been considered as overpack materials which are economically acceptable.

A third way is the so called corrosion allowance concept. If the overpack material corrodes without developing a protective layer, it can nevertheless be used provided it corrodes at a known rate which is low enough to allow a material thickness to be corroded away during the specified life time of the overpack without breaching the container. Cast iron, carbon steels and iron belong to this class of materials which are called consumable materials.

1.2 Testing conditions

The aim in selecting testing conditions for the candidate materials is to obtain results which allow valid prediction for the container [2].

Electrochemical measurements are suitable for decreasing the duration of testing and are able to classify the performance, i.e. the corrosion behaviour of the materials in situ.

1.2.1 Classification of the corrosion processes

Corrosion damages can be classified into two main categories: general corrosion which is mainly observed in high temperature reactions and localized corrosion, more typical for wet corrosion processes.

General corrosion affects uniformly the surface of the specimen and during a given length of time transforms the same thickness of initial metal or alloy into corrosion products. If these are eliminated as fast as they are formed, the corrosion rate is then controlled by the supply of the corroding agent. They may also accumulate on the specimen surface forming a corrosion layer which may protect more or less the underlying alloy from further corrosion, the material is then corrosion-resistant under these specific conditions.

Localized corrosion processes are subdivided into several categories: pitting and crevice corrosion, grain boundary, galvanic and stress corrosion.

1.2.1.1 Pitting corrosion

This is the phenomenon in which the destruction of the alloy proceeds at discrete points of the surface. In the first case, it is characterized by an induction period during which no pitting is observed, followed by a propagation period during which the pit grows at a catastrophic rate [1]. These two characteristics of pitting corrosion resistant alloys poses a difficult problem for the application of these materials to overpack: how to suppress the initiation and/or propagation of pits and how to assess the induction period in real service.

Pitting corrosion can occur only within a definite potential range lying within the passive range. With the exception of active pit bottom areas the alloy surface is passive [3].

Electrochemical methods have been widely used in examining pitting behaviour of iron and steels in media containing aggressive ions, like e.g. Cl^--ions [4]. Starting from the active range, the sample becomes passive with increasing potential (fig. 1) and is then subjected to pitting corrosion. The potential value where pitting is observed first, is called the pitting nucleation potential E_{np} (fig. 1). The initial stages of pitting may be caused by several mechanisms [5]: incorporation of aggressive ions into the preformed passive oxide is able to cause pitting initiation, adsorption of anions on the oxide surface or simply destruction of the oxide film may start the pitting process (fig. 2).

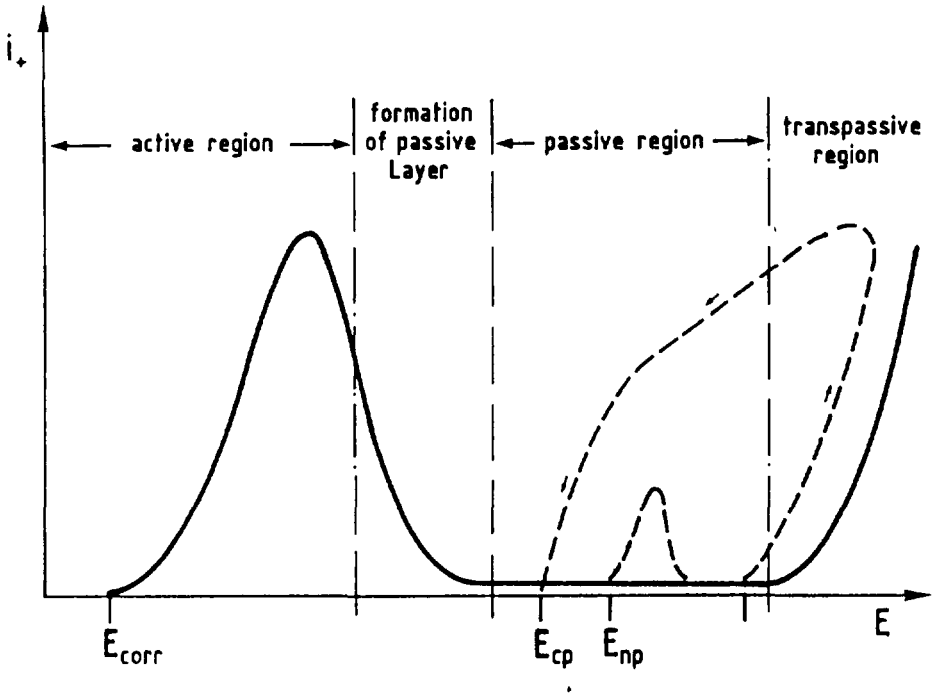

E_{corr} = corrosion potential
E_{cp} = critical pitting potential
E_{np} = pitting nucleation potential

Fig. 1: Schematics of a Current-Density-Potential Curve with Positions of Pitting Potentials.

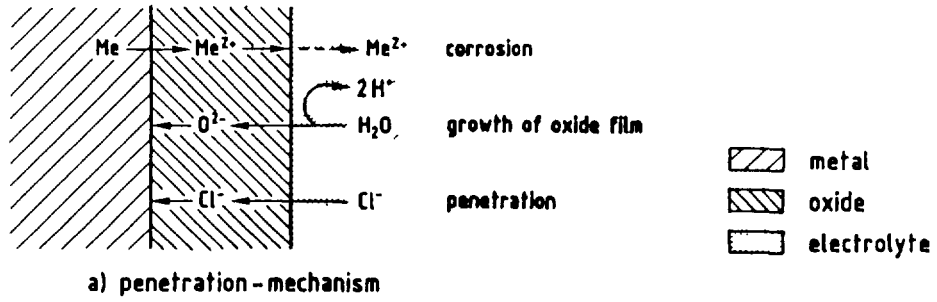

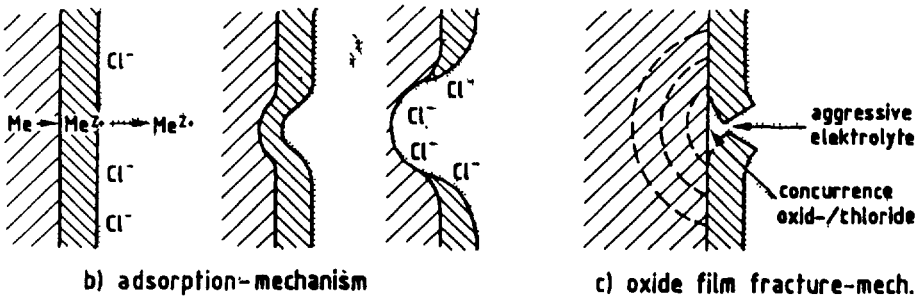

Fig. 2: Schematics of possible initial stages of pitting:

a) Incorporation of Anions into the Oxide,
b) Adsorption of Anion Islands on the Oxide Surface,
c) Destruction of the Oxide Film by Fracture

Transition into the pitting range is not sharply defined. The pits occurring at first may be repassivated completely at potentials below a certain value, called the pitting potential. At potentials changing into the pitting range beyond this value [3], the repassivating effect of the pits decreases while the rate of growth increases and finally, stable pits occur in the alloy surface.

2. Experimental

A computerized experimental equipment was used for the investigations; the electrochemical cell with working electrode, counter electrode and reference electrode is shown in fig. 3.

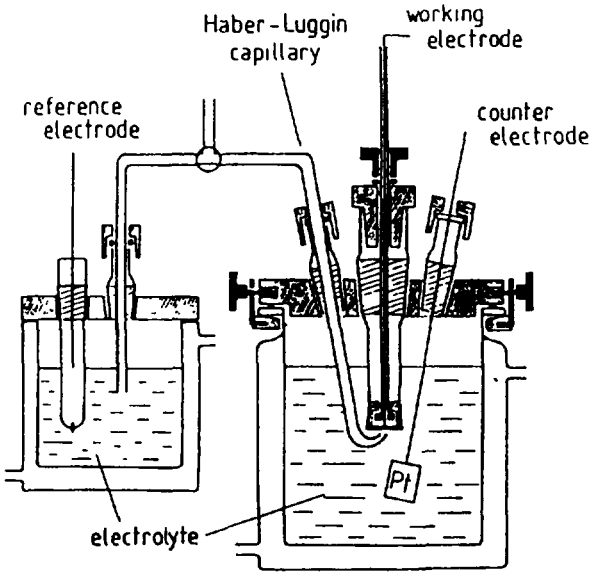

Fig. 3: Schematics of the electrochemical cell

As electrolyte 1 m H_2SO_4 was used, as parameters temperature, chloride content and pH-value were varied. The electrolytes were prepared from deionized water and reagent grade chemicals and were deareated with hydrogen for 1 h.

The materials tested and the experimental conditions are summarized in table 1. Besides the chemical composition, the pitting resistance equivalent "PRE" (i.e. weight % Cr + 3 × weight % Mo) is listed in the last column of the table.

Tab. 1: Composition of alloys and experimental conditions.

Chemical composition of the tested alloys

Alloy	weight %											PRE
	C	Si	Cu	Fe	Mn	Cr	Ti	Al	Co	Mo	Ni	wt% Cr + 3·wt% Mo
HASTELLOY C4	0,003	0,02	-	0,53	0,13	15,65	0,24	-	0,1	15,31	(68,0)	61,6
INCONEL 625	0,02	0,26	0,02	2,33	0,05	22,6	0,12	0,12	-	9,04	(62,7)	49,7
SANICRO 28	0,011	0,61	0,97	(35,8)	1,67	26,72	-	-	-	3,42	30,74	37
INCOLOY 825	0,009	0,22	1,98	31,0	0,13	22,18	0,8	0,16	0,63	3,28	(39,4)	32
INCONEL 690	0,01	0,3	-	10,26	0,42	29,1	0,29	0,22	-	-	(59,4)	29

PRE = pitting resistance equivalent

Experimental conditions:

Temperature range	300 K ≤ T ≤ 365 K
Electrolyte	1 m H_2SO_4 + x m KCl, x = 0, 0.2, 0.5, 1.0, 2.0 / H_2 (≥ 99,999 %) / different pH-values
Surface finish	1200 SiC wet grit
Reference electrode	$Hg/Hg_2SO_4, K_2SO_4$ (sat.), E_{NHE} = +648 mV

The electrochemical techniques used for the investigation of the different alloys were:

- Measurements of the open circuit potential (free corrosion potential) for 1 h before any polarization routine was applied.
- Potentiodynamic polarization measurements to obtain current density - potential curves (scan rate dE/dt = 0.2 mV/s) and thus to determine characteristic potentials, passive current densities, and critical pitting potentials.
- Potentiostatic measurements in order to get current density - time dependences, and thus to evaluate the duration of the incubation period of pitting at various potentials.
- Galvanostatic measurements to obtain potential - time dependences in order to characterize critical pitting potentials.

3. Results

At first, temperature dependences of the current density - potential curves were determined for the different alloys. The current density - potential curve of HASTELLOY C4 in pure H_2SO_4 with the temperature as parameter (fig. 4) is representing the various characteristics such as height of active peak, active/passive transition, passive current density and passive/transpassive transition. The increase in temperature leads to an increase of the critical passivation current density, the passive potential bandwidth decreases slightly and the passive current density increases with rising temperature.

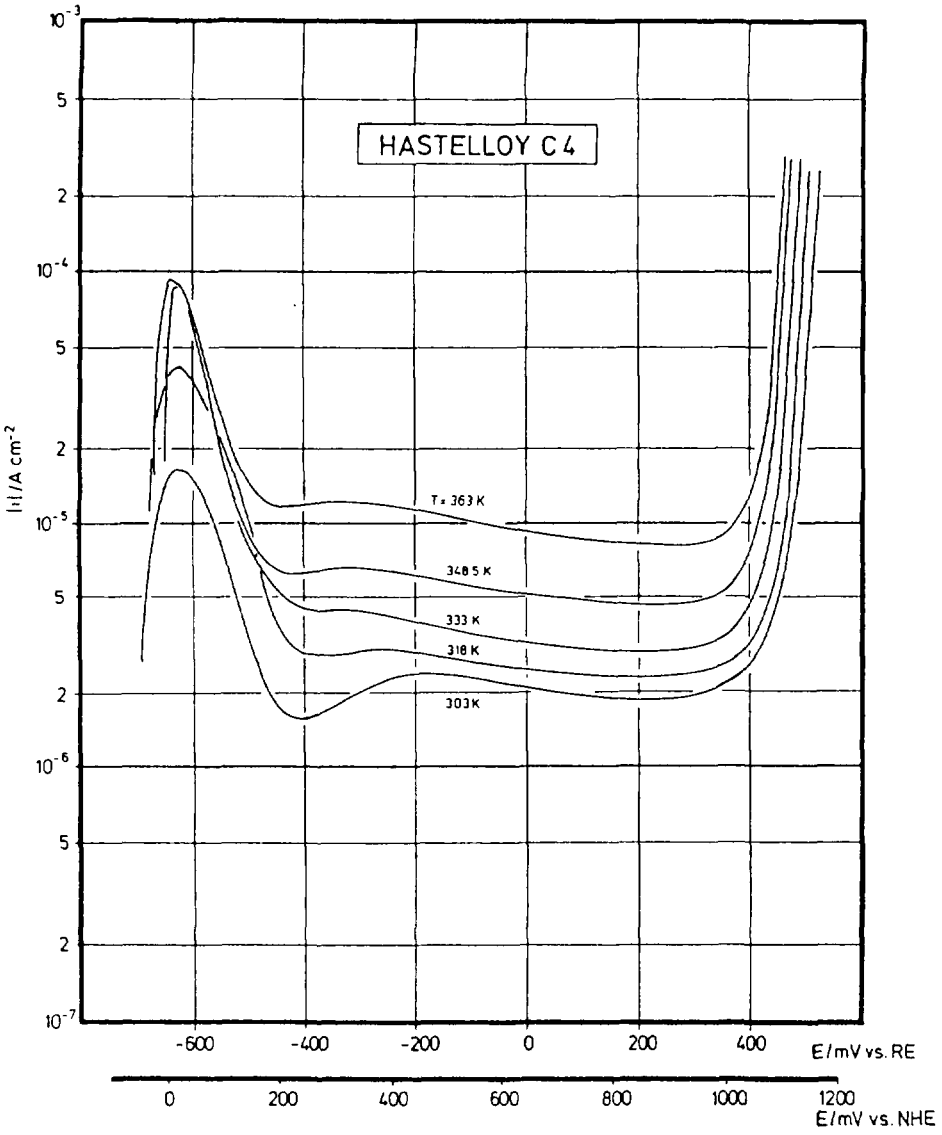

Fig. 4: Potentiodynamic Current-Density-Potential Curves ($dE/dt = 0.2\ mVs^{-1}$)
System: HASTELLOY C4 / 1 m H_2SO_4 / H_2

Fig. 5 shows the temperature dependence of the current density - potential curves for HASTELLOY C4 in a 1 m H_2SO_4 + 0.5 m KCl solution. At higher temperatures a hysteresis in the curves indicates the appearance of pitting corrosion processes.

The criteria for the evaluation of the pitting resistance of the five tested alloys were:

- current density in the passive range,
- shape of the hysteresis in the current density - potential curves, if there was pitting corrosion,
- incubation time of pitting,
- critical pitting potentials, and
- microscopic inspection of the surface of the specimen after electrochemical polarization (hereby also determining whether crevice corrosion at the edges of the specimen had occurred or not).

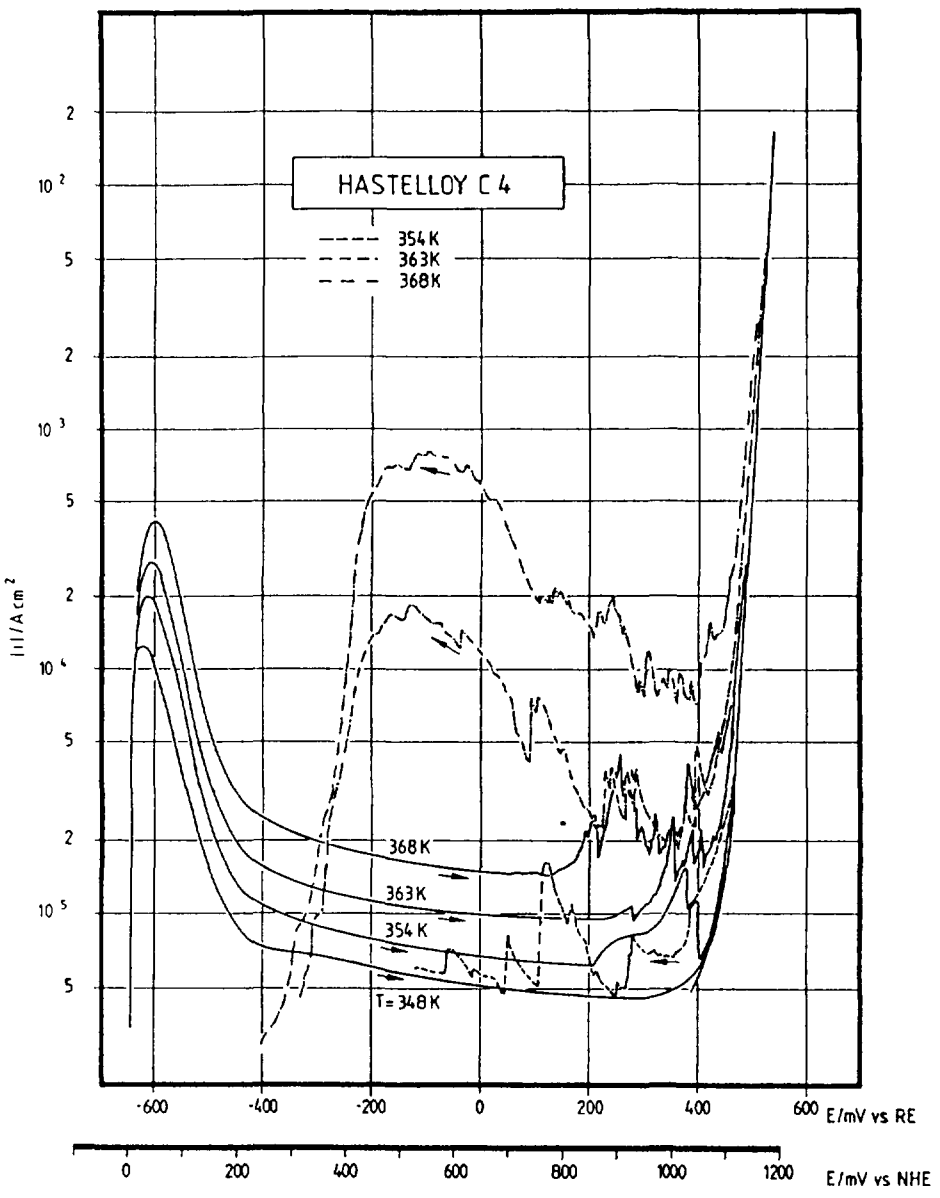

Fig. 5: Potentiodynamic Current-Density-Potential Curves
(dE / dt = 0.2 mVs^{-1})
System: HASTELLOY C4 / 1 m H_2SO_4 + 0.5 m KCl / H_2

From these criteria, an evaluation of the ranking order of the tested alloys was possible which is in accordance to the PRE - values given in table 1. The pitting resistance decreases in the following order of alloys: HASTELLOY C4 > INCONEL 625 > SANICRO 28 > INCOLOY 825 > INCONEL 690.

The further investigations were focussed on HASTELLOY C4 and INCONEL 625, which in so far proved to have the highest corrosion resistance of the fice alloys. As parameters the chloride concentration and the pH-value of the electrolyte were varied.

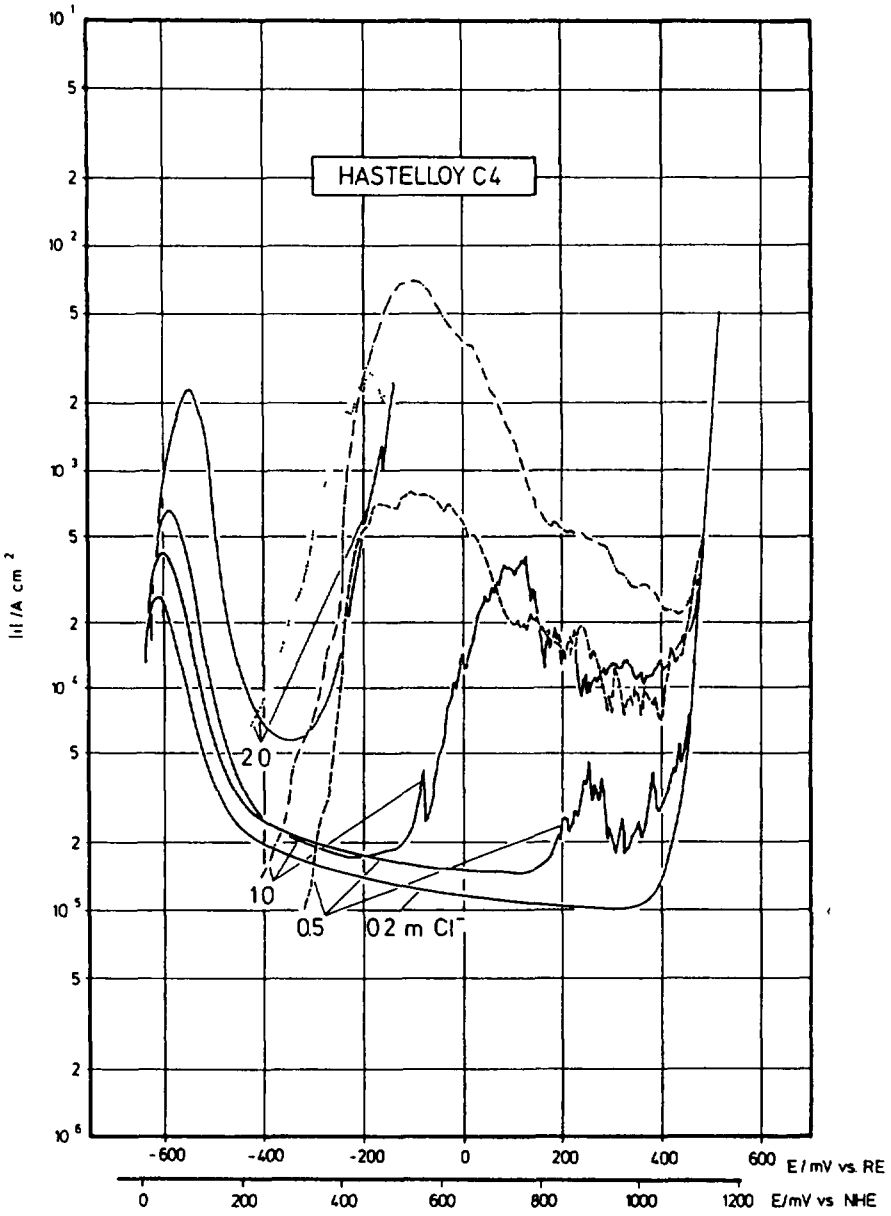

Fig. 6: Potentiodynamic Current-Density-Potential Curves ($dE/dt = 0.2\ mVs^{-1}$)
System: HASTELLOY C4 / 1m H_2SO_4 + xm KCl,
x = 0.2, 0.5, 1.0, 2.0 / H_2 / T = 367 K

The addition of different chloride contents to the H_2SO_4 showed the following effects: the critical passivation current density and the passive current density increase with increasing chloride concentration and both, the critical pitting potentials and the pitting nucleation potentials shift towards negative values (fig. 6 and 7).

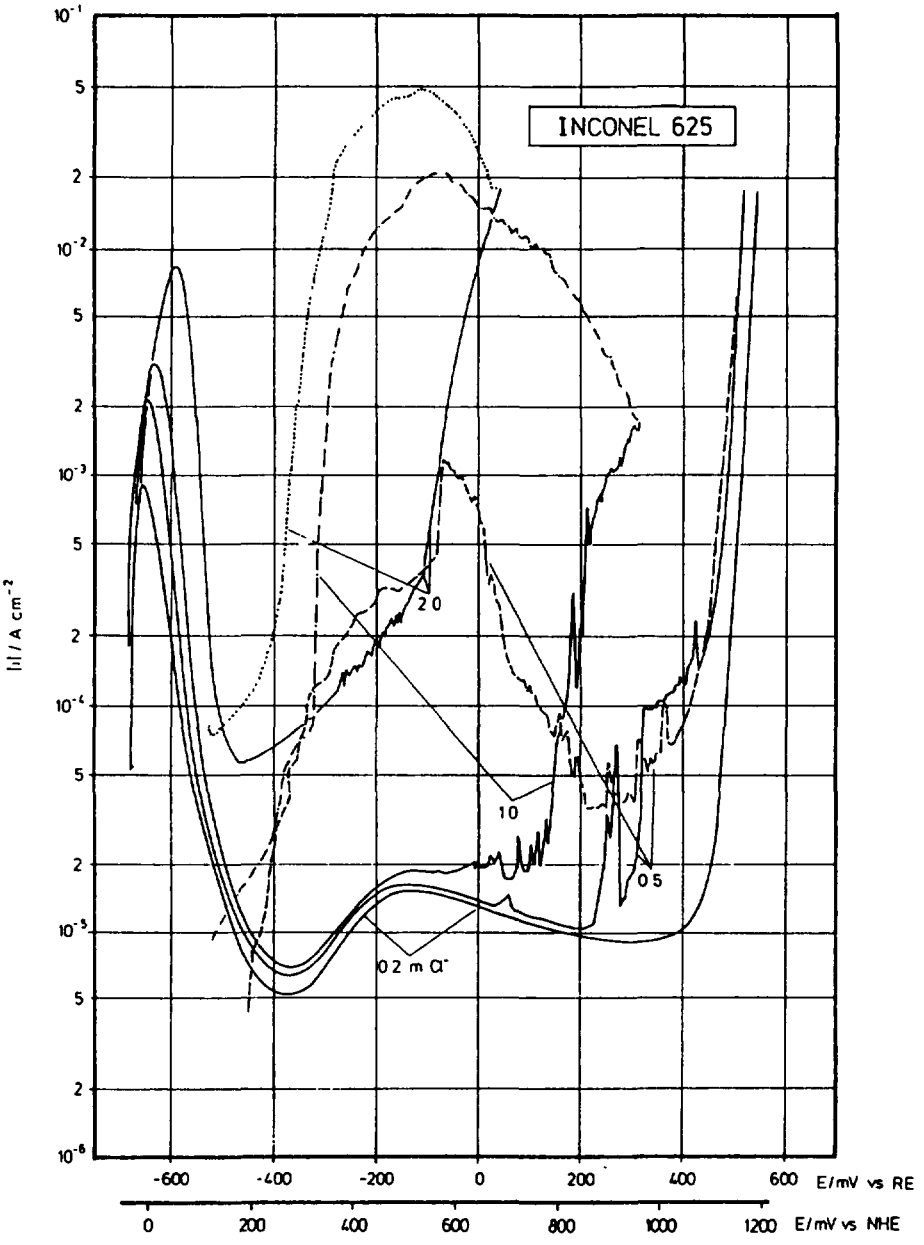

Fig. 7: Potentiodynamic Current-Density-Potential Curves
($dE/dt = 0.2\ mVs^{-1}$)
System: INCONEL 625 / 1m H_2SO_4 + xm KCl,
x = 0.2, 0.5, 1.0, 2.0 /H_2 / T = 367 K

As next parameter the pH-value was varied. As expected, an increase of the pH-value extends the passive region to more negative values, the passive current density decreases. The variation of the pH-value does not affect the critical pitting potential, as can be seen from fig. 8.

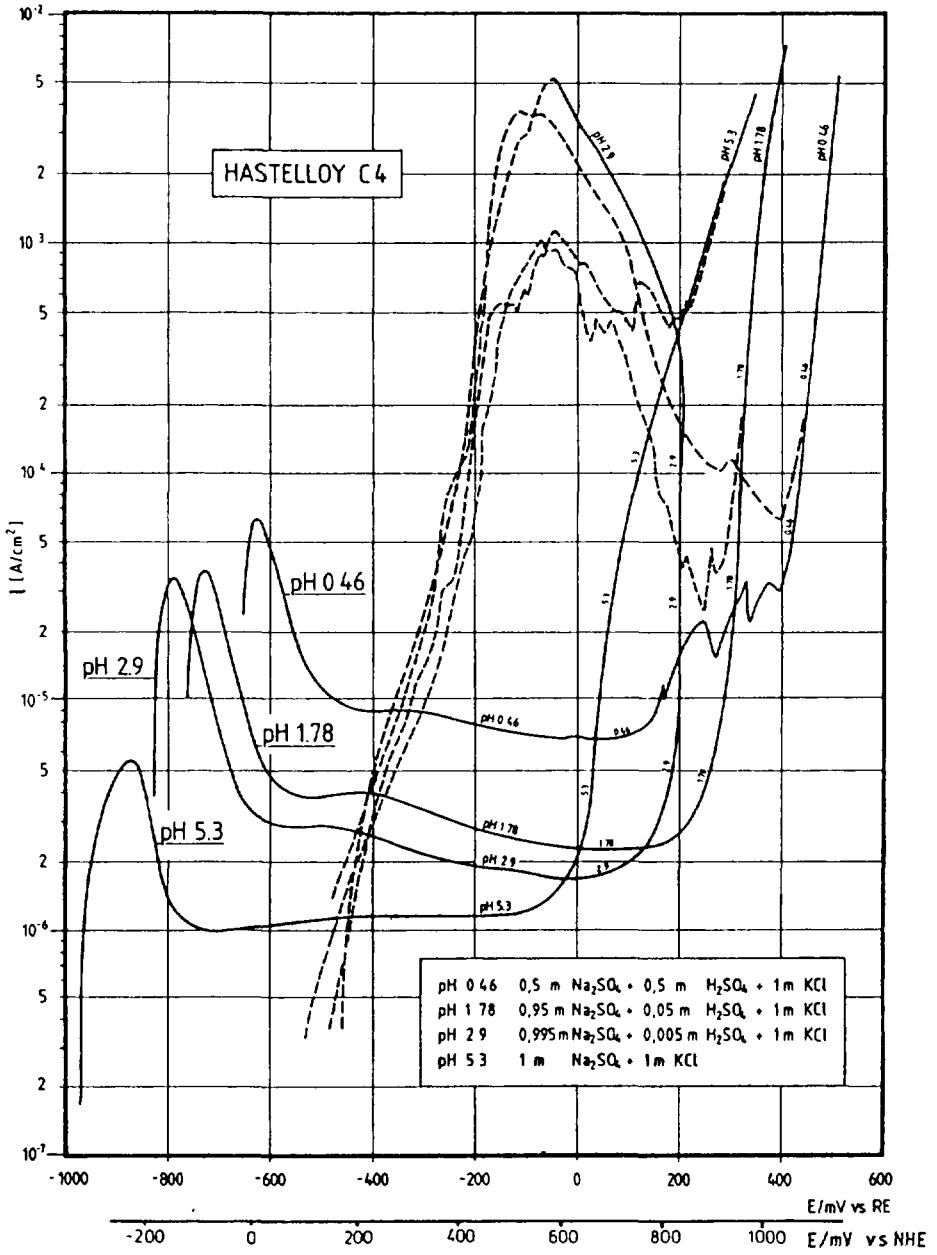

Fig. 8: Potentiodynamic Current-Density-Potential Curves
($dE/dt = 0.2\ mVs^{-1}$)
System: HASTELLOY C4 / x m H_2SO_4 + y m Na_2SO_4 + 1 m KCl /
$0 \leq x \leq 1$, $x + y = 1$ / H_2 / T = 367 K

4. Conclusions

All tested alloys showed a clearly limited resistance against pitting corrosion phenomena.

However, the best corrosion behaviour is shown by HASTELLOY C4, which has of all tested alloys the lowest passivation current density and the largest potential region with protection against local corrosion phenomena.

Further investigations will now be directed towards the corrosion allowance concept, i.e. electrochemical corrosion testing of low carbon steels under various conditions will be performed.

5. References

[1] Nuclear Science and Technology, CEC-Report, EUR 9836 en (1985)
[2] MOLECKE, M.A., RUPPEN, J.A., DIEGLE, R.B., Trans. Am. Nucl. Soc. 41 (1982) 284
[3] SCHWENK, W., Corrosion 20 (1964) 129
[4] JANIK-CZACHOR, M., Werkst. Korr. 31 (1980) 606
[5] STREHBLOW, H.-H., Werkst. Korr. 35 (1984) 437

MATERIAL CORROSION UNDER SPENT NUCLEAR FUEL STORAGE CONDITIONS

V.G. KRITSKY, V.V. MOROZOV, A.F. NECHAEV,
Yu.A. KHITROV, N.G. PETRIK, N.N. KALYAZIN,
T.F. MAKARCHUK
All-Union Project and Research Institute
of Complex Power Technology,
Leningrad, Union of Soviet Socialist Republics

Abstract

The decision is taken in the USSR to build additional independent spent fuel storage facilities for 10 or more years of NPP operation.

The longer is the time of SFA storage, the more severe are the requirements for fuel element cladding integrity and for all fuel assembly and storage components safety. Investigations of zirconium alloy and some steels corrosion under storage pool conditions indicated the possibility of long-term safe storage in water pools. However, model experiments indicated the probability of significant steel corrosion accelleration due to radiation exposure.

The most developed thermal neutron reactor types in the USSR are:

boiling water-graphite one-circuit reactors and two-circuit pressure-vessel water-water reactors /1,2/.

LWR reactors use low enriched uranium fuel (uranium dioxide) with zirconium alloy cladding. After cooling in the reactor the fuel is placed in cooling pools.

Some characteristics of the main types of spent fuel are given in Table 1.

At present the decision is taken in the USSR to build additional independent spent fuel storage facilities for 10 or more years of NPP operation /3/. Such storage facilities are accomodated as a rule on NPP sites in separate buildings.

Table 1 Characteristics of the main types of spent nuclear fuel /2,3,4/

Characteristics	Reactor	
	pressure-type	boiling-type
Capacity, MW(th)	3000	3200
Initial charge, tU	66	180
Average burn-up, MWd/kg	27 - 40	15.5 - 22.3
Length of a fuel assembly (FA), mm	4570	10030
Outer diameter of a fuel element, mm	9.1	13.5
Thickness of a fuel element cladding, mm	0.67	0.90
Activity after three year cooling, MCi/tU	0.78	0.5
Heat-rate after three year cooling, kW/tU	3.6	2.5

In this case the following technological requirements are imposed upon structure of the storage facility and storage conditions from the point of view of safety of equipment operation and fuel element storing:

- fuel accomodation providing nuclear safety during storage and transfer operations;
- pool water cooling to the temperature not higher than 50°C with decay heat removal from fuel;
- radiation safety of the personnel during the storage operation according to the existing standards;
- prevention of water leakage into environment by the storage structure eliminating water ingress into ground during operation and localization of leakages.

It is known, that the longer is the time of spent fuel assembly storage, the higher are the requirements to the safety of fuel element claddings and all structural elements of fuel assemblies and storages.

To meet the above requirements in the storage construction, principal technological solutions are accepted at NPP to reduce the impact of the storage environment

(water and radioactivity) on the storage pool equipment and FA claddings.

Mainly these are:

- use of water cleaning and purification systems in the storage;
- maintaining of the required water level;
- special ventilation of the above-water space;
- process and radiation monitoring.

The following structural solutions are adopted in this case:

- Water purification according to the two-stage principle: at the first stage water is purified from suspended corrosion products, and at the second stage it is cleaned from dissolved salts, with simultaneous decontamination from radioactive matters at both stages.
- Installation of light removable roofing over the pool which provides stable ventilation of the above-water space.
- Stainless steel lining of the pool inner surfaces.

However, the measures indicated above do not completely eliminate radiation and storage medium impact upon corrosion in the cooling pool water. For more efficient and safe operation of pools investigations of the material behaviour in actual and simulated conditions are carried out.

Below the results of steel and zirconium behaviour in pool water and that of stainless steel in simulated conditions are given.

A. Zircalloy

In the set of investigations of irradiated fuel assemblies of the boiling water reactor, zircalloy mechanical properties and its corrosion resistance were studied. Fuel element cladding mechanical properties were also examined on samples cut from fuel elements of fuel assemblies with different burnup (up to the reserve) and up to 8 year storage time in reactor cooling pools both with canned and uncanned ways of storage. The results of inves-

tigations showed that spent fuel assembly storage in cooling pools up to 8 years does not result in significant change of mechanical properties and remains within the following limits: 500÷670 MPa ultimate strength, 400÷600 MPa yield point, 7.8÷22% elongation /5,6/.

The greatest attention was paid to the examination of fuel element cladding corrosion properties, as this is important for long-term storage in pools. It should be noted that chlorine- and fluorine-ion content in pool water prior to additional purification changed within large ranges. Thus, chlorine-ion concentration for the first two years of operation reached 1200 ppb and that of fluorine-ions 200 ppb.

Investigations were carried out using samples cut from both inner and outer raw fuel elements with 400 mm pitch along the FA height of different burnup and different residence time in the cooling pool. It is of importance, that during FA operation the most intense corrosion of a fuel element cladding takes place at points of highest burnup. Oxide film in the area of highest burnup under spacing grids was 80-100 μm thick, while in the gas-collector area it was 10-15 μm thick /5/.

It was found that the fuel element cladding material in the reactor conditions is susceptible to nodular corrosion /5/. Nodular corrosion up to 100 μm deep was also found in boiling water reactors of Japan, FRG, Finland on claddings of zircalloy-2 fuel elements with burnup up to 30 GWd/t U.

In the process of fuel assembly storage in the cooling pool the maximum oxide film growth took place under the spacing grids and their surrounding areas, 1.0-1.5 m above and below the core and comes to 3-5 μm a year.

It was found in some samples that during FA storage, up to 8 years, after 1.5-2 years of FA storage in the cooling pool the hydrogen content increases by 30-40% as compared to that in the claddings.

Estimates may be of pessimistic character, as for the examination the FA were used, which were stored for a long time in cooling pools filled with water of lower quality

than it is shown in Table 2. After introduction of the water purification system its quality in cooling pools significantly improved, as the total content of chlorine and fluorine ions decreased to $\leq$ 100 ppb . This resulted in the descrease of fuel element cladding material corrosion-rate.

Table 2 NPP pools water quality

pH	5.3 - 8.0
Cl^- content, ppb	500
Conductivity, Sm/cm	3
Dissolved salt content, ppm	1 - 2
Corrosion product content, ppm	0,5

B. Pool lining materials

Full-scale testing of steels

X18H10T steel corrosion in reactor pools is < 1 mg/m^{2}d, and according to the estimates this steel may be classified as an absolutely stable material.

In Tables 3-5 data are given concerning water composition and corrosion of samples of structural steels in WWER reactor pools /7/.

Survey of the results shown in Tables 3-5 allows to consider that the main factors determining the corrosion-rate are the following:

- chemical composition of steel;
- way of sample accomodation;
- chemical composition of the medium.

Cl^--content in pool "A" periodically increased up to 1140 ppb that, in its turn, led to higher corrosion rate of steel in contrast with pool "B".

Such processes as sedimentation and suspended corrosion products deposition are very important for increasing of surface film thickness and γ-radiation sorption (Tables 4 and 5).

Table 3 Quality characteristics and water chemistry for cooling pools under process of tests

System	Quality characteristics and water chemistry						
	pH	Cl^- mkg/kg	NH_3 mg/kg	H_3BO_3 g/kg	F^- kg/kg	K^+ mg/kg	ΣAi Ci/L
Unit "A"	7.2÷9.0	50÷1140	15÷37.5	0.06÷0.81	-	-	$1.1\ 10^{-5}$
Unit "B"	5.0÷6.2	50÷150	0.8÷12	9.3÷16.7	20÷1000*	3.4÷10.1	10^{-6}÷$3\ 10^{-6}$

* during fuel reloading period only (scheduled preventive maintenance)

Table 4 Corrosion test results for steel samples in cooling pools of units "A" and "B" with WWER reactors

System	Material	Way of treatment	Rate of total corrosion		Corrosion nature	Notes
			mg/m^2d	mm/a		
1	2	3	4	5	6	7
Pool (A)	08Х14МФ	as-supplied	1.5 ± 0.6	$0.7.10^{-4}$	total corrosion	horizontal arrangement of samples, depth - 12 m
	Х18Г16	- " -	3.2 ± 1.3	$0.15.10^{-3}$	- " -	
T_{test} 340 days	Х18Н10Т	- " -	0.8 ± 0.2	$0.5.10^{-4}$	- " -	
	Cm.20 (carbon steel)	polished	1700	$0.8.10^{-1}$	pitting corrosion	
	08Х14МФ	as-supplied	1.4 ± 0.5	$0.65.10^{-4}$	total corrosion	vertical arrangement of samples, depth - 8 m
	Х18Г16	- " -	2.3 ± 0.1	$1.1.10^{-4}$	- " -	
	Х18Н10Т	- " -	0.2 ± 0.1	$0.09.10^{-4}$	- " -	
	Cm.20 (carbon steel)	polished	2800	$1.3.10^{-1}$	pitting corrosion	
Pool (B)	08Х14МФ	as-supplied	0.9 ± 0.2	$0.4.10^{-4}$	total corrosion	horizontal arrangement of samples, depth - 12 m
	Х18Г16	- " -	1.2 ± 0.3	$0.6.10^{-4}$	- " -	
T_{test} 370 days	Х18Н10Т	- " -	0.60 ± 0.2	$0.3.10^{-4}$	- " -	
	Cm.20 (carbon steel)	polished	850	$0.4.10^{-1}$	pitting corrosion	
	08Х14МФ	as-supplied	0.8 ± 0.2	$0.4.10^{-4}$	total corrosion	vertical arrangement of samples, depth - 8 m
	Х18Г16	- " -	1.0 ± 0.2	$0.5.10^{-4}$	- " -	
	Х18Н10Т	- " -	0.2 ± 0.05	$0.1.10^{-4}$	- " -	
	Cm.20 (carbon steel)	polished	1400	$0.7.10^{-1}$	pitting corrosion	

Table 5 Radionuclide analysis data on steel sample surfaces and deposits after residence in the Unit "B" cooling pool

Radioisotope	Specific activity					
		10^{-9} Ci/cm^2			10^{-7} Ci/kg	
	X18H10T steel	08X14MФ steel	X18Г16 steel	Cm.20 steel	Deposits from Cm.20, 12 m depth, horizontally	Deposits from Cm.20, 8 m depth, vertically
^{58}Co	1.3	1.9	1.1	6.6	5.3	3.4
^{54}Mn	1.5	1.8	1.1	18	15	4.5
^{110}Ag	0.33	0.7	0.39	5.5	29	14
^{60}Co	3.6	3	2.7	31	34	9.7
Total activity	6.7	7.4	8.8	61.1	83	32

Thus, pool water purification from corrosion products and decontaminftion from radioactive material released into pool water from fuel rod surfaces are obligatory technological processes.

Model water corrosion of stainless steel under gamma radiation

Behaviour of X18H10T austenitic Cr-Ni-stainless steel in distilled aerated water was studied. The samples were exposed to gamma-quantum dose from ^{60}Co-source at the dose rates, 0.9 ± 0.05 and 3.3 ± 0.15 Gy.S^{-1}, and temperatures 307 ± 2 K and 330 ± 2 K, respectively. A set of representative samples situated out of radiation zone were thermostatted under the same conditions. Disk samples (26x1 mm) were placed in 0.2 l glass ampules filled with water. The samples were removed at definite intervals, then the solution was analyzed for Fe-, Cr- and Ni-contents by atomic absorption spectroscopy. Sample mass changes were monitored.

Three groups of samples were studied, differing in their surface conditions. The first group included electropolished samples. Surface investigation by X-ray photoelectron spectroscopy (XPS) revealed a surface oxide film a few

atomic layers thick. The second group included as-supplied samples with rough surfaces and thin oxide film more than 5 nm thick was detected on the sample surfaces. Cr-content in that oxide film was three times higher than in metal with no Ni at all. The chemical state of Cr- and Fe-atoms corresponded to that of trivalent metal hydroxides. The third group included samples which were autoclaved in $NaOH + KNO_3$ solution for 8 hours at 570 K. On their surfaces a thick magnetite film, Fe_3O_4, was registered.

While sample irradiation in water Fe was released from the steel surface into water (mainly as hydroxides). On the other hand, Cr and Ni were not found there up to the dose of 0.6 MGy. Fe selective dissolution was accompanied by surface film enrichment in Cr: Cr-content in the oxide increased by a factor of 1.5 at 0.1 MGy. For all groups of samples Fe-release rate grew with the dose rate: by a factor of 2-14 at 0.9 $Gy.S^{-1}$ (Fig.1) and by a factor of approximately 30 at 3.3 $Gy.S^{-1}$ (Fig.2). It is evident (from Fig.1) that at different steps radiation corrosion rate begins to increase significantly with increasing of initial oxide film thickness (curves 1-2-3). Corrosion kinetics of the samples with thin surface films was characterized by two steps: a rapid step and a slow one (Fig.1, curves 1 and 2). For the specimens of the second group the amount of Fe dissolved at the slow kinetic step, approached that of the initial oxide film. Evidently, under the radiation impact the oxide film dissolution was a more rapid process compared to the oxidation of metal surface (particularly at different corrosion steps). Therefore, the steel oxidation didn't lower the Fe-release rate into the solution but, on the contrary, promoted it in the presence of radiation.

Our previous results /8/ showed that γ-radiation greatly increased the dissolution rate of some metal oxides (Fe-oxides included). The radical products of water radiolysis were important for this process. At the same time, as it is known, the radical products of water radiolysis intensified the steel oxidation as well. In our tests this

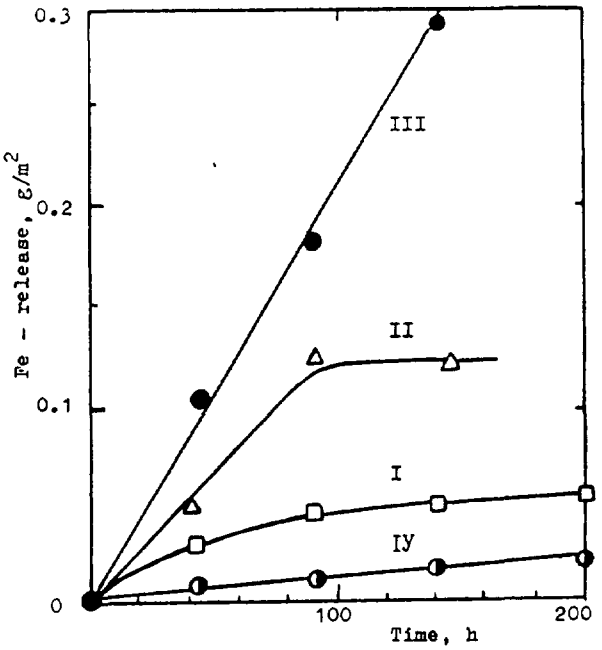

Fig.1. Kinetics of stainless steel water corrosion at γ-dose rate 0.9 Gy.s^{-1} and in the absence of radiation(IV).

I - electropolished samples; II - as-fabricated samples; III - autoclaved samples

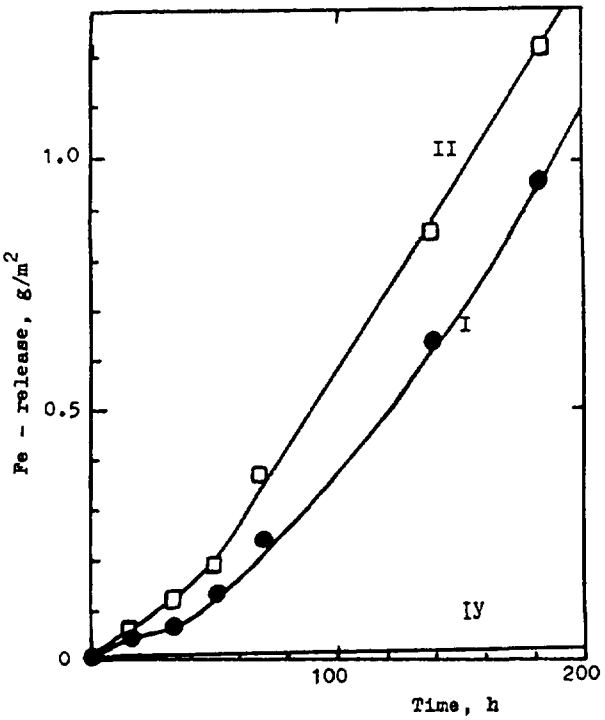

Fig.2. Kinetics of stainless steel water corrosion at γ-dose rate 3.3 Gy.s^{-1} and in the absence of radiation(IV).

I - electropolished samples; II - autoclaved samples

effect became obvious at later corrosion steps appearing with greater dose rate (Fig.2). On passing from 0.9 to 3.3 $Gy.S^{-1}$ Fe dissolution rate both from oxidized and polished samples started to increase. Difference in corrosion rates between the first and the third groups of samples levelled off with time.

In the solution Fe-ions became hydrolized and formed colloid hydroxides. The hydrolysis led to acidification of the medium to pH = 4.1. After 150 hours of exposure at 0.9 $Gy.S^{-1}$ a reverse process was observed, namely deposition of colloids (crud) on the steel surface. Fe-release rate into the solution was reduced. XPS-analysis revealed a steady rise of the Fe-content in the surface oxide film (despite of its intense dissolution). At higher dose rate, 3.3 $Gy.S^{-1}$, Fe dissolution exceeded again that of the crud deposition.

Spent nuclear fuel is the source of ionizing radiation. Therefore the problems of radiation-induced corrosion of cooling pool structural materials, containers and fuel cladding are urgent and need investigation.

Based on the radiation-corrosion kinetics study, the main factors influencing the corrosion under irradiation and a significant number of radiation-induced corrosion models are found in literature. These models in total describe the following corrosion kinetics under irradiation:

1 - corrosive medium radiolysis (practically in all models);
2 - radiation effect on the oxide morphology: the phase changes, nucleation effects. An oxide morphology changes under medium radiolysis products;
3 - oxide radiation injury (defect formation, embrittlement, creep, electric properties changes);
4 - metal radiation injury (embrittlement, creep, ageing).

The first two corrosion mechanisms in the cooling pool water may be caused by spent fuel fission product radiation. The rest, in principle, may be realized only for spent fuel assembly materials because of fast neutron fluence during the reactor campaign.

Conclusion

Thus, the investigations showed that mechanical properties of SFA structural materials practically remain unchanged at long-term wet storage. The estimated values of SFA structural part corrosion rates as well as those of concentrations and deposit activity on their surfaces allow to arrive at the conclusion about the possibility of SPA long-term storage up to 30 years, of its transportation to independent storages and radiochemical plants.

The investigations carried out have shown that X18H10T stainless steel corrosion in water environment is accelerated by one order of magnitude under γ-radiation. The radiation stimulates the following process: steel oxidation; iron oxide film dissolution, Fe-ion hydrolysis followed by crud formation, crud deposition. The corrosion rate even more accelerated by radiation appears to be insufficient to limit the life-time of stainless steel structural elements. It is approximately 10 μm/a for uniform corrosion process. More considerable radiation effects, apparently, will be the increased radionuclide release into the cooling pool water from active deposits on fuel cladding as well as from activated stainless steel structural elements.

References

I. Александров А.П., Коченов А.С., Рязанцев Е.П. и др. Ядерная энергетика в СССР// Атомная энергия, 1983, т.54, вып.4. - С.243.

2. Бакуменко О.Д., Ихлов Е.М., Кулаковский М.Я., Орлов В.В., Троянов М.Ф., Ширин В.М. О транспортировании отработавшего топлива быстронейтронных энергетических реакторов// Доклады совещания специалистов стран-членов СЭВ по вопросам транспортирования отработавших твэлов и неразрушающим методам определения в них содержания делящихся материалов. - М.: СЭВ, 1976. - С.134.

3. Петросьянц А.М. Ядерная энергетика. - М.: Наука, 1981. - С.59-70.

4. Усынин Г.Б., Кусмарцев А.Б. Реакторы на быстрых нейтронах. - М.: Энергоиздат, 1985. - С.202-203.

5. Варовин И.А., Еперин А.П., Уманец М.П. и др. 10-летний опыт эксплуатации Ленинградской АЭС// Атомная энергия, 1983, т.55, вып.6. - С.349-353.

6. Варовин И.А., Покровский А.С., Никифоров С.А. и др. Материаловедческие исследования твэлов РБМК-1000 с оболочками из сплавов: цирконий-ниобий, цирконий-ниобий-железо-олово, цирконий-железо-олово. - Препринт НИИАР 38/603. - Димитровград, 1983.

7. Krutikov P.G., Makarchuk T.F., Nechaev A.F., Kchitrov Yu.A. The USSR Experience in Spent Fuel Storage (Report BEFAST Coord., Agr. N 3428/CF-IAEA). - USSR: SCUAE, 1983. - 10 p.

8. Калязин Н.Н., Нечаев А.Ф. Радиационно-кинетические эффекты растворения гидроокиси хрома в перекиси водорода// Тез.докл. III Всесоюзного совещания по воздействию ионизирующего излучения и света на гетерогенные системы, Кемерово, 1982. - Кемерово: Изд.Кем.ГУ, 1982, ч.I. - С.376.

MATERIAL SELECTION FOR FINAL STORAGE OF SPENT FUEL IN A SALT REPOSITORY — THE POLLUX CASK SYSTEM AS AN EXAMPLE

K. EINFELD, F.W. POPP
Deutsche Gesellschaft für Wiederaufarbeitung
von Kernbrennstoffen mbH,
Hannover

U. KNAPP
Kernforschungszentrum Karlsruhe GmbH,
Karlsruhe

Federal Republic of Germany

Abstract

In the framework of the development of containers for the final disposal of radioactive waste in salt deposits DWK conceived the Pollux Cask System. This cask system is highly flexible in so far as it is capable of bearing extremely different types of waste such as integral fuel elements, consolidated rods, HTR-pebble elements, consolidated structure materials, solidified high active waste etc.

The Pollux cask system is characterized by an anticorrosive coating of Hastelloy C4 which is applied to by surface welding. With regard to its long term behaviour comprehensive corrosion tests on Hastelloy C4 were performed in Q-brain. This reports presents a survey on results of these corrosion tests; especially recent results of long term integral tests (lasting about two years) on two cask models will be reported about. Moreover investigations on surface corrosion and local corrosion in depence of the temperature will be reported about in order to demonstrate the limits of application of the anti-corrosive coating.

---

1. Introduction

The POLLUX cask System ist designed for the final disposal of spent fuel in a salt repository. The materials of POLLUX cask are selected in accordance with the special safety criteria of final storage. The mechanical properties and the anticorrosive behaviour of the selected materials ensure safe containment of radionuclides during final storage.

The POLLUX Cask System is based on investigations which were conducted in the Project PAE "Project for Alternative Disposal Techniques" - an R & D program of the German Ministry of Research and Technology (BMFT) - during the years 1980 - 1984. DWK continued this development since that time on their own for planning and construction of a pilot plant for conditioning and encapsulation of spent fuel. Both tasks are part of the overall R & D "Program Direct Disposal " as shown by fig. 1. The other tasks of this programme are coordinated by KfK, the Karlsruhe Nuclear Research Centre. Major contributions to the programme are made by KfK, DBE, the German Company for Planning and Construction of Repositories for Radioactive Waste, GSF[1] and BGR[2]. The objective is to demonstrate the feasibility of the new techniques of disposing final storage casks in a salt mine.

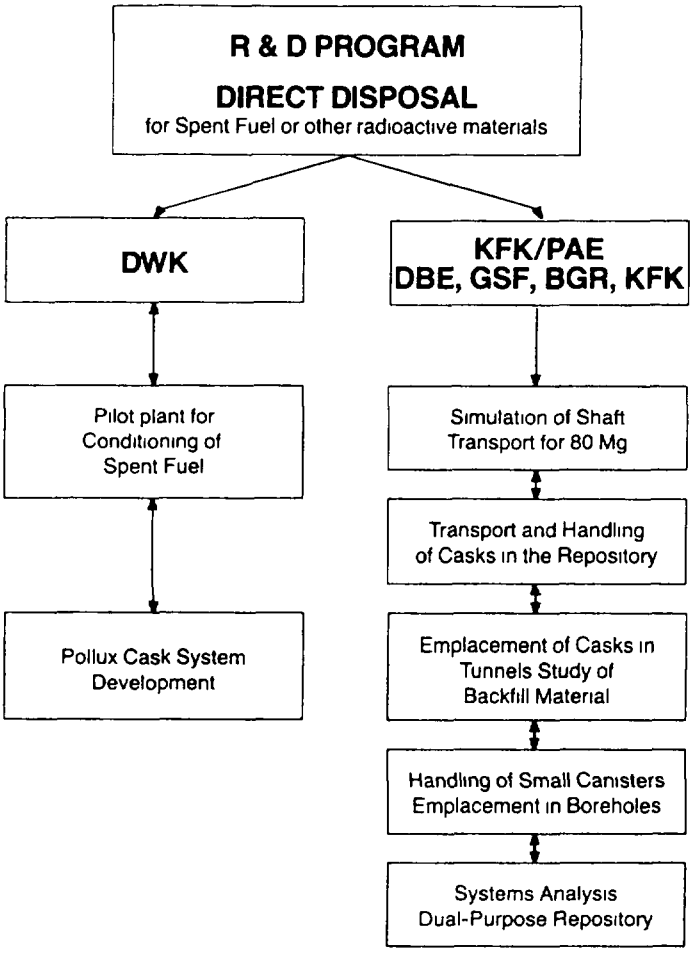

FIG. 1. R & D program direct disposal.

1) Gesellschaft für Strahlen- und Umweltforschung, Institut für Tieflagerung, Braunschweig
2) Bundesanstalt für Geowissenschaften und Rohstoffe

2. POLLUX-CASK

The objective of the POLLUX Cask System is safe containment of spent fuel with regard to

- long term intermediate storage and
- final disposal in a geological repository.

The POLLUX-Cask-System is defined by

- the waste form of radioactive materials
- the final disposal cask to assure inclusion of waste in a steel containment
- the anticorrosive coating to assure final disposal in a geological repository
- the overpack to assure shielding, handling and transport.

The containment of POLLUX-Cask is shown in fig.2. It consists of the following multiple barriers:

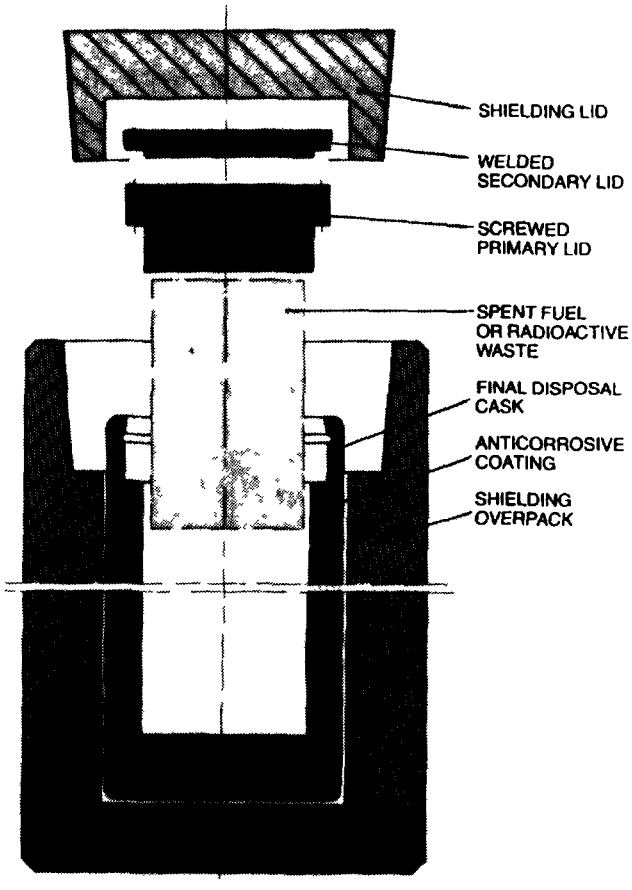

FIG. 2. Pollux containment concept.

The Final Disposal Cask

which assures

- gas tightness by means of a screwed primary lid and a welded secondary lid
- protection against mechanical loads and impacts.
  The dominant mechanical load is given by the pressure in the geological repository
- protection against corrosion during final storage in the geological repository. The protection against corrosion can be realized with Hastelloy C4 resurfacing by welding.

The Shielding Overpack

which assures

- shielding of gamma- and neutron-radiation under transport, storage and corresponding accidental conditions
- mechanical protection unter operational and type B(U) test conditions, and shock absorber function for the inner final disposal cask (no gas tightness function necessary because this is already guaranteed by the steel containment of the final disposal cask).

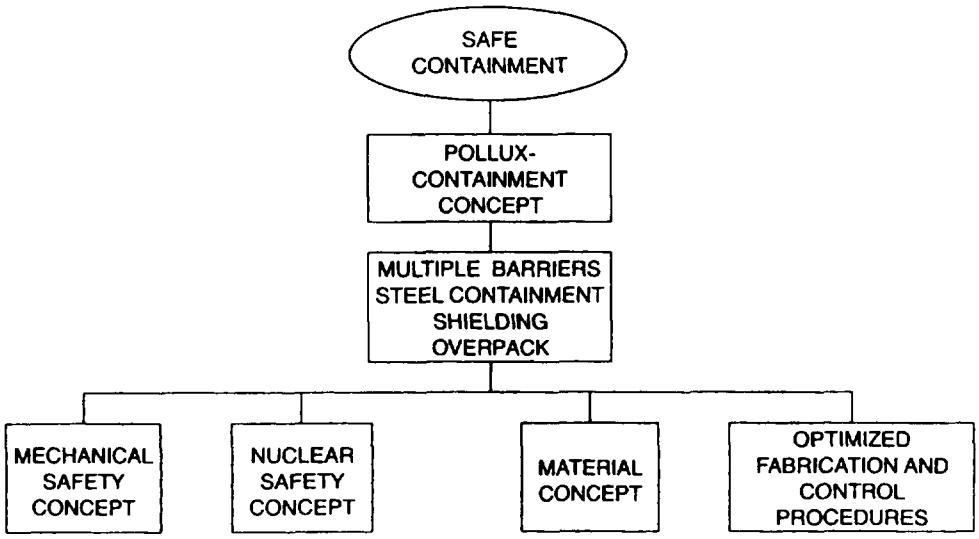

FIG. 3. Safety concept.

3. Safety Concept

The safety concept of POLLUX containment cask includes (fig.3)

- the mechanical safety concept
- the nuclear safety concept
- the material concept
- optimized fabrication and quality assurance.

3.1 Mechanical Safety Concept

The safety of the POLLUX containment cask under type B (U) test conditions will be fulfilled by analytical calculations in accordance with regulations for operational and accidental loads.

The gas tightness of the final disposal cask will be ensured under operational and type B (U) test conditions by

- limitation of mechanical loads
- conservative limitation of stresses and strains.

The calculations will be performed by the method of finite elements (fig. 4).

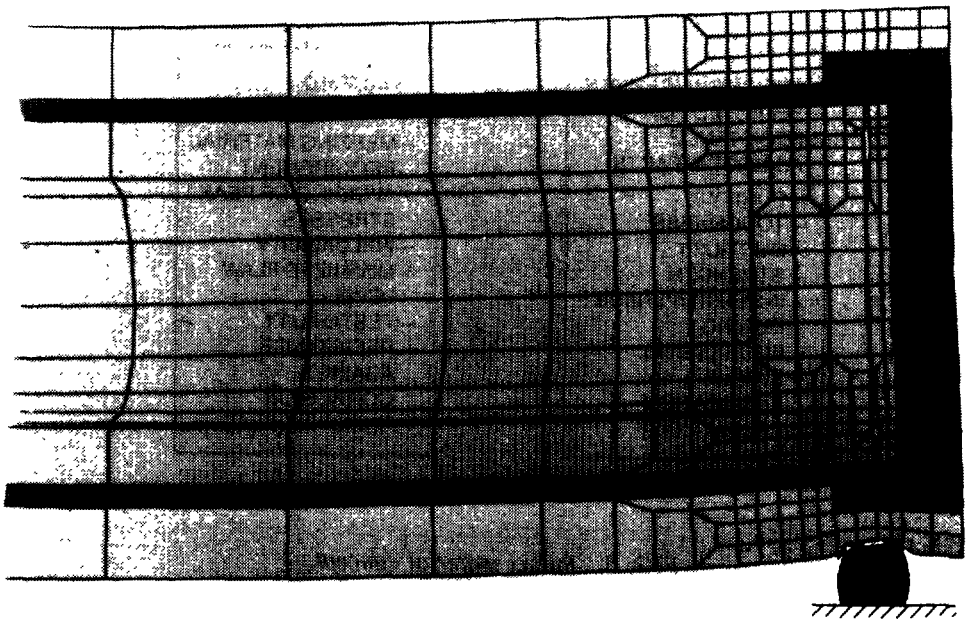

FIG. 4. Pollux safe-containment analytical calculation of stresses.

3.2 Nuclear Safety Concept

The nuclear safety concept assures for all operational and the considered test conditions (type B (U) et.al.)

- undercriticality
- sufficient shielding
- integrity of containment
- removal of decay heat .

3.3 Material Concept

The material concept is based on specific selected well-tried materials for the final disposal cask and the shielding overpack (fig.5).

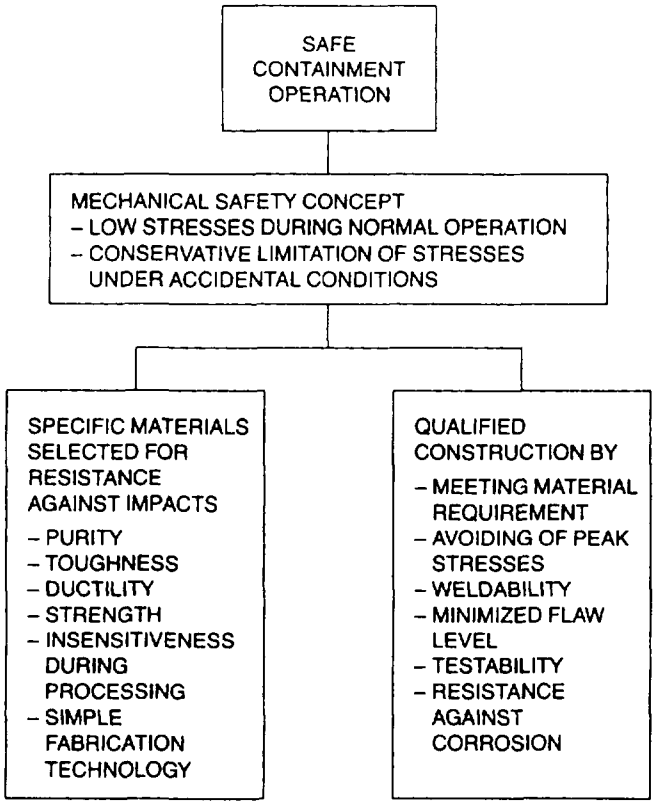

FIG. 5. Pollux material concept.

The Final_Disposal_Cask is a steel containment of the steel grade 15 Mn Ni 6.3, which is also applied as containment in modern nuclear power plants in Germany.

The selected materials for the Shielding Overpack are ductile cast iron (GGG 40) and polyethylene.

The reliability is achieved by proper material selection with respect to

- application of conventional fabrication technologies and experiences especially concerning welding techniques
- minimized flaw level by optimized manufactoring
- weldability
- testability and quality assurance which forms the basis for the reliability during transport, intermediate storage and in the final repository in combination with
- sufficient ductility and toughness
- sufficient strength combined with low stress levels
- corrosion resistance.

3.4 Optimized fabrications and quality assurance

The optimized fabrication and quality assurance supervise the compliance with all fundamentals required to obtain the reliability of the POLLUX cask system.

4. Closing Techniques

4.1 Closing procedures

The POLLUX closing procedures after loading are characterized by the following steps:

- closing final disposal cask by srewing in primary lid in a hot cell
- closing steel containment of final disposal cask by welding secondary lid in direct operation mode.

- closing anticorrosive coating by hot wire surfacing in direct operation mode

- closing shielding overpack by screwing in shielding lid

4.2 Welding of steel containment

The welding of steel containment is performed by a welding gantry in direct maintenance technique (fig.6). The narrow spaced gap between the secondary lid and the final disposal cask is closed by submerged arc welding. The narrow gap welding technique has been employed for thick wall components of nuclear power plants. The advantages are considerably shorter welding times and a provable reduced coarse grain area in the heat affected zone. The welding procedures are automated. Control of welding parameter assures quality and tightness of the welding seam.

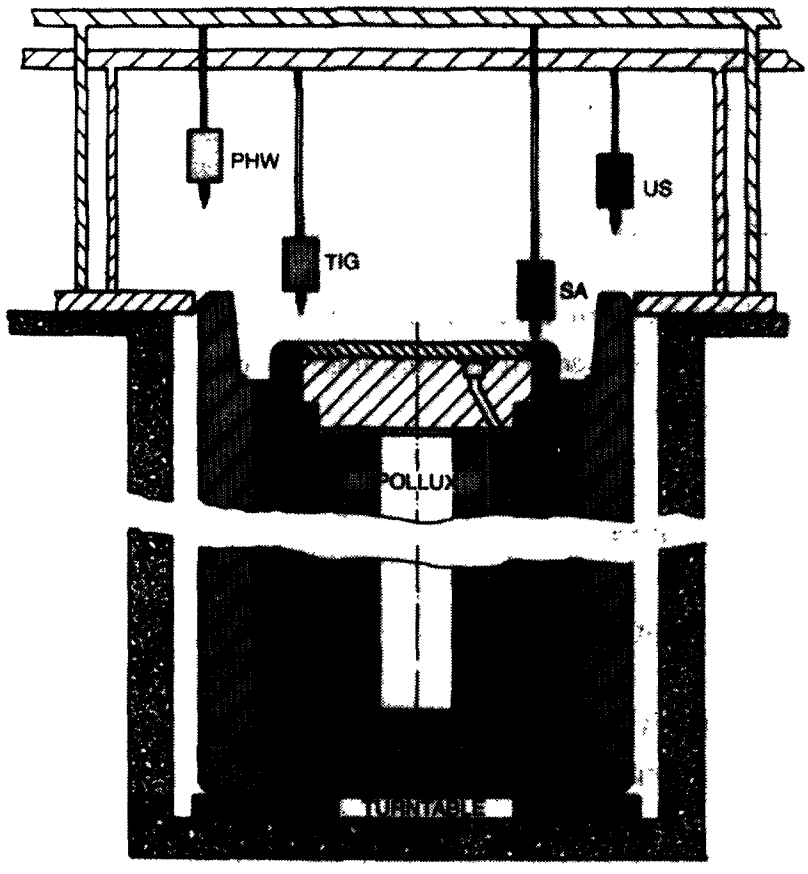

US = ULTRA SONIC TEST
PHW = PLASMA HOT WIRE WELDING
SA = SUBMERGED ARC WELDING
TIG = TUNGSTEN INERT GAS WELDING

FIG. 6. Pollux welding gantry.

The steel grade 15 Mn Ni 6.3 has been selected for final disposal cask and welding lid because of his quality features of weldability.

The welding gantry and closing of POLLUX final disposal cask are shown in figures 7 to 9.

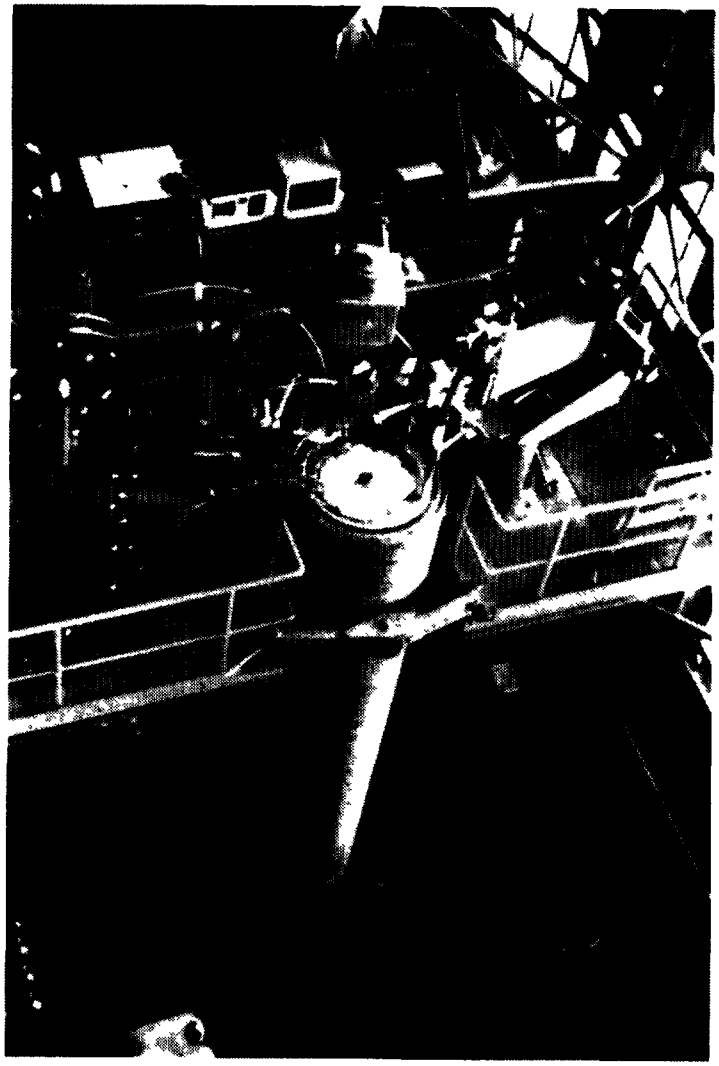

FIG. 7. Pollux: closing final disposal cask welding of secondary lid.

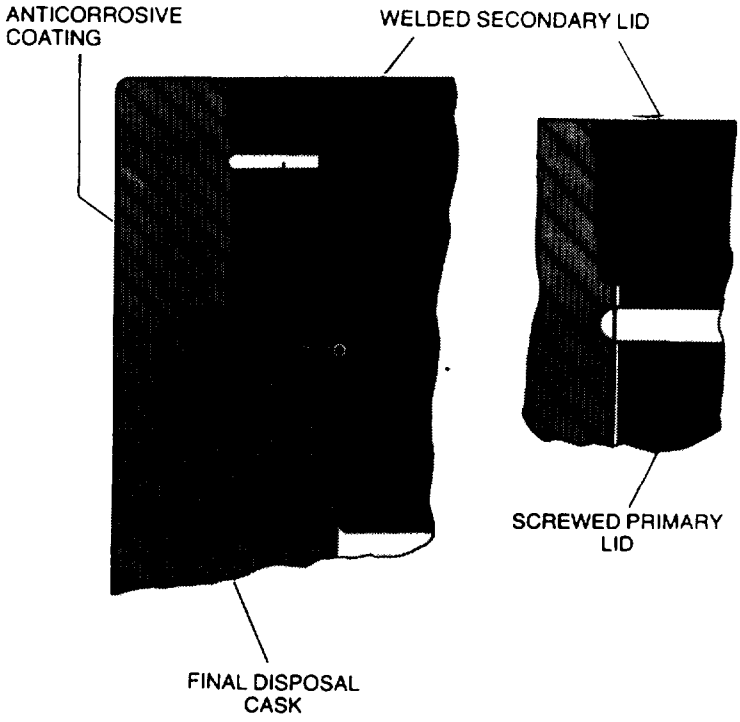

FIG. 8. Pollux containment concept narrow gap welding.

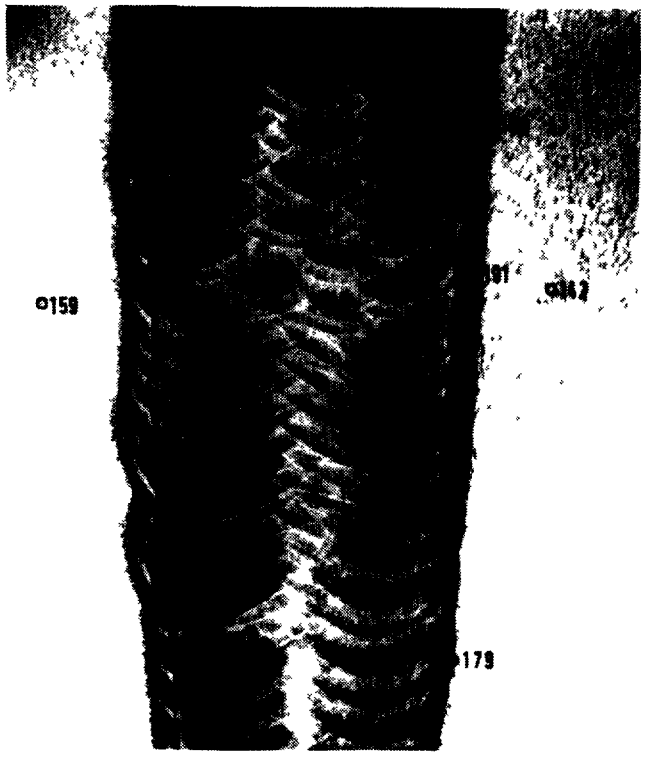

FIG. 9. Structure of welded secondary lid (scale 1:3).

4.3 Plasma Hot Wire Surfacing

Plasma hot wire surfacing (PHW) of the final disposal cask (steel grade 15 Mn Ni 6.3) combines a base material well-known in nuclear technology with a provable welding process (fig. 10.).

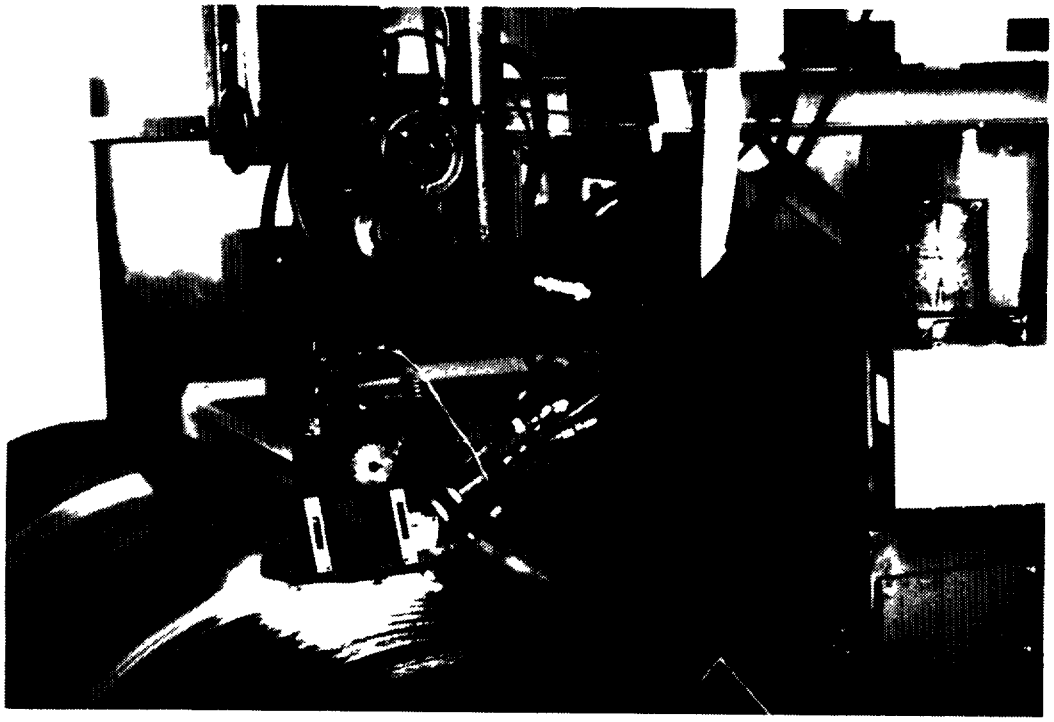

FIG. 10. Pollux: coating of final disposal cask Hastelloy C4 resurfacing by welding.

Plasma hot wire surfacing is a welding procedure. Filler metal will be fed as hot wire into the melting bath and heat input will be procedured through a separately working plasma arc. PHW surfacing is characterized by

- low heat input
- low depth of penetration
- low mixture of base and filler metal
- uncritical structure in the heat affected zone
- favourable residual welding stress distribution
- annealing effect by multilayer surfacing
- realization of thin layers with mandatory chemical composition
- no influence on welding metallurgy by flux
- flexibly applicable and optimally controllable welding process.

Especially the low heat input and the low mixture of base and filler metal have a positive influence on the structure of the heat affected zone. It ensures the stability of the chemical composition of the coating and the mechanical properties of the compound materials (surfaced components) (fig. 11). Therefore welding defects such as underclad cracking do not appear during PHW surfacing.

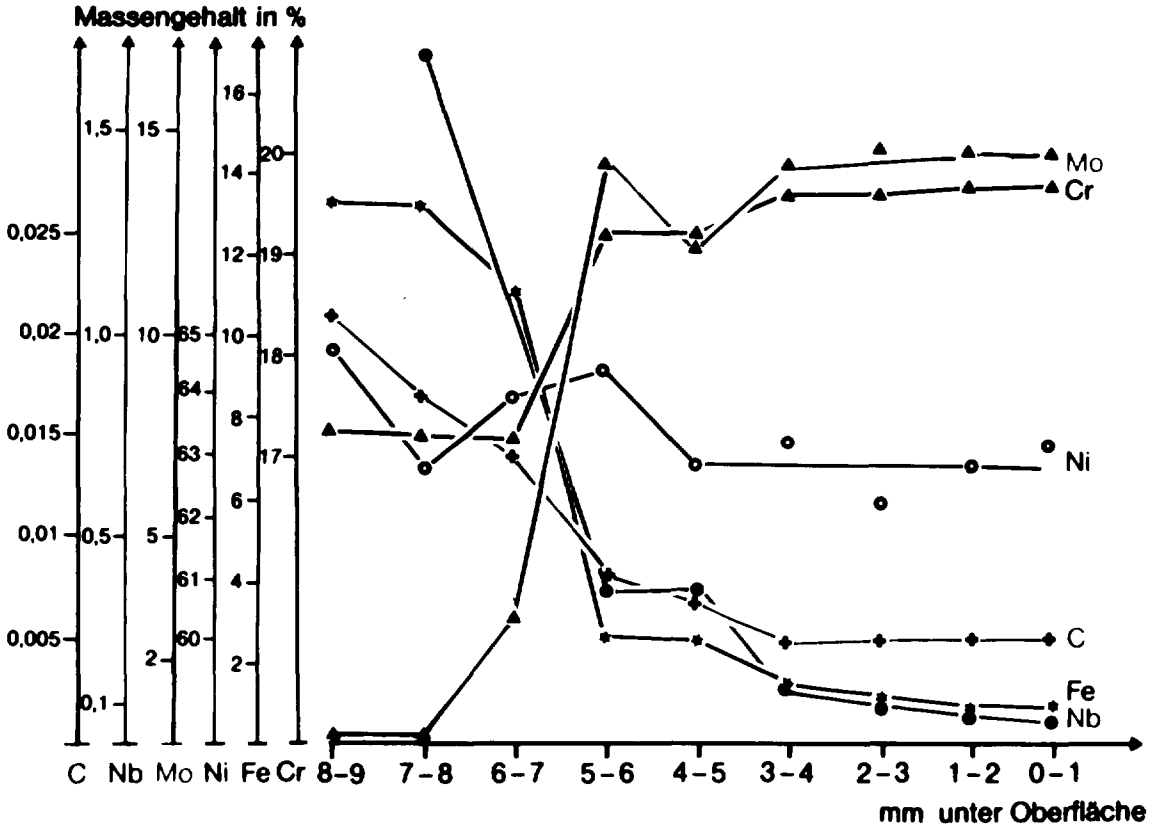

FIG. 11. Hastelloy C4 resurfacing material analysis.

5. Corrosion Tests

Within the Project PAE "Project for Alternative Disposal Techniques" corrosion tests on different materials were carried out with regard to the unrealistic case, that the POLLUX will be exposed to hot salt solution. These investigations are continued by DWK and KfK.

5.1 Corrosive Media

Corrosive media were selected according to a recommendation of a PTB meeting dated Oct. 1980, where altogether 11 different brines were listed. The most serious conditions can be expected from the Q-brine ($NaCl-KCl-MgCl_2-H_2O$) which was used in most corrosion studies.

$MgCl_2$	26.5 %
$MgSO_4$	1.5 %
NaCl	1.8 %
KCl	4.7 %
H_2O	65.5 %

In planning of the final disposal repository PTB intends not to touch any salt formations containing larger amounts of $MgCl_2$.
Consequently, it can't be expected that in the unrealistic case of an exposure of POLLUX to a hot salt solution the brine contains larger amounts of $MgCl_2$.

The performed corrosion experiments in Q-brine with a high amount of $MgCl_2$ must therefore be considered as very conservative.

5.2 Results of corrosion tests

Built-up welds/quinary salt solution/100 °C (fig. 12 and fig. 13)

The corrosion rates are calculated from the measured mass losses. Corrosion rates of

$$< 1.10^{-3} \text{ mm/a}$$

are obtained after test durations of 84 and 168 days. The mass loss rates are not affected by sensitization from welding (2 to 8 hours at 850 °C).

No special effects were found on any of the material samples tested up to 84 days.

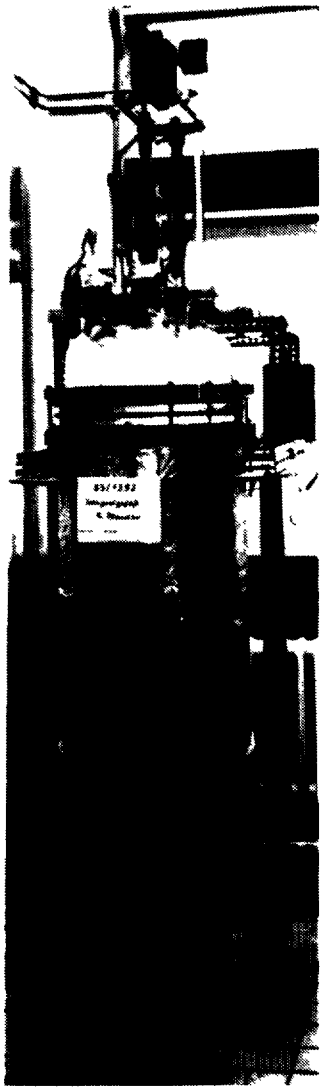

FIG. 12. *Corrosion program.*

Built-up welds, type Hastelloy* alloy C-4
in the quinary salt solution / 168 days / 100 °C

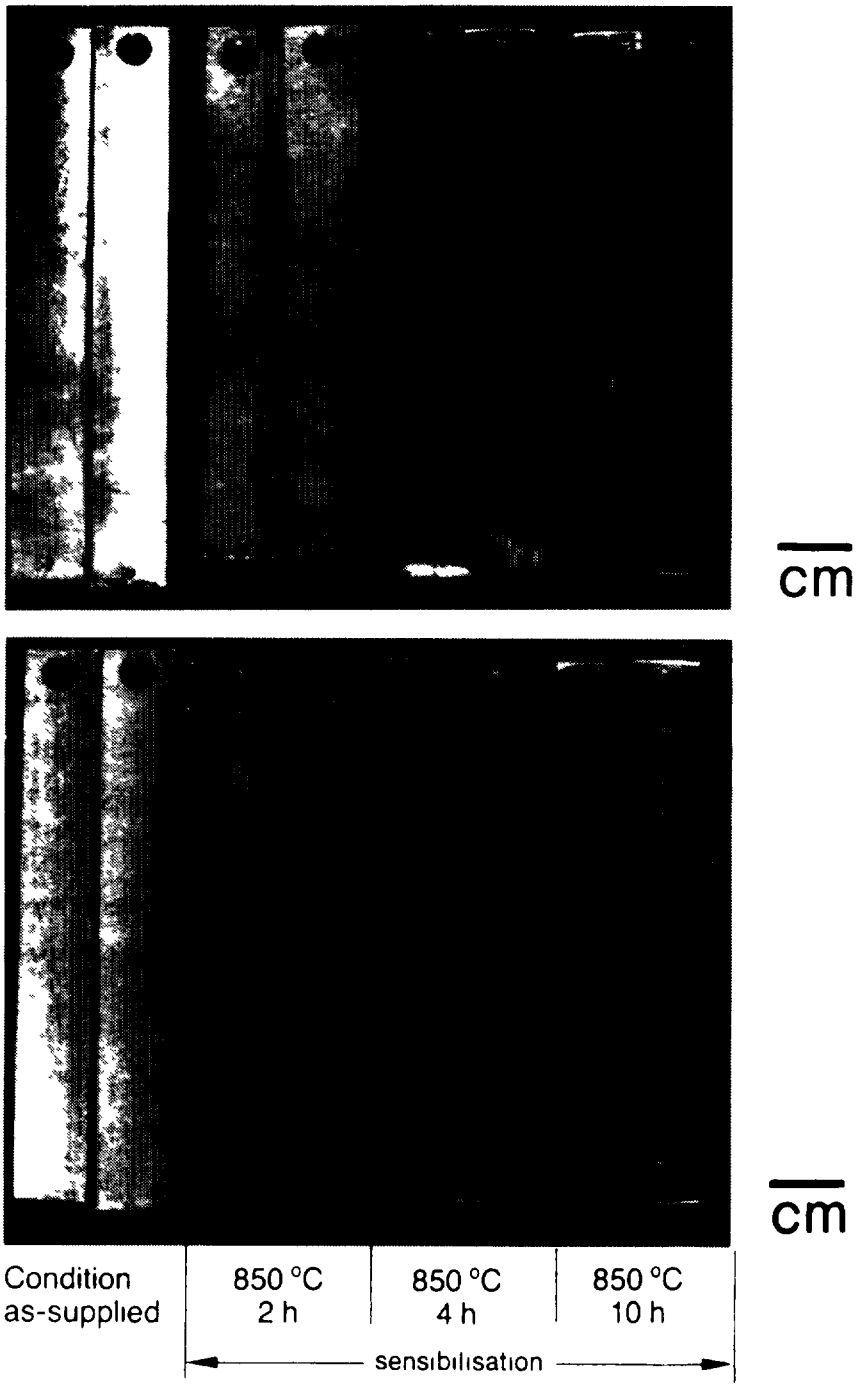

Sample dimensions: B: usually 50 x 10 x 5 mm

FIG. 13. *Corrosion program.*

Built-up welds/quinary salt solution/150 °C

It was found that the first serie of metal samples (1982) led to poor results since they had been manifactured under unfavourable conditions. Foreign particles were pressed into the material surface during grinding. Therefore this serie of material samples was discarded. New samples (1984) which had been finished using new grinding wheels revealed considerably better properties. They showed after 50 days no signs of corrosion; furthermore the mass losses were very low, corresponding to corrosion rates of

$$< 1.1 \times 10^{-3} \text{ mm/a}$$

Corrosion tests in 150 °C quinary brine are continued.

Built-up welds/quinary salt solution/175°C/200°C (fig. 14)

Results for an exposure period of 365 days are available. Parent metal samples and weld joints made of the corresponding wrought material Hastelloy C4 were included in the tests. No differences have been found. The following corrosion rates are obtained

175° C	$1 \times 10^{-3} - 1.8 \times 10^{-3}$ mm/a
200° C	$3 \times 10^{-3} - 5.7 \times 10^{-3}$ mm/a

With both temperatures the samples showed locally corroded areas. As a result of these test it can be stated that Hastelloy C4 is not suitable for corrosion protection in quinary brine with temperatures of 200 or 175° C

Integral test

A model container with anticorrosive layers of Hastelloy-C4 and ceramic was tested in quinary salt solution heated to 100° C from 1st during 264 days (1983/84) (fig. 15)

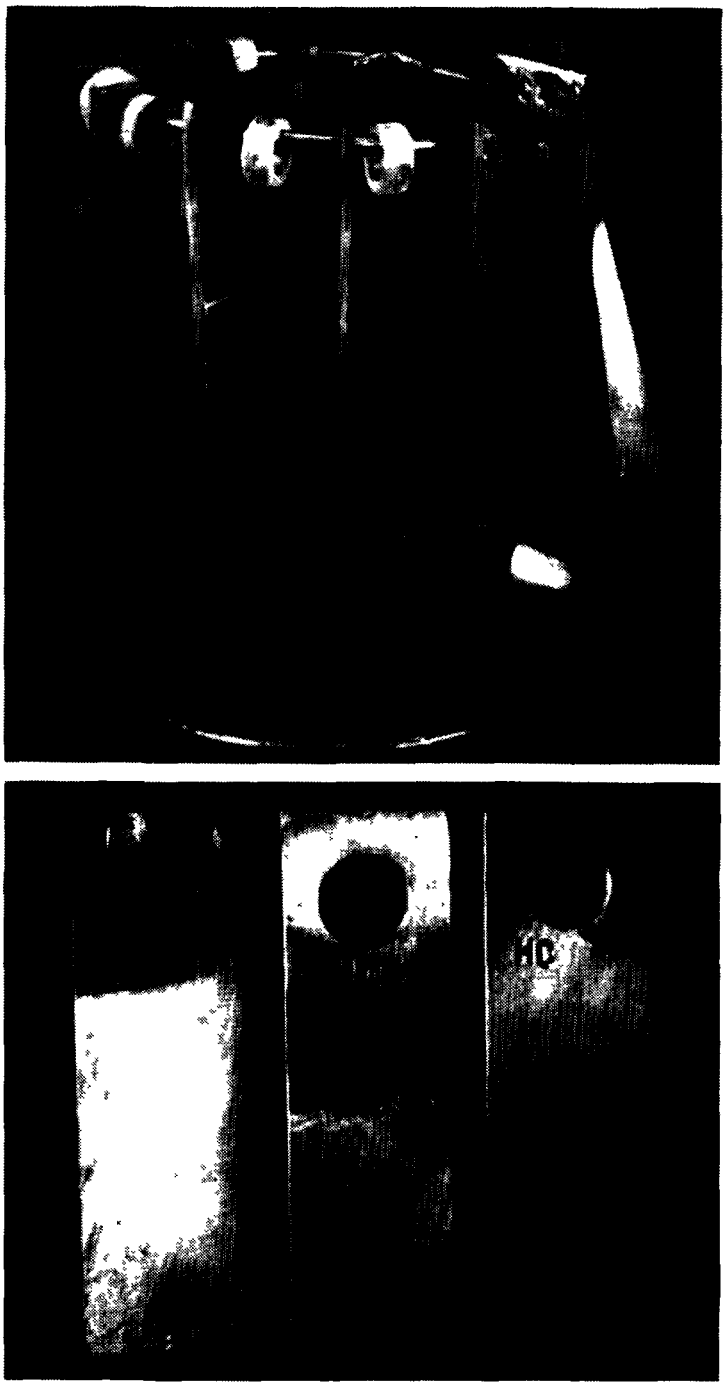

Samples including built up welds, type Hastelloy C 4 in the quinary solution / 365 days / 200 °C

FIG. 14. Corrosion program.

Model container, removed from the quinary salt solutions after 289 days: encrusted with salt

FIG. 15. Corrosion program.

The dissolved Ni component of the alloy was determined in order to estimate the corrosion rate of the built-up weld. The result corresponds to corrosion rates of

$$1.9 \times 10^{-3} \text{ and } 1.7 \times 10^{-3} \text{ mm/a}$$

respectively.

When removed from the salt solution, the entire surface of the container was encrusted with salt which was easily removed with warm water. The ceramic coating had remained unchanged and showed no sign of gloss reduction.

Model container
in the quinary solution
747 days / 100 °C

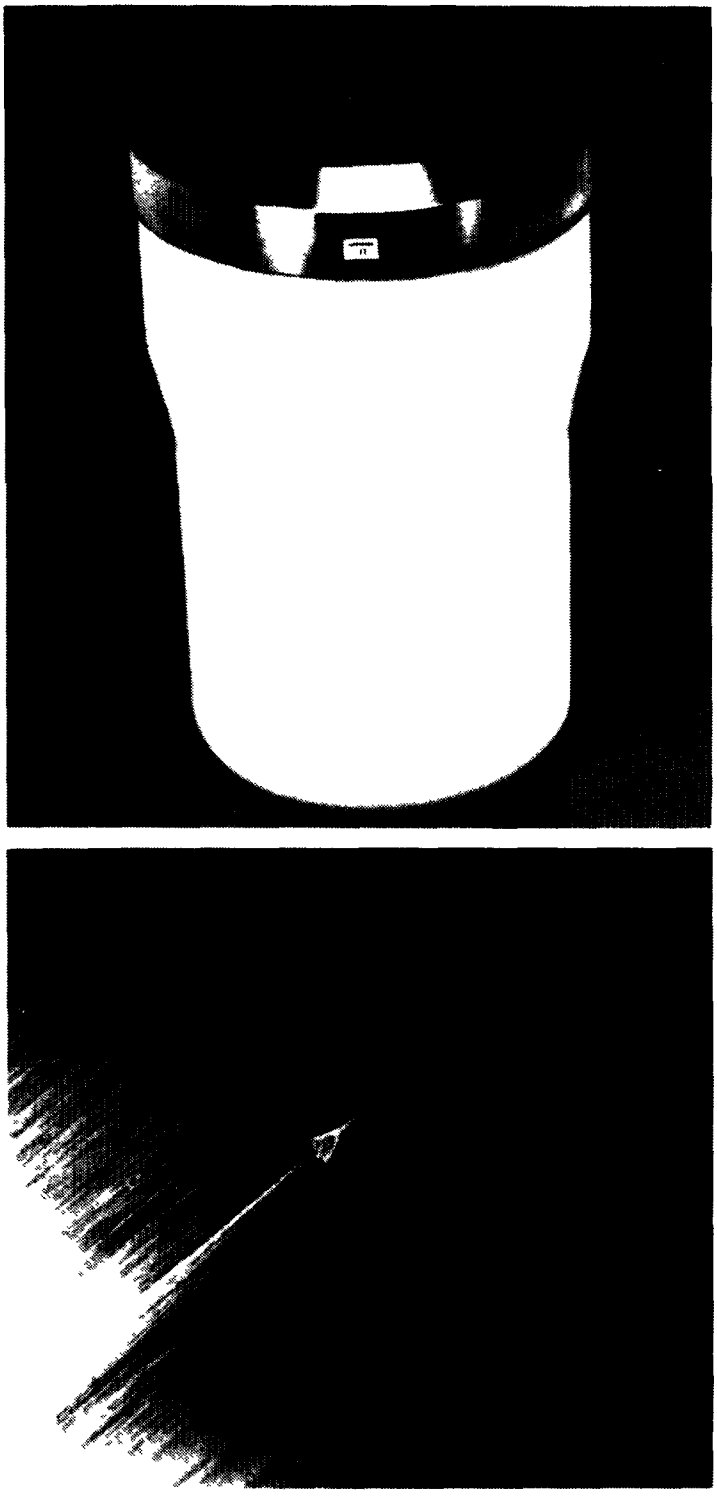

FIG. 16. Corrosion program.

The metal of the machined built-up weld (top section of the container) was bright after cleaning. The jacket surface revealed local accumulations of small scale residues in surface areas which had not been removed by metal-cutting operations.

Such areas were also found on the end surface, but to a far lesser degree. Isolated marks, usually of triangular shape and only slight depth, were also found on the end surface; these were caused by machining. A re-ground area of 2 to 3 mm in diameter was also found, surrounded by a darker halo and being the result of sparking between the earth electrode and the built-up weld when welding out the centre bore.

The model container was again exposed into 100° C quinary brine, with an exposure time of 747 days until now.
The corrosion rates found for Hastelloy are:

$$2 \times 10^{-3} \text{ to } 3 \times 10^{-3} \text{ mm/a (fig. 16)}$$

It is intended to continue the corrosion test in 100° C quinary brine with the container.

Future corrosion test programme

Corrosion tests so far were performed mainly with pure metals or alloys. Systematic investigation on special material combinations are still missing. Therefore a corrosion test programme is being prepared at KfK in order to study the corrosion behaviour of the material combination which is typical for the POLLUX cask under conditions representative for a salt mine repository. Therefore these aspects will be of special interest in this programme.

The tests will be performed within three brines at 150° C

- $NaCl-KCl-MgCl_2-MgSO_4-H_2O$ (Q-point)
- $MgCl_2-CaCl_2-H_2O$ (NaCl-KCl)
- $NaCl-CaSO_4-H_2O$ ($KCl-MgCl_2$)

The samples will be worked out of original surface welded layer of Hastelloy C4. For crevice corrosion tests they will be built up sandwichlike between a layer of the material from the shielding overpack (mainly Fe) will be added to the brine in order to investigate the combined effect of the different materials selected in the POLLUX cask system.

First results of this corrosion programme are expected spring 1987.

HLLW STORAGE TANK MATERIALS: TECHNICAL OPTIONS AND OPERATING EXPERIENCE

J. BACHELAY*, J. DECOURS**, R. DEMAY[+], M. PELRAS[+], L. ROZAND[++], G. TURLUER[+]

* Société générale pour les techniques nouvelles, Saint-Quentin en Yvelines

** CEA, Institut de recherche technologique et de développement industriel, Saclay

[+] CEA, Institut de recherche technologique et de développement industriel, Fontenay-aux-Roses

[++] Cogéma, Saint-Quentin en Yvelines

France

Abstract

Storage tanks for concentrated fission product solutions are made of Z 2 CND 17-12 (AISI 316 L) stainless steel. The solution temperature is cooled below 60°C and permanent stirring of the medium keeps the insolubles in suspension preventing the formation of wall deposits.

This stainless steel was selected after a number of corrosion tests conducted "in situ" in the tanks of nuclear facilities and in radioactive fission product solutions prepared in the laboratory. All these tests demonstrated a superior localized corrosion resistance under radioactive deposits for AISI 316 L steel, when compared to AISI 304 L steel.

Laboratory tests were also performed up to 100°C in fission product solutions containing ferric ions (up to 20 $g.l^{-1}$). Under these conditions, more severe than nominal operating conditions, 316 L steel exhibits some risks of intergranular attack.

The operating conditions adopted, and the experience gained in France over the past 30 years, clearly vindicate the choice of 316 L steel.

---

1. INTRODUCTION

After reactor use, fuel elements are treated in nitric medium in order to chemically separate U and Pu on the one hand and fission products on the other. Upon completion of the cycle, the fission products are found grouped in a low acidity aqueous solution. Fission product solutions are then concentrated and stored in stainless steel tanks, pending treatment in vitrification units prior to disposal.

In order to limit corrosion phenomena in the storage tanks, the following precautions are taken :

- each tank has two independent cooling systems
- an efficient stirring system maintains the insolubles in suspension
- quality of the stainless steel used is chiefly defined according to its best possible general and localized corrosion resistance so as to guarantee a maximum lifetime of the installation.

The last point has resulted in various tests being performed in order to assess corrosion hazards and to choose those grades of stainless steel which present the highest degree of safety for the construction of fission product solution storage tanks.

2. "IN SITU" CORROSION TESTS IN A STORAGE TANK

2.1. Experimental conditions

Stainless steel test specimens were immersed for 10 years in a fission product storage tank in the Marcoule reprocessing plant.

Grades studied were in the form of welded, 10 to 12 mm thick plates the composition of which is given in Table I.

TABLE I - Steel chemical composition in wt%

Steel Grades	C	Cr	Ni	Mo	Cu
URANUS 50 T (Z2 CNDU 17-13)	0 018	16 8	13 0	2 55	1 60
ICN 164 BC (Z2 CND 17-12)	0 030	17 4	18 1	2 20	—
ICN 472 BC (Z2 CN 18-10)	0 027	18 4	11 4	0 18	—

Each grade was given 4 test specimens, measuring 50 x 10 x 10 mm for URANUS 50 T and ICN 472 BC, and 50 x 10 x 12 mm for ICN 164.

After degreasing and pickling, the specimens were fastened to a support and immersed in a tank containing a fission product solution with the following properties :

- volume 57 m^3
- temperature < 50°C (average 35°C)
- composition :

HNO_3	Na	Mg	Al	Fe	Cr
1.4N	31g.l^{-1}	39g.l^{-1}	98g.l^{-1}	17g.l^{-1}	2.7g.l^{-1}

Ni	Mo	Pu	FP(γ)
2g.l^{-1}	1.4g.l^{-1}	1.4mg.l^{-1}	15Ci/l

2.2. Results

After test periods of 4 and 10 years, the specimens were analyzed and measured and results obtained are given in Table II.

TABLE II - Long-term corrosion testing

Steel Grades		Weight loss in mg / dm ^{2}	
		After 4 years	After 10 years
URANUS 50T STEEL	Average	45 0	74 2
	Standard deviation	1 3	0 9
ICN 164BC STEEL	Average	29 7	50 0
	Standard deviation	1 2	0 8
ICN 472BC STEEL	Average	28 3	51 8
	Standard deviation	1 2	1 8

Weight loss corresponds to extremely low corrosion rates and to metal removal lower than 1 micrometer after 10 years.

The general appearance of the test specimens after completion of tests is showned in Fig. 1. Surface texture appeared sound, both on the base metal and on the weld seam, and no pitting or localized attacks were observed.

Micrographic inspections were made and revealed no special corrosion on any of the 3 grades experimented, nor was there any notable difference when compared to the surface state of the original specimens.

2.3. Conclusion

After a residence time of 10 years in a fission product solution, the different stainless steel grades experimented revealed a highly satisfactory behaviour. It should be noted, however, that during these tests the specimens were in contact with solid particles maintained in suspension by permanent stirring but were not representative of the walls of certain sections of the tank where deposits could form and develop hot spots.

Supplementary laboratory tests enabled the action of these deposits to be studied, as well as the influence of temperature.

3. LABORATORY TESTS - INFLUENCE OF DEPOSITS

3.1. Experimental conditions

3.1.1. Definition of media

Both active and inactive tests, were performed.

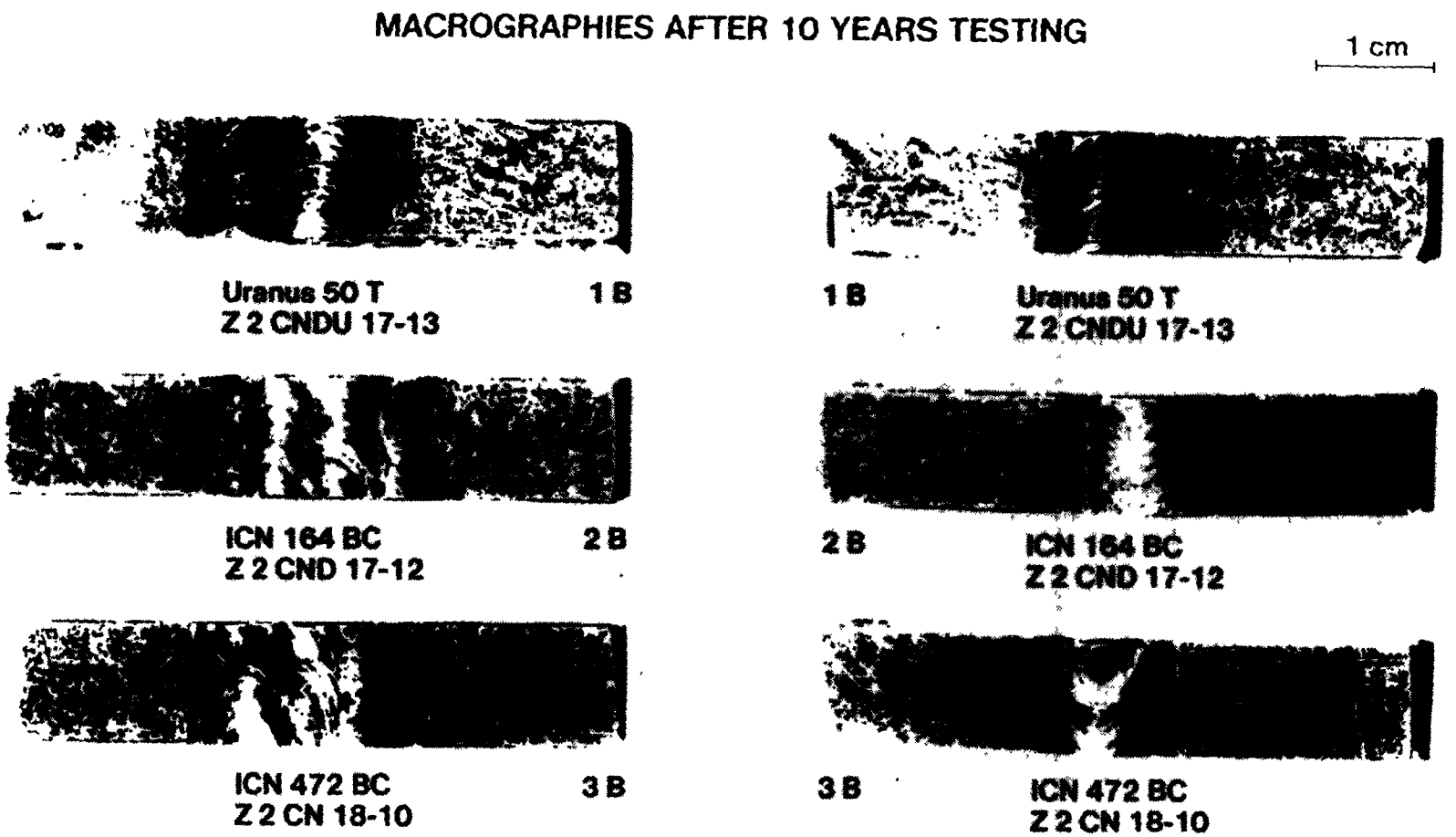

Figure 1 : Welded stainless steel samples

TABLE III - Concentrate overall composition (solution + precipitate)

HNO_3 1 N	PO_4H_3 5 05 g l^{-1}	
Zr 6 5 g l^{-1}	Mo 6 15 g l^{-1}	Cs 4 85 g l^{-1}
Ce 5 15 g l^{-1}	Sr 1 60 g l^{-1}	Cl 1 mg l^{-1}
Cr 1 0 g l^{-1}	Fe 3 00 g l^{-1}	I 0 6 mg l^{-1}
		Br 3 0 mg l^{-1}

An inactive medium was prepared from a synthetic extraction raffinate solution which was concentrated with formaldehyde up to 560 l.t^{-1}. Table III shows the total concentrate solution composition (solution + precipitate) at this stage.

The active medium was prepared with extraction raffinates obtained from the treatment of EL_3 reactor elements, irradiated at 30,000 MWD.T^{-1} concentrated at 560 l.t^{-1}. In principle, this solution has the same composition as that above after having been adjusted with Zr, Fe, Cr, Cl, Br, I and P to the inactive medium concentration. This solution had a radioactivity of 1,500 Ci/l.

Fractions of 200 ml of inactive and active media were homogenized and distributed among containers made of very low carbon content Z 2 CN 18-10 and Z 2 CND 17-12 stainless steels, whose compositions are given in Table IV. The solutions were evaporated by dry air sparging for periods of 5 and 7 days in order to obtain concentration ratios of 350 l.t^{-1} and 150 l.t^{-1} respectively. The composition of these experimental media follows from that of the solution at 560 l.t^{-1}.

However, for the active tests, nitric acid concentration decreased from 1.0 to 0.8 N at 350 l.t^{-1} and from 1.0 to 0.6 N at 150 l.t^{-1}.

3.1.2. Temperature - Duration

Storage tests continued for 3 months at 70°C. Evaporation time (5 to 7 days) was insignificant with respect to the total time taken by the test.

3.1.3. Definition of specimens

Specimens were actually the 300 ml cylindrical containers themselves (diameter 65 mm, height 100 mm), built from 1 mm thick sheets, in a quench annealed state as delivered (Fig. 2). The formed shell and dished bottom were weld assembled (TIG welding) and degreasing was followed by pickling in hydrochloric acid solution.

In all, 8 containers were tested. Their distribution and composition, expressed in percentages, are given in Table IV.

Two additional containers (one for each grade), constructed as above, were used as references in order to compare the state of the metal before and after corrosion tests.

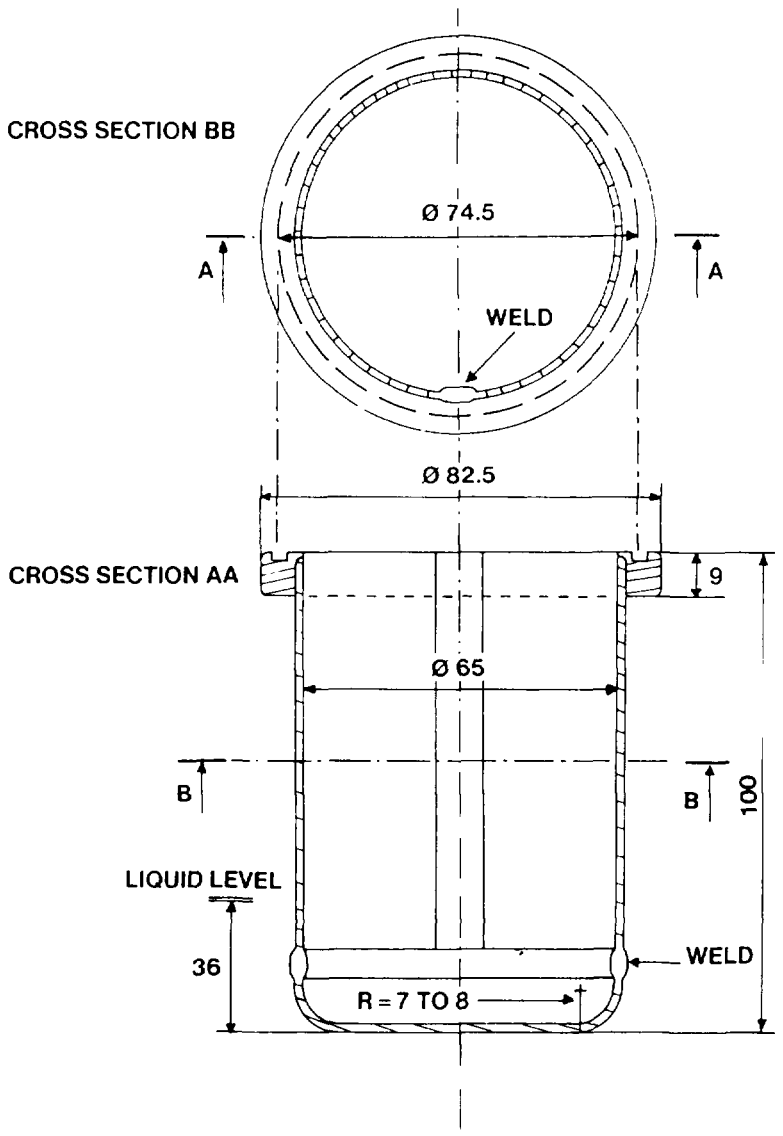

Figure 2 : Test container drawings

TABLE IV - Experimental conditions and steel chemical composition in wt%

	MEDIA			
	Active		Inactive	
Concentration ratio in $l.t^{-1}$	150	350	150	350
Z2 CN 18.10 (304L) Steel C Cr Ni 0.026 18.9 10.3	X	X	X	X
Z2 CND 17.12 (316L) Steel C Cr Ni Mo 0.021 17.3 11.7 2.2	X	X	X	X

3.2. Results

After completion of the tests, the solutions were drained and a large quantity of deposits were observed on the shell of the containers tested in active medium. These deposits had a whitish, greenish appearance for concentration ratios of 150 $l.t^{-1}$ and a brownish aspect for 350 $l.t^{-1}$.

On the other hand, no deposits were found on container walls in inactive media.

Figure 3 illustrates this pronounced difference between inactive and active tests.

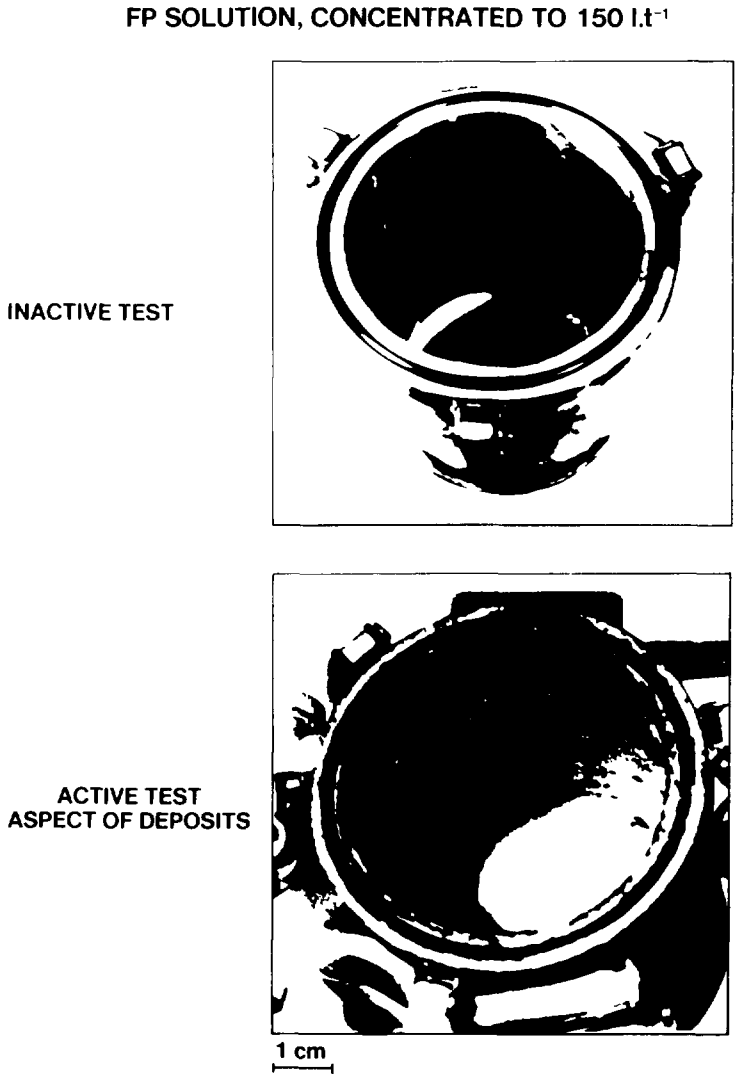

Figure 3 : Inside view of Z2 CN 18-10 stainless steel containers after 3 month testing

After removal of the deposits, it was noted that the surface of Z 2 CN 18-10 (304 L) steel was more scored than that of Z 2 CND 17-12 (316 L). Moreover, corrosion increased with the concentration of the fission product solution. Corrosion areas were also observed on the walls above liquid level.

3.2.1. Micrographic inspection

The containers were cut up as shown in Figure 4.

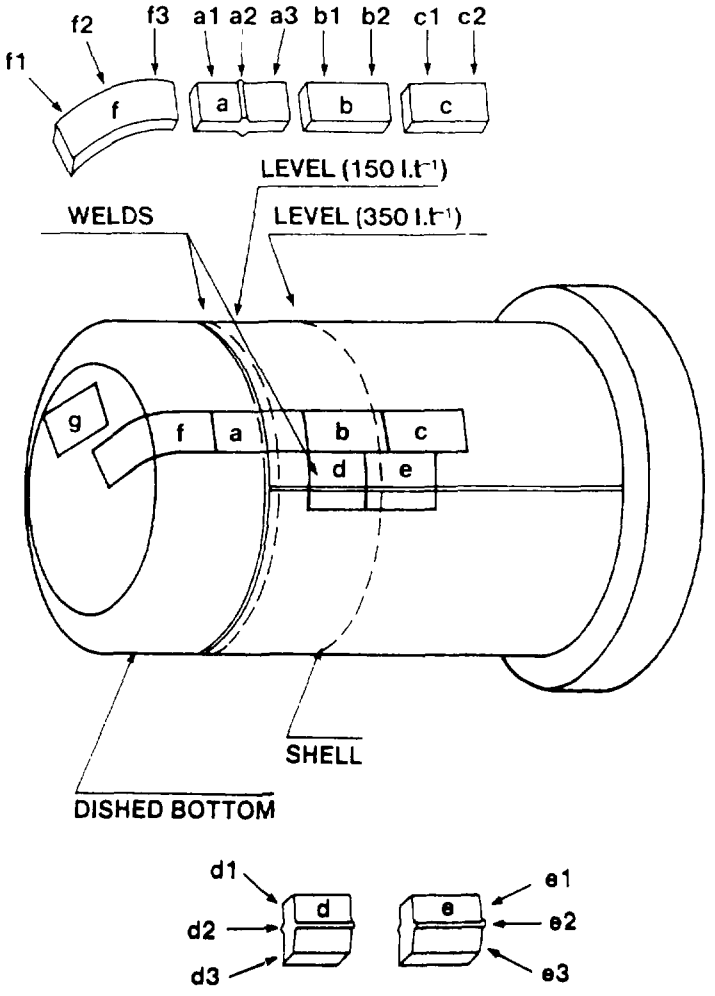

Figure 4 : Container sampling scheme for post-testing examination

. Active medium containers

Tests made in solutions concentrated at 150 $l.t^{-1}$ resulted in higher corrosion than in solutions concentrated at 350 $l.t^{-1}$, as illustrated in Figures 5 and 6. There is, furthermore, a more pronounced difference in the behaviour of the two grades tested.

Z 2 CN 18-10 steel shows under-deposit corrosion with a maximum depth of 100 to 130 µm in the most highly concentrated solutions and from 40 to 50 µm in the less concentrated ones. For Z 2 CND 17-12, some localized corrosions with depths of 40 µm were observed only in the most concentrated solutions.

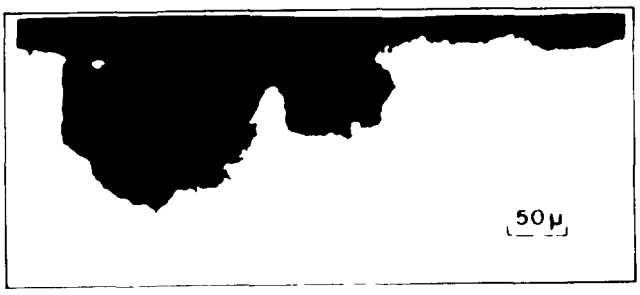

Z 2 CN 18-10 steel (304 L)

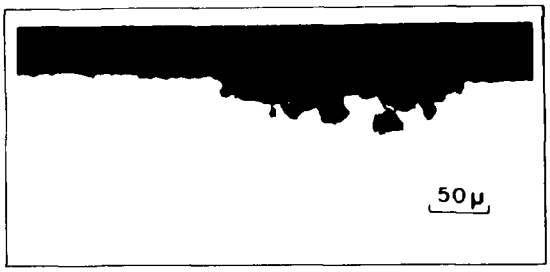

Z 2 CND 17-12 steel (316 L)

Figure 5 : Micrographies of localized attacks observed in FP solution concentrated to 150 $l.t^{-1}$

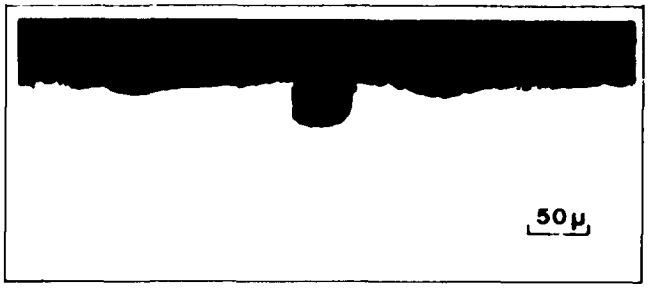

Z 2 CN 18-10 steel (304 L)

Z 2 CND 17-12 steel (316 L)

Figure 6 : Micrographies of localized attacks observed in FP solution concentrated to 350 $l.t^{-1}$

. Inactive medium containers

Inspection of the different containers revealed no specific corrosion, whatever the steel grades and solution concentrations.

Finally, inspection of the weld assembly and the heat affected zone revealed no defects or evidence of corrosion more pronounced than those observed on the base metal.

3.3. Conclusion

Research on the storage of fission products from spent fuel leads to the following conclusions :

. a corrosion hazard exists in active solutions,

. this hazard increases with the fission product concentration.

Z 2 CND 17-12 is more corrosion resistant than Z 2 CN 18-10. It should be observed that the two first points are closely related, activity being proportional to concentrations.

Damage observed is due to corrosion, which is usually most severe on the walls above liquid level. Formed deposits, which are adhesive and unevenly distributed over certain areas, cause heterogeneity that could result in preferential corrosion. It could also be assumed that under certain deposits, elements such as halogens concentrate in the medium and may cause pitting. This action may be enhanced by the depletion of nitric acid which is destroyed by intense radiation (5,600 Ci/l at 150 $l.t^{-1}$). For those wall deposits situated above liquid level, this destruction could be total. The better behaviour of molybdenum-content steel would seem to favour this interpretation.

Finally, intense activity under the deposits should prevent the formation of chromium VI, which confirms the absence of intergranular corrosion.

In summary, these tests have demonstrated that the risk of localized corrosion under deposits exists in fission product storage tanks. Safety in this area is increased by the use of very low carbon stainless steel grades containing molybdenum.

Moreover, the influence of deposits is minimized by permanent stirring of the solution in order to keep the insolubles in suspension and to prevent the formation of wall deposits.

4. LABORATORY TESTS - INFLUENCE OF TEMPERATURE

4.1. Experimental conditions

4.1.1. Definition of test specimens

The specimens were in the form of a cylindrical container, identical to those of the preceding test, 1 mm thick, 65 mm diameter and 100 mm high.
The dished bottom and the shell were weld assembled (TIG welding) as shown in Figure 2. They were degreased and pickled prior to tests.

The nominal steel composition was :

Z 2 CND 17-12 C ≤ 0.03% - Cr 17% - Ni 12% - Mo 2 to 2.5% (316 L)

4.1.2. Medium

The solution was prepared from Borssele fuel elements, irradiated at 32,500 MWD.t^{-1}. After separating by extraction and concentrating to 300 l.t^{-1}, this solution (described in Table V) was distributed by fractions of 120 ml between 2 containers which were tested under the following conditions :

	HNO_3	Fe
Test at 100°C	2N	2. 4 g.l^{-1}
Test at 60°C	2N	16 g.l^{-1}

TABLE V - Composition of fission product concentrate used for corrosion testing

H^+	2N
U	20 g.l^{-1}
Pu	200 mg.l^{-1}
Mo	2 - 4 g.l^{-1}
Zr	2 - 8g.l^{-1}
Fe	2.4 g.l^{-1} (100°C testing)
	16 g.l^{-1} (60°C testing)
βγ activity	≈ 800 Ci.l^{-1}
iodine	not detectable
bromine	not detectable

4.1.3. Test procedure

The containers were sealed by a lid fitted with a cooler and were heated in an isothermal bath.

Medium renewal : nil

$$\text{Ratio} \quad \frac{\text{metal surface}}{\text{solution volume}} = 7.5 \text{ dm}^2.\text{l}^{-1}$$

Test period = 1 year.

4.2. Results

At the end of the experiment, the containers were drained and inspected in a shielded cell.

Following a visual inspection, the containers were cut in the areas which appeared defective and were presented for a more precise metallographic examination, as the in-cell macrographic examination only showed an overall aspect of the surface state, certain minor defects or pits being mistaken for deposits or vice versa.

Deposits were observed on the walls and at the bottom of the container. Samples were taken from the characteristic areas, metallographic examination of the cross-sections prompting the following comments :

4.2.1. Test at 100 °C

The container presented intergranular corrosion in the form of surface indentations on the walls and heavier corrosion in sensitized areas adjoining the weld seams and under certain deposits (Figure 7).

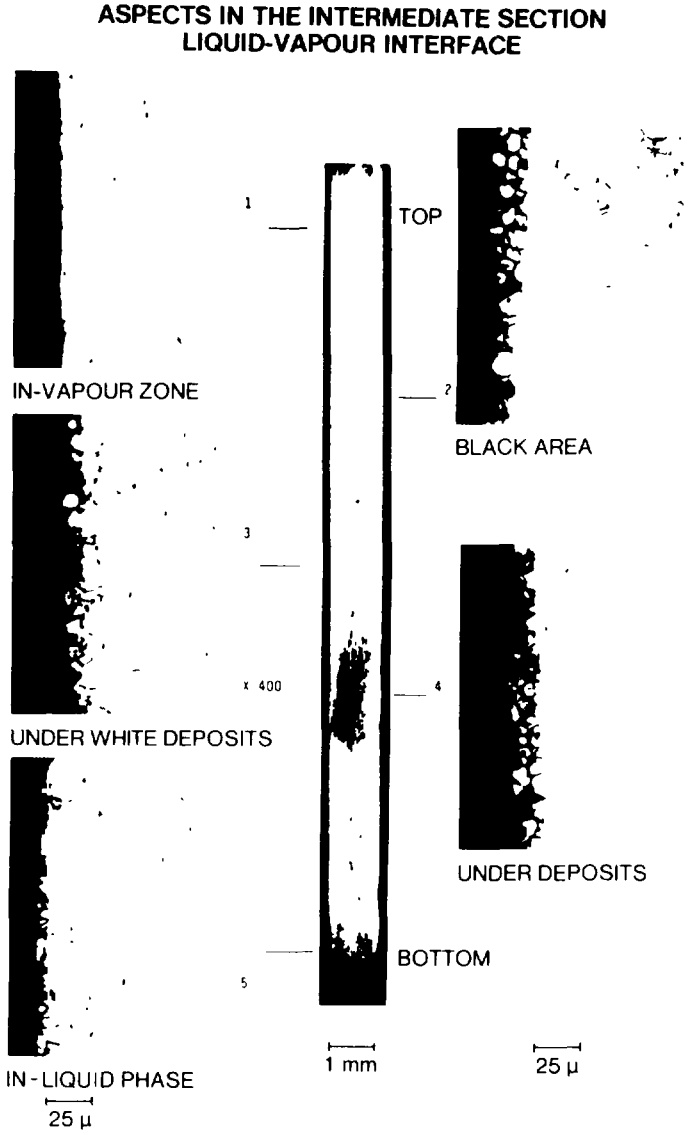

Figure 7 : Z 2 CN 17-12 steel at 100°C

4.2.2. Test at 60 °C

No intergranular corrosion, or localized or pitting corrosion were seen on the walls and bottom of the container in contact with the fission product solution. Above the liquid level, however, surface exposed irregularities with a depth of approximately < 10 µm were observed which could be ascribed to original flaws rather than to localized corrosion.

The different areas inspected are shown in Figure 8.

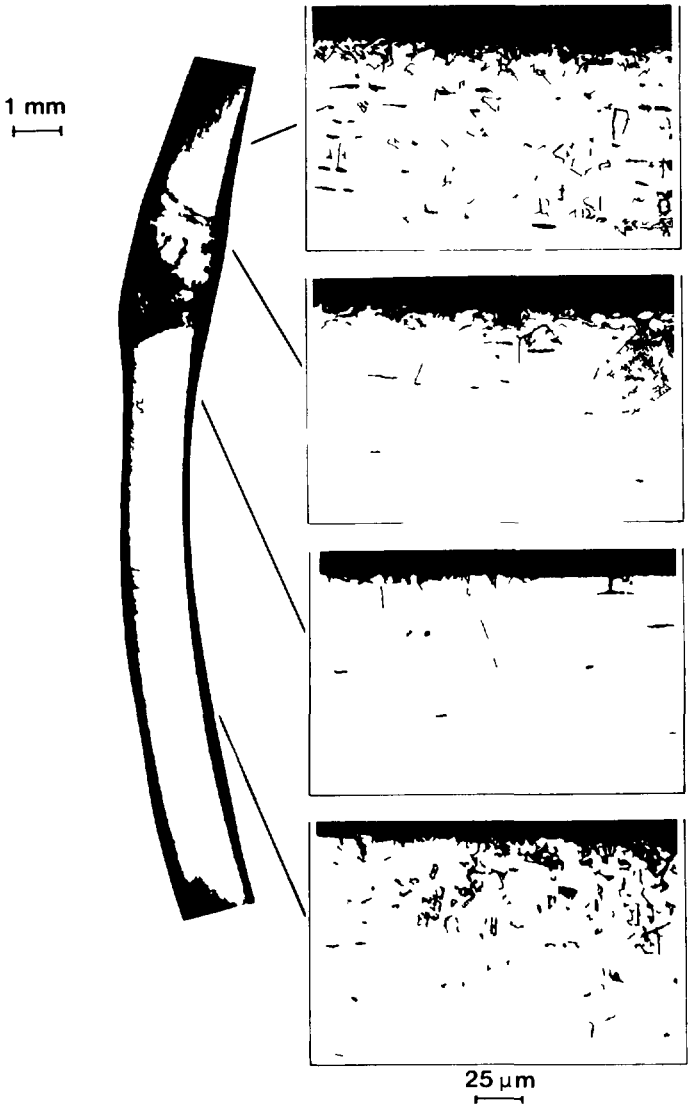

Figure 8 : Z 2 CN 17-12 steel at 60°C

4.3. Discussion and Conclusion

The various laboratory testings have demonstrated a satisfactory behaviour of stainless steel grade Z 2 CND 17-12 in fission product solutions at 60°C. This was easily confirmed as, after 12 months testing, no pitting or intergranular corrosion was observed.

Tests at 100°C were conducted to simulate the influence of hot spots formed by deposits on the walls. For grade Z 2 CND 17-12 these tests were too pessimistic as the medium was not renewed throughout the entire duration of the tests. It was therefore enriched by corrosion products such as iron and chromium, which stimulate stainless steel corrosion. This experimental process explains the intergranular corrosion observed at 100°C, as the influence of corrosion products is known to be higher at 100°C than at 60°C.

Reference tests performed in inactive solution with the same surface/volume ratio of 7.5 $dm^2.l^{-1}$ on grade Z 2 CND 17-12 test specimens yielded the results shown in Table VI. Intergranular corrosion is observed at 100°C.

TABLE VI - Corrosion rate in mdd influence of temperature and of ferric ion

	EXPERIMENTAL CONDITIONS 6 months testing, unrenewed media Surface to volume ratio = 7 5 dm^2 l ^{1}	
	2 5N HNO_3 - 60°C 15 g l ^{1} Fe	2 5N HNO_3 100°C 0 g l ^{1} Fe
Instantaneous corrosion rate in mdd		
2 nd month	<1	2
6 th month	<1	60

To conclude, for grade Z 2 CND 17-12 no pitting or intergranular corrosion hazard is to be feared at the mean temperature of 60°C prescribed for fission product storage, and under conditions used for the above tests. Intergranular corrosion hazard exists if there are hot spots, at 100°C for example, but this hazard is slight; in fact the corrosion would only affect a restricted area, freeing a limited amount of corrosive products which would progressively diluted in the high volume of the tank. Despite the barrier formed by deposits, these should not be sufficiently impermeable to prevent exchange between the confined volume and the fission product solution. Moreover, due to stirring the location of hot spots is liable to change, which means that a same area is not permanently endangered. Finally, it should be pointed out that the test containers used at 100°C are only an imperfect replica of the real tanks and most certainly give pessimistic results.

The choice of grade Z 2 CND 17-12 , from among the range of stainless steels available would therefore appear to be the best compromise for fission product storage installations.

5. INDUSTRIAL EXPERIENCE :

The above mentioned material testing and selection have been confirmed by the very reliable operating experience now accumulating 310 tank.years* with 25 tanks in service. The oldest of these tanks has been used for over 28 years.

---

* Concerning merely storage tanks, not to mention transfer tanks.

GLASS MELTER MATERIALS: TECHNICAL OPTIONS FOR THE FRENCH VITRIFICATION PROCESS AND OPERATING EXPERIENCE

R. BONNIAUD*, R. DEMAY**, R. RICHTER[+], L. ROZAND[++],

* CEA, Institut de recherche technologique et de développement industriel, Marcoule

** CEA, Institut de recherche technologique et de développement industriel, Fontenay-aux-Roses

[+] Société générale pour les techniques nouvelles, Saint-Quentin en Yvelines

[++] Cogéma, Saint-Quentin en Yvelines

France

Abstract

The French vitrification process for solidifying high-level radioactive waste which has been under industrial application since 1978, is mentioned briefly. This technique involves glass melting at 1,150°C, using an induction heated metallic vessel.

The molten glass pouring is controlled by a thermal gate, which is also heated by induction.

Two types of vessel are in use. Both are remotely removable and disposable to permit replacement at regular intervals. The technical criteria that the materials have to meet are described.

The behaviour of the materials has been investigated using the industrial experience gained in the AVM facility during 8 years of operation, as well as with operation of a prototype for the new vitrification facilities under construction at La Hague.

A short description of the use of these materials is also presented.

INTRODUCTION

Three industrial installations for the vitrification of fission product concentrates are operating or being built in France. They include the AVM installation for Cogema at Marcoule, in operation since 1978, and two additional facilities also for Cogema at La Hague : R7 associated

with the UP2 800 reprocessing plant, currently being tested, and T7 associated with UP3, now under construction. An other one is under construction for BNFL at Sellafield (U.K.).

These installations implement a CEA continuous vitrification process which combines calcining with a glass melting furnace. Inactive prototypes for R & D are operating in the CEA laboratories at Marcoule.

1. PROCESS PRINCIPLE

This principle is shown on Figure 1. The solution to be vitrified is a mixture of fission product concentrates, alkaline effluents and dissolution fines. It is continuously fed at the inlet of a rotary calciner together with calcination additives to obtain a calcinate with a structure and a particle size distribution which facilitate its incorporation into the glass. The electrically-heated calciner is made of URANUS 65 and is tilted at 3%. In this equipement solution evaporation and calcining of most of the metallic salts take place. The calcinate thus produced is mixed at the bottom of the calciner with glass frit introduced to yield the required vitrification forming elements. The mixture then flows by gravity into the glass melting furnace.

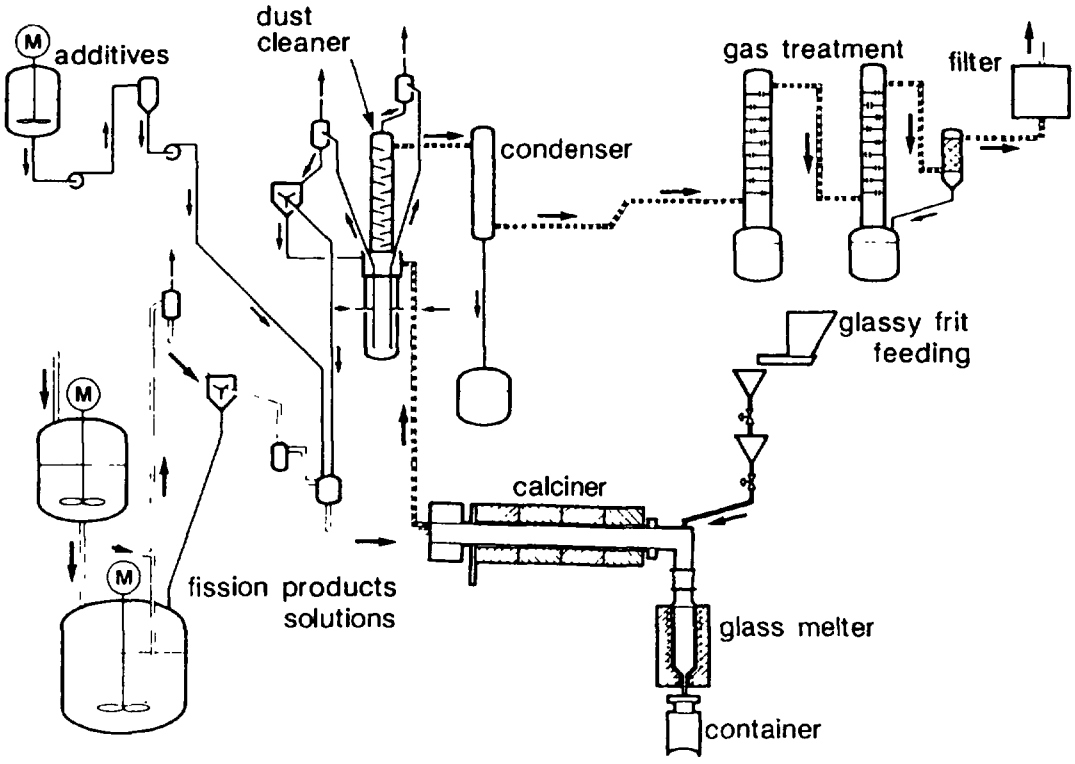

Figure 1 Flow sheet of vitrification process

The furnace is constituted by a metal reactor heated by medium-frequency induction (10,000 Hz or 4,000 Hz). Even heat distribution is ensured by the superposition of several inductors working independently. Temperatures are set at each inductor to a value determined according to the glass level.

The melter is fitted with draining nozzles, which are also induction heated. The nozzles act as thermal gates.

The glass level in the reactor varies progressively during feeding. Glass is poured into a preheated cylindrical canister as soon as the load is sufficient, generally every 8 hours. Several pourings can be made in the same canister.

An off-gas treatment system condenses steam produced, recombines nitrous fumes, recovers volatile chemical substances which are recycled to the calciner, and purifies non condensable gases before release.

There are two types of metallic melters :

. the AVM facility uses a cylindrical reactor (Fig. 2) with a diameter of 350 mm, constituted by a 1,030 mm high cylindrical shell ending in a 300 mm cone fitted with a pouring nozzle. It weighs approximately 120 kg .

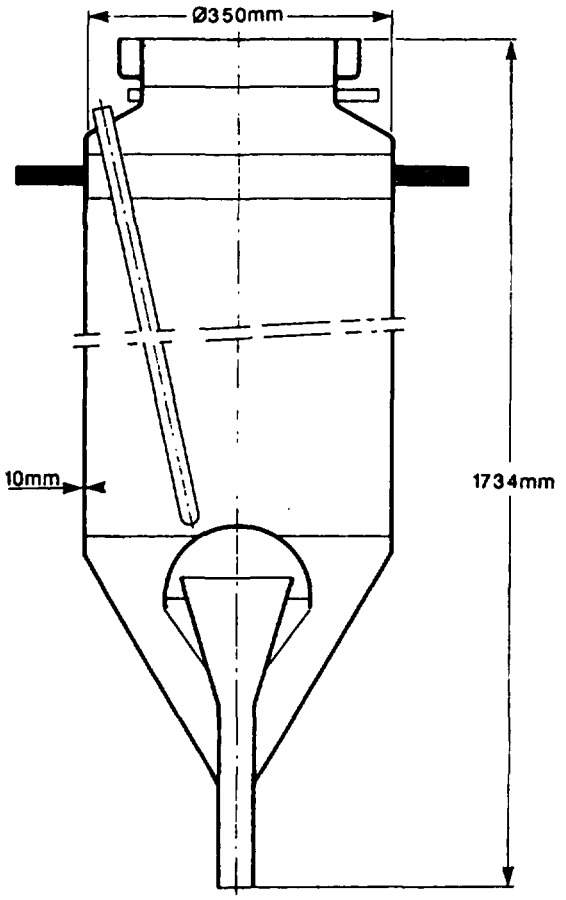

Figure 2 Cylindrical metallic melter

. the R7 and T7 facilities use an ovoidal reactor with a height of 950 mm and a width of 1,000 mm over its largest axis and 350 mm over the smallest. It is equipped with two pouring nozzles, one for partial, and one for total drainage. It weighs approximately 300 kg (Fig. 3).

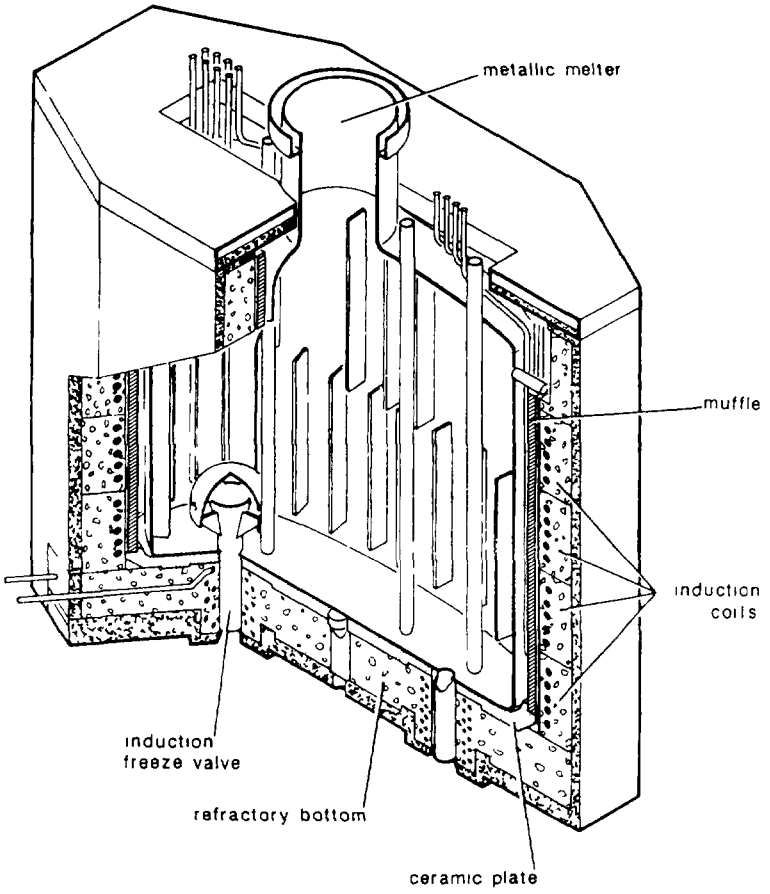

Figure 3 Ovoïd melter and induction furnace

The thickness of the melter walls is now 10 mm for both types. They are fitted with internal vertical fins for improving heat diffusion.

Glass is prepared at temperatures ranging between 1,120°C and 1,150°C. In view of the high thermal stress involved, melters are disposable components and have therefore been designed for remote replacement.

The maximum glass load for the AVM cylindrical melter is approximately 150 kg , that of the ovoidal melter is 250 kg to 300 kg.

The cylindrical melter is suspended with free expansion at the bottom. The ovoidal melter has a flat bottom resting on a ceramic slab and freely expands upwards by means of bellows attached to the tube connecting the calciner to the furnace.

2. STRESSES RECEIVED BY THE REACTORS

The constituent material of these melters is subject to several significant stresses.

2.1. Thermal stress

The metal reactors operate at high temperatures, which are in fact not far from the acceptable limit for rolled alloys. Furthermore, induction heating is not perfectly uniform, especially for ovoidal melters with different bending radii. Design philosophy, together with insertion of a protective insulating muffle made of alumino-silicate fibers between the inductor and the melter, have however contributed to homogenizing the temperature and mitigating this disadvantage.

As induction heating is rapid, furnace temperature control is achieved by means of moderate and carefully controlled voltage steps in order to avoid any local metal overheating.

2.2. Mechanical stress

All the mechanical stresses gradually result in creep and localized distortion at hot areas. They are caused by the following factors :

- melter weight (300 kg for the ovoidal model)
- glass load (300 kg at the highest level)
- stress caused by reaction and gas release
- stress caused by negative pressure maintened at 150 mm WG in the reactor.

2.3. Corrosion

Corrosion can be considered at different levels :

2.3.1. At glass contact

Molten glass dissolves the protective oxide layer, causing chromium release into the bath and possibly penetration of the glass components into the grain boundaries. The corrosive nature of the glass depends on its composition, and especially on the nature and content of the glass array modifiers. However, the molten glass bath exerts a protection of the metal with regard to the direct oxidation by the atmosphere.

2.3.2. Glass-atmosphere interface

The combined action of melting glass and ambient oxygen may lead to localized corrosion (flux line) especially severe for certain glass (heavy Na_2O, Li_2O, P_2O_5 concentrations). In the process used, the constantly fluctuating glass level considerably reduces this risk.

2.3.3. Above the glass bath

Corrosion is due to off-gas entraining volatile glass components at high temperatures. This specially applies to borosilicate glass. Upwards

of 1,050°C, alkaline borates become extremely volatile and could be redeposited on the upper part of the furnace held at medium temperature. These extremely aggressive salts dissolve the chromium oxide surface layer and could result in substantial localized corrosion under unfavorable thermal and aerodynamic conditions. Moreover, the metal above the bath is subject to corrosion by the released fumes, actually nitrous fumes possibly containing traces of F^-, P_2O_5 and SO_4^{--}.

During normal operation, the volatility of glass components is however limited by the layer of calcinate and glass frit above the melting bath, which considerably reduces the evaporation surface.

3. ALLOYS USED

Alloys chosen for melters must therefore provide a suitable trade-off with respect to the following criteria:

- oxidation resistance with respect to the atmosphere,
- hot mechanical strength,
- resistance to corrosion by liquid glass or its volatile components
- good weldability.

The main alloys under consideration are listed in Table I.

Table I Alloys tested for melters

		Ni	Cr	Fe	Co	Mn	Si	Cu	Mo	Al	Ti	C	W
	Inconel 600	72	14-17	6-10		1	0 5	0 5				0 15	
Rolled	Inconel 601	60 5	23	14 1		0 5	0 25	0 25		1 35		0 05	
	Nimonic 81	63	30	1	2	0 5	0 5	0 2	0 3	0 9	1 8	0 05	
alloys	Coronel 230	60	35-37	< 5		< 1	< 0 6	< 1		< 0 5	< 1	< 0 08	
	Inconel 690	60	30	9 5						0 25	0 25		
Cast	Manaurite 50 w	50	28	14		< 1 5	1 5					0 4	5
alloys	More 2	50	33									0 15	15

They are all chromium nickel base alloys. Most are rolled with the exception of the last two, which are tungsten enriched cast alloys with excellent heat proof properties. Coronel 230 has also been used in cast alloys.

From a hot mechanical strength aspect, these alloys all present practically the same hot creep characteristics.

Deformation of the melter after 1,000 hours of prototype testing have been observed in the most exposed areas on those rolled alloys for which a 0.1% creep deformation is reached after 1,000 hours for a stress close to 2×10^4 Pa (2 newton/ mm^2).

These deformations appear in the form of a swelling of the cylindrical shell below the maximum glass level and, for the ovoidal shell, by a swelling of the large radius lateral faces. This swelling can be accompanied by a concave deformation of the melter below the glass level.

For melters made of cast, tungsten-containing alloys which have a higher hot creep resistance, these deformations are relatively slight.

Taking into account the glass load and the internal negative pressure, the maximum stress at 1,150°C is estimated at 0.25 newton/mm^2 for the cylindrical melters and 1 newton/mm^2 for the side elements of the ovoidal melters. This last value corresponds to a theoretical creep of 0.01% in 1,000 h.

Figure 4 plots iso-deformation curves established after a 1,500 hour operating period with an ovoidal melter. This was used on an inactive prototype under conditions more stringent than those of normal continuous industrial operation since testing was not fully continuous but rather performed in cycles of one week, an operating rate which leads to additional fatigue.

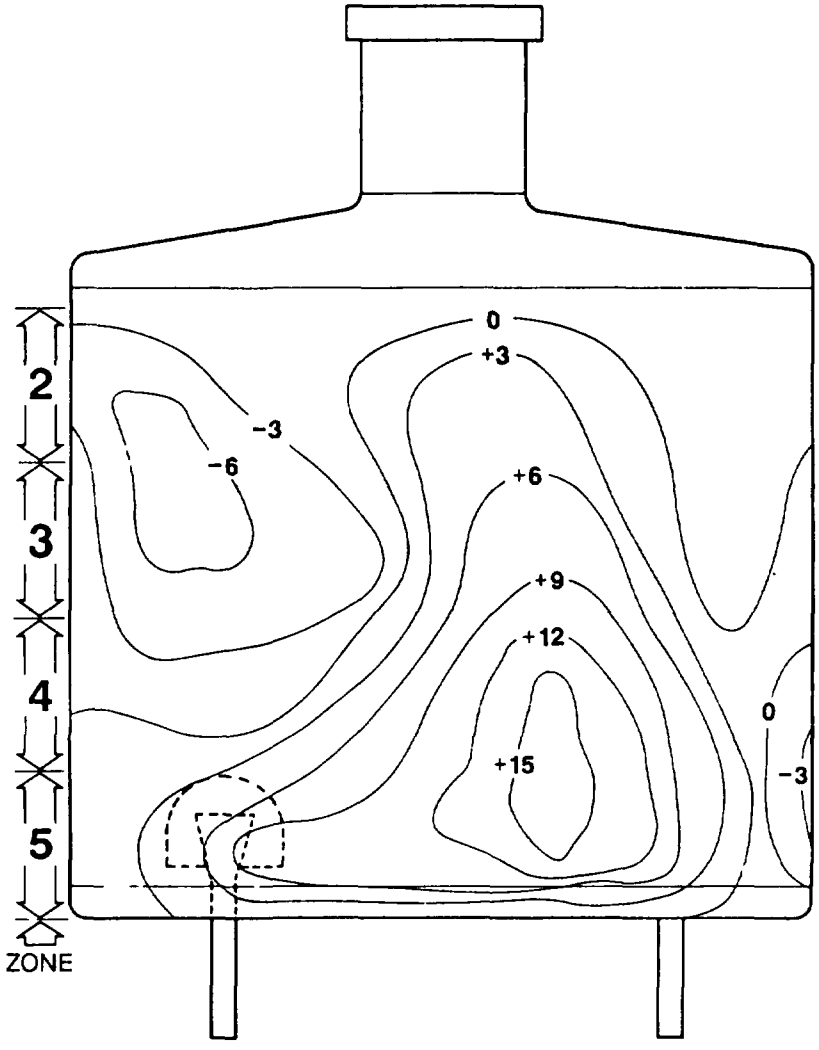

Figure 4 Deformation of ovoïd melter; operating time 1,500 hours

As far as corrosion is concerned, behaviour obviously depends on the glass composition used. The following general observations are proposed:

- corrosion at glass contact is generally much lower than that on the metallic section above the bath ;

- behaviour, with respect to weight loss, thickness reduction or the depth and evenness of intergranular corrosion improves with the chromium content of the material. This observation not only applies to behaviour at glass contact, but also and especially at interface level and above the glass ;

- material of the type Coronel 230, Inconel 690 and 601 have a more consistent behaviour ;

- glass containing a substantial proportion of P_2O_5 (greater than 5%) causes more intensive corrosion at interface and above the bath and, under these conditions, high chromium content alloys such as Coronel 230 or Nimonic 81 have the highest resistance. It can be assumed that Inconel 690, which was not tested with this type of glass, could also be favourably placed.

For cast alloys, the best results from a corrosion aspect were obtained by Manaurite 50 w, but its metallurgical state does not enable definite conclusions to be drawn.

Generally speaking, when examined by micrography, these alloys placed at glass contact typically display 3 different layers : the outer most chromium oxide layer contains some metallic particles, followed by an intermediate layer showing internal oxidation precipitates of chromium oxides (aluminum or titanium oxides when those elements are present) ; below a chromium depleted zone is observed for depths of several hundred microns. As an example, for the glass used for vitrifying light water reactor concentrates in the R7 and T7 facilities, metallographic examination revealed, for Inconel 601, a surface 40 to 80 µm chromium oxide layer, a 60 µm internal corrosion layer reaching 80 µm above the bath and a chromium depleted area of 200 µm ; in the case of Inconel 690, these values were 60 µm for the chromium oxide layer, 40 µm for the internal corrosion and a chromium depleted area of also approximately 200 µm.

From prototype results, it was seen that the life of the metallic melters was basically determined by the hot mechanical strength of the equipment. Corrosion, especially that observed in areas unwetted by the glass, is secondary. Increase of melter mechanical deformation in the course of operation can be indirectly assessed by the evolution of the electric phase shift values for the inductor circuits as a function of time.

The lifetime of a melter, determined by prototype experiments, is roughly 2,000 hours. After rinsing with inactive glass, its replacement is remotely performed, following established procedures.

4. USE OF MATERIALS

Materials were implemented following different methods :

• Construction of the cylindrical or ovoidal shell and the end cones using rolled steel sheets, stamping of bottoms and domes and assembling by TIG welding. The internal fins are placed in the shell prior to welding of the end fittings.

• Electron beam welding of a machined metallic assembly including the internal fins : bending the side elements of the ovoidal pot, electron beam welding on the fillets, followed by TIG welding of the stamped bottoms and domes as above (Figure 5).

This process, still under development, has been used for the construction of one ovoidal melter prototype, in order to strengthen the rigidity by incorporating the vertical fins in the structure. Moreover,an additional transverse reinforcement of the side elements in the deformation areas consolidates the assembly and decreases its deformation.

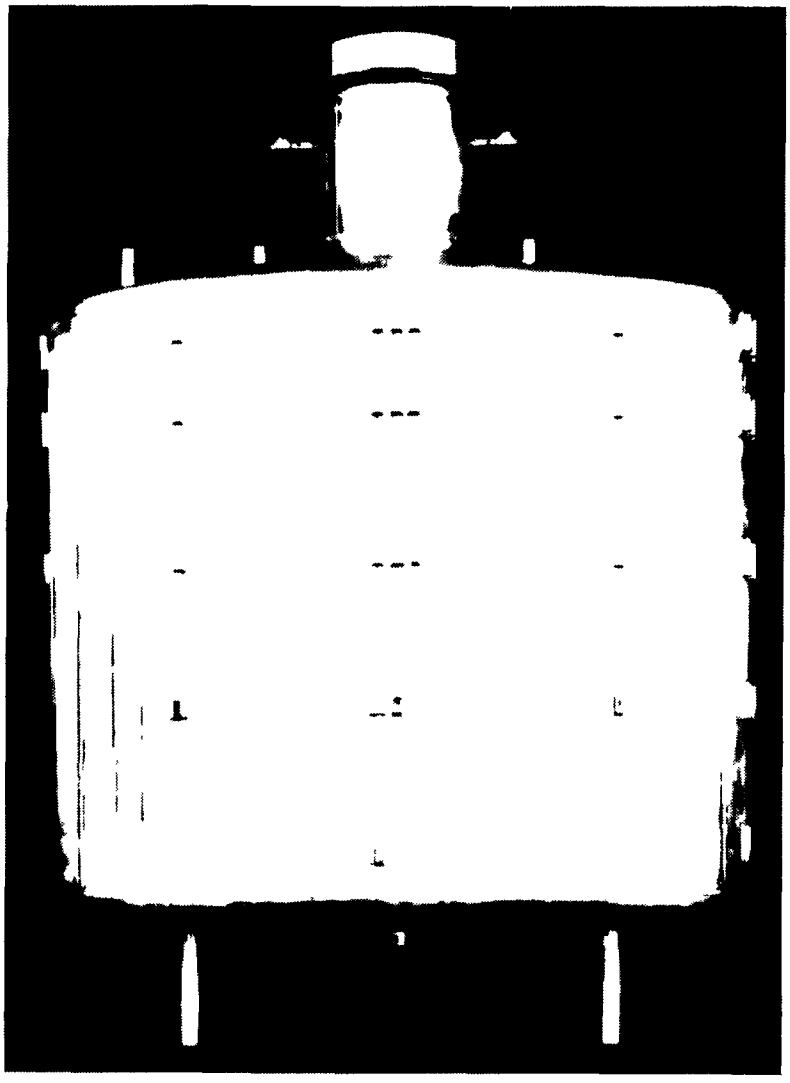

Figure 5 Ovoïd melter welded by electron beam.

• Casting which is reserved for the cylindrical melter. The shell is centrifuged and joined to the cast cone section and the machined dome by conventional TIG welding. This method can be used for alloys such as Coronel 230.

5. INDUSTRIAL EXPERIENCE

Inconel 601 was chosen for the melters of the present industrial installations, because of its satisfactory overall properties relative to heat and corrosion resistance, its acceptable price,and its workability.

The Cogema AVM vitrification facility, constructed by SGN at Marcoule, was commissioned in June 1978. It has since vitrified 1,100 m^3 of fission product concentrates, measured at the calciner feed point, in 37,000 hours of operation. A total of 1,412 canisters have been filled, representing 4,230 pourings and 490 tons of glass (cumulated figures up to July 1986). During this time, 13 cylindrical melters have been used.

Table II gives the service life of these melters.

Table II COGEMA vitrification facility (AVM); service lifetime of the melters.

Reactor	Wall thickness (mm)	Lifetime (hour)	Comments
1	6.35	2,150	
2	6.35	880	Local overheating
3	6 35	1,590	Local overheating
4	6 35	1,235	
5	6 35	1,714	
6	6 35	2,213	
7	6 35	1,908	
8	6 35	2,085	
9	8	5,024	
10	10	6,545	
11	8	2,700	Local overheating
12	6 35	2,537	
13	10	5,151	

Not counting the 3 melters prematurely withdrawn due to local overheating resulting in glass leakage, the average lifetime is established at 1,980 hours for 6.35 mm thick pots and 5,500 hours for the currently used pots, which are much thicker.

CONCLUSION

The metallic melters used in the French process for fission product concentrate vitrification are made of Ni-Cr alloys with a high chromium content. In particular, Inconel 601 is being used for the reactors of the Marcoule vitrification facility. These highly stressed components are considered as disposable equipment requiring remote replacement.

Their service life is basically determined by the hot mechanical strength of the alloys used. Under continuous operating conditions, industrial experience has proven a melter is able to function for several thousand hours before being replaced.

SELECTION OF SUITABLE STAINLESS STEELS FOR NUCLEAR REPROCESSING PLANTS: APPLICATION OF CHEMICAL AND ELECTROCHEMICAL TESTING METHODS TO AUSTENITIC CrNi STEEL AISI TYPE 304L IN VARIOUS CHEMICAL COMPOSITIONS

S. LEISTIKOW, R. KRAFT
Institut für Material- und Festkörperforschung II,
Kernforschungszentrum Karlsruhe GmbH,
Karlsruhe

R. SIMON
Lehrstuhl für Metallurgie und Metallkunde,
Technische Universität München,
Munich

M. SCHNEIDER
Siemens AG,
Erlangen

Federal Republic of Germany

Abstract

DIN Standard Huey testing has been performed in boiling 14.4n nitric acid during 5-15 periods (240-720 h) for selection of appropriate nitric acid resistant materials for nuclear fuel reprocessing applications.

The paper describes the testing process during which the intermediate and final results of metal loss by dissolution are directly transfered from the balance to the computer, stored and activated - besides material properties data - for documentation purposes. Further routine evaluation of these experiments includes metallography in cross-section and surface microscopy to look after uniformand localmetal dissolution phenomena and their relationship to the bulk structure. A large variety of materials have been tested this way through the last years. It was shown how sensitively the chosen testing conditions are able to differ between materials of the same nominal composition AISI 304L/Material No. 1.4306 in different contents of residual elements. Especially, for the purest electroslag-molten steel (ESU) results of parameter studies concerning the influence of sensitization, cold deformation, grain size and sheet thickness (in respect to end grain attack) are given.

Within an attempt to define faster methods of corrosion testing, e.g. to differ within a group of materials of similar composition, but different corrosion behaviour, electrochemical tests in heated nitric acid were performed under potentiostatic conditions. The necessary electrochemical equipment and the results of its application by potentiostatic tests on AISI 304L in above mentioned three chemical compositions at 1250 mV, 14n HNO_3 are presented. The evaluation by light and electron microscopy of the corroded surfaces, supported by measurements of current density, weight change, metallography and surface roughness, proved that

within one hour a remarkable differentiation of the corrosion behaviour took place which can serve as a basis of materials preselection and to diminish the extent of expensive Standard Huey testing.

---

1. Introduction

Since long time the unstabilized austenitic CrNi Steel AISI Type 304L, corresponding to the German Material No. 1.4306, is generally applied as vessel, container and tubing material in reprocessing plants of nuclear fuel. However, corrosion problems have been reported of those parts of the plant which are exposed to an environment of concentrated acid, fuel and fission product solutions at high temperature (dissolver, evaporator etc.). The insufficient corrosion resistance could be explained as caused by the alloy composition, especially in respect to the content of minor elements, and inhomogeneous distribution of those elements as consequence of production and processing.

The German chemical industry in parallel uses this material for production, application and storage of nitric acid. It has initiated the development of improved versions of the above mentioned steel by propositions for optimizing the chemical composition, full use of the secondary metallurgy, and improved heat treatment as part of the processing. The result of successful development was a fully austenitic and homogeneous product, rich in Cr and Ni, and very poor in corrosion active elements as C, P, S, Si, Mo and suitable for application in nitric acid of lower and medium concentration up to the respective boiling point. The CrNi steel is being sold under the designation material No. 1.4306s, in which s stands for Salpetersäure = nitric acid grade. The abbreviation ESU is added when in addition, the electroslag remelting process is applied for further improvement of purity and especially homogenity of this steel in respect to macrosegregations. Tab. 1 shows the steps of development of the AISI Type 304L (Material No. 1.4306) for application in nitric acid.

Tab 1 Results of AISI Type 304 L (Material No 14306) Development Chemical Analyses of Normal and Special Qualities

Material No.	Chem. Analyses (Weight%)							
	C	Si	Mn	P	S	Cr	Mo	Ni
1.4306 n	0.020 - 0.025	0.29 - 0.63	1.38 - 1.6	0.024 - 0.033	0.003 - 0.017	17.9 - 18.8	0.17 - 0.37	10.2 - 11.4
1.4306 s	0.006 - 0.017	0.02 - 0.20	0.72 - 1.8	0.008 - 0.022	0.002 - 0.010	18.5 - 19.7	0.006- 0.05	10.9 - 12.5
1.4306 s ESU	0.007 - 0.019	0.01 - 0.02	1.59 - 1.7	0.017 - 0.022	0.002 - 0.005	19.1 - 20.2	0.05 - 0.09	12.3 12.6

This modern melting process allows the production of CrNi steels (equally on the basis of 17/14/4 CrNiSi and 25/20 CrNi) which practically undergo only uniform metal loss and no localized corrosion in nitric acid of various concentrations.

This paper deals with the response of those CrNi steels in the above mentioned range of composition (normal, nitric acid and improved nitric acid electroslag remelted quality) to chemical (Huey) and electrochemical testing - whether the applied methods are able to differentiate between the materials behaviour within the given range of quality and a limited duration of testing.

2. Experimental Procedure

2.1 Material Composition, Specimen Shape and Pretreatment

The various CrNi steels were delivered in solution annealed plates of 2-12 mm thickness. The chemical compositions are given in Tab. 2. While chemical testing of all four steels has been done, electrochemical testing was performed only in case of steel No. 1, 3 and 4. Sheet specimens (30 x 30 mm) and cylindrical specimens (20 Ø x 5 mm) were cut of these plates and tested in the as-received, solution (re-) annealed and specially heat treated conditions. Cold deformation was performed by rolling to 10-80% cold work.

Table 2 Chemical Composition of Various Sheet Materials No 14306

Material No	Producer	Melt No	Thickness mm	Chem. Analyses [Weight %] C	Si	Mn	P	S	Cr	Mo	Ni
1.4306n	Thyssen	681870	5	0.024	0.60	1.44	0.025	0.003	18.00	0.17	10 23
1.4306n	Krupp	537095	6	0.026	0.65	1.72	0.017	0.010	17.90	0.21	10.15
1.4306s	Krupp	293783	12	0.017	0.03	1.58	0.019	0.007	19.10	0.02	12.50
1.4306s ESU	Krupp	010457	2 10	0.007	0.020	1.59	0.022	0.005	19.13	0.08	12.40

2.2 Corrosion Testing by Chemical Methods

In principle, corrosion testing was performed according to the DIN Standard Huey Test [1] in boiling aceotropic nitric acid. Instead of surface grinding or pickling as pretreatment, the specimens were usually electropolished in a mixture of sulfuric and phosphoric acid. Thus, the surfaces became smooth and shiny, etching did not take place under the chosen electropolishing conditions. Instead of prescribed 5 x 48 h testing (48 h = 1 period) and extended exposure of in total 15 x 48 h - interrupted after each period by weight measurements and refreshing of the acid - was performed. While exposed to the boiling acid, the specimens were suspended on glass hooks. The surface volume ratio was 1 cm^2 metal surface area to 20 ml HNO_3. The metal loss was measured by weighing and calculated to give the results in terms of uniform surface area or thickness related rate of metal loss. The sequence of testing in respect to the evaluation by gravimetry and data processing directly from the balance is given in Fig. 1.

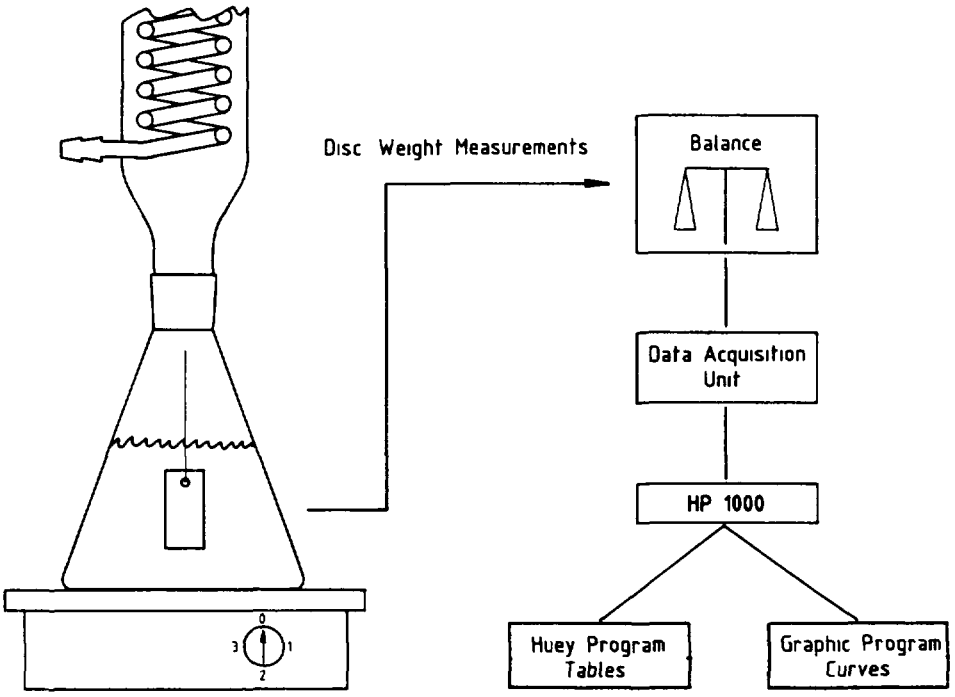

Fig. 1: Process of Huey Testing: Generation, Evaluation and Presentation of Experimental Results.

2.3 Corrosion Testing by Electrochemical Methods

To perform the electrochemical corrosion tests in nitric acid a special electrochemical cell (Fig. 2) was built up and applied, which had the following characteristics:

- a thermostat for heating the acid containing flask (directly by heater or indirectly by heat exchange with oil), the reference electrode and the conductive connection to the Haber-Luggin capillary,
- an acid resistant specimen holder.

Otherwise the usually applied electrochemical devices (as potentiostat etc.) were used. The free corrosion potentials of the materials were measured as function of time and environment, specially under Huey test conditions. Redox-potential measurements were performed in 1-14 n nitric acid and nitric acid solutions containing 50-1000 mg/l Cr (VI) ions. Mainly potentiostatic measurements were performed at the critical potential of +1250 mV at which a massive destruction of the surface grain structure took place within a short time of exposure.

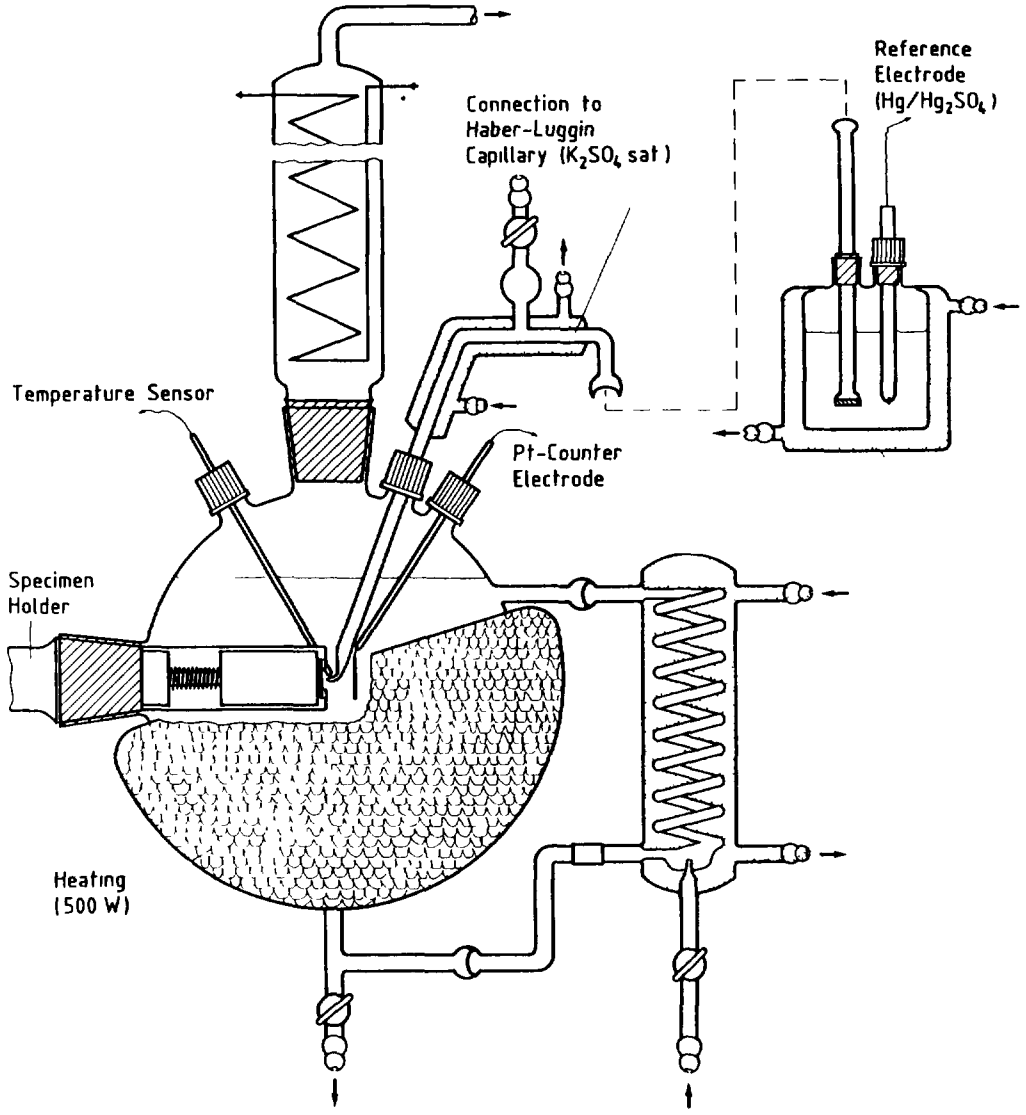

Fig. 2: Electrochemical Cell with Specimen Holder for Corrosion Tests in Nitric Acid.

3. Experimental Results

3.1 Corrosion in Nitric Acid by Extended Huey Testing

Extended Huey testing resulted in rate of metal loss/time functions (Fig. 3) which show that the normal quality material can be of very different long-time corrosion resistance. While during the beginning exposure a rather similar weight loss was found, the rate through long times can increase drastically.

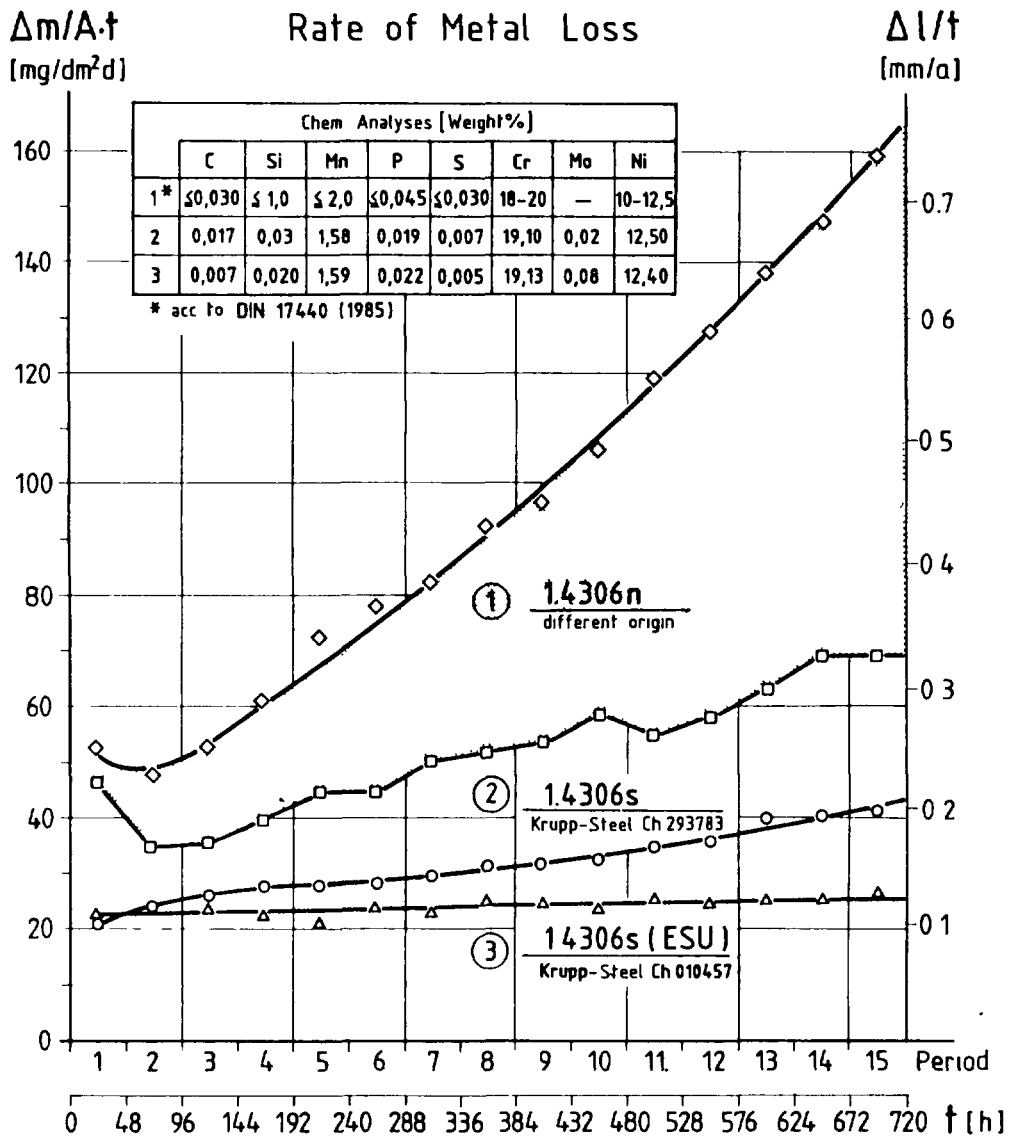

Fig. 3: Huey-Testing of Various AISI Type 304L (Material No.1.4306) Sheet Materials in the Solution-Annealed Condition. 65% HNO_3, 120°C, 720 h

The reason can be explained as follows: Material which corrods quickly because of its relative low purity in minor elements undergoes a more or less pronounced grain-boundary selective attack. The deeper the grain boundary areas of the metal surface are dissolved the more difficult becomes the cleaning process at test interruption. Corrosion products will concentrate on the bottom of each single gap and will start its own chemical activity as soon as rewetted by fresh acid. A solution of oxidizing ions and increasing potential penetrates into the rough metal surface speeds up the rate of attack and leads to untolerable losses of wall thickness.

In contrast, material of lower content in minor elements show a less pronounced tendency to grain boundary attack. Grain and grain boundary dissolution are observed in equal proportion, i.e. not in a selective manner.

In conclusion the results of extended Huey testing of various 1.4306 steels show roughly the following:

- for normal quality steels a wide range of corrosion behaviour is noticeable, during the 15. period ending with corrosion rates of more than 0.3-0.7 mm/a,
- for the special nitric acid quality steel a considerably lower rate of metal loss takes place, ending at about 0.2 mm/a,
- for the special electroslag remelted nitric acid quality steel a metal loss of only 0.1 mm/a was measured.

The Huey-test extended to 15 periods clearly is able to distinguish between the various qualities of the most commonly used material in the nuclear reprocessing industry.

Based on these findings, the best quality Material No. 1.4306s ESU was tested in respect to the influence of special material related parameters on the nitric acid corrosion behaviour:

- sensitization and grain size, adjusted by various heat treatments,
- cold deformation, adjusted by cold rolling to 10-80%,
- sensitivity to end grain corrosion attack, checked by testing of sheet material in two different thicknesses (2 and 10 mm).

The results are given in Fig. 4. The only remarkable effect was shown by numerous 1 h heat treatments between 650 and 750°C. The maximum rate of metal loss was measured for 700°C: an increase from 0.124 up to 0.180 mm/a. Since these sensitizing time-at-temperature conditions (in respect to welding) seem to be highly exaggerated, one has to keep in mind the highly pessimistic kind of procedure and thus the unimportance of the effect. The other sensitizing and grain size increasing heat treatments, the cold deformation, and end grain attack - related exposures (except those being sensitized at 700°C) did not show any effect on the rate of metal loss. The corrosion rate during the 15. period did not show an increase beyond the level established by testing of the solution annealed material, that is 0.100-0.125 mm/a, during the same time. A more detailed description of the experimental results is given in [2,3].

3.2 Electrochemical Testing in Nitric Acid by Application of Potentiostatic Methods

The evaluation of the free potential measurements as function of time of the various steels No. 1.4306 under nitric acid and Huey test conditions showed that the upper limit of measured free potentials is about +1200 mV (nhe). The time in which the potentials

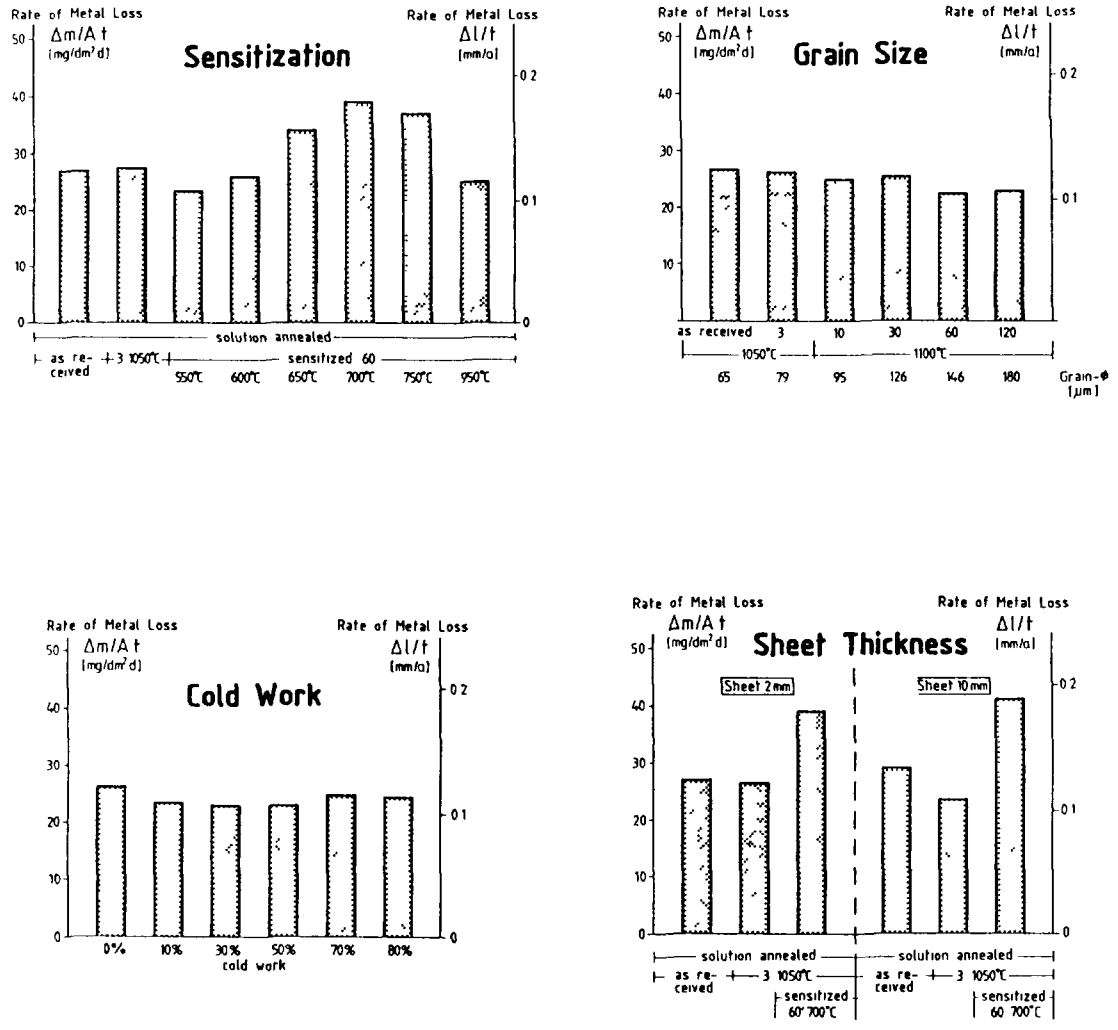

Fig. 4: Huey-Testing of AISI Type 304L (Material No. 1.4306s ESU) Sheet Material in Electroslag Remelted Quality. Parameters: Sensitization, Grain Size, Cold Work, Sheet Thickness; 65% HNO_3, 120°C, 720 h

remained at this level was decreasing with increasing content in minor elements. The evaluation of those curves lead to the conclusion that when a constant critical potential of +1250 mV (nhe), which in fact is a limiting condition in practice, is applied quick dissolution in 1-14 n nitric acid can be induced by potentiostatic polarization. When the above given potential was established a surface corrosion attack was observed which - in its rate and appearance - clearly depends on minor elements content and distribution, kind of heat treatment etc., thus enabling us to differ within a short time of testing between various steels of nominal equal material designation. Below +1250 mV (nhe) the attack losses its intensity and does not occur at $\leq$ +1150 mV (nhe), always resulting of a 1 h lasting exposure.

When all the solution annealed 1.4306 steels of category n,s and s ESU after a 1 h polarization at +1250 mV (nhe) in 14.4 n HNO_3, 120°C are compared by light microscopic evaluation (Fig. 5),

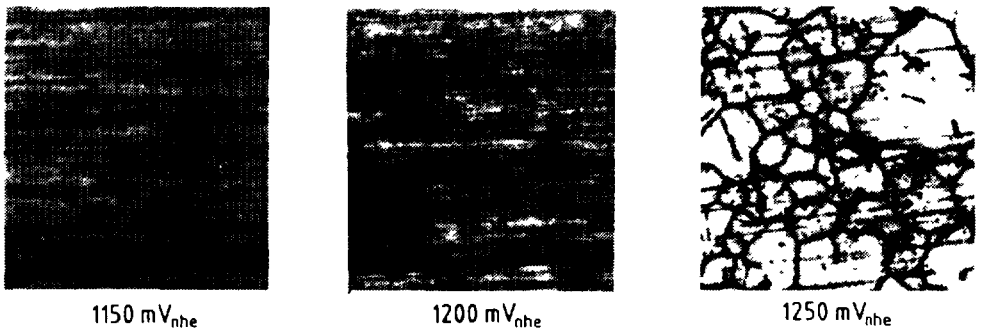

Fig. 5: Potentiostatic Experiments Using AISI Type 304L (Material No. 1.4306) of Various Chemical Compositions during 1 h at 1150-1250 mV. 65% HNO_3, 120°C

the influence of composition on the extent of surface dissolution becomes visible. The normal material shows grain boundary dissolution, while the attack on the special and especially on the remelted quality was either much weaker or only an indication that some kind of attack will happen after longer exposure. Thus the classification of metal dissolution could be done first of all by microscopy, but was supported by comparative measurements of current density, surface roughness, and metallography. So it becomes necessary to value in each case the need to gain results of long-time Huey testing of 240-720 h or even longer duration in contrast to those of short-time potentiostatic tests of about 1 h. A more detailed description of the experimental results is given in [4,5].

4. Conclusions

By application of chemical and electrochemical methods it was shown that quality control of materials nominally belonging to the same family of CrNi steel AISI Type 304L = Material No. 1.4306 and being applied to nitric acid service is a matter which can be done quantitatively by Standard Huey testing or at least qualitatively by means of electrochemical methods. But since the true conditions of material application in nitric acid rarely correspond to those of the Huey test it is more or less a test on CrNi steel purity and homogenity for preselection or quality control purposes. Under these aspects it seems us advisable to apply and further elaborate - in competition to the standard chemical procedures - the method of potentiostatic testing at critical potentials.

5. References

[1] DIN 50921 (1984)
EURONORM 121-72 (Dec. 1972), Stahl-Eisen-Prüfblatt 1870 (1979)
[2] KRAFT, R., LEISTIKOW, S., POTT, E., KfK-Report No. 3802 (1984)
[3] KRAFT, R., LEISTIKOW, S., POTT, E., KfK-Report No. 3878 (1985)
[4] SIMON, R., SCHNEIDER, M., LEISTIKOW, S., KfK-Nachrichten 18 2 (1986) 90
[5] SIMON, R., Dr.-Ing. Thesis Technische Universität München (1986) to be published

AUSTENITIC STAINLESS STEELS: ASSESSMENT OF PROGRESS IN MATERIALS PERFORMANCE FOR REPROCESSING APPLICATIONS

J. DECOURS*, J.-C. DECUGIS**, R. DEMAY***, M. PELRAS***, G. TURLUER***

* CEA, Institut de recherche technologique et de développement industriel, Saclay

** Société générale pour les techniques nouvelles, Saint-Quentin en Yvelines

*** CEA, Institut de recherche technologique et de développement industriel, Fontenay-aux-Roses

France

Abstract

Spent fuel reprocessing involves various operations in which nitric acid is used at relatively high concentrations and at temperatures up to the boiling point.

The choice of Z 2 CN 18-10 stainless steel (AISI 304 L) is a satisfactory solution to mitigate corrosion problems when using solutions with a maximum concentration of 8N, up to the boiling point. Above this concentration, since the corrosion rate is significantly higher, it is better to use Z 2 CN 25-20 stainless steel (Creusot-Loire's URANUS 65).

Despite these advantages, these stainless steels are not immune to intergranular corrosion, if the medium containing oxidizing species or ions (such as Cr VI, Pu VI or higher concentrations of Fe III) places the material in transpassive conditions. In this case it is recommended to use silicon-rich stainless steel (4% Si) Z 1 CNS 17-15 (Creusot-Loire's URANUS S1N).

Whatever the steel grade used, however, when cross-sections of plates pipes, or forgings are exposed to the corrosive medium, the development in the rolling direction of end-grain attack (tunnel corrosion) can hardly be prevented.

End-grain attack most usually spreads from non-metallic line inclusions caused by working, forging and rolling operations (sulphides being the most dangerous inclusions). This form of corrosion may also occur in oxidizing media, along zones segregated in chromium, molybdenum or silicon, and/or along second-phase alignments such as ferrite or σ phase.

A very-low carbon material with good inclusion cleanliness can be obtained by a specially designed argon vacuum process .

The proper control of the preparation and transformation processes yields, for this material, semi-finished products perfectly suitable for use in nitric acid media with respect to hazards in developing end-grain attack, regardless of the presence or absence of oxidizing species or ions.

---

1. SPECIFIC PROBLEMS OF REPROCESSING PLANTS

Spent fuel reprocessing operations implement different processes in which nitric acid is used at varying concentrations and at temperatures up to boiling point. After dissolution of the spent fuel, very fine insoluble products remain, mixed with nitric solutions of uranium, plutonium and fission products. All these elements are present throughout reprocessing, and are separated, concentrated, mixed with other reagents, stored, etc.

Construction materials used for reprocessing plant equipment and its connections must be chosen and used with precaution. Careful consideration must be given to :

- the nature of the medium encountered
- its concentration
- its temperature
- plant operating conditions
- its radioactivity

Corrosion resistance problems encountered in the use of stainless steel in spent fuel reprocessing plants may be more or less serious, depending on the metallurgical state of the steel and the redox properties of the acid solution.

1.1. Passive behaviour

Austenitic stainless steels, composed of iron, chromium, Nickel, owe their good corrosion resistance properties in most nitric acid solutions to the formation of a chromium rich passive oxide layer, in so far as the redox properties are adequate for the stability of Cr_2O_3 in the oxide layer. The passive conditions may no longer be met in the situations described below.

1.2. Active behaviour

Dissolution as Cr^{+++}, Fe^{++}, Ni^{++} may occur if medium conditions are made sufficiently reducing, entailing corrosion rates similar to pickling rates.

1.3. Transpassive attack

If the medium becomes excessively oxidizing so as to provoke Cr_2O_3 to dissolve into chromate, passive film dissolution results in a rapid accelerating "transpassive corrosion". This form of attack is all

the more severe as it is preferentially intergranular whether or not the steel grain boundaries are depleted in chromium i.e. sensitization as caused by intergranular carbide precipitation would not in those circumstances be the primary factor liable for intergranular attack.

For HNO_3 solutions, transition between relatively oxidizing conditions (passive region) and highly oxidizing conditions (transpassive) occurs at concentrations of 70 to 80% at ambient temperature ; the transition concentration decreases as the temperature rises.

Figure 1 illustrates the behaviour of Fe Cr 18, Ni 10 steels in acid media according to the electrochemical potential of the steel determined by oxidizing properties of the solution.

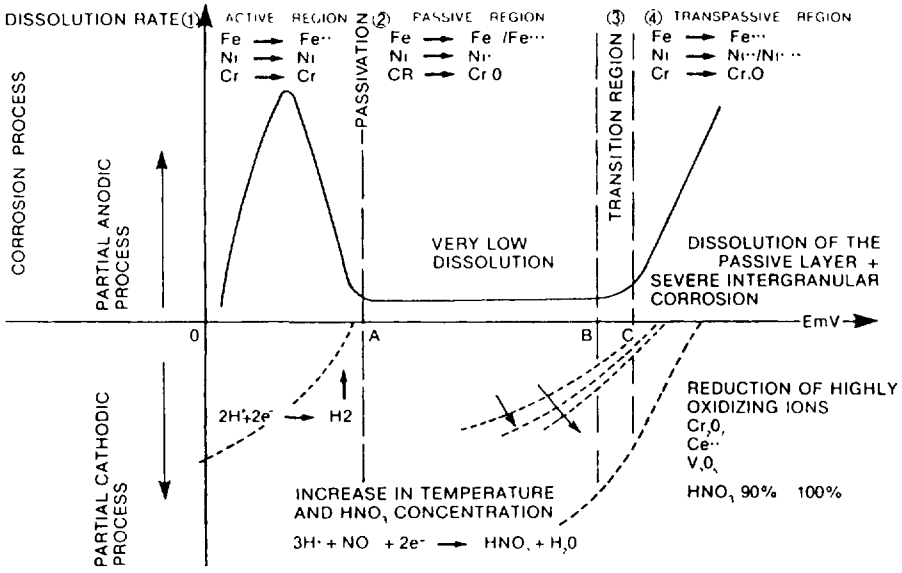

FIG. 1 — DIAGRAM ILLUSTRATING THE BEHAVIOUR OF Fe-Cr 18 Ni 10 STAINLESS STEELS IN ACID MEDIA ACCORDING TO THE ELECTRO-CHEMICAL POTENTIAL OF THE STEEL DETERMINED BY THE OXIDIZING CAPACITY OF THE SOLUTION. (SOURCE : CREUSOT-LOIRE)

2. VARIOUS FORMS OF CORROSION ENCOUNTERED

2.1. General corrosion

This form of corrosion, characterized by a uniform attack and a rather even thinning of vessel walls is predictable and can be controlled. It is quantified as weight loss and may be expressed in milligrams per square decimeter over a period of 24 hours ; 1 mdd standing for 1 $mg.dm^{-2}.day^{-1}$ equals approximately an even metal removal rate of 4.5 µm per year.

2.2. Intergranular corrosion

This corrosion is characterized by attack along the grain boundaries or in adjoining regions of the metal. It is hazardous and cannot be expressed in terms of weight loss. It is observed under two different conditions.

2.2.1. Passive state

During heat treatment between 1,050°C and 1,150°C (quench annealing), stainless steels acquire a uniform structure in which carbon is dissolved in the austenite. If such a steel is heated to between 500°C and 800°C, it undergoes "sensitization" caused by precipitation of the chromium carbide at the grain boundaries, thus creating a chromium depleted path in the adjoining regions. In the passive state of the base metal, the chromium depleted regions may undergo heavy corrosion. This form of corrosion may affect all austenitic steels, all the more as their carbon content is high and even those with very low carbon content, if their surface is contaminated by carbon.

2.2.2. Transpassive state

Under this condition, austenitic stainless steels undergo heavy intergranular corrosion in process media containing oxidizing ions such as hexavalent chromium and to a lesser extent trivalent iron, whatever the sensitization of the grain boundaries.

2.3. End-grain attack (tunnel corrosion)

This type of corrosion is caused by the attack of non-metallic inclusions and of internal zones in the metal segregated in chromium. The type, shape, quantity and distribution of these inclusions depend on the metal preparation process and on operations performed to transform the metal into a semi-finished product. The most hazardous are the sulphides. End-grain attack probably caused by the dissolution of local areas more prone to depassivation may further develop into more severe forms of corrosion possibly due to the build-up of corrosion products in semi-occluded volumes of nitric acid solution ; Fe III and occasionally Cr VI build-up may be responsible for some forms of local transpassive behaviour.

3. STAINLESS STEEL GRADES

3.1. General

The basic grade used is Z 2 CN 18-10 with a carbon content below 0.03% or below 0.02% if possible, to prevent intergranular corrosion in the chromium depleted areas caused by welding. The general corrosion rate of this steel is acceptable for nitric acid concentrations of up to 8N at temperatures close to boiling point. This steel is subject to intergranular attack in the transpassive state in highly oxidizing media.

Stabilization with titanium must be completely excluded as this encourages knife-line corrosion in the welded areas, even in passive conditions with 0.8N nitric solutions at boiling point.

Addition of molybdenum is detrimental in boiling nitric acid solution, as this element considerably increases corrosion rate. However, the addition of 2 to 3% molybdenum makes the steel more resistant to pitting corrosion in the event of accidental contamination by chlorides or in the presence of deposits.

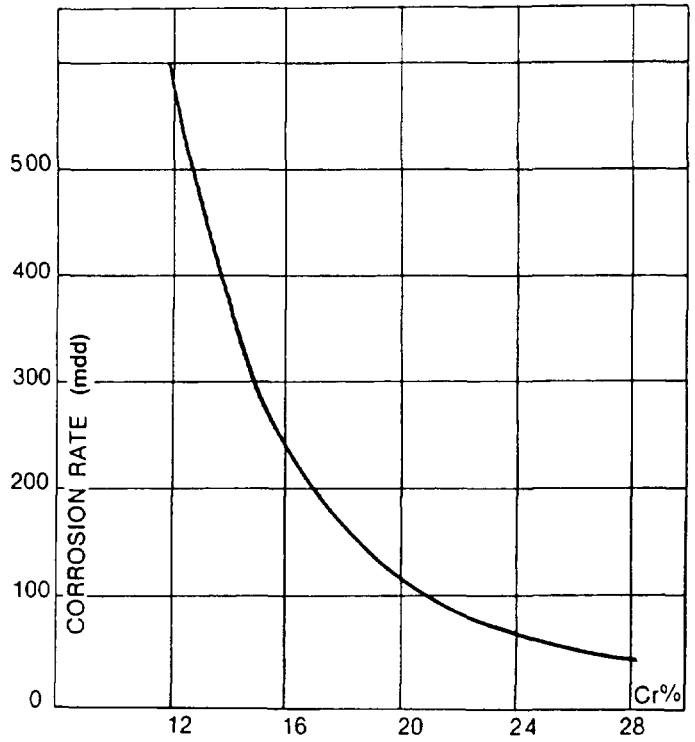

FIG. 2 — INFLUENCE OF THE CHROMIUM CONTENT ON THE CORROSION RATE IN 65% wt% NITRIC ACID.
(SOURCE CREUSOT LOIRE)

An increase in chromium content reduces the corrosion rate (see Figure 2) but favors the emergence of ferrite. In order to retain a stable austenitic structure, the nickel content is increased since its concentration is not very critical for corrosion resistance in nitric acid solutions considered in the Purex process.

This led Creusot-Loire, in collaboration with the CEA, to produce a steel called URANUS 65 which corresponds to AFNOR grade Z 2 CN 25-20. This steel has an excellent behaviour in boiling nitric acid solutions with concentrations up to 14N, with corrosion rate remaining below approximately 0.1 mm.year^{-1}. It is however subject to intergranular corrosion, of the type caused by chromium carbide precipitation due, for example, to surface carbon pollution, or resulting from sensitizing treatment such as welding.Also despite a low carbon content, this steel is not immune to transpassive intergranular attack in highly oxidizing process media.

Figures 3, 4 and 5 illustrate the comparative behaviour of Z 2 CN 18-10, Z 2 CND 17-13 and URANUS 65 (Z 2 CN 25-20) steels depending on acidity and on the metallurgical state (quench annealed vs sensitized).

The curves of Figure 5 illustrate the excellent behaviour of URANUS 65. Even in 14 N boiling HNO_3 medium, the corrosion kinetics curves confirm this behaviour, the other two grades showing rapid acceleration due to intergranular attack.

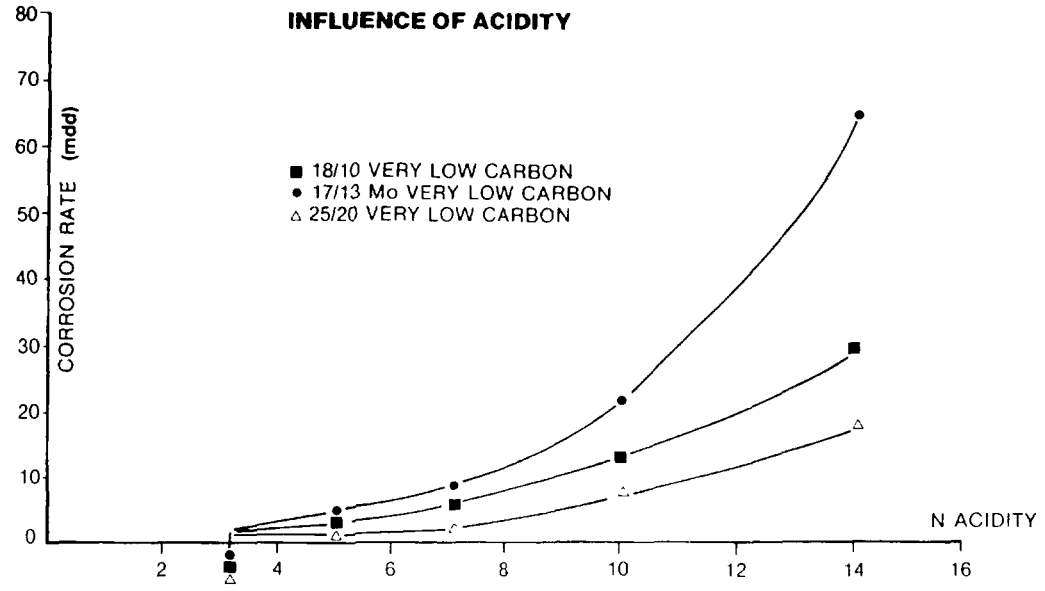

FIG.3 — BEHAVIOUR OF QUENCH ANNEALED STAINLESS STEELS IN BOILING NITRIC ACID (SOURCE : CEA/IRDI)

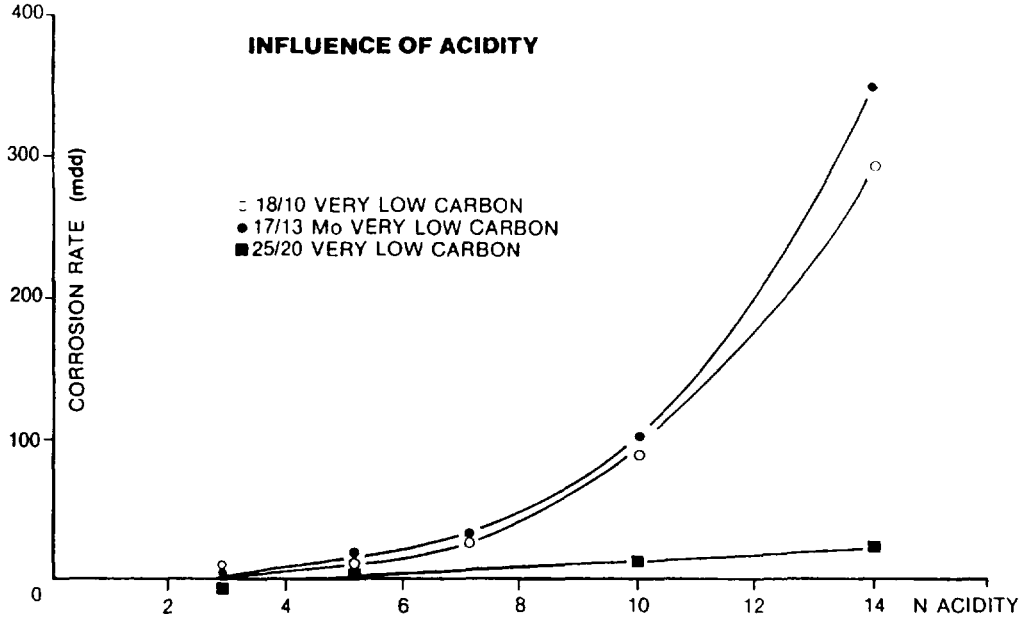

FIG.4 — BEHAVIOUR OF SENSITIZED STAINLESS STEELS IN BOILING NITRIC ACID (SOURCE : CEA/IRDI)

The influence of the presence of oxidizing ions (hexavalent Pu) clearly shows the occurence of intergranular corrosion. For the sake of comparison, corrosion rates for titanium and zirconium in the same medium are also presented (see Fig. 6).

Behaviour of stainless steels in the transpassive region is strongly affected by its silicon content (CEA - Creusot-Loire study).

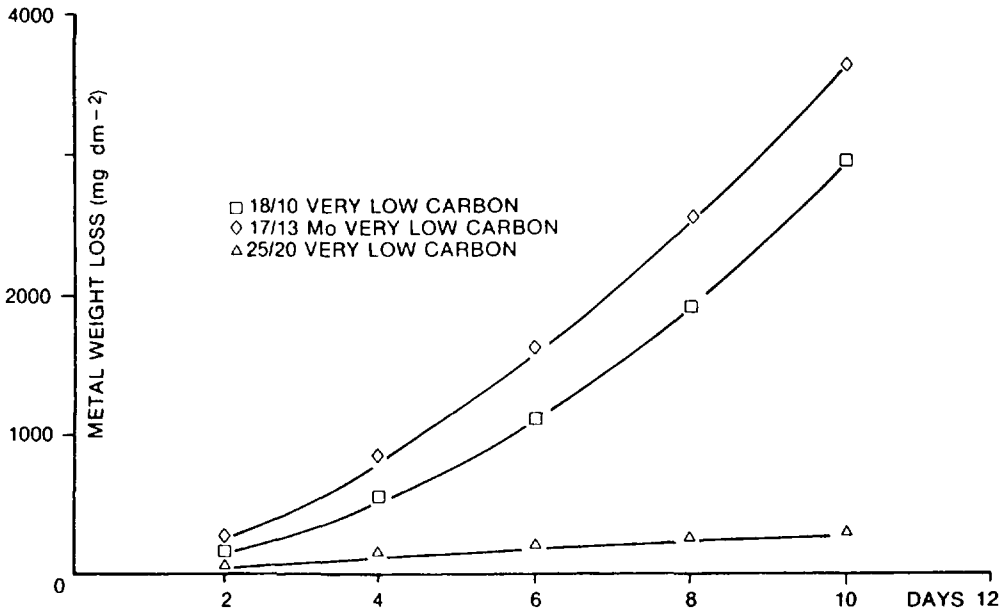

FIG.5 — CORROSION KINETICS FOR SENSITIZED STAINLESS STEELS IN BOILING 14 N NITRIC ACID (SOURCE : CEA/IRDI)

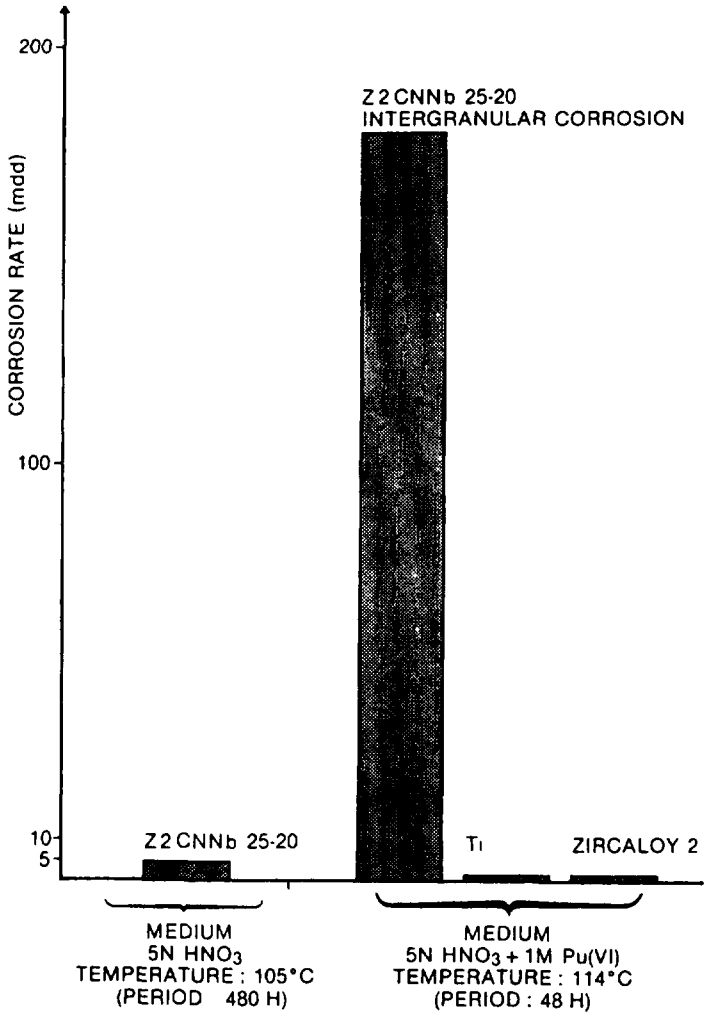

FIG.6 — INFLUENCE OF Pu VI
(SOURCE : CEA/IRDI)

Maximum penetration is observed for a Si content of around 1%. The absence of intergranular corrosion is noted for Si values greater than 3% (Fig. 7).

It has also been observed that steel containing 3 to 4% silicon has an excellent behaviour in a 5N HNO_3 solution containing 1 $g.l^{-1}$ hexavalent Cr, with no intergranular corrosion (Fig. 8).

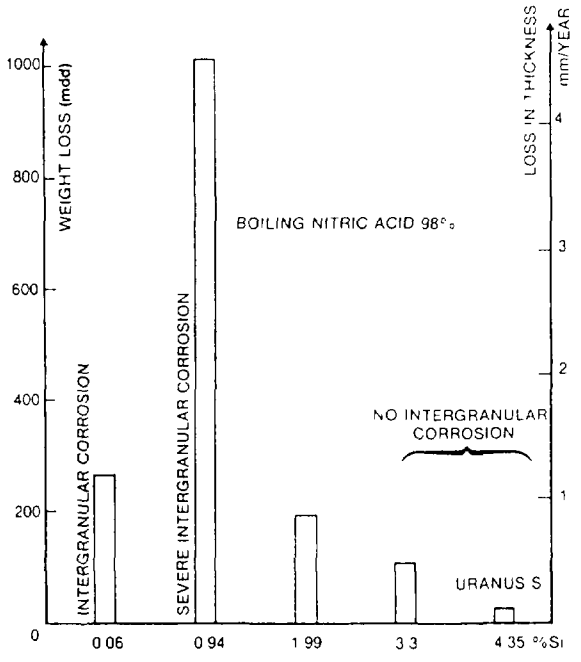

FIG.7 — INFLUENCE OF THE SILICON CONTENT ON CORROSION RESISTANCE IN CONCENTRATED NITRIC ACID
Cr 18-Ni 14-Si 0.1 TO 4 ($C \leqslant 0.015$) STEELS.
(SOURCE CREUSOT LOIRE)

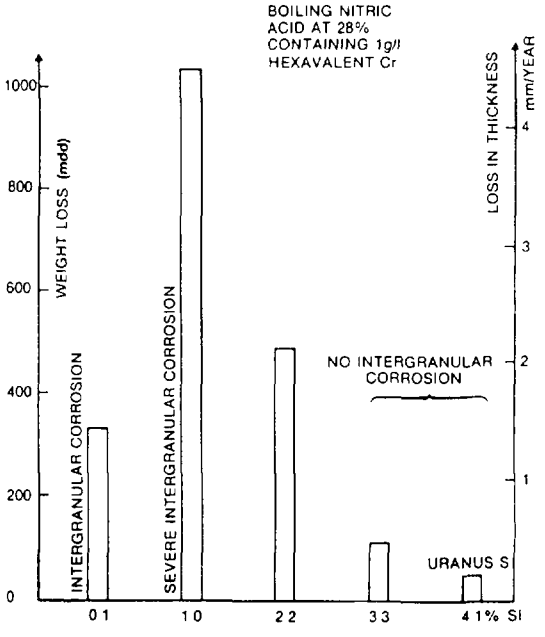

FIG. 8 — INFLUENCE OF THE SILICON CONTENT ON CORROSION RESISTANCE IN NITRIC ACID
Cr 18 Ni 14 - Si 0.1 TO 4 ($C \leqslant 0.015$) STEELS.
5N HNO_3 + Cr (VI) 1g/l

Steels with a higher silicon content (4%) are extremely sensitive to intergranular chromium carbide precipitation which can seriously compromise their behaviour in highly oxidizing acid media. Consequently their maximum permissible carbon content should be 0.015%. Creusot Loire has developed a steel called URANUS S1N - AFNOR grade Z 1 CNS 17-15 which contains 4% silicon with the addition of niobium.

Figure 9 shows the behaviour of the different steels in boiling HNO_3 5N medium containing 1 $g.l^{-1}$ of hexavalent chromium. Steels with very low carbon content, Z 2 CN 18-10 and URANUS 65 (Z 2 CN 25-20), show heavy intergranular corrosion whereas URANUS S1N (Z 1 CNS 17-15), although showing a relatively high general corrosion rate, has no intergranular corrosion.

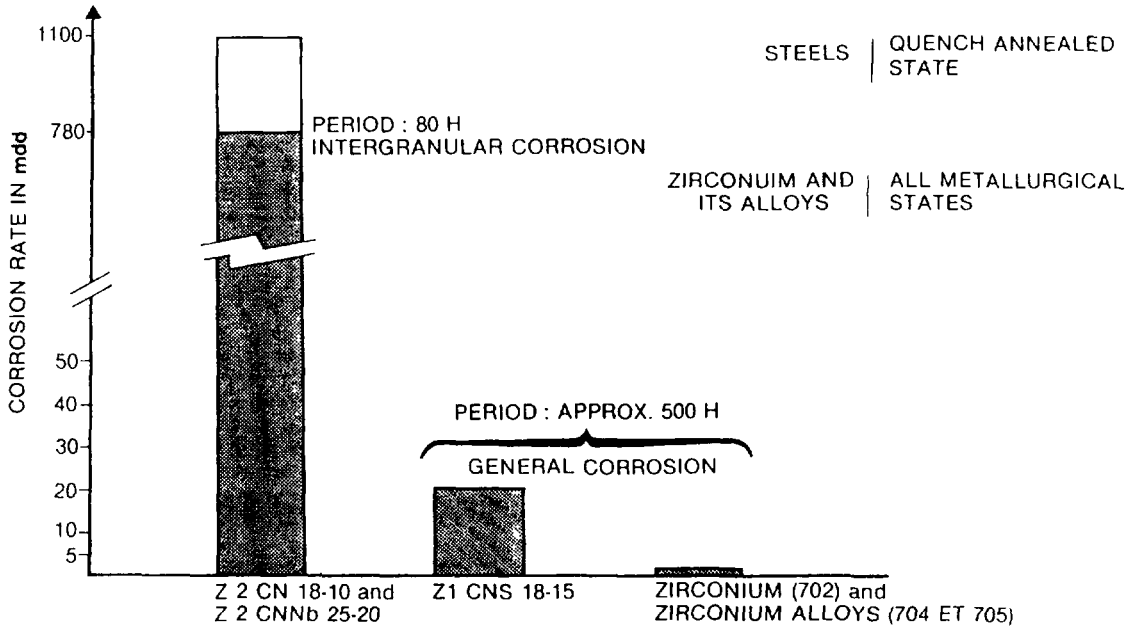

FIG. 9 — PRESENCE OF Cr(VI) · MEDIUM : BOILING 5N HNO_3 + 1g.l^{-1} Cr (VI)

3.2. Influence of inclusions and segregations

Silicon and phosphorus segregations, as well as precipitations of chromium rich phases as, for example, chromium carbide, σ phase and intergranular ferrite are the main sources of heavy, localized corrosion, accelerated in oxidizing medium.

Moreover, non-metallic inclusions with heterogenous shapes, sizes and distribution can cause end-grain attack and these are considerably influenced by steel preparation operations such as working, forging, and rolling.

To correct these defects, selected steels will therefore have a sulphur, phosphorus and carbon content as low as possible. With the exception of URANUS S1N, silicon will also be reduced to a minimum.

Considerable attention must be given to the solution heat treatment (quench annealing) which should be performed for a period sufficiently long to ensure good homogeneity.

3.3. Stainless steel grades used

The different austenitic stainless steel grades used are given in Table I.

Table I : Steel chemical composition in wt%

DESIGNATION		C	Cr	Ni	Si	S	P	Mo	Mn	N	Nb
AFNOR	COMMERCIAL										
Z 2 CN 18-10		≤0 03	18	10	≤1 0	≤0 02	≤0 03				
Z 2 CND 17-12		≤0 03	17	12	≤1 0	≤0 02	≤0 03	2-2 5			
Z 2 CND 17 13		≤0 03	17	13	≤1 0	≤0 02	≤0 03	2 5-3			
Z 2 CN 25 20	URANUS 65	≤0 015	24 26	19-22	≤0 25	≤0 005	≤0 025	≤0 5	≤2		addition
Z 1 CNS 17-15	URANUS S1N	≤0 015	16 5-18 5	13 5-15	3 8-4 5	≤0 005	≤0 025	≤0 5	≤2	≤0 035	addition

Quench annealing temperatures range between :
- 1,050 and 1,150°C for Z 2 CN 18-10, Z 2 CND 17-12 and Z 2 CND 17-13,
- 1,100 and 1,150°C for Z 2 CN 25-20 and Z 1 CNS 17-15.

Heating time varies between 5 and 60 minutes depending on the size of the part. Cooling is performed quickly either with air or water. Cleanliness, i.e. the type, shape and distribution of inclusions is measured following AFNOR standards NFA 04 106 or ASTM E 45 methods.

The detection of possible Nb carbonitrides has not been considered. Corrosion tests mainly used to reveal surface carbon pollution which could lead to chromium-depleted areas along the grain boundaries during sensitizing treatments (e.g. welding) will be performed according to procedures adapted to each metal.

3.4. Influence of alloy preparation

The above data confirm the importance of controlling :
. the chemical composition
. the carbon content
. inclusion cleanliness.

These parameters are controlled by using a specifically adapted procedure called ASV (argon under vacuum) which has enabled Creusot-Loire to supply products made of URANUS 65 (Z 2 CN 25-20) and

URANUS S1N (Z 1 CNS 17-15) that meet specifications for welded vessels used in spent fuel reprocessing plants and operating with nitric media.

Examples of construction given below illustrate the perfect control of special grades used (see Figure 10).

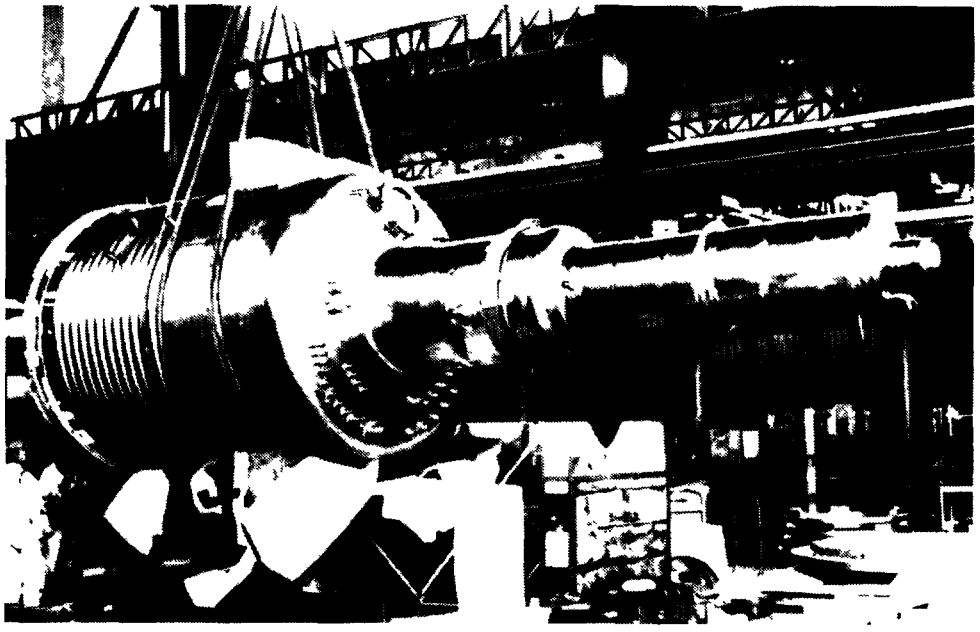

FIG. 10 — FISSION PRODUCTS CONCENTRATOR IN URANUS S1N STEEL (Z 1 CNS 17-15)

EXPERIENCE OF CORROSION PROBLEMS AND MATERIAL DEVELOPMENTS IN THE TOKAI REPROCESSING PLANT

T. YAMANOUCHI, A. AOSHIMA, N. SASAO,
S. TAKEDA, N. ISHIGURO
Power Reactor and Nuclear Fuel Development Corporation,
Tokyo, Japan

Abstract

In Tokai Reprocessing Plant, several problems on the main process equipment have occured due to the corrosion of the austenitic stainless steel.

Under these circumstances, the plant operation was stopped for a long intermittent period in order for us to investigate the corrosion conditions and take necessary measures such as repair or replacement of failed equipment.

In this paper, such problems and measures are summarized together with the description of the corrosion behaviors in reference to the dissolvers and acid recovery evaporator in the plant.

1. Introduction

In Tokai Reprocessing Plant, the total amount of about 260tU of spent fuels has been processed to date since 1977 (FIG.1). Through the plant operation, the fundamental reprocessing techniques have been established by proving the validity and safety of the process, except for the relatively low availability of the plant.

Among several reasons of the low plant availability, the most serious one was the radioactive leakage caused by the corrosion in the main equipment, although such equipment was made of high Cr-Ni stainless steel resistant to corrosion in boiling nitric acid solution.

Such equipment as acid recovery evaporator, which could be replaced because of relatively low radiation ambience, has been replaced with domestic one for considering improvements on material selection, structure, operation method, etc.

On the other hand, the in-situ repair was developed and carried out remotely for dissolvers which could not be replaced easily because of their high activities. This remote repair technology will be applied to similar failures and preventive maintenance of the dissolvers in future.

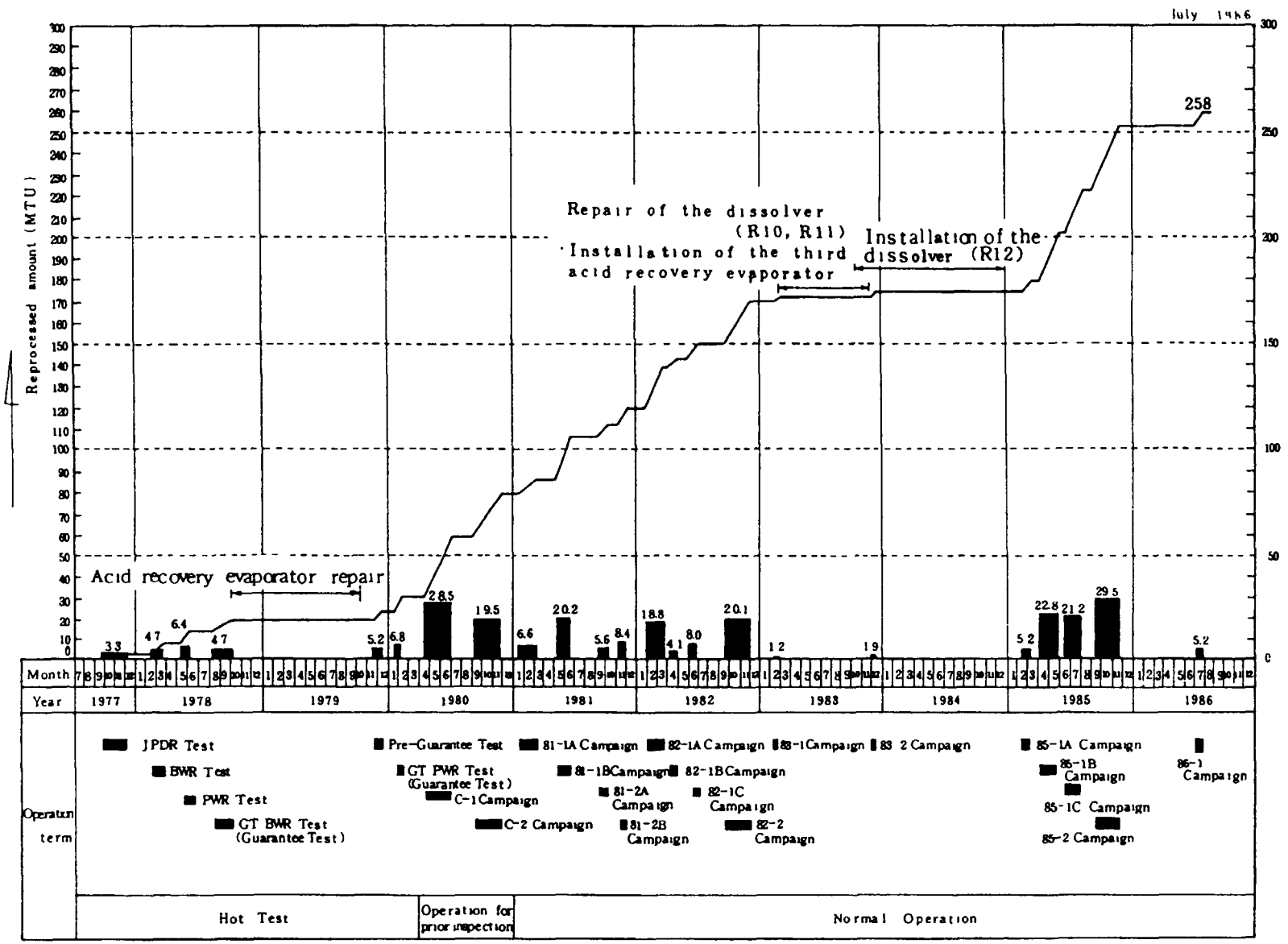

FIG 1 Operation of Tokai Reprocessing Plant

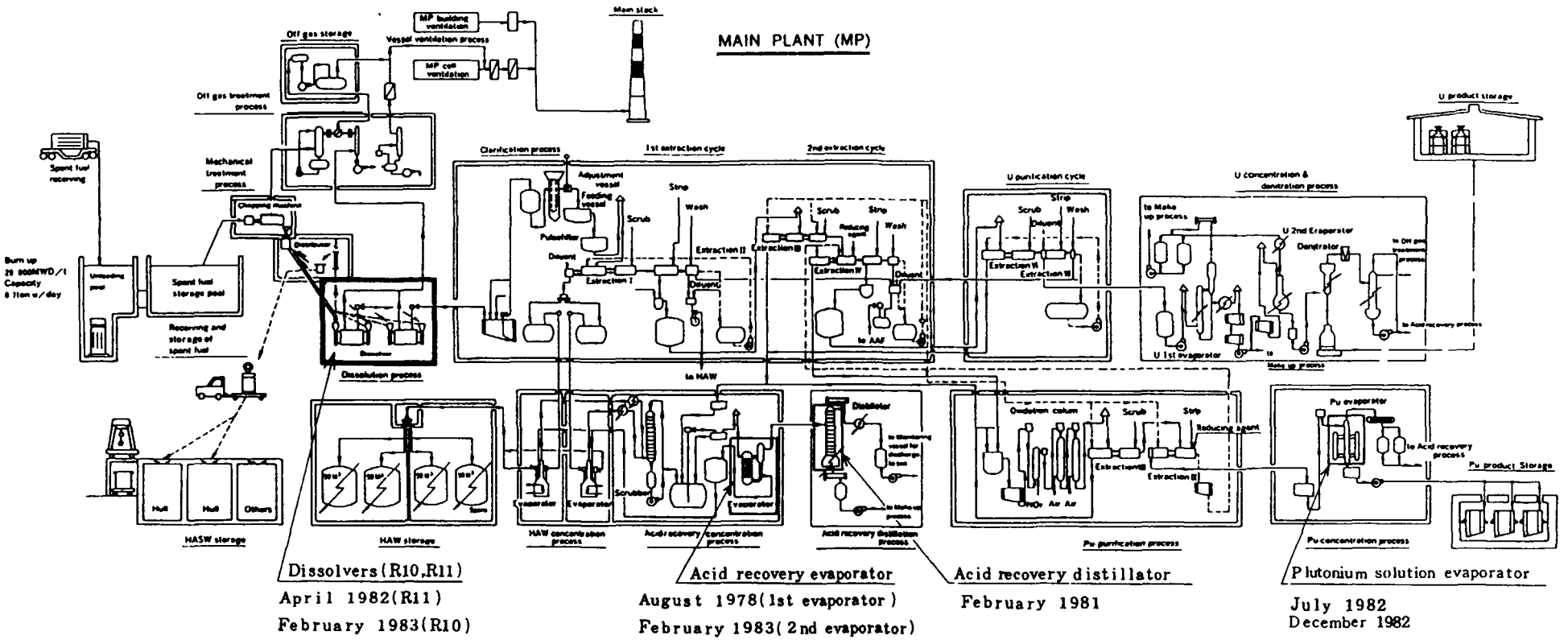

FIG. 2 Corrosion probrems in main equipments of Tokai Reprocessing Plant

Table I Corrosion problems experienced in Tokai Reprocessing Plant

Equipment	Occurence of leakages	Measures	Remarks
Dissolver (R10, R11) R10 R11	 February 1983 April 1982	 Repaired (September ~ November 1983)	•Installed new one (R12) in 1984 •Additionally repaired in 1986 (R10, R11)
Acid recovery evaporator 1st evaporator 2nd evaporator	 August 1978 February 1983	 Replaced with new one (January ~ October 1979) Replaced with new one (June ~ October 1983)	
Acid recovery distillator	February 1981	Repaired (April 1981)	Replaced with new one in 1984 (Only lower part)
Plutonium solution evaporator	July 1982 December 1982	Repaired (August ~ September 1982) Repaired (January 1982)	Replaced with new one in 1984

2. Corrosion problems experienced in Tokai Reprocessing Plant

FIG.2 and Table I show significant failures of equipment caused by corrosion experienced in Tokai Reprocessing Plant since the start of the plant operation in September 1977.

(1) Dissolvers

Following the shearing process, the dissolvers are used for dissolving chopped fuels with nitric acid. At the start of hot operation in 1977, there installed two dissolvers (R10,R11) made of URANUS 65.

The leakage failures of R11 and R10 due to corrosion occurred in April 1982 and February 1983, respectively. All of leaking points, one for R10 and two for R11, appeared on welding lines in heating jackets of the dissolvers.

These dissolvers were repaired remotely from September through November 1983. Also, the third dissolver (R12) made of NAR310Nb was installed in a neighbouring cell in 1984.

(2) Acid Recovery Evaporator (FIG.3)

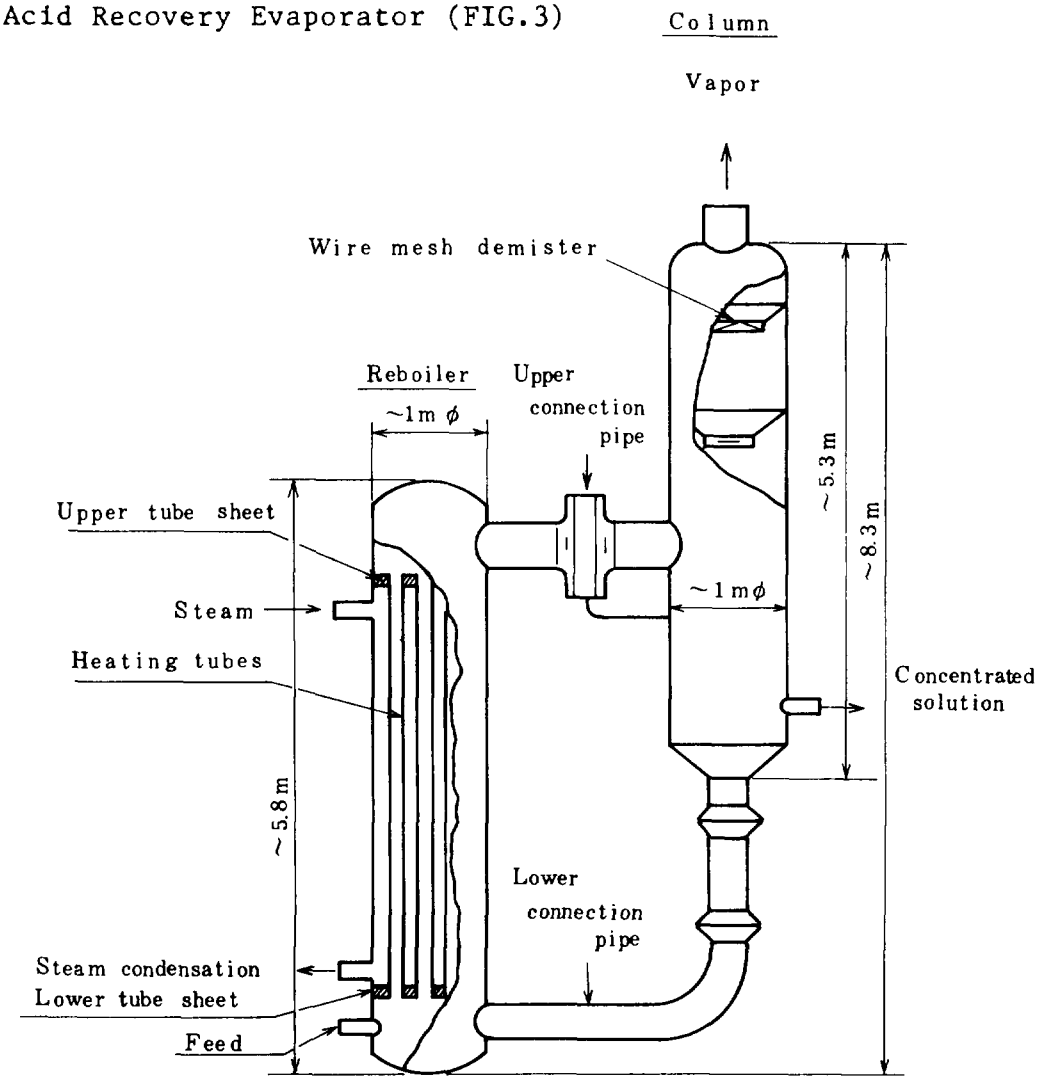

FIG. 3 Scheme of the acid recovery evaporator

The acid recovery evaporator made of URANUS 65 was installed in the acid recovery process which is used for concentrating the MAW solution from the extraction process and from HAW concentration process as shown in FIG.2.

The first leakage failure of the evaporator occured in August 1978, after about 6,000hrs operating duration. Five pin-holes were detected and all of them was located on welding lines between the upper tube sheet and heating tubes in the reboiler. The failed evaporator was replaced with new one made of CRONIFER25-20Nb from January through October 1979. This second generation evaporator was manufactured domestically with raw material imported from West Germany. Several improvements were considered, especially for the welding between tube sheets and heating pipes to avoid simillar failures (FIG.4).

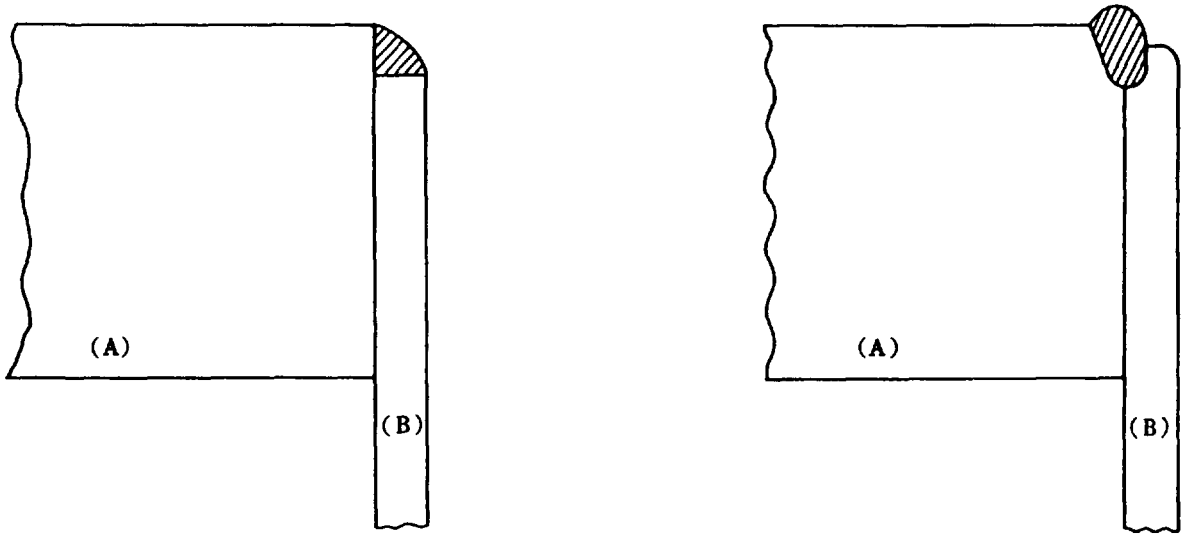

The 1st evaporator

The 2nd evaporator

(A) : Tube sheet(34mm in thickness)

(B) : Heating tube(42mm in outside-diameter)

FIG. 4 Shape of the groove between heating tubes and tube sheet

However, the second leakage failure occured in 1983, after about 13,000hrs operating duration.

The inspection revealed that leakages were caused by defects of two heating tubes in the reboiler due to corrosion of base metal. There was no defect on welding lines between tube sheets and heating tubes. After detailed inspections, only the reboiler portion of the second generation evaporator was replaced with spare one made of NAR310Nb from June through October 1983.

(3) Acid Recovery Distillator (FIG.5)

The acid recovery distillator was installed in the acid recovery process for distillating the acid fume from the acid recovery evaporator.

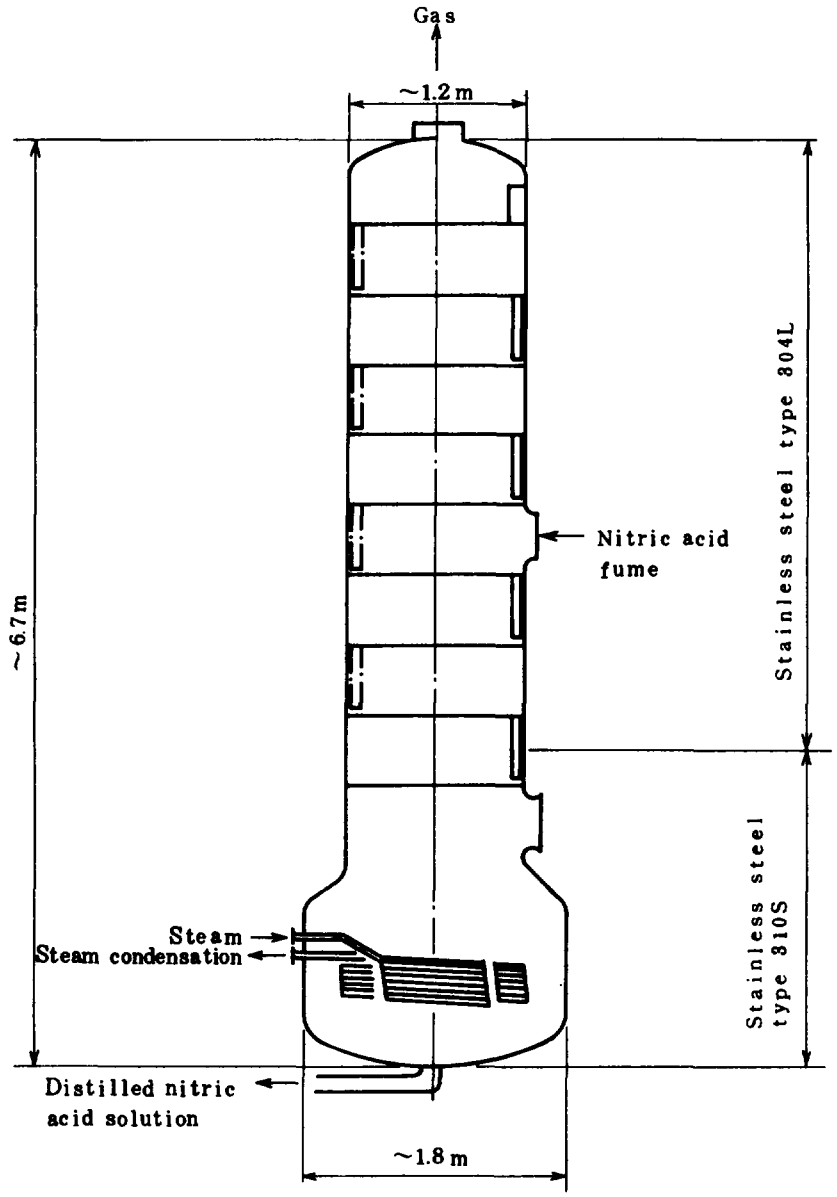

FIG. 5 Acid recovery distillator

A leakage failure of the distillator occured in February 1981. There were three leaking points on butt welding lines of heating pipes and around welding portion between heating pipes and piping support. The failed portion of the distillator was repaired directly because of relatively low levels of radiation dose in ambience.

Futhermore, the lower portion of the distillator which might suffer corrosions was replaced with spare one in 1984.

(4) Plutonium Solution Evaporator (FIG.6)

The plutonium solution evaporator, composed of an evaporator and a scrubbing tower, is used for concentrating the plutonium nitrate solution from the plutonium purification process as shown in FIG.2. The tower is made of stainless steel type 304L and the evaporator of titanium.

In July 1982, a leakage occured in the tower. The leaking point was located on a instrumentation nozzle neck in the gaseous phase near the liquid surface. The in-situ repair welding was carried out directly in the cell in 1981. Also in 1984, the plutonium solution evaporator was replaced with spare one in terms of the preventive maintenance.

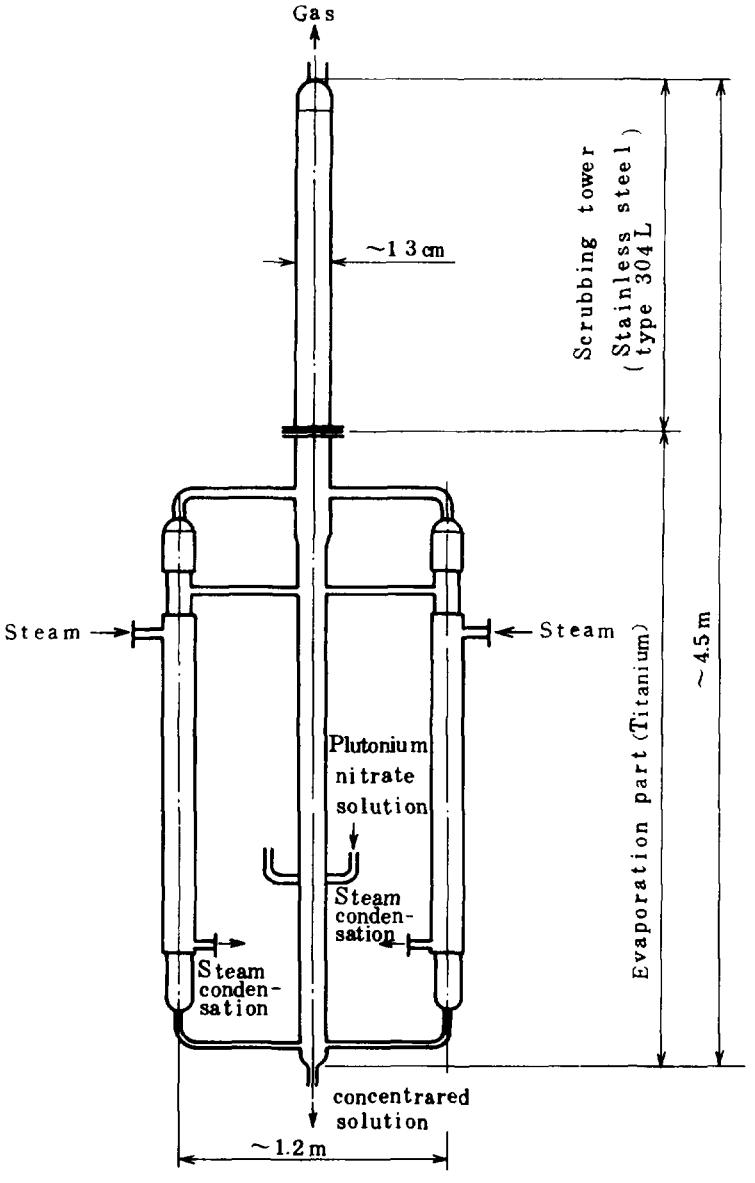

FIG. 6 Plutonium solution evaporator

3. Development of remote repair technique for the dissolvers

3.1 Development program (FIG.7)

The development of remote repairing technique for the failed dissolvers was classified roughly into four steps as follows:

① Development of remote devices for inspection and repair
② Development of welding procedure
③ Actual repair work
④ Certification of the validity of the remote repairing technique

Since item ①, ② and ③ were already reported at the international conferences [1], [2], this paper discribes mainly on item ④.

The remote repairing technique including the ISI methods was certified through the test operation of the dissolvers using spent fuels.

3.2 Description of failed dissolver

Each of dissolvers (R10,R11) consists of two cylindrical barrels containing baskets for holding chopped fuel elements and a slab tank connected with the barrels by four pipes each as shown in FIG.8. The inside diameter of the dissolver barrel is about 27cm and the length is about 6m.

The leaking points were observed on welding lines of the barrels that located on or near the heating surface in the liquid phase as shown in FIG.8.

3.3 Certification of the validity of remote repairing technique

(1) Test dissolution

Test dissolution using spent fuels was carried out from December 1983 through November 1985 with the repaired dissolvers (R10,R11) as shown in FIG.9.

The test dissolution consisted of three small runs named the first run, the second run and the third run, respectively and each dissolver was operated for about 400hrs in total, as listed in Table II.

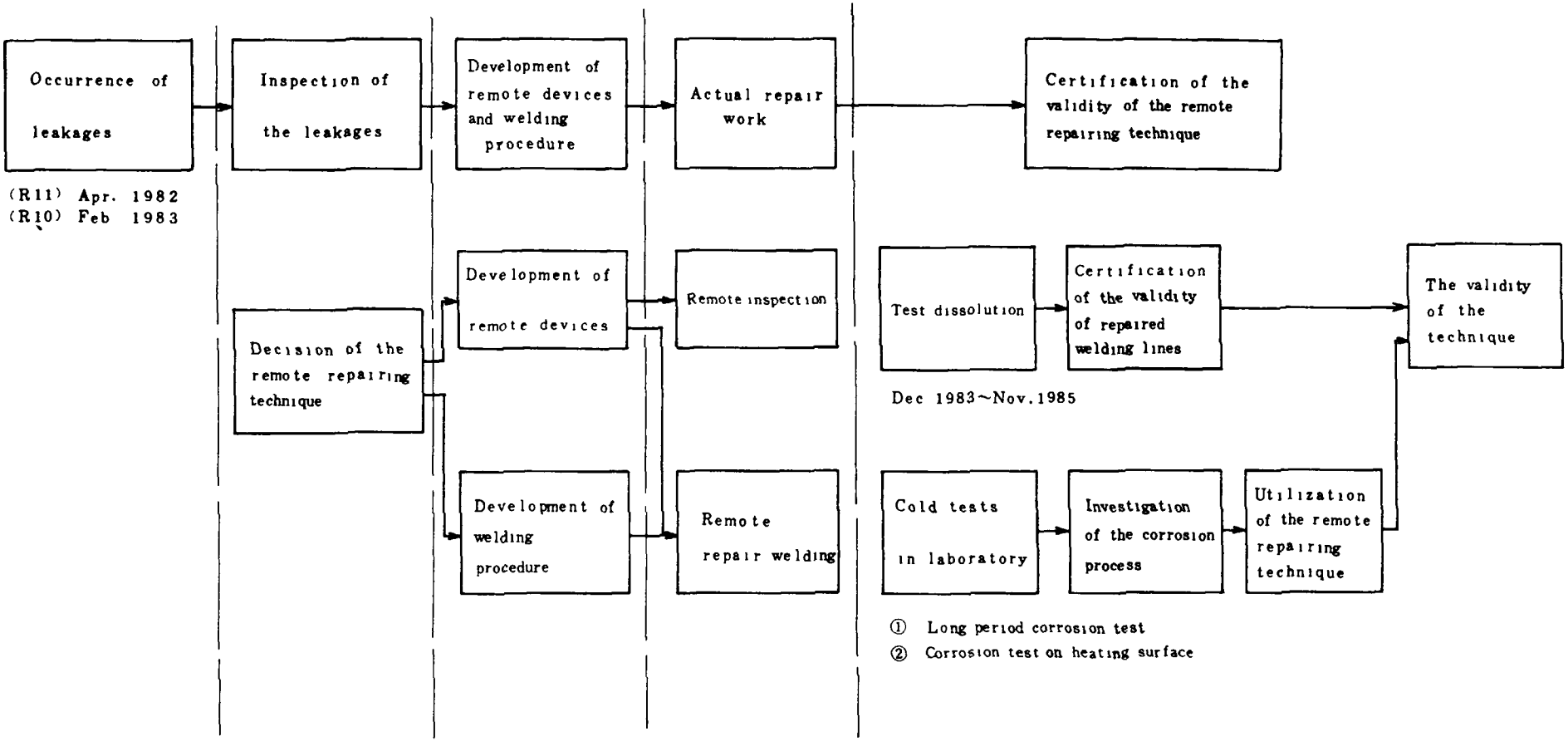

FIG. 7 Flow diagram for development of the remote repairing technique

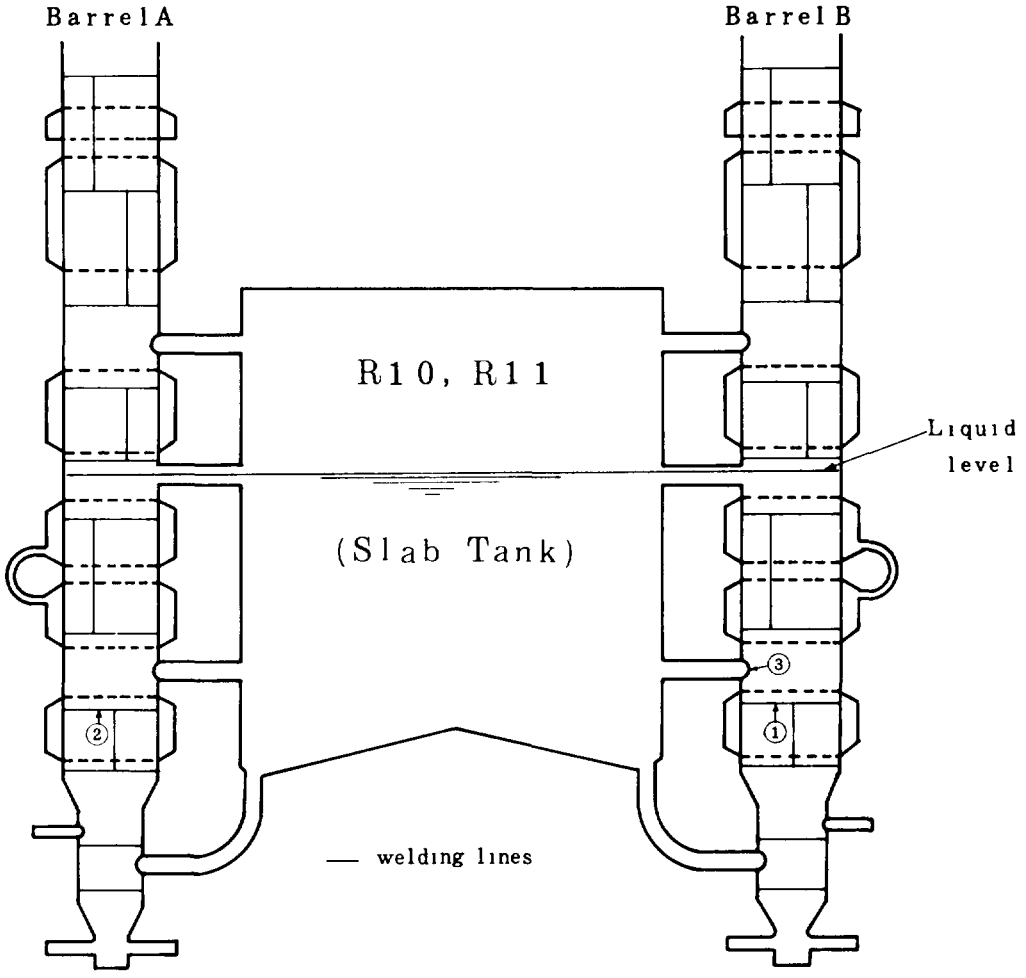

Dissolver	Barrel	Occurence of leakages	Location of leaking points
R10	B	February 1983	Circumferential weld ① covered with the steam jacket
R11	A	April 1982	Circumferential weld ② covered with the steam jacket
	B	July 1982	Weld ③ of the third connecting pipe

FIG. 8 Location of leaking points in the dissolvers (R10, R11)

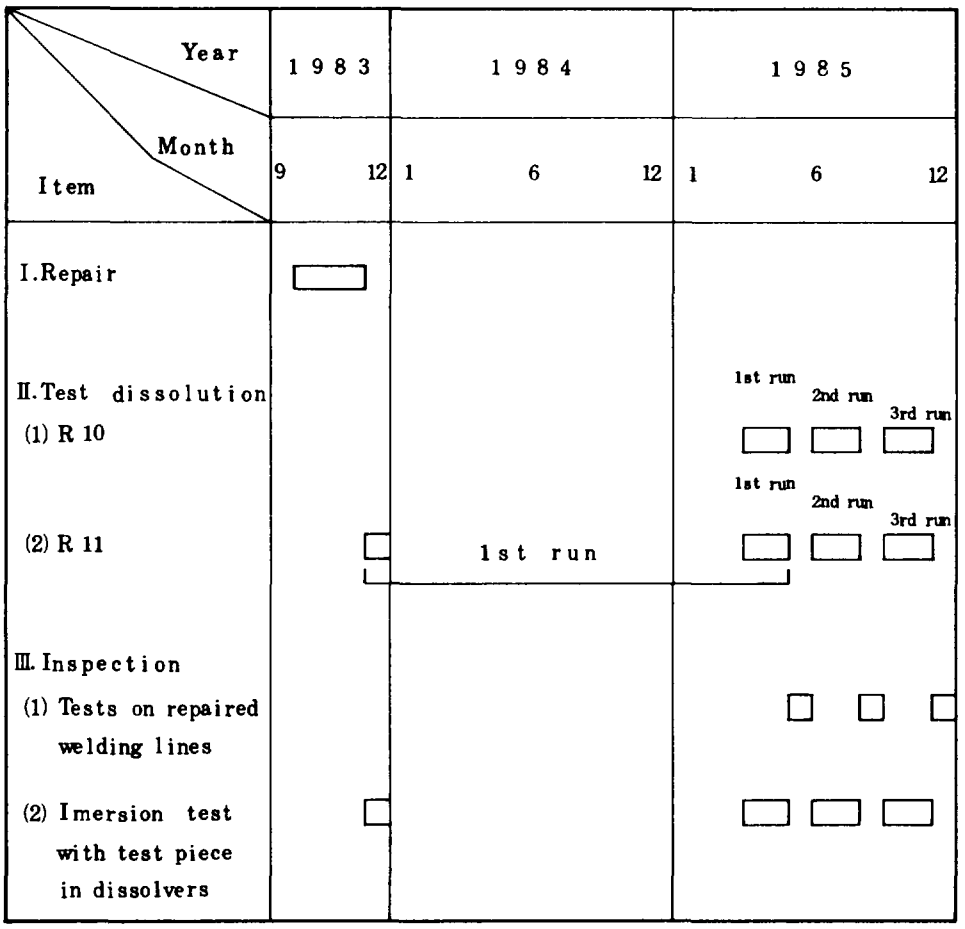

FIG. 9 Schedule of test operation

Table II Test dissolution time

Run	Test dissolution time (hrs)		Term
	R10	R11	
1st	127	130	December 1983 April ~ May 1985
2nd	135	136	June ~ August 1985
3rd	143	150	September ~ November 1985
Total	405	416	

Table Ⅲ Inspections in test dissolution

Object of inspection	Items	Results
I. Tests on repaired weld beads	I. Visual test of repaired welding lines	Good
	Ⅱ. Visual test of outside of barrel (R11 B side barrel)	Good
	Ⅲ. Air leak test	No bubble
	Ⅳ. Ultrasonic test	No defect
Ⅱ. Immersion test with test piece in dissolvers	I. Weight loss Ⅱ. Surface observation etc.	·No defect ·A slight weight loss

At each intervals of three runs, the soundness of the repaired welding lines were checked by several inspections listed in Table III. The results of the inspections were listed in Table II.

(2) Corrosion tests in laboratory

Besides the test operation, following cold corrosion tests were carried out in laboratory.

① Long period corrosion test
② Corrosion test on heating surface

① Long period corrosion test
The purpose of this test was to investigate basic corrosion behaviors of dissolver materials.
The corrosion test was performed in boiling 65%HNO_3+5mol/l of Ru^{3+} solution that was renewed every 100hrs.
Specimens were tested for a maximum 4,000hrs to get as much information as possible.

The main results of this test were as follows:

-In base metal, corrosion proceeds as falling of grains, so the uneveness of about 200μm (eaqual to two grains) is observed on the corroded surface through the test period (FIG.10).

After 4,000hrs Immersion

FIG.10 SEM observation of base metal(URANUS65)

-In welding lines, corrosion proceeds as the intergranular corrosion along with dendritic structure boundaries.
In the stage of corrosion proceeded considerably, the falling of dendritic structure occured like the grain falling in base metal.
The shape of the residual dendritic structure was grass-shaped as shown in FIG.11.

After 4,000hrs Immersion

FIG.11 SEM observation of welding lines (WEL MIG SW310)

② Corrosion test on heating surface

The corrosion process of the repaired welding lines was investigated using test plates which have heating surfaces on them.

The test plates with buttering weld beads, shown in FIG.12, were used for the test that were simulated the repaired portion of the dissolvers (R10,R11).

These test plates were put together into the box-shaped test apparatus that contained the test solution heated by an outside heater.

The test plates were corroded for a maximum 1,000 hrs in boiling 65%HNO_3+5mol/l of Ru^{3+} solution that was renewed every 100hrs.

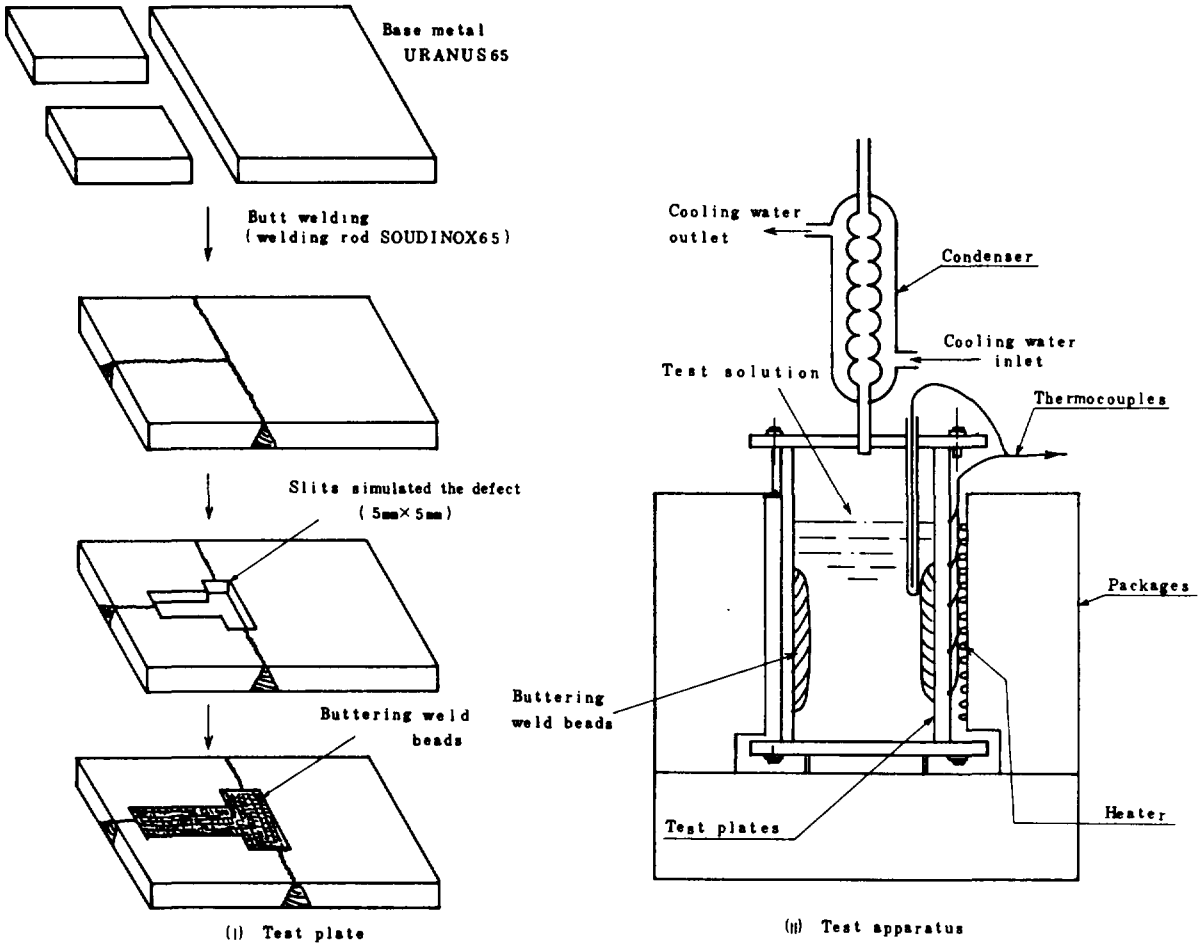

FIG. 12 Test apparatus for the corrosion test on heating surface.

The corrosion process of the buttering weld beads were divided into following three stages according to their characteristics of the external appearances as shown in FIG.13.

(i) First stage
The intergranular corrosion starts at first and it makes the dendritic structures of the beads clear. In the final stage, lipple lines on the buttering weld beads disappeare.

(ii) Second stage
The corrosion proceeds along with the boundary of the dendritic structures and results in falling these structures. The residual dendritic structure looks like grass-shaped.
At the end of this stage, the width of the buttering weld beads decreases somewhat.

(iii) Third stage
In this stage, the decrease of the bead width by the falling of dendritic structures is observed apparently.

(3) Soundness of repaired welding lines of dissolvers after test dissolutions

The soundness of the repaired welding lines of the dissolvers (R10,R11) was confirmed by the remote observation with peliscopes.

The corrosion state of the repaired welding lines after 400 hrs test dissolution was revealed to be very slight as the results of inspections carried out after each run. This corrosion state corresponded to the first stage obseved in the corrosion test on heating surface. It is concluded that the validity of the remote repairing technique was certified including the remote inspection technique.

This remote repairing technique can be adopted to the dissolvers (R10,R11) in future, if necessary.

4. Replacement of the acid recovery evaporator

(1) As stated before, the acid recovery evaporator has been replaced twice. Presently, the third generation evaporator has been operated for about 5,000hrs in total since 1983. Little amount of corrosion is estimated for the evaporator by analysing Cr and Ni concentrations of the concentrated solution in the evaporator.

The corrosion state of the evaporator will be inspected directly in the cell in spring 1987, after about 10,000hrs operating duration. The inspection items will be as follows:

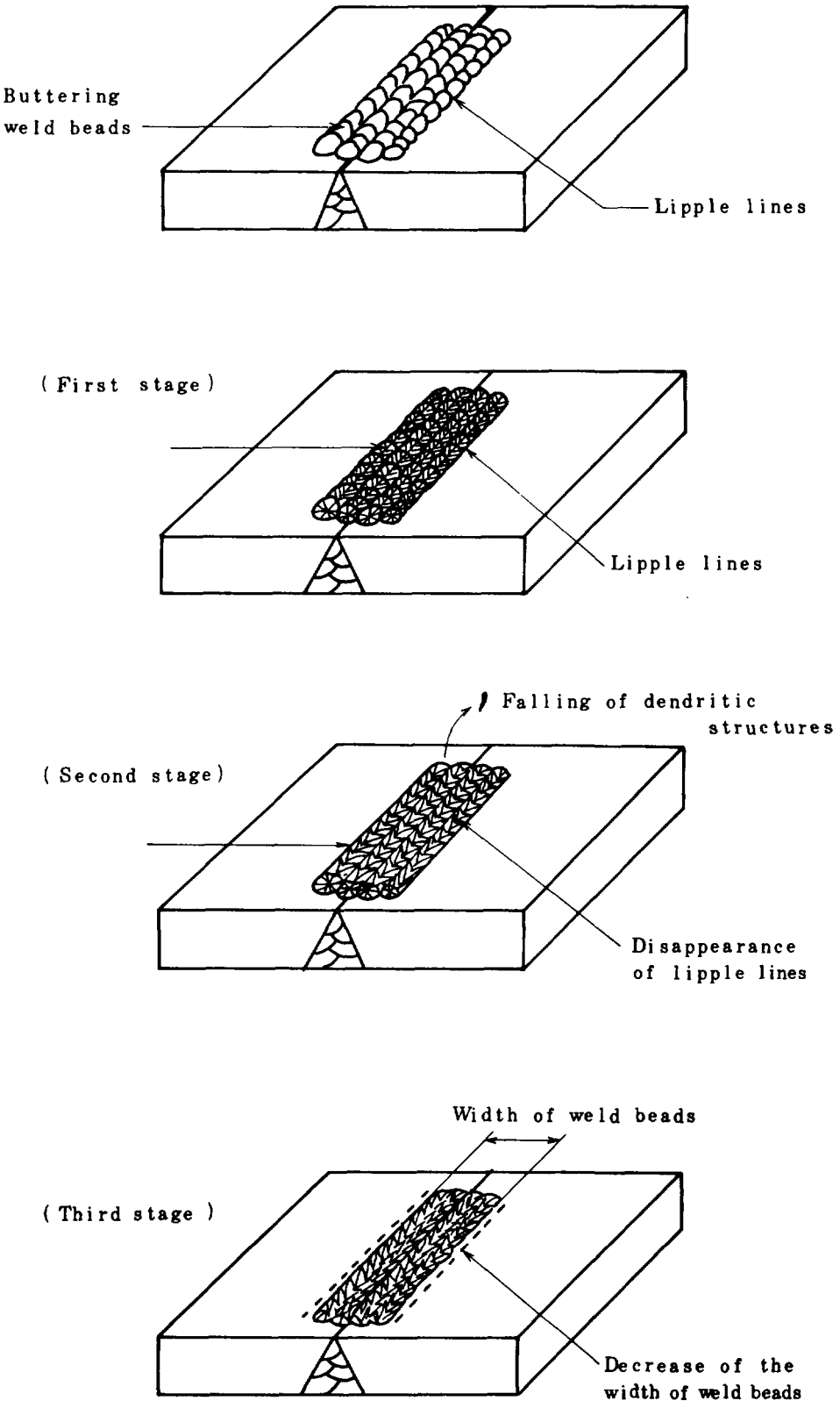

FIG. 13 Corrosion stages of buttering weld beads

① Inspection of heating tubes

The heating tubes in the reboiler will be inspected by the eddy current test for measuring the wall thickness of heating tubes and the surface observation to find out possible defects inside tube walls.

② Measurement of wall thickness of the evaporator

The wall thickness of the evaporator will be measured by the ultrasonic method. The measurement will be carried out from the outside of the evaporator, not only for the reboiler but also the column and connection pipes.

(2) It is planned to replace the third generation evaporator in 1988 with new one made of Ti-5%Ta alloy.

Ti-5%Ta alloy was sellected as the raw material for the new evaporator according to the result of design study including the corrosion test for Ti-5%Ta, Zr, and stainless steels in 1984. In the design study, these materials were examined and compared each other in three viewpoints: material production, corrosion resistance, and equipment manufacturing. A pilot scale equipment made of Ti-5%Ta alloy was already manufactured in 1985. The test operation will be started in this year to evaluate the corrosion resistance of this new material in detail.

Applications of new materials to dissolvers and other equipment will be examined in future considering the operation result of the new evaporator.

5. Conclusion

In Tokai Reprocessing Plant, corrosion problems on the main equipment have been experienced which caused stoppages of the plant operation. For the failed equipment, proper measures have been taken successfully to resume the plant operation.

In the case of the failed dissolvers, the remote repairing technique was developed and applied. The validity of the technique was certified by confirming the soundness of repaired welding lines with peliscopes. On this occasion, the third dissolver was installed in the spare cell.

The acid recovery evaporator has been replaced twice. The current evaporator will be inspected on the corrosion state next year. New materials such as Ti-5%Ta have been examined for the fourth generation evaporator. The pilot scale equipment made of Ti-5%Ta was fabricated and the test operation will be started soon.

References

(1) "Development of remote system technology for inspection and repair of the leaked dissolvers in Tokai Plant"
S.Hayashi, T.Yamanouchi et. al, IAEA-SR-103/8 (1984)

(2) "Remote maintenance experience of the dissolvers in Tokai Reprocessing Plant"
K.Takeda, T.Funaya, J.Masui, ANS Winter Meeting in 1985

STUDY OF THE CHEMICAL STRUCTURE OF FILMS FORMED DURING TRANSPASSIVE TO PASSIVE TRANSITIONS ON A CATHODICALLY PROTECTED AISI 430 FERRITIC STAINLESS STEEL

M. BEN HAIM, U. ATZMONY, N. SHAMIR
Nuclear Research Centre Negev,
Israel Atomic Energy Commission,
Beersheba

J. YAHALOM
Technion — Israel Institute of Technology,
Haifa

Israel

Abstract

AISI 430 stainless steel can be cathodically protected in highly oxidizing solutions. The freely corroding potential of this stainless steel in such solutions is transpassive. In the protecting process this potential is lowered from the transpassive to the passive zone by applying potentiostatic techniques. The chemical structures of the surface films formed during the various stages of this potential shift were investigated by X-ray and Auger electron spectroscopies combined with Ar^+ ion sputtering for depth profiling and by scanning electron microscopy. The shift is accompanied by two distinct phenomena: a) Increase of the concentration ratio of the oxidized to the metallic states of the iron and of the chromium present in the film. This implies that films formed in the passive zone are thicker than those formed in the transpassive one, a fact which is also revealed by the Auger depth profiles. b) Formation of a layered structure in the passive zone which is characterized by chromium surface segregation in the film. Three layers were detected. The layer at the metal film interface is composed of Cr^{+3} oxide whereas the two layers above it are composed of mixed iron and chromium oxides with the iron being primarily of Fe^{+2} type in the intermediate layer and of Fe^{+3} type in the outer one.

Introduction

Austenitic and ferritic stainless steels can be cathodically protected in highly oxidizing nitric acid solutions [1,2]. The freely corroding potential of these stainless steels in such solutions is

transpassive. In the protecting process, this potential is lowered from the transpassive to the passive zone by applying potentiostatic techniques. In order to monitor changes of the chemical nature of the surface film formed during this kind of protection, electrochemical and surface analysis techniques as Auger Electron Spectroscopy (AES) and X-ray photoelectron spectroscopy (XPS) were applied. A commercial 18%-Cr ferritic stainless steel, AISI 430 was used in these studies. The results are summarized in the following.

Experimental

The electrochemical experiments as well as the film formation processes, were performed in a one liter reactor vessel with a tightly fitting five inlet lid. 400 ml of test solution were used in each experiment. Solution contact for potential measurements was made between the contents of the cell and an external SCE, with the aid of a Luggin capillary probe and an electrolyte bridge. AISI 430 stainless steel discs, 12 mm diameter and 2 mm thick were mechanically polished to 0.25 microns finish using diamond spray and ethanol as coolant. Only a part of the specimen corresponding to a circle of 7 mm diameter was exposed to the electrolyte, while the remaining part was insulated by a Teflon housing of the working electrode assembly. The electrolyte solution, 4N nitric acid, was prepared from analytical grade chemicals and double-distilled water. Specimens for the surface studies were held at a constant potential for one hour in the test solution. The specimen of transpassive region was held at 1250 mV SCE. The specimen of the passive region was shifted from the transpassive zone (1250 mV) to 800 mV (SCE). All the anodically treated specimens were first cathodically polarized for 30 minutes at -400 SCE mV in order to reduce naturally formed films. The anodically treated specimens were quickly removed form the electrochemical cell, washed with double distilled water, rinsed in ethanol and dried in nitrogen stream. They were kept in a dessicator for about ten minutes before being inserted into the UHV chamber of a combined XPS/AES system. The samples were introduced via an introduction chamber to the surface analysis system equipped with a double pass cylindrical mirror analyzer (CMA) electron gun, differentialy pumped raster ion gun and X-ray source (Perkin Elmer,

Physical Electronics Division, Model 548). All the samples were analyzed in the same position, being perpendicular to the CMA axis. The Mg X-ray source was operated at 10 KeV and 40 mA with pass energy of 25 eV.
XPS and AES measurements were performed on each sample in the as received (AR) and after various times (up to 40 minutes) of Ar^+ sputtering. The sputtering was performed by a 2 KeV Ar^+ beam rastered on a 4x4 mm area. Full AES and detailed partial XPS spectra of the Fe $2p_{3/2}$ and Cr $2p_{3/2}$ were measured.

Results

The anodic polarization curve for the AISI 430 stainless steel in 4N nitric acid, at 600 mV/hour is presented in figure 1. The current-potential curve exhibits Tafel behavior at the passive-transpassive transition range with a slope of about 60 mV/decade. A limiting current density of 2.5 mA/cm^2 is reached at the transpassive zone.

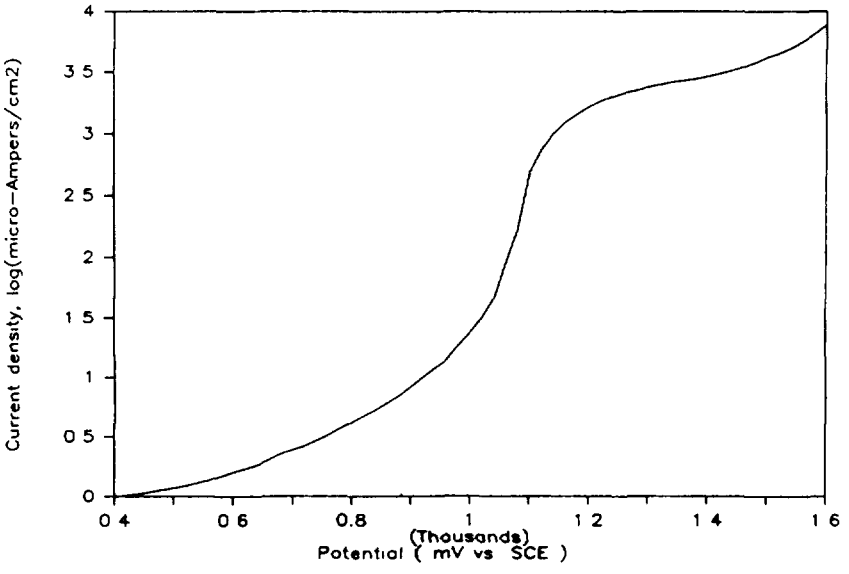

Fig. 1 Potentiodynamic polarization curve of AISI 430 stainless steel in 4N nitric acid.

XPS spectra of the Fe $2p_{3/2}$ and Cr $2p_{3/2}$ lines for the two samples are presented in figures 2, 3 for passive and figures 4, 5 for transpassive films. The Fe^{+3} and Fe^{+2} lines are shifted by about 4.2 and 2.5 eV respectively relative to metallic Fe [3]. The Cr^{+3} line is shifted by about 2.5 eV relative to metallic Cr [3]. Similar spectra of chromium and iron for passive films were reported [4, 5].

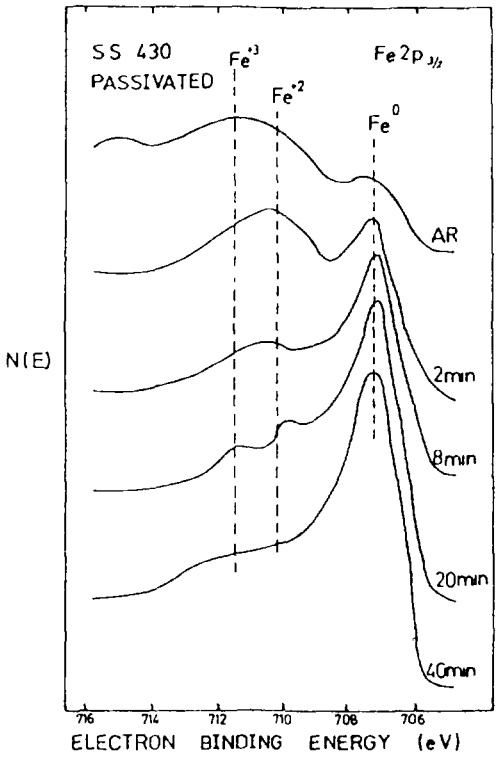

Fig. 2 Fe $2p_{3/2}$ XPS spectra of AR and of sputtered AISI S.S. 430 in the passive state. Dashed lines indicate the binding energies of Fe^{0}, Fe^{+2} and Fe^{+3}.

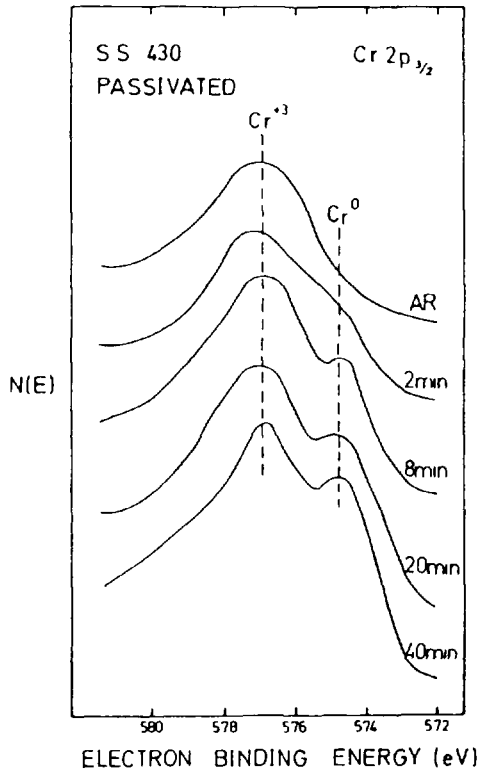

Fig. 3 Cr $2p_{3/2}$ XPS spectra of AR and sputtered AISI S.S. 430 in the passive state. Dashed lines indicates the binding energies of Cr^{0} and Cr^{+3}.

In the passive formed film, (figures 2, 3) enrichment of the Cr^{+3} is observed, especially at the metal-film interphase. Beyond this zone, a mixture of Cr and Fe oxides is observed, with Fe^{+3} at the outermost zone and Fe^{+2} at the inner section of the film. In the transpassive formed film, (figures 4, 5) only a slight Cr enrichment is observed in the film, with some presence of Fe^{+2} and Fe^{+3} at the outermost section of the film. No Cr^{+6} was observed.

The AES results describing the Cr/(Cr+Fe) ratio for the passive and transpassive zones are presented in figure 6. An appreciable chromium enrichment is observed for the passive formed film while the chromium enrichment of the transpassive formed film is observed to a lesser extent and may be attributed to the specimen exposure to atmosphere while being transferred form the electrochemical to the UHV system.

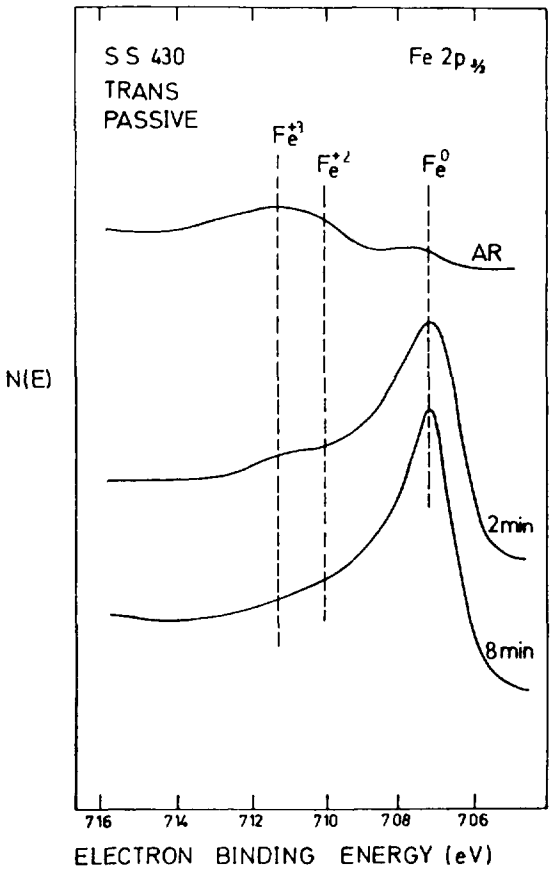

Fig. 4 Fe $2p_{3/2}$ XPS spectra of AR and sputtered AISI S.S. 430 in the trans-passive state.

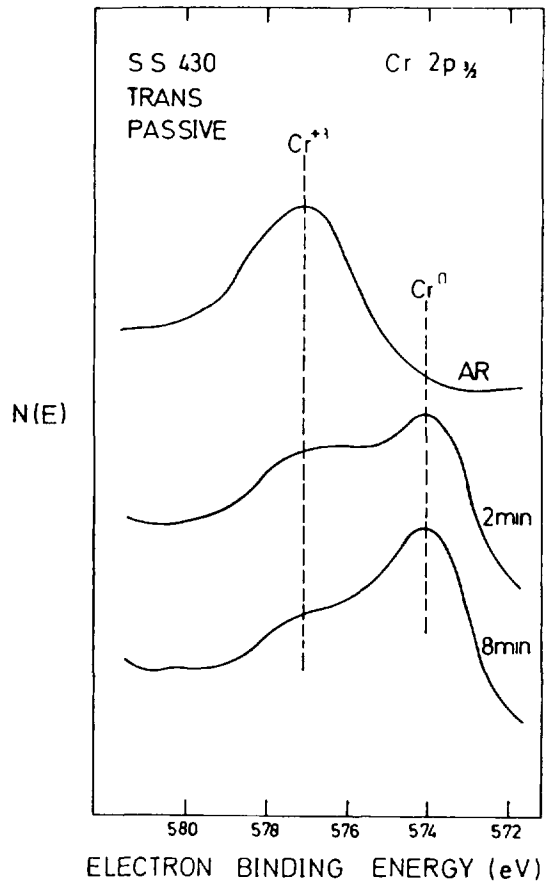

Fig. 5 Cr $2p_{3/2}$ XPS spectra of AR and sputtered AISI S.S. 430 in the trans-passive state.

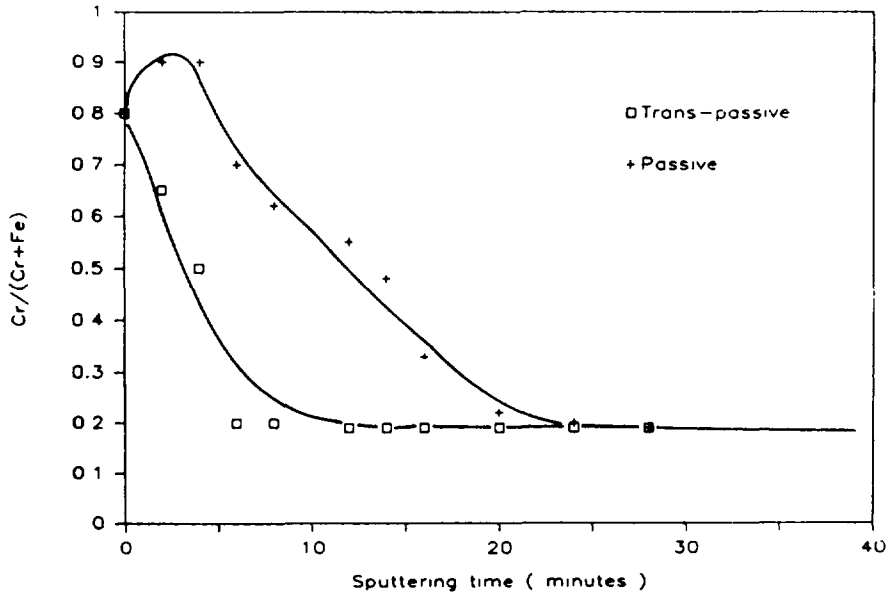

Fig. 6 Depth profiles of the AES Cr(LMM) line intensity of AISI S.S. 430 in the passive and trans-passive states.

Discussion

These experimental results imply that the shift form the transpassive to passive zone (the cathodic protection process) is characterized by formation of a well established passivating film. This conclusion was derived due the detection of two distinct phenomena:

a. Increase of the concentration ratio of the oxidized to the metallic states of the iron and chromium present in the film. This implies that films formed in the passive zone are thicker than those formed in the transpassive one, a fact which is also revealed by the Auger depth profiles.

b. A layered structure is formed in the passive zone, with a general surface chromium enrichment revealed throughout all the film profile. Three layers were detected: the one at the metal-film interphase composed mainly of Cr^{+3} oxide, and the two layers above it are composed mainly of mixed oxides of Cr^{+3}, Fe^{+2} and Fe^{+3}. The ratio of Fe^{+2}/Fe^{+3} is higher at the intermediate one and lower in the outer one. This layered structure characterizes a typical passive film as far as chromium enrichment [6] and Fe^{+2}/Fe^{+3} ratio are concerned [7].

References

[1] M. Ben-Haim, 3rd Israel Material Engineering Conference, (1985) 2.1.3.

[2] M. Ben-Haim, M.Sc dissertation, University of Manchester Institute of Science and Technology, (1980).

[3] C.D.Wagner, W.M.Riggs, L.E.Davis, J.F.Moulder, G.E.Muilenberg (Ed.), Perkin Elmer Co. Physical Electronic Div., (1979).

[4] J.E.Castle, C.R.Clayton, Corros. Sci., 17, (1979) 7.

[5] F.Mansfeld, J.V.Kenkel, A.B.Harker, Passivity of Metals, R.P.Frankenthal and J.Kruger, Eds., Electrochem. Soc., Princeton, NJ, (1978) 752.

[6] K.Asami, K.Hashimoto, S.Shimodaira, Corros. Sci., 16, (1976) 378.

[7] G.Okamoto, T.Shibata, Passivity of Metals, R.P. Frankenthal and J.Kruger, Eds., Electrochem. Soc., Princeton, NJ, (1978) 646.

LONG-TERM STORAGE PROBLEMS OF SPENT LWR FUEL ELEMENTS

B. ČECH, E. KADEŘÁBEK, J. KOUTSKÝ
Nuclear Research Institute,
Řež, Czechoslovakia

Abstract

The concept of spent fuel storage in Czechoslovakia is based on storage for 5 years followed by transport to the reprocessing plant. General considerations on fuel assembly integrity during its prolonged pool storage and transport of spent fuel container were given taking into account the possible effects of fuel burnup increase and load following mode of reactor operation.

---

1. Mechanisms of failures of LWR spent fuel assemblies during the long-term storage

The requirement of prolonged storage periods (3 – 5 – 10 years) of light-water power reactor spent fuel assemblies leads to a re-evaluation of mechanisms able to affect fuel element tightness and the release of fission products into the cooling water. Since the time, when a number of authors evaluated optimistically the potential mechanisms of failures of LWR spent fuel assemblies /1/, some changes of conditions have occurred. Knowledge of conditions of fuel loads during operational regimes has deepened and preconditions of increased time and power utilization of fuel have been established. Fuel burnup is being gradually increased so that the material margins, which guaranteed fuel integrity during its storage, have decreased. For the near future, load following mode of power reactor operation is being considered. As has been evidenced, the cyclic changes of power have specific effects from the point of view of fuel loading. These effects, though not decreasing fuel reliability under operating conditions, can manifest themselves adversaly during storage of spent fuel. From the point of view of these conditions it is reasonable to evaluate the probable mechanism of degradation with delayed or long-term effect, which would be able to threaten the stability of spent fuel element cladding and

which would require further examination. It is also necessary to consider the changes brought about by the development of fuel assembly design.

Supposin g that the hermetic fuel assemblies only are deposited for the long-term storage, tightness of cladding can fail because of corrosion effects from inner or outer sides of a fuel element. Mechanical failure caused by external forces can occur only under special circumstances (handling, impact, etc.). The stresses in fuel element cladding, caused by the inner force, are therefore especially important.

1.1 Mechanical stresses in spent fuel elements during the long-term storage

Spent fuel is under operational conditions deformed by sufficiently known mechanisms. Mechanical interaction of fuel pellets and cladding (PCI) leads to cladding deformation. Fuel element cladding deformation is characterized by the localization according to the conditions of PCI. Non-homogeneous stress from local contact of pellet and cladding is superimposed on the homogeneous stress caused by inner and outer overpressures of gases on the walls of cladding.

Many studies have been carried out enabling us to assess the mechanical stress in the cladding under the fuel operating conditions in the reactor. These studies led to some modifications of fuel elements, mainly to the increase of the filling gas (He) pressure. It is not possible to assume that, after the modifications, the stress in the cladding walls will thoroughly relaxe itself before storage. The response to inner stress is complicated by a pronounced anisotropy of mechanical properties of zirconium alloys for fuel element cladding as has been experimentally verified for Zr-1Nb, Zircaloy 2, and Zircaloy 4 alloys /2/, /3/. It can be concluded, that the localized stress in the cladding walls can lead to a delayed failure under the pool conditions despite no reliable experimental evidence has been given so far. The stress in the cladding wall is of fundamental importance in appreciation of possibility of stress corrosion cracking (SCC) of the cladding.

1.2 Corrosion of spent fuel elements during storage

On the basis of present knowledge of corrosion mechanism, there is a low probability of existence of a time-delayed process, which would lead to rapid deterioration of fuel cladding ability to retain the radionuclides.

Fuel cladding failure caused by homogeneous corrosion can be practically excluded because the corrosion rate of zirconium alloys in water under the given conditions is very low. Local corrosion under the layer of corrosion products, corrosive reactions of fission products on the inner surface, and local corrosion at the positions of welds, slots, and joints of fuel components is to be considered. Even the local precipitation of hydrides after a high level of hydriding of spent fuel during temperature variations cannot be omitted. These processes increase the danger of loss of tightness of fuel elements during handling of spent fuel, but it is not possible to prove their connection with the changes of conditions of fuel exploitation because they develop themselves not before the period of fuel disposal.

1.3 Oxidation of fuel in defective spent fuel elements

It is known that oxidation of UO_2 leads to its transformation into U_3O_8 and to an increase of volume of fuel pellets. The so called hairline crack, which is temporarily closed by corrosion products after pressure equalizing, is one of the types of cladding defects. As is presented in /4/, fuel volume expansion by oxidation is little probable under the conditions of storage, because formation of U_3O_7 with no substantial volume expansion occurs at temperature below 250 °C. Behaviour of spent fuel during dry transport, when fuel temperature can achieve higher values, is, however, an important question. Total oxidation of UO_2 can be then prevented by maintaining the inert environment. In the opposite case the oxidation of UO_2 will lead to an increased stress in cladding.

1.4 Simultaneous effects of inner and outer stresses during spent fuel storage

Under the conditions of high quality of pool water, the corrosion deposits from the reactor primary circuit have also real significance. Their

effect must be considered simultaneously with the mechanisms of fuel element cladding failures. From the point of view of corrosion, the porous deposits are more dangerous than adhesive layers. It is presented in /5/ that thin layers of corrosion sediments, which could be wiped off by a pad, were found on the surfaces of spent fuel elements of VVER-365 reactor (burnup of 19 100 MWd/t U). This fact is significant when the period of storage is being increased and the present components of corrosion are evaluated in a complex way. The presence of chemically active fission products inside the fuel elements and corrosive deposits on the outer surface of claddings can participate in the stress corrosion cracking and in a delayed formation of leakage of the stored fuel. A check of residual stresses in the cladding after high burnup would be certainly a complex problem, but it is possible to expect its considerable significance for the loss of tightness probability evaluation of the long-term-stored spent fuel assemblies. With parameters of fuel utilization increasing, it is possible to expect also changes of long-term behaviour of spent fuel under the storage conditions.

2. Storage of spent fuel assemblies of the VVER-type reactors in Czechoslovakia

2.1 Present conditions of storage

Development of the Czechoslovak nuclear power is based on construction of VVER-type LWRs with unit capacity of 440 and 1000 MW. Five units with the VVER-440 reactors are in operation at present and units with VVER-1000 reactors are in the stage of construction. In Table 1, the parameters of the VVER-type reactors, which are applicable to storage of spent fuel, are presented.

The concept of storage of spent fuel is based on storage for 5 years followed by transport to reprocessing plant. For the first three years, at-reactor storage (AR) is assumed. For the remaining two years, the fuel is supposed to be stored in away-of-reactor interim store (AFR).

TABLE 1. SELECTED PARAMETERS OF THE VVER REACTORS

	VVER-440	VVER-1000
Reactor core uranium inventory, t	42	66
Fresh fuel enrichment	3.5	3.3 - 4.4
Fuel burnup	28.6×10^3	$(26.0-40.0) \times 10^3$
Spent fuel enrichment	1.2	1.26
Number of assemblies in the reactor	349	151
Mass of uranium in an assembly, kg	120	437
Dimensions of an assembly, mm	144	238

Spent fuel assemblies are stored vertically in a basic rack, on which it is possible to locate an additional storage rack with simultaneous increase of water level in the pool. Fuel assemblies with loss of tightness detected during outage are stored in sealed capsules. Most assemblies are, however, stored freely. The upper level of water (+21 m) enables transport of spent fuel under the protective water layer above the transport channel head. Heat removal is ensured by two independent cooling circuits with capacity of 350 m^3/hr. Water in the pool contains 12 g of boric acid in 1 kg and its temperature must not exceed 50 °C at the exchanger inlet. The design assumes the possibility of periodic purification of water in case of necessity. Transport of fuel assemblies is carried out in transport containers, the parameters of which are presented in Table 2.

TABLE 2.

Containers VVER-440	Vertical cylinder, D=2.2 m, H=4.1 m Wall thickness of 360 mm Mass of uranium of 3.8 t UO_2 Number of fuel assemblies: 30
Containers VVER-1000	Horizontal cylinder, D=2.1 m, L=6.1 m Wall thickness of 410 mm Mass of uranium of 3 t UO_2 Number of fuel assemblies: 9

2.2 Perspective concepts of storage

In design studies, the possibility of increase of at-reactor (AR) storage capacity by means of more dense arrangement of the stored spent fuel assemblies has been also considered. A specific feature of VVER-type reactor storage pools consists in the fact, that the cooling water contains boric acid, which by itself enables a relatively dense filling of the storage rack. For reconstruction, a decrease of triangular rack pitch from the original 225 mm to 160 mm was proposed.

2.2.1 Cooling for compact arrangement

Supposing that the cooling system remains unchanged, it is important to verify, whether the cooling capacity is sufficient with simultaneous preservation of safe subcriticality /6/. It is assumed, that the water purification system will be satisfactory because of its periodic mode of operation.

It is assumed for the store with the current rack:

Basic rack	379 storage locations
Additional rack	350 storage locations

For the store with the compact arrangement:

Basic rack	712 storage locations
Additional rack	350 storage locations

The determination of decay power was based on the following sources of heat:

a) the aftermath of fission reaction
b) β - and γ - radiation of fission products
c) β - and γ - radiation of the Np chain
d) α - radiation of decay chains of transuranides
e) radiation of activated structural material

Only the components b) and c) were practically considered in calculation.

The component caused by β - and γ - radiation of fission products:
The relative power is given generally by the relation

$$\overline{P}_A = \frac{P_A(t, \tau)}{P_o} = K_A \left[Q_A(t) - Q_A(t+\tau) \right]$$

The component caused by β - and γ - radiation of the Np chain: This component applies only in time interval from 10^4 to 10^5 s.

The equation for relative power is similar to that for the fission products.

t is time after the reactor shutdown /s/

τ is time of fuel operation at power /s/

P_o is fuel assembly power during operation /MW/

K_A is safety factor

The total relative power is, therefore, given by the relation:

$$\bar{P} = \bar{P}_A + \bar{P}_B$$

The following values were considered in calculation:

P_o = 3.94 MW

τ = 7500 hrs

t_o = 8760 hrs

The results of calculations of decay power are shown in Table 3.

TABLE 3.

Year of storage	normal rack store		compact rack store	
	number of filled storage locations	gross power of fuel in the store MW	number of filled storage locations	gross power of fuel in the store MW
1.	126	1.101	118	1.031
2.	252	1.306	236	1.223
3.	376	1.456	354	1.364
4.	378	1.518	472	1.448
5.	378	1.540	590	1.553
6.	378	1.540	708	1.576
7.	378	1.540	708	1.586
8.	378	1.540	708	1.586
9.	378	1.540	708	1.586
10.	378	1.540	708	1.586

It can be seen from the Table 3 that, in case of filled store with the current rack, the total power transferred to water is 1.54 MW; the power in the case of compact rack is 1.58 MW and, after re-calculation on the case of filled store (712 locations), the power would be 1.60 MW. The power for compact rack is, therefore, only by 3 % higher compared to the store with the current arrangement.

Also in the case of reactor scram and discharge of fuel from the reactor after three operational fuel cycles the heat transferred to the coolant for the compact store is only by 1 % higher and amounts to approximately 5 MW.

From the analysis and calculation, it is therefore possible to conclude that the present cooling system, dimensioned for removal of 8 MW, enables application of dense arrangement of spent fuel in the storage pools of VVER reactors.

A preliminary calculation of subcriticality has been also carried out. Metal sheet with 1.1 % of boron was considered as the rack material. The results of subcriticality calculations for various enrichments and burnups are presented in Table 4.

TABLE 4. RESULTS OF SUBCRITICALITY CALCULATION

assembly designation	No. of fuel cycle	enrichment (%)	length of fuel cycle (d_{eff})	burnup (MWd/t)	k_{∞}
A	1	1.6	317	10680	0.52
B	1	3.6	317	9900	0.68
C	2	2.4	254	20555	0.56
D	2	3.6	254	19836	0.64
E	3	3.6	271	29674	0.60
F	0	3.6	0	0	0.73

As can be seen in the Table 4, the quantity k_∞ is sufficiently low to meet the required safety.

Lately, the problems of suitable material of absorptive capsules an basis of boron is being solved. Functional tests of various materials were carried out and verification of their absorptivities is in progress in a research reactor.

References

/1/ NEA Seminar on Storage of Spent Fuel Elements, Madrid 1978, ISBN 92-64-01840-9.

/2/ Tenckhoff, E.: Operable Deformation Systems and Mechanical Behaviour of Textured Zircaloy Tubing... in Zirconium in Nuclear Applications, ASTM STP 551, 1974, p. 179.

/3/ Čech, B., Hamouz, V.: Experimental Research of Cladding Tubes for VVER Reactor Fuel Elements from the Point of View of Operational Stresses. Report ÚJV 7535-M, Řež, 1985. (In Czech).

/4/ Boase, D. G., Vandergraaf, T. T.: Nucl. Technology, 32, 1977, p. 60-71.

/5/ Operational Regimes of Light Water Power Reactors. Atomizdat, Moscow 1977. (In Russian).

/6/ Schubert, , Hrouda, .: Compact Storage of Spent Fuel. EGP Study, 1985. (In Czech).

ZIRCONIUM USE FOR LARGE PROCESS COMPONENTS

H. CHAUVE*, J. DECOURS**, R. DEMAY[+],
M. PELRAS [+], J. SIMONNET[++], G. TURLUER[+]

* Société générale pour les techniques nouvelles,
Saint-Quentin en Yvelines

** CEA, Institut de recherche technologique et de développement industriel,
Saclay

[+] CEA, Institut de recherche technologique et de développement industriel,
Fontenay-aux-Roses

[++] Cogéma,
Saint-Quentin en Yvelines

France

Abstract

ZIRCONIUM BEHAVIOUR IN NITRIC MEDIA

Austenitic stainless steels display satisfactory behaviour in reprocessing facilities. However, certain failures are occasionally observed and usually ascribed to corrosion in oxidizing nitric media capable of bringing these materials close to or within the transpassive range.

Zirconium does not present this drawback and helps to solve corrosion problems in these particularly aggressive conditions for stainless steels.

Zirconium generally displays an outstanding general corrosion resistance in nitric acid media. In practice, however, its use in reprocessing facilities leads to the consideration of certain factors that may either restrict its application, or should be closely investigated.

The most important among these are :

- fluoride content of the medium
- nitrogen content of the metal
- formation of possible insoluble compounds despite very low ionic release rates
- stress corrosion cracking observed only in some severe laboratory testings.

DEVELOPMENT AND APPLICATION TO REPROCESSING EQUIPMENT

It was decided to use zirconium in the new facilities at La Hague for most of the weld-fabricated equipment treating boiling nitric solutions and for a number of specific process units (for example, reactors containing sulphides in acidic media). A total of 80 tons of zirconium will be employed, and 5,500 meters of piping circuits are being installed with this material.

This was achieved through the development of semi-finished products (plates, pipes, etc.) with properties adapted to the construction of the large weld-fabricated units of nuclear chemistry. Shaping, welding and inspection specifications have been developed. Finally, the choice and development of zirconium were facilitated by the use of zirconium-stainless steel junctions allowing the connection of a zirconium unit to a stainless steel piping system.

---

1. ZIRCONIUM BEHAVIOUR IN NITRIC MEDIA

1.1. Introduction

Stainless steels with very low carbon content are the most widely used in nitric media. Their behaviour is generally satisfactory but, when used in extreme conditions, they are subject to intergranular corrosion that can lead to failures.

Zirconium and its alloys in nitric acid display much better characteristics regarding general corrosion and are insensitive to intergranular corrosion.

The advantage of zirconium over stainless steels and titanium will be detailed. Then the results of tests concerning the influence of the metallurgical states and composition, and the effects of galvanic coupling with stainless steel in nitric media will be given. Finally, the influence of some adverse factors which may be met in industrial environment will be shown. These factors are :

- presence of fluoride ions in the medium
- presence of nitrogen in the metal
- presence of phosphoric acid in the medium
- presence of stresses under corrosive conditions [1].

1.2. Comparative corrosion resistance of zirconium, stainless steel and titanium

Various tests were carried out on these three metals. The main results are summarized in Fig. 1, 2, and 3.

In boiling nitric acid, the corrosion rate of zirconium and its alloys is considerably lower than that of stainless steel. With the presence of oxidizing ions, such as Cr VI, Pu VI, this advantage is even more evident in view of the very high corrosion rate of stainless steel, with the exception of that containing 4 % silicon, which has a good resistance to intergranular attack in oxidizing nitric medium.

Titanium also displays a low corrosion rate in these media, but a specific form of corrosion can be observed in vapour phase. Such corrosion appears in the form of white, non-adhesive oxide (TiO_2) above liquid level, in the condensation zone. This can be explained by the constant trickling of acid condensate, which prevents the formation of a sufficiently stable passive oxide film. A vessel filled with uranyl nitrate acid solution at 120°C during one month is shown in Fig. 4. A similar phenomenon was also observed on samples partially immersed in boiling nitric acid [2] [3].

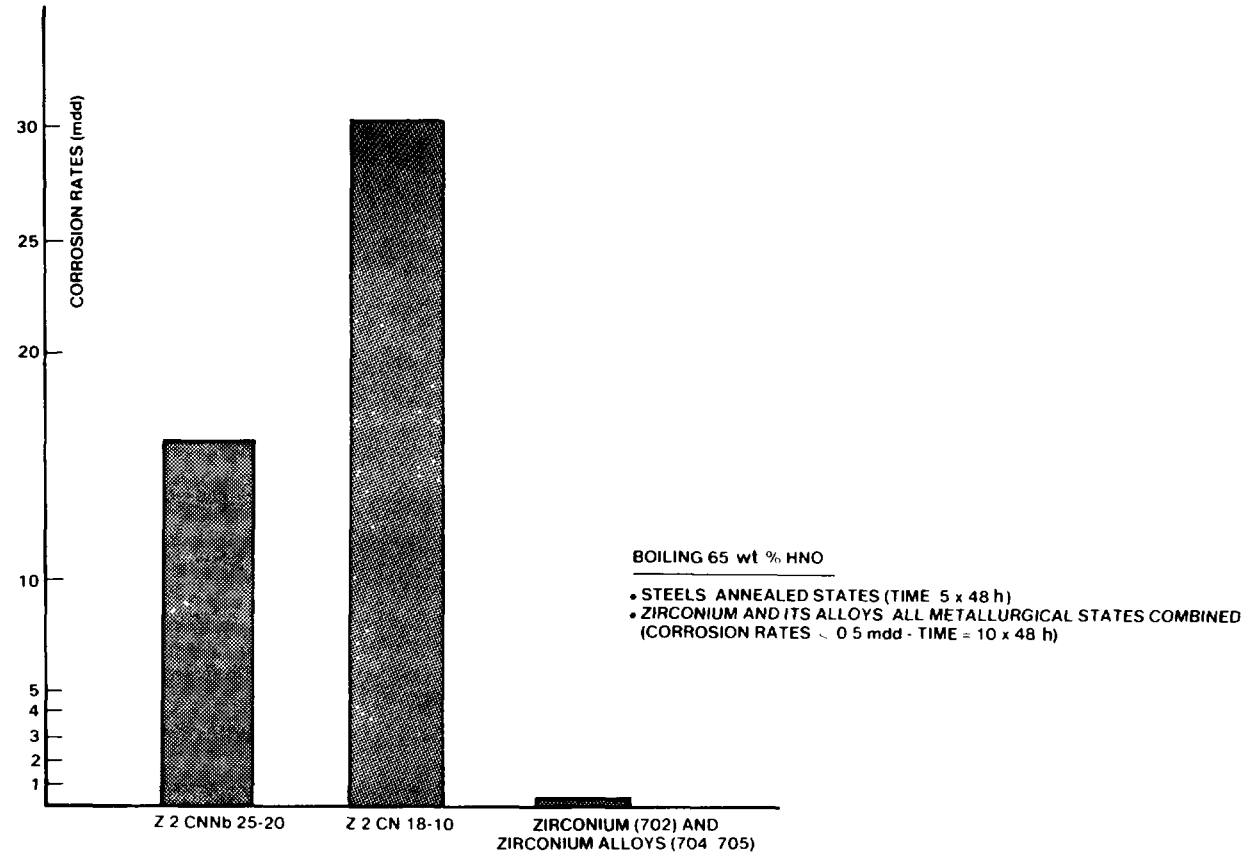

Figure 1 : Corrosion rates of zirconium and stainless steels in boiling nitric acid

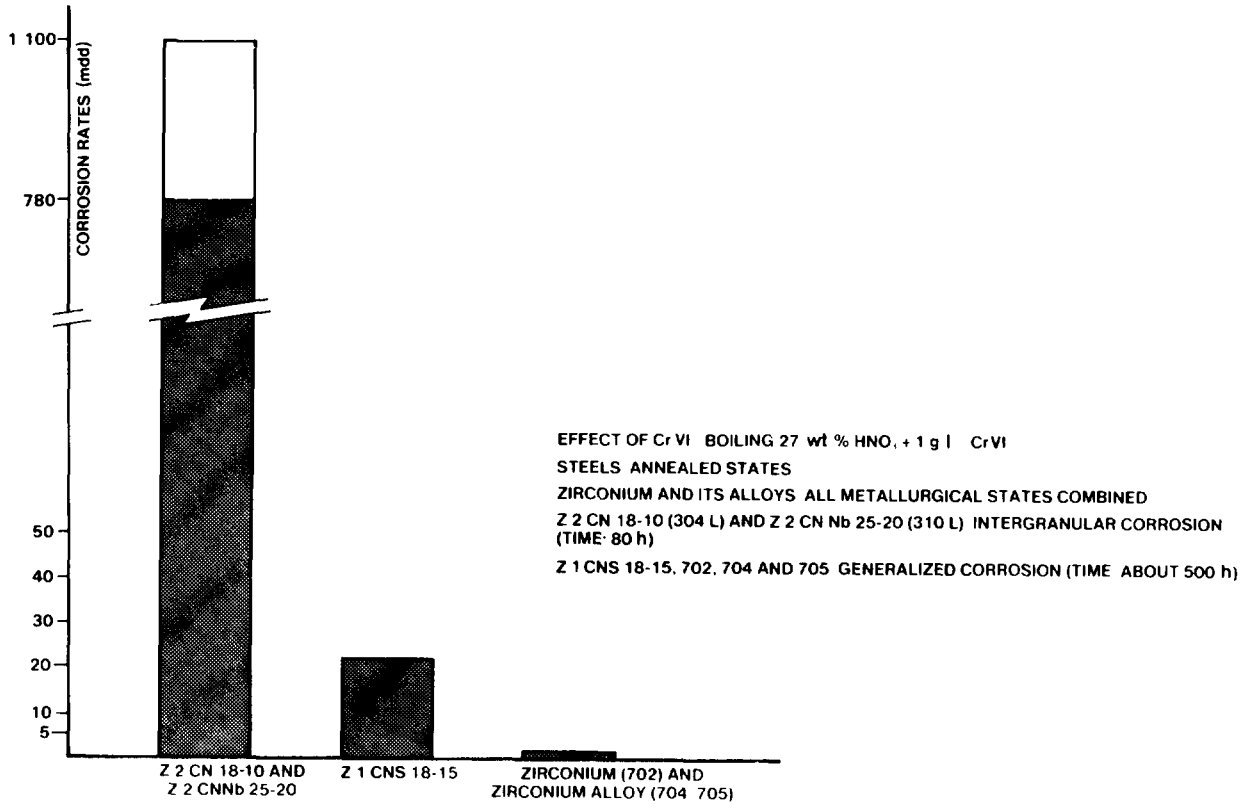

Figure 2 : Corrosion rates of zirconium and stainless steels in boiling nitric acid containing Cr VI

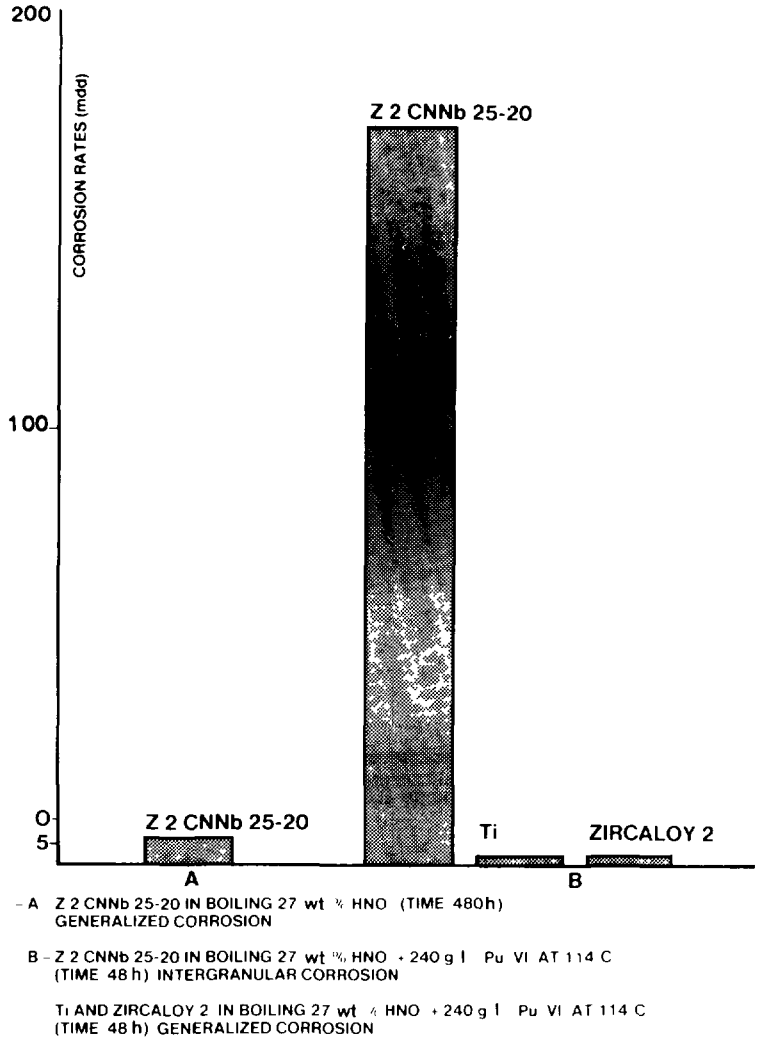

Figure 3 : Corrosion rates of zirconium and stainless steels in boiling nitric acid containing Pu VI

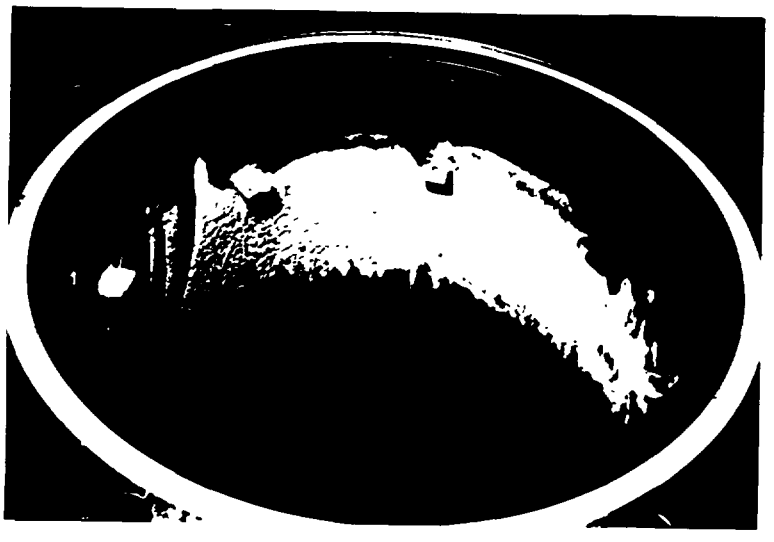

Figure 4 : Titanium grade 2 vessel (40 dm^3) containing uranyl nitrate solution at 120°C - Testing time : one month

Under identical conditions, zirconium and its alloys remain insensitive to this form of corrosion.

1.3. Behaviour of zirconium and its alloys in nitric medium

1.3.1. Influence of the metallurgical states

This influence was studied for the three usual zirconium alloys, (grades 702, 704, and 705) in eight different metallurgical states and in two different media. See Table 1 for details of the composition, the metallurgical states and the test conditions.

TABLE I - Influence of the metallurgical states

METAL COMPOSITION, ppm, AS-RECEIVED			
Elements	Grade 702	Grade 704	Grade 705
Al	58	32	...
C	54	114	220
H	3	1	14
Hf	2,600	<30	90
N	30	26	50
Ni	20	<50	...
O	1,200	1,200	...
Si	30	78	...
Ti	31	21	...
Cr	93	1,100	...
Fe	475	2,300	...
Sn	<10	14,900	...
Nb	...	...	25,000
Fe+Cr	...	...	800

- Metallurgical states
  - fine-grain recrystallized (650°C)
  - strain-hardened
  - coarse-grain recrystallized (650°C)
  - annealed in α region (800°C)
  - annealed in α + β region (900°C)
  - β quenched (1,000°C) (water cooled)
  - β annealed (1,000°C) and cooled under argon
- Test specimens
  - taken from 2mm thick plate
  - dimensions 30 by 40 mm
  - treated in nitric/hydrofluoric acid pickling bath (thickness loss about 30 μm)
- Definition of environments
  - 65 wt% HNO_3 at 121°C
  - 27 wt% HNO_3 + 1 $g.l^{-1}$ Cr VI at 106°C

In all cases, the corrosion rates proved to be extremely low, less than 0.5 mdd ($mg.dm^{-2}.day^{-1}$). Examination of the test specimens revealed a uniform brown or black appearance, and no form of intergranular or local corrosion at all. This confirms the excellent results cited in the literature [4], showing that for these grades, the corrosion resistance does not depend on the metallurgical state.

1.3.2. Zirconium / austenitic stainless steel galvanic coupling

In a plant, the use of zirconium for exposed equipment raises the problem of connections with the other stainless steel portions of the installation. The effects of galvanic coupling between these two types of material was investigated by corrosion tests performed under the following conditions :

- Type of coupling :
  - . Zircaloy 2 (grade 704) / Uranus 65 (310 L) Cr 25 wt%, Ni 20 wt%, Nb 0.2 wt%, C < 0.02 wt%.
  - . Zircaloy 2 (grade 704) / Z 2 CN 18-10 (304 L) Cr 18 wt%, Ni 10 wt%, C < 0.03 wt%.
- Environments :
  - . HNO_3 27 wt% at 106°C,
  - . HNO_3 65 wt% at 120°C,
  - . HNO_3 27 wt% + $Ca(NO_3)_2$ at 545 $g.l^{-1}$ at 119°C.
- Coupled test specimens were equal in surface area, interconnected by a stainless steel conductor kept outside the solution, to avoid any crevice effect.
- Weight loss measurements and metallographic examinations were carried out.

After ten days of testing, the behaviour of the Zircaloy 2 and Uranus 65 were unaffected by the coupling.

For the 304 L steel, a coupling effect was observed in 27 wt% nitric acid at 106°C which was a slight increase in the generalized corrosion rate. In 65 wt% nitric acid at 120°C, some incipient intergranular corrosion was also observed. To prevent this effect, junctions between the two materials have to be kept at lower temperature, for instance 60°C, at which no effect can be seen.

Additional electrochemical coupling tests were performed on industrial junctions kept at this temperature. Continuous monitoring of galvanic current and coupling potentials and the interpretation of the data with potentio-dynamic polarization characteristics showed that, under steady-state design conditions, the galvanic coupling of Zircaloy 2 with 304 L steel has no significant effect on steel corrosion.

1.4. Tests in industrial environments

1.4.1. Influence of hydrofluoric acid in the medium

The addition of hydrofluoric acid or fluoride ions to nitric acid produces conditions that can be highly corrosive to zirconium. Tests were undertaken to determine maximum fluoride concentrations leading

to moderate zirconium corrosion rates, e.g., less than 5 mdd. The same types of test specimen as those described in Table I were tested in the following boiling environments :

- HNO_3 27 wt% ; HF additions ($mg.l^{-1}$) : 0, 1, 2, 10, 20.
- HNO_3 40 wt% ; HF additions ($mg.l^{-1}$) : 0, 1, 2, 10.

Table II shows the results obtained after 240 hours of immersion.

TABLE II - Influence of hydrofluoric acid in the medium

Grade	Hydrofluoric acid (HF), mg-1 1				
	0	1	2	10	20
			Boiling 27 wt% HNO_3		
702	<0 5	1 to 2	7 to 9	103 to 120	240 to 270
704	<0 5	1 to 2	8 to 12	115 to 166	240 to 300
705	<0 5	0 5 to 1	5 to 9	48 to 60	140 to 170
			Boiling 40 wt% HNO_3		
702	<0 5	4 to 6	10 to 20	130 to 200	
704	<0 5	4 to 5	12 to 20	120 to 240	
705	<0 5	1 to 2	10 to 18	80 to 100	

Corrosion rates of zirconium are expressed in mdd (1 mdd = 5 5 μm year ^{1})

It can be seen that grades 702 and 704 display closely comparable behaviour, whereas grade 705 exhibits a substantially lower corrosion rate. Above a fluoride concentration of about 2 $mg.l^{-1}$, the corrosion rate of zirconium increases much faster than fluoride concentration.
To make a comparison with stainless steel, the maximum fluoride concentration to maintain a corrosion rate below 5 mdd is 1 $mg.l^{-1}$ for zirconium, whereas it is about 10 $mg.l^{-1}$ for stainless steel.

Possible effects of metallurgical states were investigated. No significant difference was observed.

1.4.2. Influence of nitrogen in the metal

Nitrogen contamination of zirconium can alter its corrosion resistance to water at high temperature. Since some zirconium equipment is heated by water at 150 to 200°C flowing in tubes or in double walls, tests were performed to investigate this effect. Samples of grade 702 only, with a nitrogen content of 150 and 300 ppm were used, together with grade 702 and 704 with usual nitrogen content (about 30 ppm). Figure 5 shows the results in the form of corrosion kinetics, plotting weight gain versus time.

For the samples with standard nitrogen content and for the grade 702 sample with 150 ppm content, the shape of the curve indicates that corrosion kinetics is controlled by the build-up of a protective oxide layer. This is not the case for the grade 702 sample with 300 ppm content; the corrosion kinetics curve is linear, which means that the oxide formed provides less protection. The service life of a component built with grade 702 having a 300 ppm nitrogen content will necessarily be much shorter than that of a component built with the same grade, but with a normal nitrogen content.

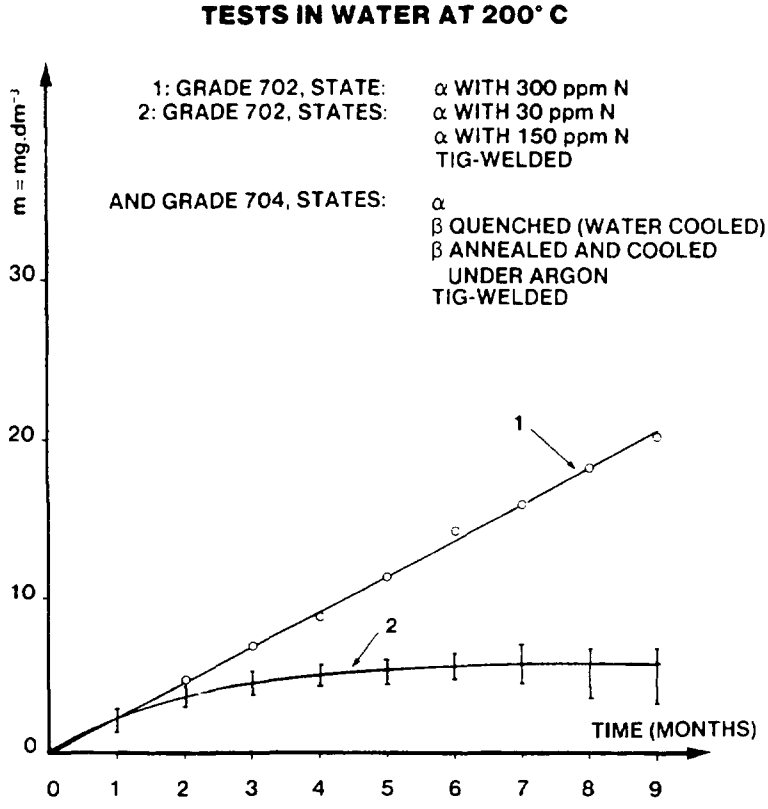

Figure 5 : Influence of nitrogen in the metal . Corrosion kinetics (weight gain)

For equipment submitted to high temperature water, nitrogen content of grade 702 should not be in excess of 100 ppm.

1.4.3. Influence of phosphoric acid in the medium

Some solutions in reprocessing equipment contain phosphoric acid in nitric acid medium. The literature considers that corrosion resistance is satisfactory in a medium consisting of 30 wt% phosphoric acid [5]. The effects of phosphoric acid additions (between 1 and 10g.l^{-1}) to boiling 24 and 40 wt% nitric acid were investigated. Under these conditions, white stains and marbling were observed on the samples, certainly due to insoluble zirconium phosphate. Very low weight increases were recorded at less than 0.5 mdd after 70 days, which is quite satisfactory. However, care must be taken for the insoluble phosphates sent to the process.

1.4.4. Stress corrosion cracking (SCC) experiments

Some laboratory investigations [6] [7] have shown that zirconium and its alloys display sensitivity to SCC in nitric acid environment for a concentration above 20 wt%, raising a doubt about the use of these materials in industrial service. Two series of SCC tests were performed in boiling 32 and 65 wt% nitric acid on grades 702 and 704, with the following objectives :

- to demonstrate a possible sensitivity to SCC by constant strain rate tests,

- to check whether this possible sensitivity was confirmed under conditions of industrial service, which are far less severe than those of the constant strain rate tests. Constant strain tests, which are easy to implement, were considered more representative and were chosen to get practical results for engineering purposes.

- Constant strain rate tests

Constant extension rate tests (CERT) were actually performed, on a tensile testing machine at very low strain rates (10^{-6} to $10^{-7}.s^{-1}$), at different temperatures. The metallurgical state of the cylindrical (3 mm diameter) test specimens was that of fine-grained recrystallization at 650°C for 2 hours. The specimens had been machined from a rolled plate, with the axis in the transverse direction. The tensile stress direction was thus perpendicular to the rolling direction. In certain cases specimens were submitted to an imposed potential to simulate specific oxidizing conditions. Table III describes experimental conditions.

TABLE III - Experimental conditions for the constant strain rate tests

Grades	wt% HNO_3	Temperature °C	Potential	Strain rate s^{-1}
702, 704	65	25	free	10^{-6}
704	65	121	and imposed	10^{-6}
704	32	25	free	10^{-6}
704	32	106	free	10^{-6} and 10^{-7}

TABLE IV - Constant strain rate tests results

Grade	wt% HNO_3	T, °C	Potential, mV / SCE	Maximum stress, MPa	Maximum strain, %	Remarks
			...	412	25. 8	reference test, air 25°C
702	65	25	+ 500	378	28. 4	no crack
			(free) + 850	378	35	cracks
			+ 1,100	381	22. 8	many cracks
			...	271	25. 3	reference test 100°C
704	65	25	+ 800	399	19. 33	many cracks
			(free) + 950	378	29. 2	many cracks
			+ 1,000	390	20. 6	many cracks
			+ 1,100	408	12. 5	many cracks
			+ 600	297	36. 5	cracks
			+ 800	279	38. 6	many cracks
704	65	121 (boiling)	(free) + 950	306	35. 6	many cracks
			+ 1,100	300	25. 3	many cracks
			+ 1,200	280	6. 2	cracks
704	32	25	free	...	...	no crack
704	32	106 (boiling)	free	...	...	cracks

The results given in table IV indicate that a SCC phenomenon may be involved, as shown by a reduction of the maximum strain observed in some instances and confirmed by the result of fractographic scanning electron microscope inspections performed after the complete rupture of the specimens.

Cracking, when observed, was not accompanied by any significant decrease of the apparent mechanical characteristics. In particular, maximum stress observed during the test was not changed. Moreover, it appeared that most of the strain occurred at an almost constant stress level, very close to the ultimate tensile strenght, scattering being taken into account. These observations indicate that an occasional SCC phenomenon would occur only in a range of stress and strain close to mechanical rupture, which is far from the range of industrial use.

- Constant strain tests

The test specimens were taken from 10 and 4 mm plates, rolled by successive passes to a 1 mm final thickness. The final cold rolling rate was 50%. The specimens were then subjected to two types of heat treatment :

- fine-grain recrystallization at 650°C for 2 hours,
- annealing in the β region at 1,000°C for 5 min, with slow cooling under argon.

Both longitudinal and transverse cut specimens were used. All the samples were cut in the form of rectangle parallelipipeds, 50 × 10 × 1 mm, and tested in U-bend and four-point loading test rigs under the conditions recorded in Table V. Transversally TIG-welded specimens were also tested, with direction of tensile strength parallel to that of rolling.

TABLE V - Experimental conditions for the constant strain tests

Type of mounting	wt% HNO_3	Phases	Temperature °C	Additional species
"U-bend"	65	liquid	25	...
ASTM n° G 30	65	liquid	121 (boiling)	
Rolled specimens	32	liquid	106 (boiling)	
	32	liquid	106	I_2 (2g . l^{-1})
"U bend"	65	liquid	121 (boiling)	
ASTM n° G 30	32	liquid	106 (boiling)	
Rolled and	32	liquid	106	I_2 (2g . l^{-1})
transversally	32	vapor	106 (liquid	I_2 (2g . l^{-1})
TIG-welded			phase)	
specimens				
Four-point	65	liquid	121 (boiling)	
loading	32	liquid	106 (boiling)	CrVI (1g . l^{-1})
ASTM n° G 39				

Optical examination (binocular microscope, magnification = 50) was carried out monthly. Micrographic examinations were performed at the end of the tests.

Whatever the type of assembly and loading employed, after one year of immersion no single test revealed any sensitivity to stress corrosion cracking. Micrographic observation revealed cracks (depth 100 μm) of mechanical origin on β-quenched transverse cut specimens.

It is quite remarkable that these cracks did not show any tendency to grow in the HNO_3 65 wt% at 121°C test.

1.5. Conclusion

The experiments described above confirm that zirconium is an excellent material for service in nitric environment. Its behaviour is much better than that of stainless steels, over which its advantage is decisive, especially in environments leading stainless steels into transpassive conditions, such as in boiling 65 wt% nitric acid. Unlike titanium, it is unaffected by trickling condensates above boiling nitric acid.

The addition of phosphoric acid to nitric acid in zirconium vessels may cause the formation of insoluble salts, and a possible release of precipitates to the process. For phosphoric addition up to 10 $g.l^{-1}$, corrosion rate of zirconium is not significantly affected.

The addition of hydrofluoric acid increases zirconium corrosion rate higher than those of stainless steels. The corrosion rate remains acceptable for fluoride concentration below 1 $mg.l^{-1}$.

When zirconium is in contact with water at 150 to 200°C, the nitrogen content of zirconium must be closely followed in order to limit it to about 100 ppm.

The tests carried out in nitric acid up to 65 wt%, prove that for industrial use the risk of stress corrosion cracking is extremely low and does not have to be taken into account.

2. USE OF ZIRCONIUM IN WELDED EQUIPMENT

2.1. Introduction

Since the tests described above proved that zirconium offers decisive advantage, the use of this material was considered for the equipment of the La Hague extension facilities, which are subjected to severe corrosion conditions. Before making the final choice, it was necessary to get a fuller knowledge of the product for this application (characteristics of zirconium used as fuel cladding are well known) and to check practical aspects of its implementation. Important technological developments were necessary to achieve these goals.

The most important stages of these developments will be described first, then the various items of equipment involved and their main characteristics will be described.

2.2. Technological developments

The main problems concern :

- procurement of plates, pipes, and other items
- zirconium forming
- large-scale zirconium equipment welding
- heterogeneous connections for joining zirconium equipment to austenitic stainless steel piping.

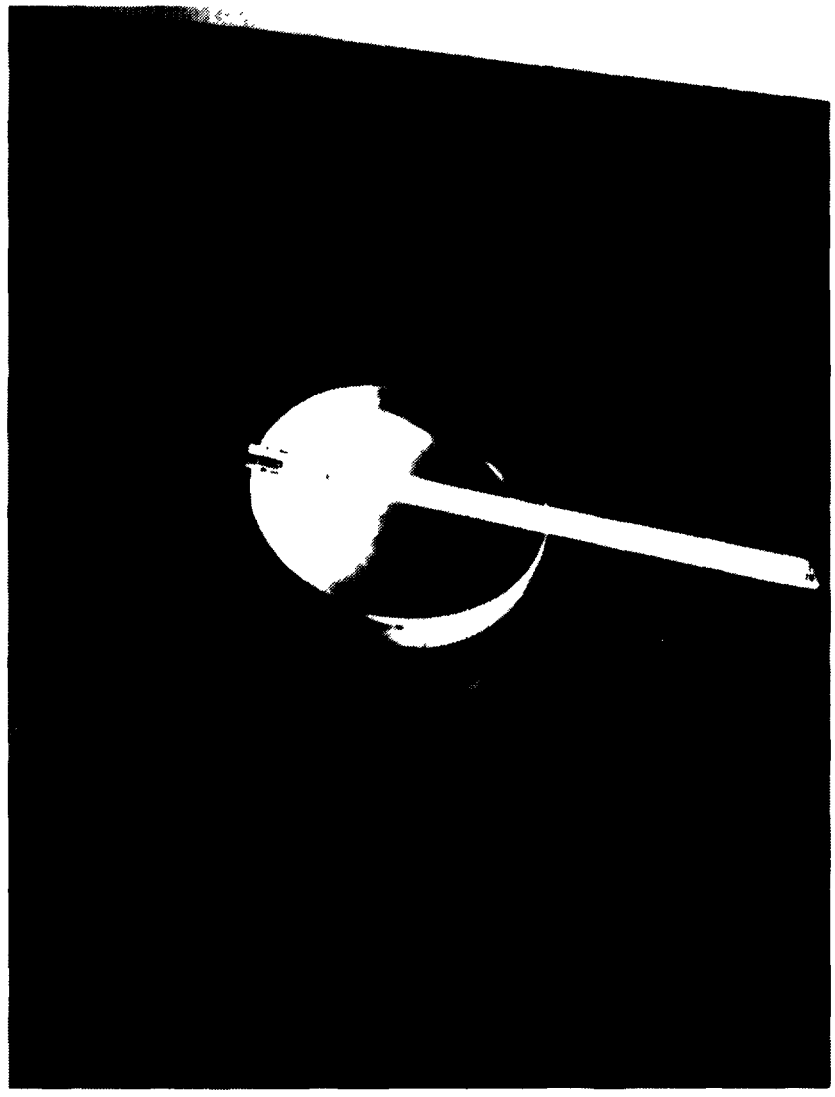

GRADE 702
THICKNESS 4 MM
220 MM DIAMETER
TRANSFORMATION PERFORMED AT 300°C

Figure 6 : Forming of an end

2.2.1. Procurement

No special technical difficulties were encountered in the manufacture of zirconium plates and tubes. Some arrangements were made with the manufacturers to obtain large or special size plates and pipes (seamless or welded) different from the usual fabrication.

2.2.2. Zirconium forming

The grades considered were 702, 704 and 705, with some additional requirements concerning the composition and the metallurgical state.

Forming limit curves were established at ambient temperature. Ductility by elongation is rather low, ductility by contraction is greater. Compared to grade 702, grade 705 is considerably better in elongation, but poorer in contraction.

Ductility increases with temperature and becomes substantial in the β region. But there is considerable oxygen pollution at high temperature. The best compromise is found between 400 to 500°C. All usual forming methods can be used. Figures 6 to 8 illustrate examples made with conventional techniques. Less commonly used methods such as hydro or isostatic forming also give very good results, as illustrated by Figures 9 and 10.

Bending of pipes up to 150 mm in diameter following a radius of 5 D proved possible without difficulty.

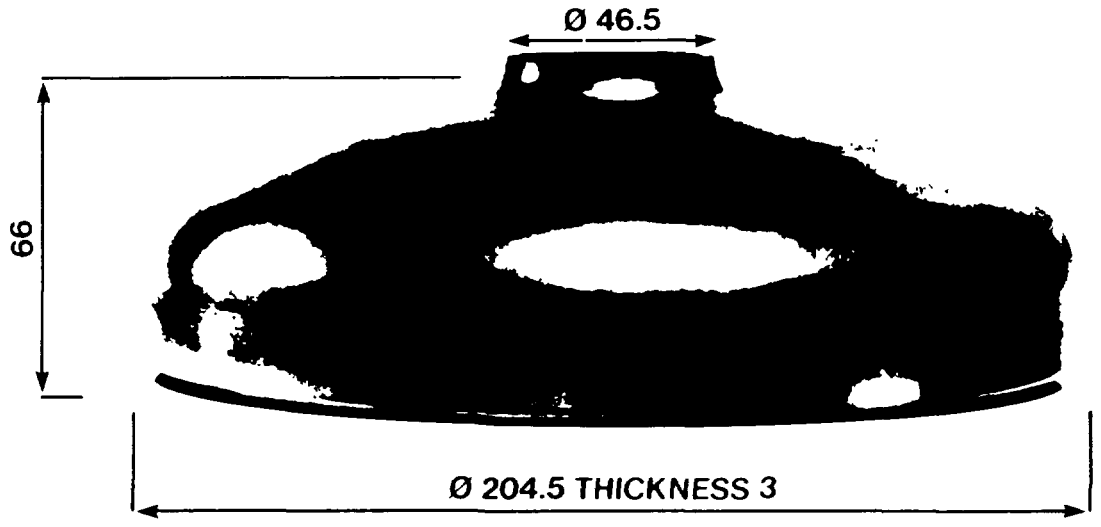

Figure 7 : Extrusion on end

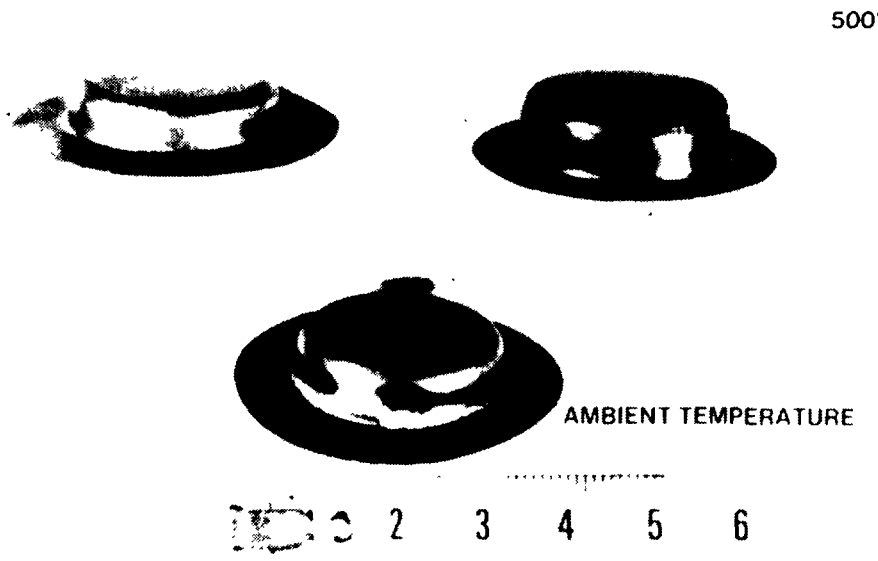

GRADE 4: IMPACT FORMING AT AMBIENT TEMPERATURE, AT 300 AND 500°C. PLATE THICKNESS 0.8 MM

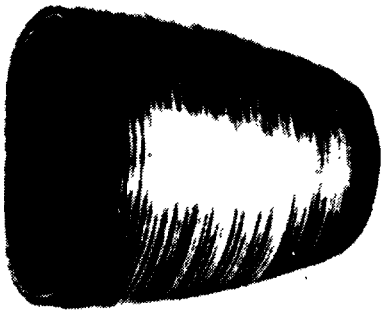

GRADE 2: DRIFT SPINNING AT 900°C

Figure 8 : Effect of forming temperature

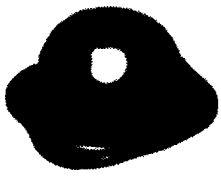

GRADE 702
THICKNESS 3 MM DIAMETER 100 MM
NUMBER OF PASSES 1

GRADE 704
THICKNESS 3 MM. DIAMETER 100 MM
NUMBER OF PASSES 1

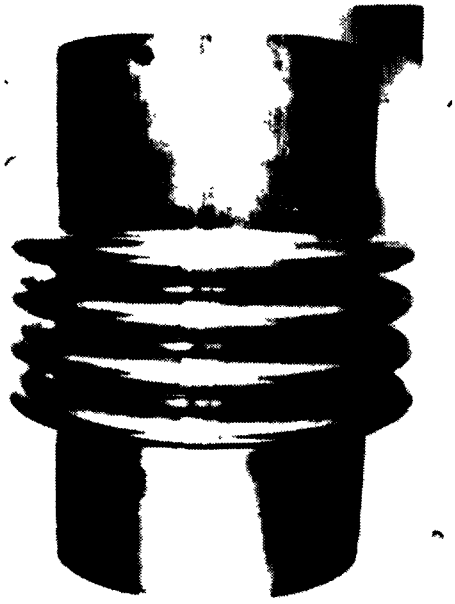

GRADE 704
BELLOWS FROM ROLLED-WELDED PIPE

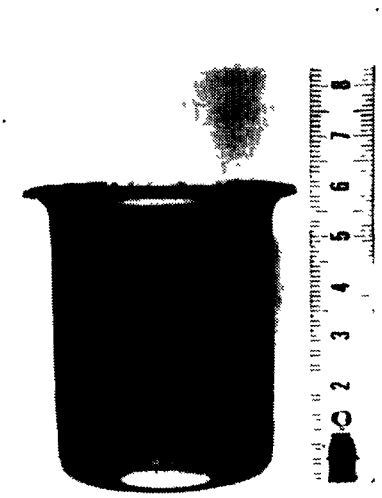

GRADE 702
NUMBER OF PASSES 2

Figure 9 : Hydroforming

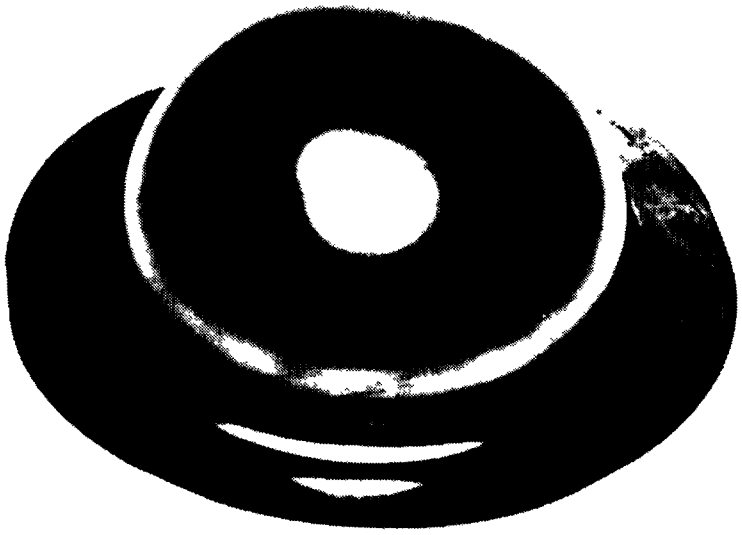

GRADE 704
THICKNESS 1 MM,
NUMBER OF PASSES 1

Figure 10 : Forming by isostatic compression

2.2.3. Zirconium welding

The topics examined were :

. weld defects and ways to prevent them
. structural modifications due to welding and their influence on mechanical properties
. risks incurred by lack of argon shielding.

Zirconium is usually welded in a glove box by the TIG process, or under vacuum by electron beam. However, the dimensions of many components were such that it was impossible to install them in a glove box or in a vacuum box. The studies were then directed to the TIG process with local shielding.

• Weld defects and ways to prevent them

Defects appearing in zirconium welds which could affect the mechanical strength of the weld (grooves, lack of penetration, excessive thickness, porosity) can be checked by conventional X-ray techniques if the conditions have been adapted to zirconium (voltage of X-ray tube, choice of screens, type of film, choice of image quality indicator).

Defects are averted by careful preparation (cleanliness, correct tolerances, proper shielding) and by determining the most suitable welding parameters.

• Structural modifications and their influence on mechanical properties

Structural modifications resulting from welding mainly depend on the welding method and parameters, which have to be adapted to the grade used.

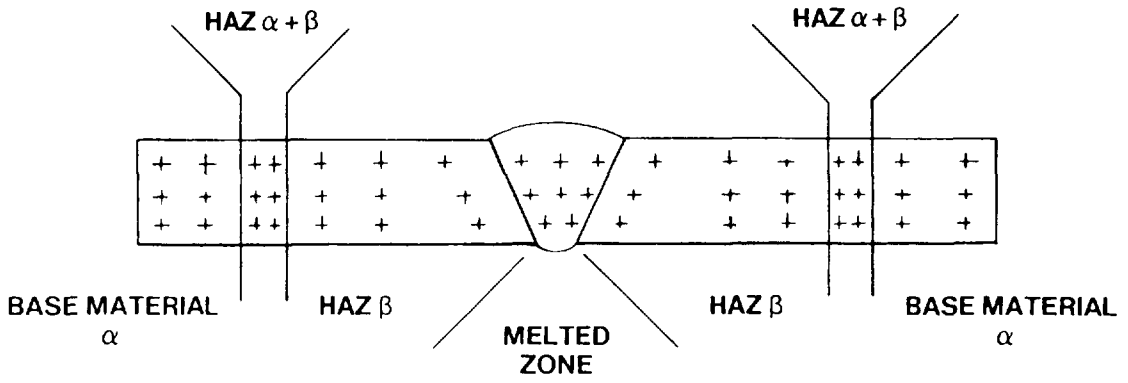

Figure 11 : Structural zones around a single passe weld

Generally speaking, a single pass weld is characterized by two main zones whose interfaces are not always well defined (Figure 11) :

- the melted area which displays rather coarse, former β grain.
- the heat affected zone (HAZ) which presents two secondary areas :
  - . an area having reached the β region with the former average β grain
  - . an area having reached the α + β region which has an intermediate structure.

For multipass welds, the basic phenomena remain the same, but the configuration becomes more complex. Each layer reaches the β region when the following one is deposited.

The overlapping of several passes tends to increase the dimensions of the former β grains, which can grow up to several millimeters. This leads to increased brittleness and loss of ductility. Tests performed on homogeneous specimens of each structure confirmed these results.

The results of these tests enabled determination of the optimum welding parameters, mainly energy, which is a function of voltage, current and welding speed.

• Risks incurred by lack of argon shielding

When welding zirconium outside a glove box, it is necessary to have three kinds of gaseous shielding (Figure 12):

- . the first one provided by the torch, in the usual way
- . the second one at the back of the weld
- . the third one on a shielding trailer, a device which follows the torch and protects the weld before it is cooled.

Different tests were performed without argon on each circuit, or by replacing argon by air or nitrogen. Hardness measurements and chemical analyses in the melted area were used to check the influence of the disturbances. The main conclusions are :

- . when the shieldings (backside and trailer) are not installed, the oxygen or nitrogen (if welded in nitrogen atmosphere) content of the melted area increases substantially. Oxygen content can increase from 1,000 to 5,000 ppm and nitrogen from 20 to 300 ppm. Hardness is raised 10 points by a 140 ppm increase in nitrogen content (for an initial content ranging between 20 and 1,000 ppm) or by a 200 ppm increase in oxygen content (for an initial content ranging between 500 and 4,000 ppm).

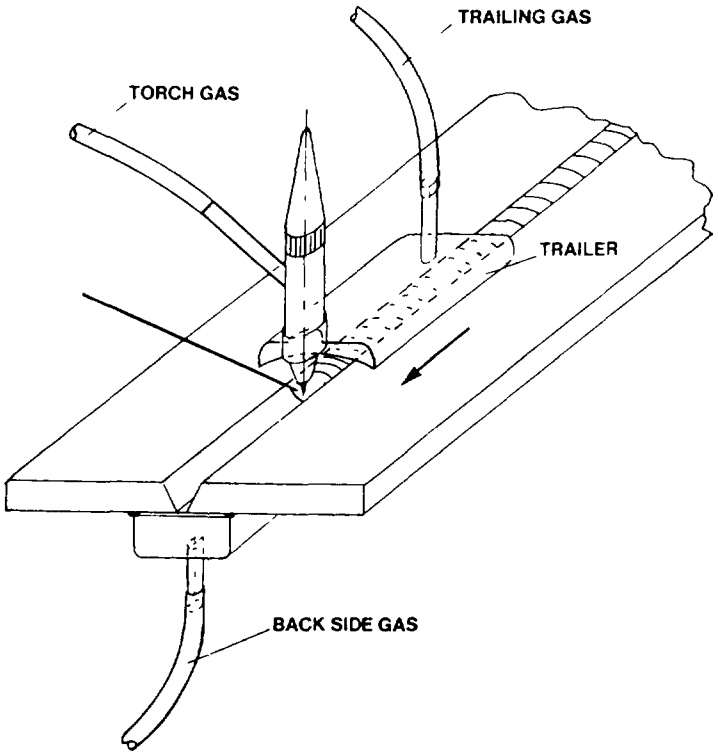

Figure 12 : Shielding arrangement

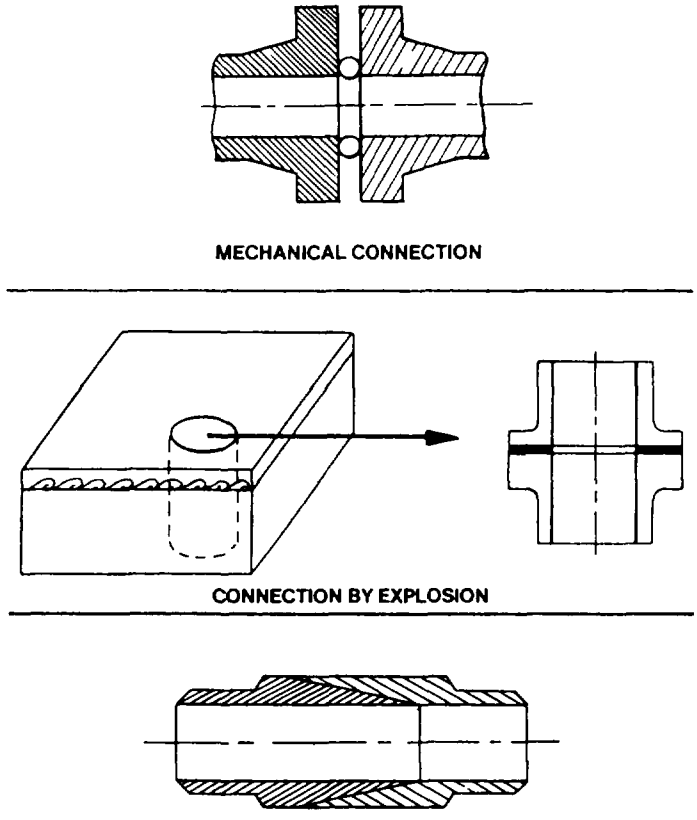

Figure 13 : Zirconium / stainless steel connections

- when the backside shielding is omitted or defective, there is formation of zirconia or zirconium nitride, which prevents correct weld penetration. This defect is revealed by X-ray examination.
- When the trailer and backside shielding are not provided with argon, a fine layer of zirconia is formed and the HAZ, including its portion next to the melted area, is not polluted by oxygen. However, the colouration is intense, matt, black or whitish.

To summarize, a serious lack of gaseous shielding is detectable by X-ray, a lesser lack is discernible by an intense colouration of the melted area and by a considerable increase in hardness.

2.2.4. Heterogeneous connections between zirconium and stainless steel

There are two ways to connect zirconium to stainless steel piping (see Fig. 13).

- by mechanical connections using flanges and gaskets,
- by metallurgical joining of the two materials using a special process, either joining by explosion or eutectic melting.

The first classical method has the drawback of creating liquid retention pockets that induce a corrosion hazard. Its use for radioactive medium requires the provision of maintenance means and access.

The second method prevents this risk and connections can be installed directly in active cells. In-depth studies have been made to ascertain the characteristics of these junctions, both with regard to corrosion resistance and to mechanical strength when cold or hot and when subjected to different stresses.

These studies have enabled the installation parameters of these junctions to be determined (optimum localization, determination of supports, etc).

During manufacture, these junctions undergo various non-destructive and destructive tests, specially designed for the verification of the zirconium/stainless steel interface.

2.2.5. Conclusion

The technological developments undertaken have provided all requisite knowledge and have permitted to take the final decision of choosing zirconium for the most exposed equipment of the La Hague extension facilities.

2.3. Description of the welded zirconium equipment

The common feature of most of these components is that they contain boiling nitric acid solutions, with acidity ranging between 3 and 12 N. Oxidizing ions such as CrVI, FeIII, PuVI, as well as insoluble platinoids are also present . Zirconium is also used for chemical reactors containing sulphide in acidic medium.

A skeleton diagram (Fig. 14) summarizes the process of the plant, with main zirconium components location indicated by a rectangle.

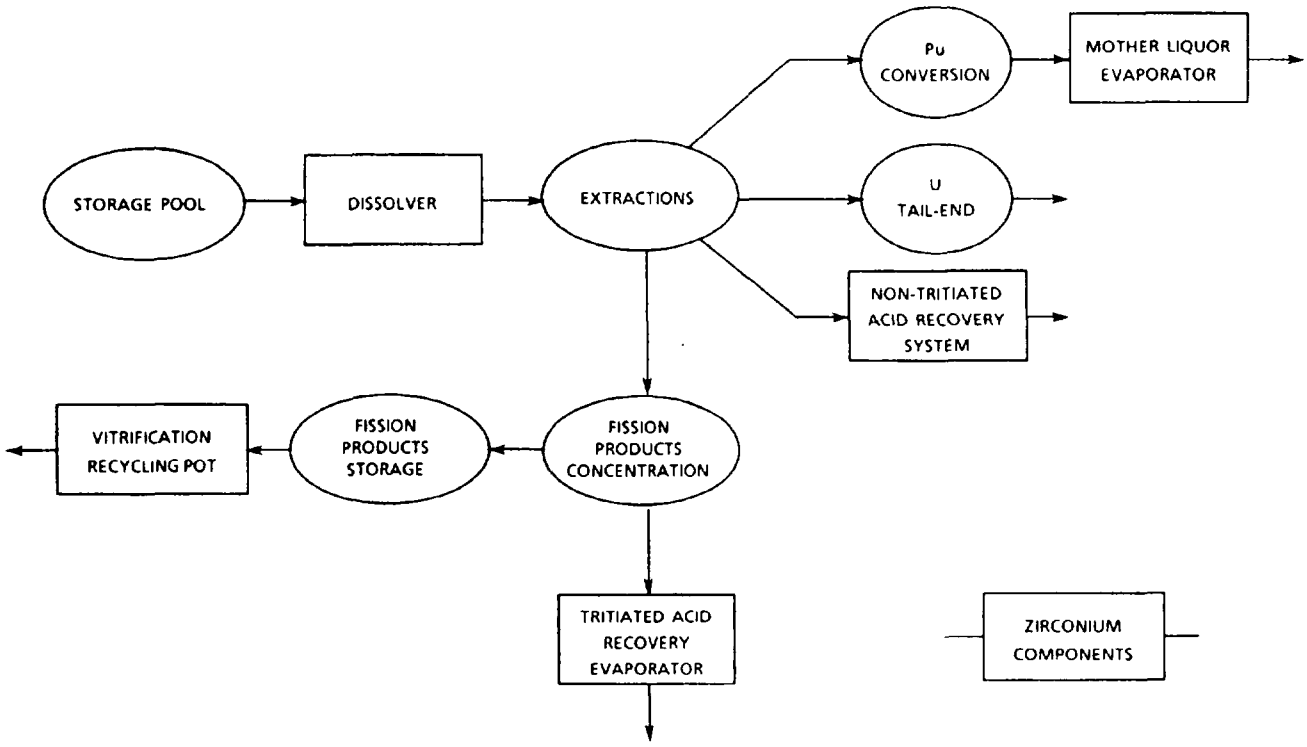

Figure 14 : Process diagram with location of main zirconium components

These components are :

. dissolvers,
. low-tritiated acid recovery system,
. tritiated acid recovery evaporator and distillation column,
. oxalic mother liquor evaporator and heat exchangers,
. vitrification dust scrubber,
. liquid waste treatment reactors.

In so far as possible, the fabrication of these components and of the piping took place in workshops, , where cleanliness conditions are more easily controlled than on a construction site. (This precaution was also taken for stainless steel equipment). Some items were built in a supporting framework with their piping networks ; this was the case for the mother liquor evaporator described below.

Zirconium equipment has roughly the same thickness as the corresponding stainless steel equipment. Zirconium is less resistant than stainless steel, and requires more thickness to support mechanical stresses (weight, pressure, temperature, reaction of piping network, possibly seismic stresses, etc), but it does not require corrosion allowance.

The components and their main characteristics are described in the following sections.

2.3.1. Rotating dissolver (Fig. 15)

This equipment is used to dissolve the oxides contained in the chopped fuel elements. It operates with a continuous supply of elements and extraction of the remaining cladding and dissolved solutions.

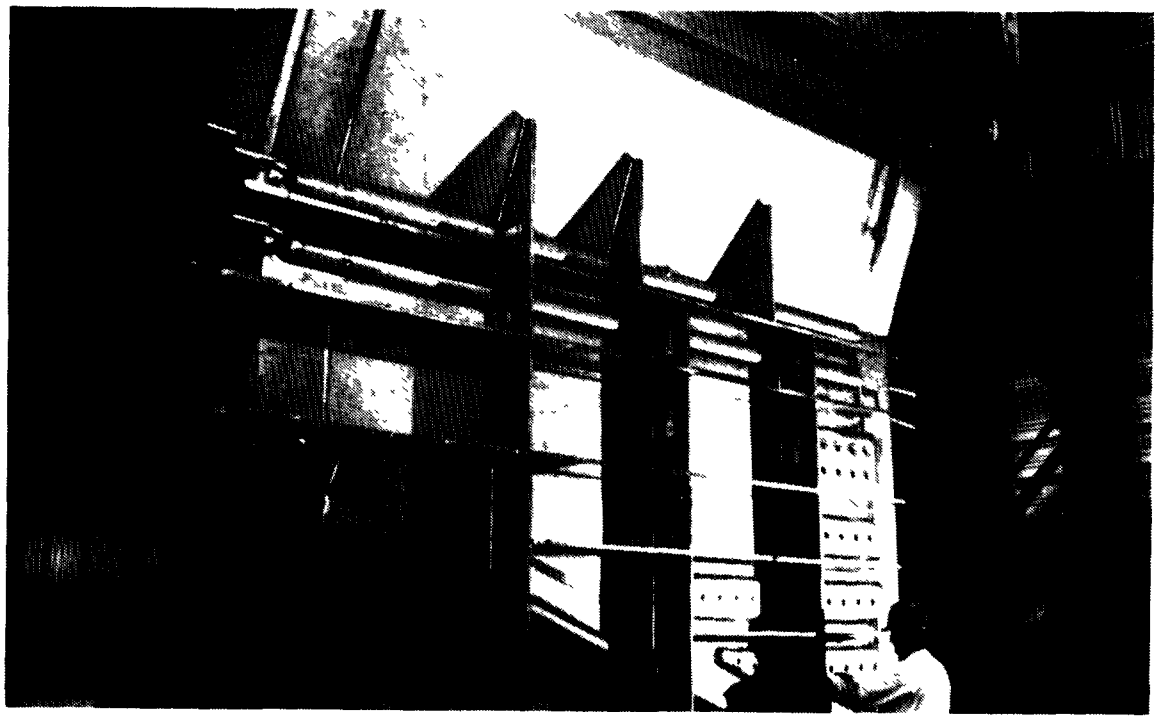

Figure 15 : Dissolver (general view)

The medium, which is boiling, has the following approximate composition :

HNO_3 3N
U 250 $g.l^{-1}$
Pu + fission products (with insoluble platinoids)
Production of nitrous vapours
Steam heated (maximum pressure 9 bar)

Only the tank and non removable parts are made of zirconium. Figure 16 shows a sketch of the dissolver. The main dimensions are :

- height 5,696 mm
- width 4,726 mm
- thickness of the slab 379 mm
- plate thickness 8 mm

2.3.2. Low-tritiated acid recovery system

This unit processes the effluents of medium activity level extraction cycles so as to recover concentrated acid and distillates with a very low activity level.

Two types of equipment are used, both having similar shape :

- thermosiphon evaporator whose function is only evaporation and decontamination of the vapours. Acidity in the boiler reaches 8N.

- evaporator with distillation column for separating recyclable nitric acid (10N) from very low acidity distillates.

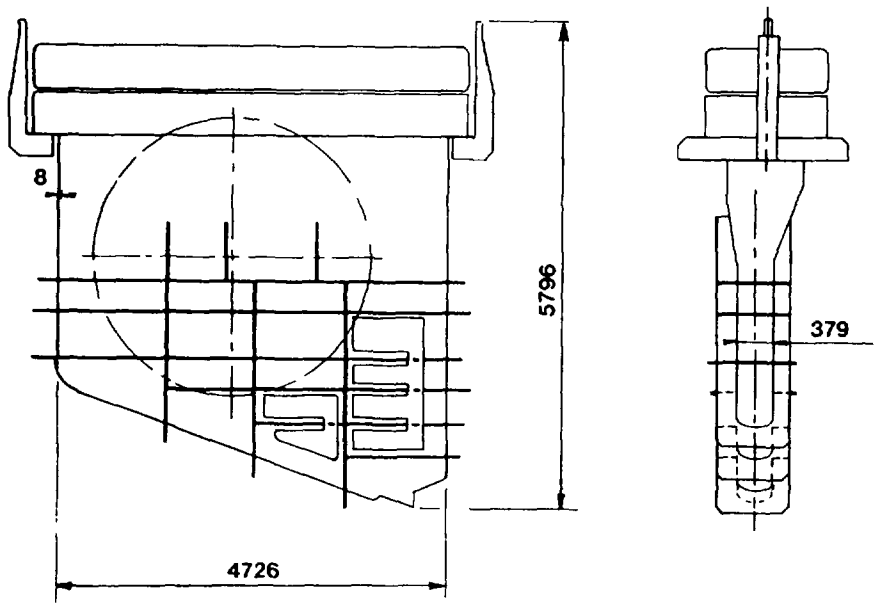

Figure 16 : Dissolver (main dimensions)

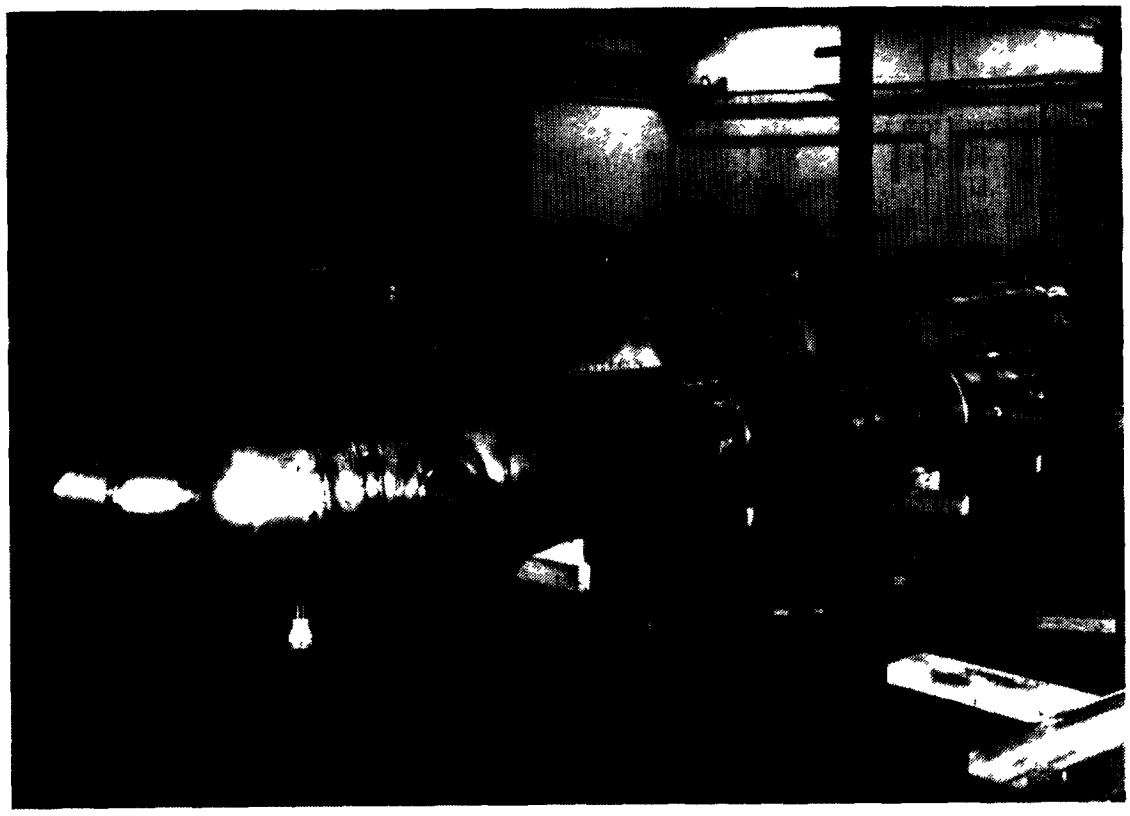

Figure 17 : Acid recovery evaporator and distillation column (general view)

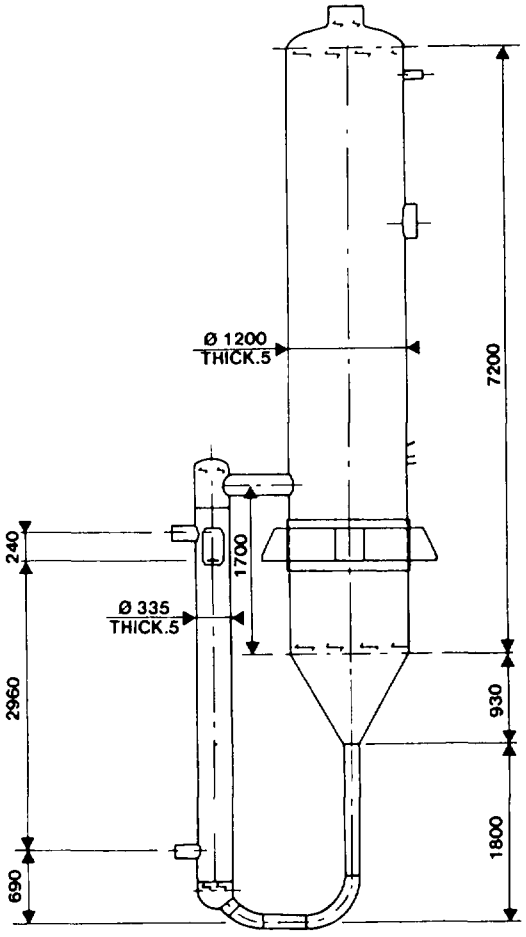

Figure 18 : Acid recovery evaporator and distillation column (main dimensions)

The main dimensions of such components are in the following range :

- height (total) 7 to 11 m
- evaporator diameter 0.3 to 0.7 m
- separator diameter 1 to 1.2 m
- thickness 5 mm

Figure 17 shows one of these components under construction and Figure 18 gives a sketch with the main dimensions of a typical component of that kind.

2.3.3. Tritiated acid recovery evaporator and distillation column

This component has the same function as the one above, for the tritiated effluents from the fission products concentration. It is of the same type, and has a similar size.

2.3.4. Oxalic mother liquor evaporator

The function of this component is to concentrate plutonium conversion effluents so that they can be recycled into the process. The equipment is sub-critical, with low-capacity thermosiphon circulation.

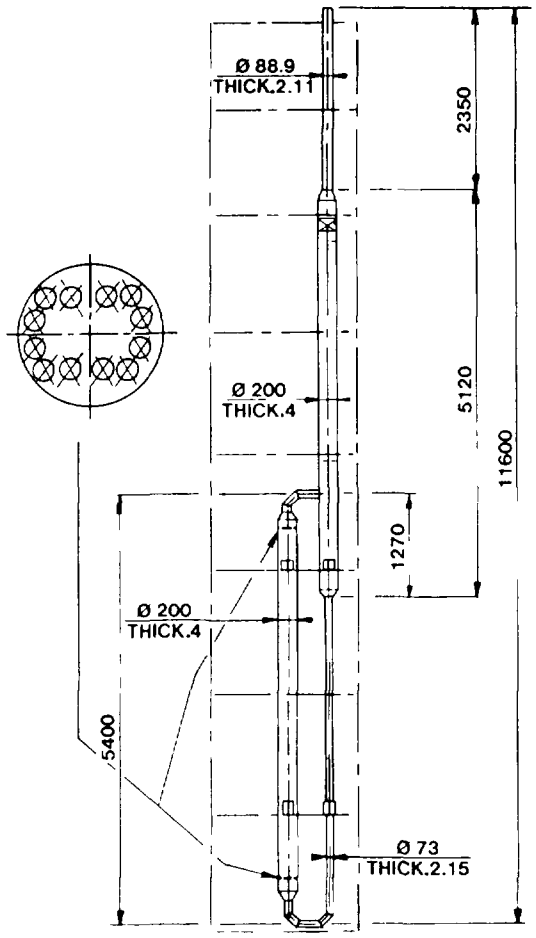

Figure 19 : Oxalic mother liquor evaporator (main dimensions)

Figure 19 is a sketch which indicates the main dimensions :

. height (total)	11,600 mm
. evaporator diameter	200 mm
. column diameter	200 mm
. thickness	4 mm

This equipment was built inside a framework (Fig. 20) and all zirconium connections have been made in workshop under favourable conditions.

The distillates flow through two series-connected heat exchangers which have also been preassembled in the workshop (Fig. 21).

2.3.5. *Vitrification recycling pot* (Fig. 22)

The function of this component is to clean the off-gas from the calciner, to dissolve removed dust in nitric acid, and to send the solution back to the calciner. Solution acidity is 5N.

The main dimensions of this vitrification recycling pot are the following:

. height (total)	4,130 mm
. cyclone diameter	500 mm
. cyclone thickness	6 mm
. column diameter	220 mm
. column thickness	4 mm

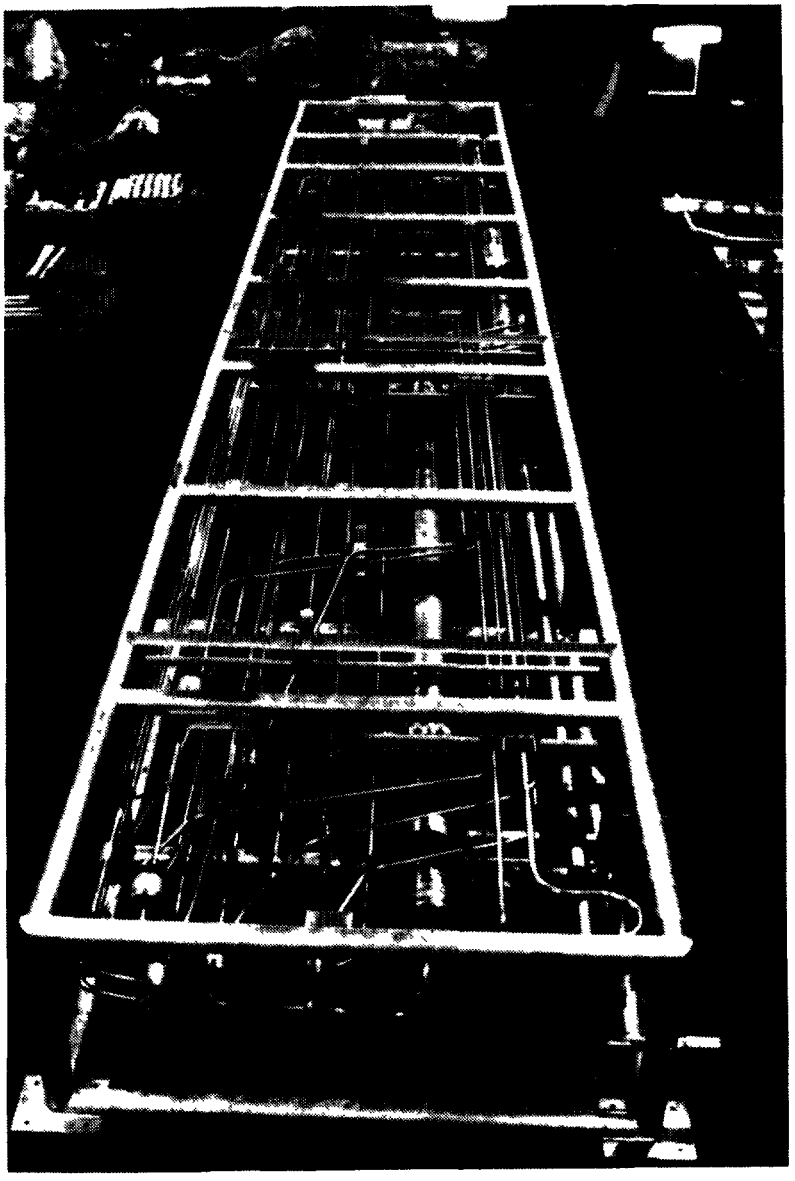

Figure 20 : Oxalic mother liquor evaporator in its frame

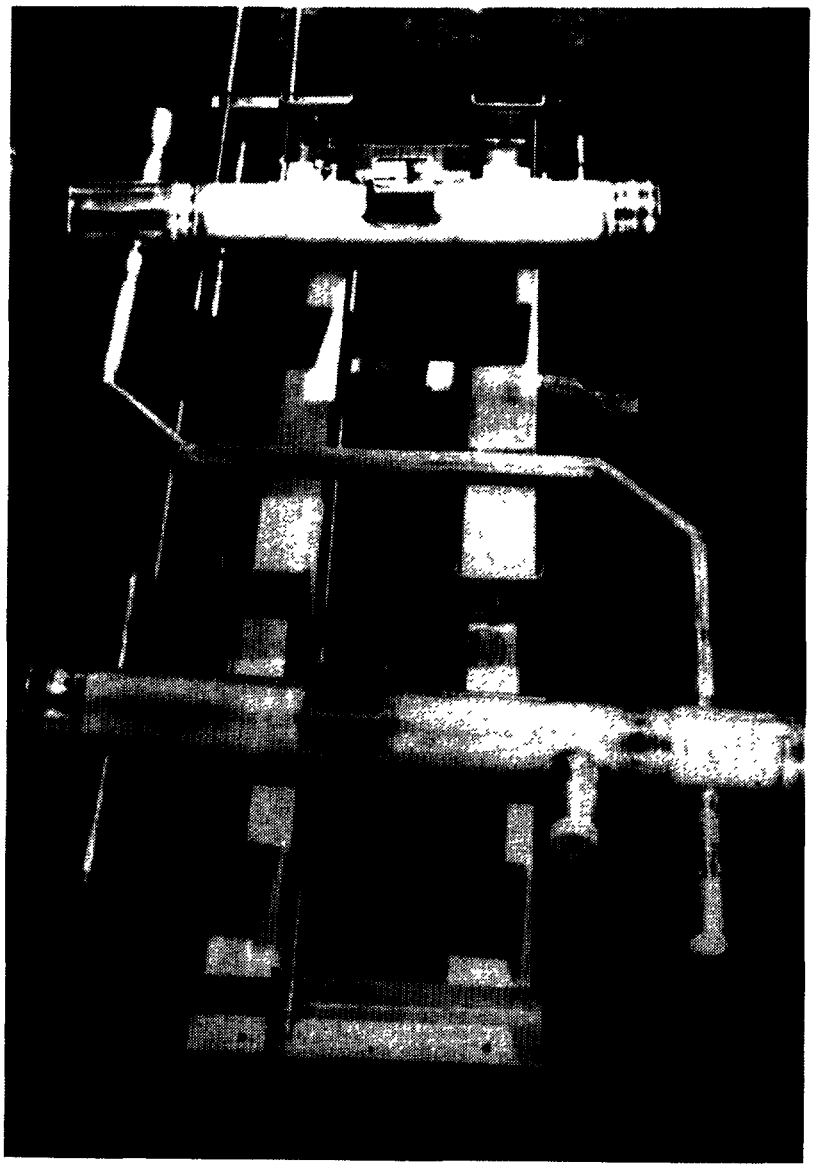

Figure 21 : Oxalic mother liquor evaporator. Preassembled exchangers in their frame

2.3.6. Liquid waste treatment reactors

These are more classical chemical reactors. They are fitted with stirrers and are used to precipitate different products. Solutions contain sulphides in acid medium which depassivate stainless steel and lead to general corrosion of this material.

2.3.7. Conclusion

Research and technological development have validated the choice of zirconium for the most exposed items of equipment of the La Hague extension facilities. The total weight of these components, with their accessories, is about 80 tons and the length of zirconium piping is 5,500 m.

Figure 22 : Vitrification recycling pot (general view)

REFERENCES

(1) LEDUC, M., LE DUIGOU, A., PELRAS, M., "The Use of Zirconium in Nitric Environment Corrosion Studies", Industrial Applications of Titanium and Zirconium : Fourth Volume, ASTM STP 917 - Philadelphia 1986.

(2) WEIMAN, S. H., "Titanium Corrosion in Aqueous Solutions", Corrosion, Vol. 22, N° 4, April 1966, pp. 98-106.

(3) TAKAMURA, A., ARAKAWA, K., and MORIGUCHI, Y., "Corrosion Resistance of Titanium and Titanium 5% Tantalum Alloy in Hot Concentrated Nitric Acid", The Science Technology and Application of Titanium, Pergamon Press 1970, pp. 209-216.

(4) BOYD, W. H., Process Corrosion Industry, National Association of Corrosion Engineers, 1975, p. 209.
(5) BISHOP, C.R., Corrosion, Vol. 19, Sept. 1963, p. 314t.
(6) YAU, T.L., "Stress Corrosion Cracking of Zirconium and Its Alloys in Nitric Acid" Corrosion, National Association of Corrosion Engineers, 1981, p. 102.
(7) BEAVERS, F. A., GRIESS, J-C., and BOYD, W.K., "Stress Corrosion Cracking of Zirconium in Nitric Acid" Corrosion, National Association of Corrosion Engineers, 1980, p. 238.

MATERIALS RELIABILITY IN THE BACK-END OF THE FUEL CYCLE: ARGENTINE EXPERIENCE

M.C. GELDSTEIN
Comisión Nácional de Energía Atómica,
Buenos Aires, Argentina

Abstract

Reliability of materials at the back-end of the fuel-cycle is a subject of permanent interest for countries that have nuclear reactors. Safety, at that stage, should be understood as the system of physical barriers to prevent radioactivity release into the environment. Those barriers must be reliable during extended periods, e.g. 50 to 100 years for interim spent fuel storage, and over 1000 years for permanent waste disposal.

The first physical barrier is the fuel itself, namely pellets and cladding. Independently of the selected intermediate storage (dry or wet storage) fuel integrity, decay heat extraction and appropiate shielding, must be guaranteed.

Two PHWR nuclear reactors are now operating (ATUCHA-I: 345 MWe; EMBALSE: 600 MWe) and one more is being built (ATUCHA-II: 745 MWe), 700 additional MWe of nuclear origin, are planned to be connected to the electrical power distribution nets during the next 15 years.

For intermediate spent fuel storage, wet technology has been selected. At present, 8200 CANDU type spent fuels are in the EMBALSE pools and 4300 ATUCHA-I type ones are in the ATUCHA-I pools.

A thorough control and maintenance program on materials that can stay under water during long periods, is being investigated. Materials used for high level waste containment, as lead, are being characterized.

Herewith is described the management of fuel pools, chemical and radiochemical controls, studies for the proper selection of structural materials and for a high level waste disposal container.

---

1. GENERAL CONSIDERATIONS

The Argentine nuclear power operating capacity is based on a nuclear program that includes 4 or 5 PHWR reactors: two of them presently operating (ATUCHA-I: 345 MWe and EMBALSE: 600 MWe), one under construction (ATUCHA-II: 645 MWe), and another 700 MWe to be installed as one or two 350 MWe stations before the end of the century.

ATUCHA-I and II were built at the Paraná de las Palmas riverside, at 110 Km from Buenos Aires, while EMBALSE Nuclear Power Plant (NPP) is

located at Embalse de Río Tercero, in the Province of Córdoba. At present, both of them use nuclear fuel with natural UO_2 and Zry-4 cladding; this type of fuel will also be used by ATUCHA-II. (See Table 1 for the characteristics of FA).

TABLE 1. FUEL ASSEMBLIES CHARACTERISTICS

F A CHARACTERISTICS	NUCLEAR POWER PLANTS		
	ATUCHA I	EMBALSE	ATUCHA II
FUEL	NATURAL UO_2	NATURAL UO_2	NATURAL UO_2
STRUCTURAL MATERIALS	ZIRCALOY-4 INCONEL STAINLESS STEEL	ZIRCALOY-4	ZIRCALOY-4 INCONEL STAINLESS STEEL
FUEL RODS	36	37	37
AVERAGE BURN-UP MW D / TU	6500	6600	7500
SPECIFIC LINEAL POWER W/ CM (DESIGN LIMITS)	531	510	531
TOTAL LENGHT MM	6028.5	495.3	6026.4
ACTIVE LENGTH MM	5300	478.6	5300
TOTAL WEIGHT KG	210.7	23.56	254
UO_2 KG	173.3	21.26	210.76

2. INTERIM SPENT FUEL STORAGE IN ARGENTINE

De-ionized water pools have been selected for spent fuels. This technology was selected and is presently being used for both operative NPP and will be also used for the one under construction (see Table 2).

Initial design parameters were chosen to provide storage for spent fuels for ten (10) years but pool storage capacity in ATUCHA-I NPP was increased to 15 years more, with a second pool house.

TABLE 2. INTERIM FUEL STORAGE IN ARGENTINA

SPENT FUEL ARE STORED IN WATER POOLS

		FA IN THE POOLS	CALCULATED Pu KG
ATUCHA I	(1974)	4145	1918
EMBALSE	(1984)	8200	520

The operation, maintenance and servicing of the pools are in charge of each one of the NPP staff, since their storage facilities are at each reactor site.

Argentine experience in this field has been, up to now, highly satisfactory but, if we consider that FA might remain in these storage pools for long periods - e.g. over 50 years - and our reprocessing program is dealing with R&D projects, possible mechanisms of degradation of irradiated fuel materials are essential.

This includes long term wet storage, as well as alternative storage technologies, e.g. spent fuels dry storage.

3. NUCLEAR POWER PLANTS: PRESENT STATE OF THE POOLS

3.1 ATUCHA-I NPP

Since 1974, fuels discharged from the reactor have been stored at the NPP site. The total amount of spent fuels in the pools, at April 1986, is 4145, with a calculated Pu content of 1918 kg. This NPP full capacity for spent fuel storage is 10340. This implies that ATUCHA-I has sufficient water pool storage capacity for its whole lifetime.

The 8 pools were built of concrete and all pools have austenitic stainless steel lining at the inner walls and floor.

Water circulates through a cooling and purification system thus guaranteeing a maximum temperature of 34°C and a pH of about 7. Chemical controls include: silica, chloride and sodium ions, pH and conductivity.

A very low chloride ion content ($\leq$ 0,2 ppm) is kept because chlorides can accelerate localized forms of corrosion in some of the materials used, e.g. stainless steel.

Radiochemical controls are carried out to keep the radioactivity levels as low as possible. The purification system (with mixed bed resins and diatomea filters) removes this type of contamination. The measured values are between 10^{-4} - 10^{-3} $\mu C/cm^3$, the 85% corresponds to γ activity from Co60 and the other 15% to Ru106, Cs137 and Cs134. (See Table 3).

TABLE 3. ATUCHA I NUCLEAR POWER PLANT

POOLS ARE OPERATING AT REACTOR SITE SINCE 1974	
TOTAL QUANTITY OF SPENT FUELS	4145
FULL CAPACITY	10340
TEMPERATURE	34°C
CHEMICAL CONTROLS	
SILICA, CHLORIDE, SODIUM, pH, AND CONDUCTIVITY	
RADIOACTIVITY CONTROLS	
THE MEASURED VALUES ARE 10^{-4} - 10^{-3} $\mu C/ML$	

Generally, no biological growth has taken place. In only one ocassion this problem has been detected but, in that case, biological contamination was brought from outside and it was removed by mechanical means.

Equipment for post-pile examinations of irradiated FA was installed in order to investigate the in-pile performance. No major problems have been found during the NPP 12 years operation.

3.2 EMBALSE NPP

Spent fuel has been stored since 1984. About 8200 CANDU type spent fuels were discharged since start-up of the NPP in 1983. Total calculated Pu in the pools is about 520 kg.

The pool storage capacity is 44648, which means ten years for a 0,85 load factor.

EMBALSE pools were built of concrete and have epoxi lining. Demineralized water circulates through heat exchangers and mixed bed resins in all the pools, thus, the average temperature is 25°C and the water is kept very clear. This is essential to make easier handling and inspection of the fuels. The radioactive material is also removed by the filtration system; this contamination arises from defective fuels or from deposits that are formed on the surface of the FA while they are in the reactor core.

Chemical controls are made to keep the water very pure. A very low chloride ion content of the water is therefore specified ($\leq$ 0.2 ppm). The average measured value is $\leq$ 0.1 ppm. The specifications of the water include pH, conductivity and chloride ion content (see Table 4).

Under normal conditions, no enhanced corrosion should be expected in the storage pools.

The radioactivity level is not specified but it is controlled: the total γ activity is about 2.10^{-3} μ Ci/cm^3.

Equipment have been installed (including disassembling for cladding inspection) to perform post-irradiation examination.

3.2.1 Possibility of galvanic corrosion and alternative construction materials for structural components in EMBALSE pools (1).

304-L stainless steel is the structural material used for the FA trays and its performance under water has proved to be satisfactory but,

TABLE 4. EMBALSE NUCLEAR POWER PLANT

POOLS ARE OPERATING SINCE 1974

TOTAL QUANTITY OF SPENT FUELS	8200
FULL CAPACITY	44648
TEMPERATURE	25 °C

CHEMICAL PARAMETERS

	SPECIFIED	MEASURED
pH (25 C)	5.5 - 7.5	6.5
Cl^-	≤ 0.2 PPM	≤ 0.1 PPM
CONDUCTIVITY	≤ 2 uS	≤ 1 uS
γ ACTIVITY	(NOT SPECIFIED)	2.10^{-3} uC/ML

TABLE 5. MATERIAL CRITERIA FROM THE CORROSION POINT OF VIEW

- GALVANIC EFFECTS
- UNIFORM AQUEOUS CORROSION BEHAVIOUR
- SUSCEPTIBILITY TO LOCALIZED FORMS OF CORROSION
  - PITTING
  - STRESS CORROSION CRACKING
  - INTERGRANULAR CORROSION
  - ETC.

since this material is not manufactured in Argentina, high strength aluminum alloys were studied as possible replacements.

To select construction materials it is mandatory to take into account the following aspects:

- galvanic effects
- uniform aqueous corrosion behavior
- susceptibility to localized forms of corrosion, such as pitting, stress corrosion cracking, intergranular corrosion, etc. (See Table 5).

AA5052 and AA5086 were proposed as alternative construction materials for the FA trays (see nominal composition of these alloys in Table 6). Both of them have Mg as the principal alloying element.

TABLE 6. NOMINAL COMPOSITION OF MATERIALS TESTED

1.- ALUMINUM ALLOYS (1)

	Mg	Mn	Cr	Rest
AA 5052	2.5	-	0.25	Al
AA 5086	4.0	0.4	1.25	Al

(1) Metal Handbook. Ninth Edition, Vol.2. Properties and Selection : Non-Ferrous Alloys and pure Metals. ASM. 1979

2.- AUSTENITIC STAINLESS STEEL AISI 304 L (2)

C	Mn	Si	Cr	Ni	P	S
0.03	2.00	1.00	18.0-20.0	8.0	0.045	0.03

(2) Metals Handbook Ninth Edition, Vol 3, Stainless Steels, Tool Materials and Special Purpose. ASM 1980

3.- ZIRCALOY - 4 (3)

Sn	Fe	Cr	Ni	Fe Cr Ni	Rest
1.2-1.7	.07-.20	.05-.15	.03-.08	.18 - .38	Zr

(3) 1974 Annual Book for ASTM Standards. ASTM B 352 - 73

The test program included electrochemical measurements to evaluate galvanic effects of dissimilar materials in contact such as aluminium alloys with either stainless steel or Zry-4. All tests were made at room temperature, in neutral aereated and deareated chloride solutions, simulating accident conditions.

Fig. 1 shows the potenciodynamic polarization curves obtained using a calomel saturated electrode as reference.

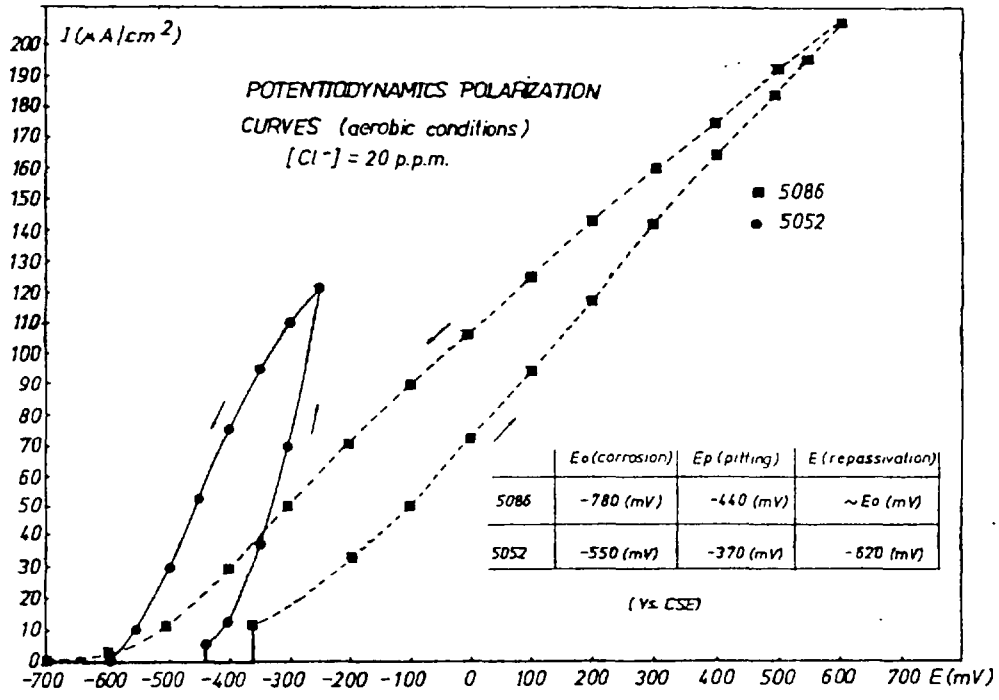

FIGURE 1

Both alloys are more susceptible to pitting corrosion in aereated halide solutions. In the presence of the cathodic reactant O_2, the Al alloys are readily polarized to its pitting potential. The passive range of overpotential is very narrow.

The reverse polarization shows higher corrosion rates than those registered in the anodic sense; this is due to the propagation of the pits that appeared during the anodic working.

In the Fig. 2 it is possible to observe the typical morphology of the "pits" in aluminum alloys in neutral chloride solutions, which is the result of a crystallographic etching with the development of (100) planes (2)(3)(4).

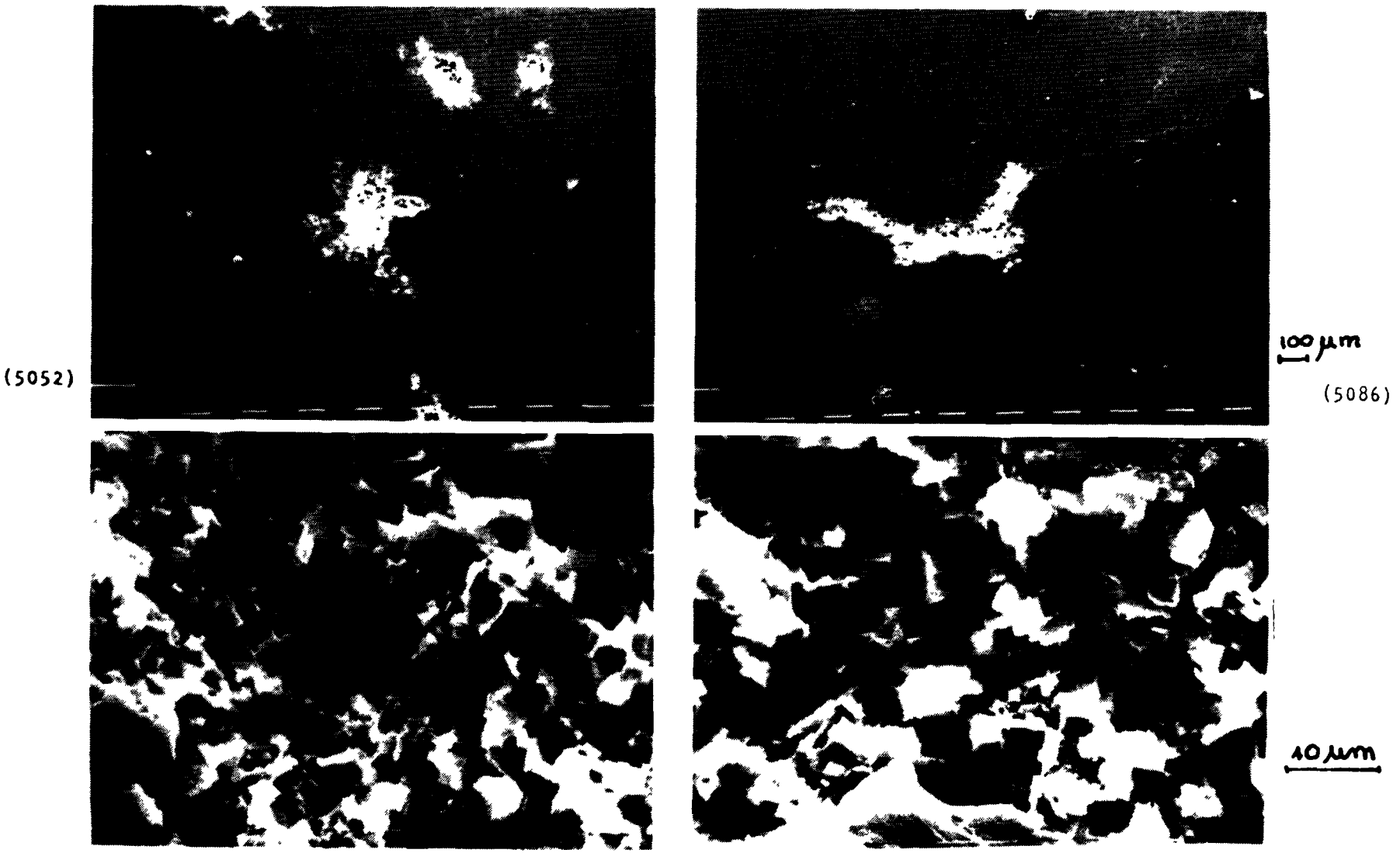

FIGURE 2

Measurements of galvanic currents between galvanic coupled materials were based on zero resistance ammeter techniques (5).

Dissimilar materials were kept coupled (on short-circuit conditions) during 100 days and the galvanic currents were measured once in a week. Results are shown in Table 7.

TABLE 7.

	GALVANIC COUPLE	GALVANIC CURRENT I_G $\mu A / cm^2$			OBSERVATIONS
I	AA 5052 - 304 L SS		4		- THE GALVANIC CURRENT IS ANODIC AND STABLE. PITTING IS OBSERVED IN AA 5052
II	AA 5052 - ZRY-4 PREOXIDIZED		0.1		- I_G IS GOING DOWN IN TIME. UNIFORM CORROSION IS OBSERVED IN AA 5052
III	AA 5086 - 304 L SS	10	4	3	- I_G INITIALLY IS VERY HIGH PITTING AND UNIFORM CORROSION IS OSERVED IN AA 5086
IV	AA 5086 - ZRY-4 PREOXIDIZED	IDEM	II		- IDENTICAL BEHAVIOUR AS IN COUPLE II

Both aluminum alloys, when coupled with stainless steel, present anodic behavior and a localized form of corrosion as pitting developes. Fig. 3 shows the pits generated as a consequence of the coupling.

Even though Zr alloys are more noble than Al alloys, accelerated corrosion is not observed in those pairs. Zirconia film has an isolating behavior and there is no electrical contact between the metals.

In addition to the effects of the galvanic coupling, these Al alloys are also susceptible to SCC and intergranular corrosion (6)(7). The use of them under long-term pool storage conditions is not advisable.

3 a: 600X

5052 vs 304-L

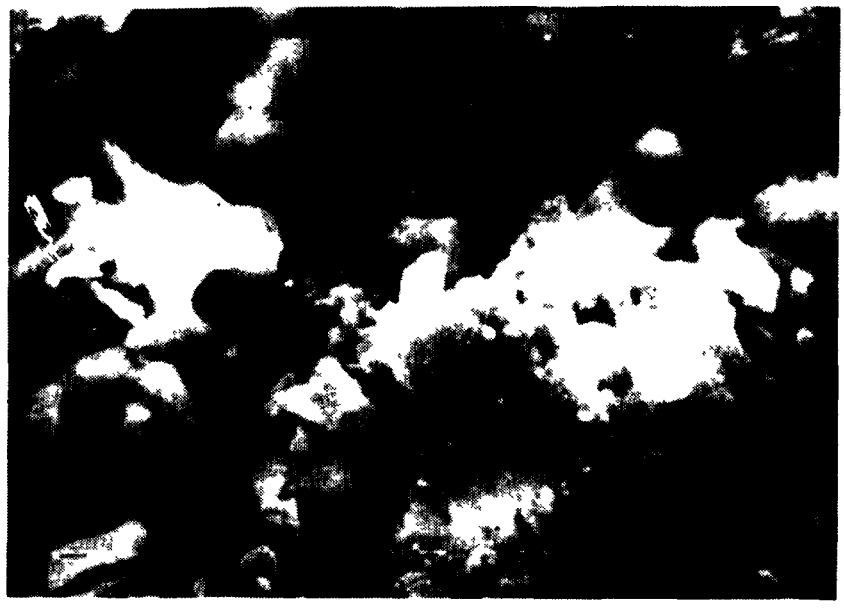

3 b: 4800X

5086 vs 304 L

FIGURE 3

Our conclusion is that the aluminum alloys are not able to stay under water for extended periods (50 years or more).

3.3 ATUCHA-II NPP

Five pools are being built: four of them for spent fuel storage and the fifth for reception and special operations. Full capacity is of 3696 spent FA. The future management of the pools will be similar to the one described for ATUCHA-I.

4. FINAL DISPOSAL (8)(9)

The Argentine Nuclear Program aims to the reprocessing of spent fuels and the recycling of Pu produced by the generation of electricity. Therefore, high level radioactive waste, that shall have to be disposed of in the long term by appropiate treatment, will be produced.

Materials to be used for high level waste containment, such as lead, are being characterized. First results were presented at the IAEA International Symposium on Settlement, Design and Construction of Underground Repositories for Radioactive Waste Disposals (9).

Experimental studies based on electrochemical measurements were carried out in underground waters and in simulated environments such as chloride, acetate and nitrate solutions. The temperature and concentration effects on lead corrosion behavior were evaluated.

Pure lead (99.999%) had good corrosion behavior in underground water uo to 80°C. High corrosion rates were observed only when soluble lead salts were detected.

Galvanic effects of several protective linings such as AISI 304 stainless steel, GR-2 Titanium and SAE-1010 carbon steel, were also investigated.

In the Pb-AISI 304 and Pb-GR2 Ti couples, lead has an anodic behavior up to 75°C. The corrosion rates are strongly dependent of the relationship between the exposed areas. Pb-SAE 1010 has a slightly

different behavior: at room temperature lead is anodic but, at 75°C, becomes cathodic. However, carbon steel seems to be the most convenient material for the lining of lead, because lead presents the lowest corrosion rates when they are coupled.

ACKNOWLEDGMENTS

We are specially thankful to IAEA for the opportunity to exchange technical aspects on the subject since our country is carrying out research and development projects on this field.

We also wish to express our thanks to the NPP for their valuable cooperation and to the personnel of the Gerencia Desarrollo for their help.

REFERENCES

(1) M.C.GELDSTEIN , A. IGLESIAS. Estudio de factibilidad de uso de aleaciones de Al como materiales alternativos al acero inoxidable AISI 304-L para la construcción de bandejas de almacenamiento de EC irradiados en la Central Nuclear EMBALSE. Informe Técnico CNEA ECn 6/86, marzo 1986.

(2) J.R. GALVELE et al. Critical potential for localized corrosion of Aluminum alloys. Localized Corrosion, NACE, p.580, 1974.

(3) S.M. de DE MICHELI. The electrochemical study of pitting corrosion of Aluminum in chloride solutions. Corrosion Sc. vol.18, N° 7, pp.605-616, 1978.

(4) A. IGLESIAS, M.C. GELDSTEIN, I. RASPINI. Estudio de compatibilidad galvánica en reactores experimentales. Informe Técnico CNEA ECn 56/84, 1984.

(5) R. BABOIAN. Predicting galvanic corrosion using electrochemical techniques for corrosion. A Symposium sponsored by NACE. Technical Committee T-3L/76.

(6) MARKUS O. SPEIDEL. Stress corrosion cracking of Aluminum alloys. Department of Metallurgical Engineering, Ohio State University (draft of a chapter prepared for Arpa-Handbook on Stress Corrosion Cracking)

(7) ROBERTO CREPALDI, PAULO EDSON CARDOSO. Estudios de corrosae da liga de Aluminio AA 5052, em agua deionizada, en temperaturas inferiores a 100°C. Instituto de Pesquisas Radioactivas, Belo Horizonte, Nuclebras SA, XX Congresso de Associaçao Brasileira de Metais, Rio de Janeiro, Junho 1975.

(8) C. ARAOZ, A. MEHLLICH, E. MONTALDO VOLACHEC. Spent fuel management in Argentina. IAEA Advisory Group Meeting on Spent Fuel Management, Vienna, Austria, 11-13 March 1986.

(9) S.M. de DE MICHELI, S.B. de WEXLER, R.O. CASSIBA, S. FERNANDEZ. Uso del plomo en contenedores de residuos radiactivos de alta actividad: estudio de resistencia a la corrosión. Simposio Internacional sobre Emplazamiento, Diseño y Construcción de Repositorios Subterráneos de Desechos Radiactivos. Hannover, Rep. Federal de Alemania, 3-7 marzo de 1986. IAEA-SM-289/22.

SELECTION OF MATERIALS FOR VARIOUS SYSTEMS IN REPROCESSING FAST REACTOR FUELS — PRESENT STATUS AND FUTURE PROGRAMME

J.B. GNANAMOORTHY, G.R. BALASUBRAMANIAN
Indira Gandhi Centre for Atomic Research,
Kalpakkam, Tamil Nadu,
India

Abstract

Choice of proper materials of construction for various applications in reprocessing of Fast Reactor fuels plays a vital role from considerations of safety and economics. A brief mention of process followed particularly for the reprocessing of mixed carbide fuel is made. The plant is classified into various functional zones based on severity of radiation and chemicals for the choice of materials such as highly radioactive cells, radioactive laboratories, low and high level waste storage areas, off-gas treatment section, etc.For each of the areas, the criteria for the selection of material is defined and based on that probable candidate materials are identified. Work carried out on corrosion studies related to the conventional and electro-chemical dissolver and its components is described.Need for development of specific code for the fast reactor fuel reprocessing industry is stressed.

Paper also describes the facilities available in the Chemical Metallurgy Section for the corrosion studies and spells out programme in the Centre for development of material needed for this part of the nuclear fuel cycle.

INTRODUCTION:

Reprocessing is a vital link in the fast reactor fuel cycle and success of fast reactor programme will depend upon the ability to set up plants for effective reprocessing of fuels discharged from the fast reactors. A well designed plant is characterised by its ability to use efficient processes that can separate valuable materials into end products satisfying prescribed specifications, its capability to achieve high recovery of these products with high degree of safety, to ensure protection to operating personnel, public and environment from exposure to radiation, its capacity to contain and safely dispose all wastes generated and demonstration of high reliability and availability of the plant to reduce the fuel cycle cost.

To achieve these objectives the plant follows a series of complex chemical processes using complicated equipment and systems. The selection of materials of construction has direct influence on the integrity of the equipment or its joints and thus the primary containment of radioactivity. Failure of equipment, apart from leading to the disruption of process and loss in productivity, will pose problems in maintenance and create high volume of radioactive waste. Hence, selection of construction materials for different applications and proper fabrication techniques with sound

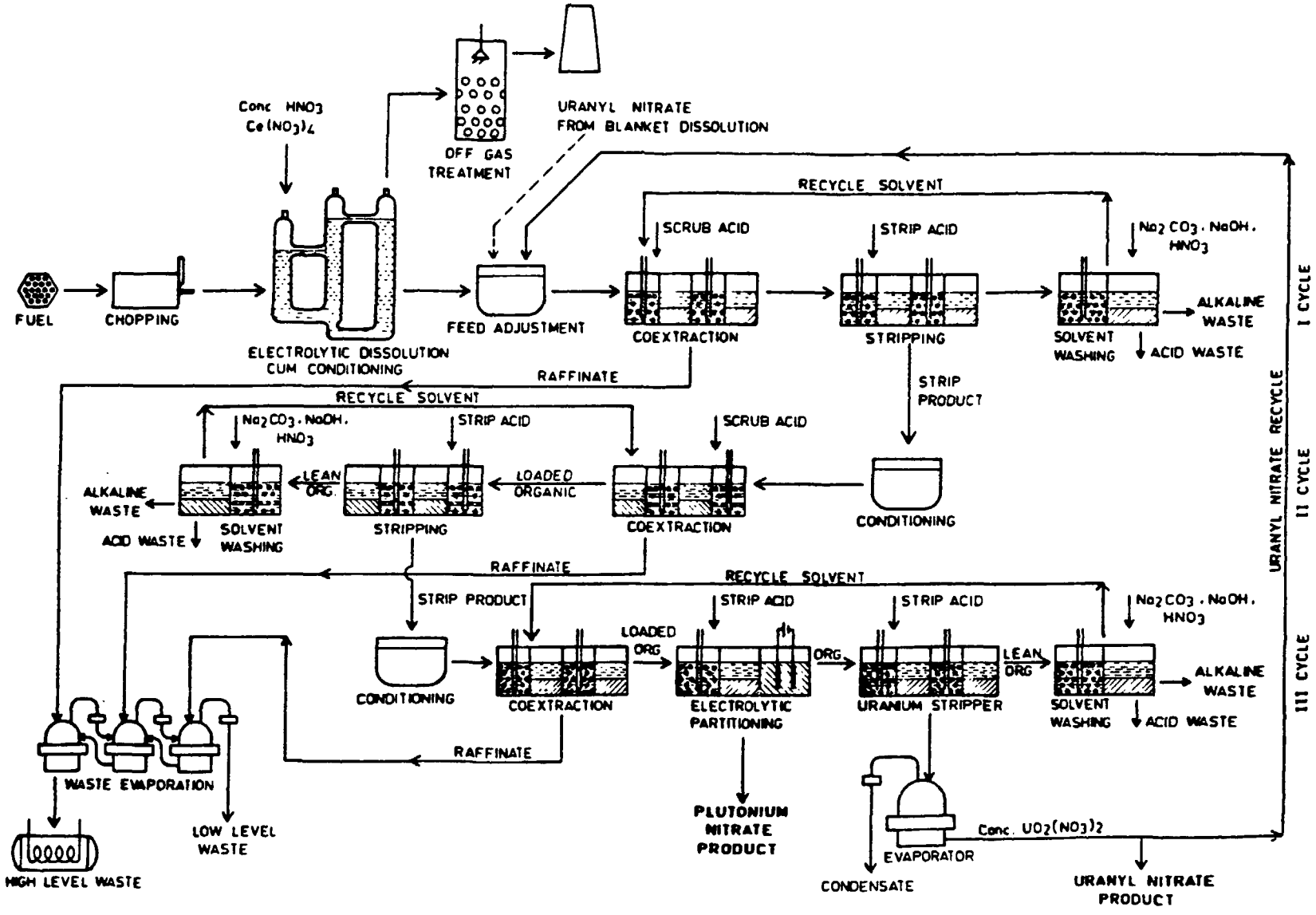

Fig.1 FBTR FUEL REPROCESSING

quality assurance programmes deserves utmost attention to ensure high reliability and long life of the plant equipment. Because of the multiplicity of the processes and complexity of the equipment and piping installations, selection of materials for different tasks becomes difficult. History of operating plants indicates that incidents such as failure of equipment, plugging of pipes due to corrosion product had contributed to the poor availability of the plants (1 & 2). Hence it is appropriate that IAEA has chosen this vital theme for the meeting at a stage when the economics of fast reactor fuel cycle is under critical review and it is anticipated that there will be a wide exchange of information.

Indian fast reactor programme:

It is expected that fast breeder reactors will be playing a major role in meeting the power requirements of the country. A dedicated research centre has been set up for the development of fast reactor technology and its associated fuel cycle . India has commissioned its fast breeder test reactor which uses mixed carbide as its fuel and other R & D labs related to its fuel cycle. The design for a 500 MW Prototype Fast Breeder Reactor is in progress.

The process folowed to reprocess fast reactor fuel is given in the flow sheet (Fig. 1)

1. The type of process and equipment used, nature of solution and environment and the criteria to be met for choice of materials are indicated for some of the important systems in Table-1. The table brings out how complex is the task for the design engineer who has to exercise the choice of material for particular applications.

2. Broad classification of systems for the choice of materials:

Following is the general classification that can be made with respect to the materials that are to be used for various applications in reprocessing plants. They are:

a) those used for equipment in process cells having nitric acid solution of varying temperature and concentration in a highly radioactive environment of alpha, beta and gamma.

b) those for application in equipment and piping installations in alpha active areas such as reconversion laboratory etc.

c) those used in amber areas such as control lab.

d) those used for handling and storage of low active effluent

e) those used for long term storage of high level waste.

f) those for lining of reprocess cells and waste vault.

g) those for handling chemicals and solvents.

h) those for various services.

Category 1.
a) Equipment of this category are associated with high beta-gamma activity and are located in process cells. They are dissolvers, process solution tanks, evaporators, condensers and solvent contactors. Dissolvers handle boiling nitric acid solution of high nitric acid concentration. High nitric acid concentration and boiling temperature can take s.s material to transpassive regions. In the electrolytic type of dissolver for mixed carbide using ceric ions as chemical oxidant, austenitic type of s.s of even low carbon content will undergo heavy corrosion. Zirconium or Titanium-5% Ta alloy is being proposed as the material for such a dissolver. TISA anode substitutes platinum anode and a special type of coating developed at this centre seems to have reasonable corrosion resistance and good performance. Even high chromium austenitic s.s seems to have high corrosion rate at boiling temperature in concentrated HNO_3 for oxide fuels. There again dissolver made of Zr seems to be better. The same argument holds good for raffinate evaporator especially when concentration of HNO_3 exceeds 6N.

b) Process vessel holding nitric acid solution up to 4N. AISI 304L type s.s seems to be adequate

c) For solvent contactors, AISI 304L s.s is generally satisfactory. It is preferable if 304ELC is used. Machined parts used must be solution annealed to have uniform grain structure.

In electrolytic type partition contactor, Ti metal and TISA anodes are used.

General precautions: It is better to avoid s.s where transpassive conditions are likely to occur. Zr or Ti-5%Ta can be used. Nitrogen concentration in Zr is limited to 100 ppm. Wherever s.s is used conditions of uniform structure in which carbon is dissolved in austenite is to be ensured. Avoid Mo content in s.s where boiling nitric acid is encountered. Corrosion allowance must be given for ease of decontamination. As far as possible semi finished product should be carefully prepared to obtain small austenite grains and fine inclusions with uniform distribution. For forgings, special attention must be paid to chemical composition of s.s to mitigate endgrain corrosion attack. Butt-welding should be preferred and any overlap should be continuously welded to prevent retention and crevice effects. Weld penetrations should be complete but without excessive thickness to avoid zones susceptible to defects. Vessels should be designed to enable complete draining. Sharp corners and recesses tending to trap stagnant acid in liquid or vapour form should be avoided. Corrosion product build-up should also be prevented. While welding, heat input has to be regulated to low values and while drilling holes, size of holes can be increased progressively to avoid excessive cold work. Quality assurance, using NDT techniques such as ultrasonic flaw detection is adopted. 100% radiography of butt-welds is to be carried out.

Mandatory: During welding, possibility of contamination of carbon is to be ruled out. At all stages of fabrication contact with iron particulate material is to be avoided. Components with end grain are to be avoided to exclude end grain attack.

Category 2: Equipment used in this area, compared to category I, have access available for repairs etc. For storage of solutions, AISI-304L s.s vessel can be used. Inconel is used for calcination and drying of oxalate

of Pu. While using glove boxes, as far as possible, combustible material is to be avoided. Stainless steel boxes painted with epoxy are used. Sometimes FRP moulded boxes are also used. Risk of fire necessitates avoiding use of perspex panels. For services s.s lines are found to be better than plastic materials such as PVC, HDPE etc.

Category 3: Here, as far as possible non-combustible materials are used. Fume hoods of s.s coated with epoxy paint are used. Exposure of s.s to boiling perchloric acid etc is controlled through scrubbers.

Category 4: For low level effluent lines, in the beginning stages, HDPE and PVC pipes are used. Stainless steel seems to be better. Delay tanks for the storage of low level effluents made of concrete, are painted with epoxy. They get attacked if the pH of the effluent is not controlled.

Category 5: Though initially vertical tanks constructed onsite were used, horizontal tanks of wider dia are being used nowadays. Since AISI-304L s.s tanks are being used it is necessary to avoid transpassive conditions. High cleanliness during fabrication, reduction of heat input and cold work are essential. Suitable allowances have to be given for reduction of thickness due to corrosion and erosion because of continuous sparging. Good fitment of the cell and the dished end is essential. Welding has to be carried out with uniform heat input to avoid distortions. Wherever necessary fixtures with suitable s.s interface should be used to contain the distortions. Though automatic metal arc welding can be used to accelerate the production rate, manual TIG welding is usually followed.

Lining of cells: The complete cell is lined with stainless steel and for the floor stainless steel angles and iron grid work are used for support. Though basic 310 type electrodes were used 309 type is suggested for the welding. Where there is ground water table, though hydraulic pressure exists, the lining part is separated with an intervening inspection space.

Utility application: Particular attention is given for use of ducts for labs. SS ducts are preferred. However fume scrubbers, to arrest fumes of acids such as perchloric acid, HCl etc should be used. Epoxy painting of the inside surfaces of the mild steel is followed if access is there for repair. Exposed external surfaces of the ducts can be covered with a concrete lining. If concrete ducts are used, they can be internally painted with epoxy to prevent attack by nitric acid vapour.

Flooring: Alpha labs and control labs are provided with PVC flooring. It is better to avoid large number of joints. Where heavy material handling is carried out heavy duty epoxy paints are used.

Fire and its influence on selection of material:

In active areas as far as possible non-combustible materials are used. Sand filters are preferred for large filter banks from this point of view.

Need for preparation of special code for fuel reprocessing plants:

Reprocessing industry represents operations involving low pressure and highly corrosive systems particularly concentrated nitric acid as compared to the high temperature, high pressure reactor system. At present the codes followed for nuclear reactors is applied to reprocessing industry also. There is also a need to develop special codes for remote welding used in hot cells.

SELECTION OF MATERIALS FOR FUEL REPROCESSING APPLICATIONS

PROCESS	EQUIPMENT	NATURE OF SOLUTION AND ENVIRONMENT	LOCATION	CRITERIA FOR SELECTION	REMARKS
Fuel transfer	Cask	Solid fuel or waste	Anywhere in shielded condition	As per the IAEA code.	Cask of steel body; lead filled for shielding
-do-	Alpha container	Fuel or solid (alpha, beta or gamma active)	Inside the cask or cell	Suitable for decontamination temperature resistance 100deg.C	Stainless steel or rigid PVC container is used
Chopping	Single pin chopper	Chopping of highly active fuel pin	Inside alpha, beta gamma process cell	High toughness and high reliability, long life for blade, chopper suitable for decontamination, no pockets for collection of dust. Temperature upto 100 deg.C	High speed steel blade for chopper; clad is of 304L
Dissolution	Dissolver	Highly concentrated HNO_3 (more than 8M) in boiling condition	Highly active alpha, beta, gamma cell	Material is likely to be transpassivated; uniform low corrosion rate and formation of uniform grain size; austenitic region; ability to stand corrosion in vapour form.	Stainless steel 304L is currently used which may not be suitable, Zr with 5% Ti is preferred (N_2 impurity content restricted to 100 ppm)
Offgas treatment	Offgas condenser	HNO_3 vapour	Process shielded cell	Withstand corrosive vapour. Crevice corrosion to be avoided.	SS 304L
-do-	Filter	HNO_3 and Iodine	Offgas room	Withstand corrosive vapour. Feasibility for remote maintenance	Deep bed fiber filter or fluidised sand bed filter
Liquid handling	Process solution tank	HNO_3 at 8M with insolubles	Process shielded cell	Withstand acid corrosion; uniform smaller corrrosion rate desired; fabrication as per stringent quality control inspection	Fabrication stringent as per quality control and inspection for SS 304L
Filtration	Centrifuge	HNO_3 at 4M with insolubles	Process shielded cell	Material should withstand stresses due to high centrifugal force and low corrosion rate	Bowl made of Stainless steel (disposed as solid waste)

Dissolution	Electrolytic dissolver	Electro oxidation of mixed carbide solution	-do-	Titanium vessel or platinum coated TSIA electrode vessel made of titanium.	SS Material likely to become transpassive; use either Ti with 5% Tantalum or High Cr Stainless steel or Zr
Conditioning	Conditioner	HNO_3 with Ce and highly radioactive materials	-do-	Ability to withstand corrosion in uniform passive region.	Though 304L is used presently, material suggested for dissolver may be preferred
-do-	Evaporator	HNO_3 solution and vapour	Hotcell	Corrosion resistance for boiling HNO_3 solution. Crevice corrosion to be avoided.	Possibility of reaching transpassive region in ss exists; though normally 304L is used material suggested for dissolver may be preferred
Extraction	Solvent contactor	HNO_3 solution in the range of 3 to 4M	Hotcell	Ability to withstand medium concentration HNO_3 solution, tolerance for vibration, crevice corrosion to be avoided.	Stainless steel 304L is used for electrolytic type solvent contactor. Ti, Pt and Tantalum are used
Piping	Process lines	HNO_3 solution and Vapour	Process cell	Intergranular corrosion resistance for weldment.	Mostly SS 304L. Stagnant liquid to be avoided
Precipitation	Precipitator	Oxalic acid	Glove box	Easy cleaning for solids, resistance to low concentration oxalic acid, resistance to fire.	Stainless steel or glass protected by stainless steel liner
High level waste storage	Storage tanks	HNO_3 at 6M; possibility of boiling	Waste vault	Resistant to boiling HNO_3, high reliability, long life, resistant to erosion by sparging, crevice corrosion resistance	
Low level waste storage	-do-	Dilute HNO_3	Delay tank and surrounding building	Ability to maintain integrity without seepage, avoiding the organic growth	Reinforced cement concrete painted with epoxy; pH to be stringently controlled. Low level effluent lines presently use HDPE; SS is recommended
Alpha material handling	Glove boxes	HNO_3 vapour in alpha environment	Reconversion lab	Fire resistance to HNO_3	Epoxy painted glove boxes are used

There is a programme to study corrosion in detail, such as inservice inspection to monitor thickness in waste tanks and corrosion studies using coupons in simulated experiments.

Facilities for R & D in corrosion.

The centre has a well equipped laboratory for carrying out simulation experiments to assess the corrosion rate of materials in different environments. Electrochemical studies using potentiostatic and potentiodynamic polarization techniques are extensively carried out. Since determination of degree of sesitization of the different grades of austenitic stainless steels is very important to avoid intergranular corrosion as well as intergranular stress corrosion cracking, tests using ASTM standard A262 practices A and E and tests using electrochemical potentiokinetic reactivation method are conducted on base materials and weldments in both annealed and cold worked conditions. Time-Temperature-Sensitization(TTS) diagrams for commercial grades of austenitic stainless steels used in the different plants are also generated. Continuous Cooling Sensitization(CCS) diagrams, of use to the designers in choosing the optimum parameters of heat treatment, have also been established using TTS diagrams and cooling curves. For studies on stress corrosion cracking of stainless steels in chloride and caustic environments, various testing methods such as slow straining rate method, constant load method, constant strain method and crack growth rate measurement method are used. Localised corrrosion studies (crevice and pitting corrosion) on stainless steels in acidified chloride media are carried out by electrochemical polarization tests. Optical and electron-optical examination of the corroded surfaces are carried out using optical microscopes, transmission and scanning electron microscopes, electron probe micro analyser and Auger electron microprobe. Failure analyses on failed plant components are also carried out using these metallographic facilities.

Presently, studies on the corrosion of titanium and its alloys (such as Ti-5%Ta) in boiling 6N HNO_3 acid are under way. Development of process for coating titanium with corrosion resistant oxide coatings for use as anodes in electro-oxidative dissolution of carbide fuels has also made significant progress. The corrosion tests on these oxide coated titanium anodes as well as assessment of the suitability of zirconium alloys as construction materials for different electrochemical process equipment in the reprocessing of spent fuels are the future programmes of the centre.

REFERENCES

1) Experiences and development status on fuel reprocessing and waste management in Japan. K.Uematsu, International Conference on Fuel Reprocessing and Waste Management, Wyoming, 1984.

2) Evolution of maintenance in Nuclear Processing facilities. John R.White, Proceedings of 30th conference on remote systems technology-1982.

3) Corrosion resistance of Zirconium, Ti, Ta alloys in HNO_3. T.Furuya et al., International conference on fuel reprocessing and waste management, American Nuclear Society, Wyoming, 1984.

4) Construction materials for Spent Fuel Reprocessing Plants by Messrs Chauve, Decours, Demay, Peltras and Simonnet, Nuclear Europe 2, 1986.

PANEL DISCUSSIONS

Summary and Conclusions

PANEL DISCUSSION I - MATERIALS FOR WASTE STORAGE

1. Long-term Interim Wet Storage

Radiation effects in regard to long-term wet storage of spent fuel on structural material and cladding were discussed.

The investigations carried out have shown that corrosion of materials is accelerated by radiolysis of water and corrosion product deposition.

Further, it was stated that laboratory tests carried out under the same level of gamma-irradiation led to lower corrosion rate of Zr-alloys than under real conditions in water pool.

Further programme: It is recommended that the above phenomena be followed up.

2. Long-term interim dry storage

Long-term interim dry storage, e.g. in the Pollux cask system in a steel containment which is closed by welding techniques, is in Germany under investigation. Those investigations include especially:

- mechanical
- thermal
- radiation
- corrosion

aspects.

Final Disposal

Development of containers for final disposal in clay and rock formations was discussed in regard to

- spent fuel
- vitrified high level waste.

This development includes especially

- mechanical aspects
- corrosion aspects.

For the mechanical aspects,e.g. the Pollux cask system for spent fuel makes use of existing standards in pressure vessel fabrication and reactor industry.

An important problem is the prediction of long-term corrosion.

In order to select materials with long-term corrosion stability, the corrosion behaviour of different materials was investigated.

The materials considered were both corrosion resistant materials such as Ni base alloys and Ti base alloys, as well as corrosion allowance materials like unalloyed steels, including commercial carbon steels, cast iron and copper.

The materials were investigated by using laboratory tests and in-situ experiments in different media with various parameters.

Most promising materials were

- Ti-Pd alloy
- Hastelloy C-4
- Unalloyed steel
- Copper.

Further programme

Further investigatons should be considered which are, in particular:

- study of effect of gamma dose rate
- hydrogen embrittlement
- stress corrosion cracking
- localized corrosion
- corrosion behaviour of coupled different materials
- different media
- especially, realistic environment media under normal and accidental conditions.

With regards to long-term extrapolation of the experimental results, the development of suitable corrosion and near field evolution models is needed.

Further, suitable corrosion monitoring techniques should be applied for in-situ corrosion evaluation under real repository conditions.

PANEL DISCUSSION II-MATERIALS FOR SPENT FUEL TREATMENT

The present experts agreed on the following points:

Existing practice and knowledge with respect to use of materials in spent fuel treatment, taking into account safety and operation aspects, are of high standards. With respect to lifetime of components, some improvements could be searched. The experts would suggest to:

(1) further differentiate the nature and localization of the various corrosion mechanisms that may shorten components service life.

(2) go on setting specific composition standards for materials which can be used in spent fuel treatment.

(3) further improve existing qualification tests for applicability closer to actual conditions of process media.

(4) establish specific design codes for spent fuel treatment equipment, rather than using too stringent codes adapted to higher pressure or temperature conditions.

(5) evaluate the feasibility of in-service monitoring of corrosion evolution.

LIST OF PARTICIPANTS

ARGENTINA

Geldstein, Maria Cristina
Comisión Nácional de Energía Atómica
Avenida Libertador 8250
Buenos Aires 1429, Argentina

BELGIUM

Tas, H.A.W.
S.C.K./C.E.N.
Boeretang 200
B-2400 Mol, Belgium

CZECHOSLOVAKIA

Koutsky, J.
Nuclear Research Institute
250 68 Rez near Prague
Czechoslovakia

FINLAND

Aaltonen, P.A.
Technical Research
Centre of Finland
Metals Laboratory
Kemistintie 3
02150 Espoo 15, Finland

Muttilainen, E.
Finnish Center for
Radiation and Nuclear Safety
P.O. Box 268
SF-00101 Helsinki, Finland

FRANCE

Bachelay, J.
SGN
1, Rue des Hérons
78182 Saint Quentin
Yvelines, France

Demay, R.
C E A/IRDI
Fontenay-aux-Roses
B. P. 6
92265 Fontenay-aux-Roses, Cedex
France

Decours, J.
CEA/IRDI
Saclay
B.P. No. 2, 91.210
Gif-Sur-Yvette, Cedex, France

FRANCE (Contd.)

Simonnet, J.

COGEMA
c/o SGN
1, Rue des Hérons
Montigny-Le-Bretonneux
78182 Saint-Quentin-En-Yvelines
France

Turluer, G.

C E A/IRDI
Fontenay-aux-Roses
B.P. 6
92265 Fontenay-aux-Roses, Cedex
France

FEDERAL REPUBLIC OF GERMANY

Leistikow, S.

Kernforschungszentrum
Karlsruhe GmbH
Institut für Material- und
Festkörperforschung II
Postfach 36 40
D-7500 Karlsruhe 1
Federal Republic of Germany

Popp, F.W.

Deutsche Gesellschaft für
Wiederaufarbeitung von
Kernbrennstoffen mbH (DWK)
Postfach 14 07
D-3000 Hannover 1
Federal Republic of Germany

Smailos, E.

Kernforschungszentrum
Karlsruhe GmbH
Institut für Nukleare
Entsorgungstechnik (INE)
Postfach 3640
D-7500 Karlsruhe 1
Federal Republic of Germany

Wolf, Irene

Kernforschungszentrum
Postfach 3640
D-7500 Karlsruhe
Federal Republic of Germany

Wolfbeiss, E.

Wiederaufarbeitungsanlage
Karlsruhe
Betriebsgesellschaft mbH
Postfach 220
7514 Eggenstein-Leopoldshafen, 2
Federal Republic of Germany

HUNGARY

Cserháti, A.	Nuclear Power Station Paks P.O. Box 71 H-7031 Paks, Hungary
Divós, F.	Nuclear Power Station Paks P.O. Box 71 H-7031 Paks, Hungary

INDIA

Gnanamoorthy, J.B.	Head, Chemical Metallurgy Section Materials Development Laboratory Indira Gandhi Center for Atomic Research Kalpakkam, 603102, Tamil Nadu, India
Balasubramanian, G.R.	Head, Reprocessing Programme Indira Gandhi Centre for Atomic Research Kalpakkam, 603102 Tamil Nadu, India

ISRAEL

Ben Haim, M.	Nuclear Research Center - Negev P.O. Box 9001 Beer Sheva, 84190, Israel

JAPAN

Ishiguro, N.	Power Reactor and Nuclear Fuel Development Corporation Reprocessing Division 1-9-13, Akasaka Minato-ku Tokyo, Japan
Yamanouchi, T.	Power Reactor and Nuclear Fuel Development Corporation Reprocessing Plant Tokai Works, PNC Tokai-mura, Naka-gun Ibaraki-ken, Japan
Yoshikawa, K.	Power Reactor and Nuclear Fuel Development Corporation 2nd Chemical Processing Section Processing Division Reprocessing Plant Tokai Works, PNC, Tokai-mura Naka-gun, Ibaraki-ken, Japan

REPUBLIC OF KOREA

Chang, H.L.	Korea Advanced Energy Research Institute Nuclear Chemical Engineering Division KAERI P.O. Box 7, Daeduk-Danji Choong-Nam, Republic of Korea

POLAND

Cholerzynski, Andrzej	Institute of Atomic Energy Isotope Production and Reactors Centre 05-400 Swierk - Otwock Poland

U.S.S.R.

Kritskij, V.G.	USSR, Leningrad-228 Dibunovskaj-57 VNiphiET

INTERNATIONAL ATOMIC ENERGY AGENCY (IAEA)

Ugajin, M. (Scientific Secretary)	Division of Nuclear Fuel Cycle
Nechaev, A.	Division of Nuclear Fuel Cycle
Onufriev, V.	Division of Nuclear Fuel Cycle

HOW TO ORDER IAEA PUBLICATIONS

An exclusive sales agent for IAEA publications, to whom all orders and inquiries should be addressed, has been appointed in the following country:

UNITED STATES OF AMERICA	BERNAN – UNIPUB, 4611-F Assembly Drive, Lanham, MD 20706-4391

In the following countries IAEA publications may be purchased from the sales agents or booksellers listed or through major local booksellers. Payment can be made in local currency or with UNESCO coupons.

ARGENTINA	Comisión Nacional de Energía Atómica, Avenida del Libertador 8250, RA-1429 Buenos Aires
AUSTRALIA	Hunter Publications, 58 A Gipps Street, Collingwood, Victoria 3066
BELGIUM	Service Courrier UNESCO, 202, Avenue du Roi, B-1060 Brussels
CHILE	Comisión Chilena de Energía Nuclear, Venta de Publicaciones, Amunategui 95, Casilla 188-D, Santiago
CHINA	IAEA Publications in Chinese: China Nuclear Energy Industry Corporation, Translation Section, P.O. Box 2103, Beijing IAEA Publications other than in Chinese: China National Publications Import & Export Corporation, Deutsche Abteilung, P.O. Box 88, Beijing
CZECHOSLOVAKIA	S.N.T.L., Mikulandska 4, CS-116 86 Prague 1 Alfa, Publishers, Hurbanovo námestie 3, CS-815 89 Bratislava
FRANCE	Office International de Documentation et Librairie, 48, rue Gay-Lussac, F-75240 Paris Cedex 05
HUNGARY	Kultura, Hungarian Foreign Trading Company, P.O. Box 149, H-1389 Budapest 62
INDIA	Oxford Book and Stationery Co., 17, Park Street, Calcutta-700 016 Oxford Book and Stationery Co., Scindia House, New Delhi-110 001
ISRAEL	Heiliger and Co., Ltd, Scientific and Medical Books, 3, Nathan Strauss Street, Jerusalem 94227
ITALY	Libreria Scientifica, Dott. Lucio de Biasio "aeiou", Via Meravigli 16, I-20123 Milan
JAPAN	Maruzen Company, Ltd, P.O. Box 5050, 100-31 Tokyo International
PAKISTAN	Mirza Book Agency, 65, Shahrah Quaid-e-Azam, P.O. Box 729, Lahore 3
POLAND	Ars Polona-Ruch, Centrala Handlu Zagranicznego, Krakowskie Przedmiescie 7, PL-00-068 Warsaw
ROMANIA	Ilexim, P O. Box 136-137, Bucharest
SOUTH AFRICA	Van Schaik Bookstore (Pty) Ltd, P.O. Box 724, Pretoria 0001
SPAIN	Díaz de Santos, Lagasca 95, E-28006 Madrid Díaz de Santos, Balmes 417, E-08022 Barcelona
SWEDEN	AB Fritzes Kungl. Hovbokhandel, Fredsgatan 2, P.O. Box 16356, S-103 27 Stockholm
UNITED KINGDOM	Her Majesty's Stationery Office, Publications Centre, Agency Section, 51 Nine Elms Lane, London SW8 5DR
USSR	Mezhdunarodnaya Kniga, Smolenskaya-Sennaya 32-34, Moscow G-200
YUGOSLAVIA	Jugoslovenska Knjiga, Terazije 27, P.O. Box 36, YU-11001 Belgrade

---

Orders from countries where sales agents have not yet been appointed and requests for information should be addressed directly to:

Division of Publications
International Atomic Energy Agency
Wagramerstrasse 5, P.O. Box 100, A-1400 Vienna, Austria